OAK RIDGE NATIONAL LABORATORY LIBRARIES
3 4456 0548293 8

CENTRAL RESEARCH LIBRARY
DOCUMENT COLLECTION

155

ORNL-3656
Special

THE JOINT NATIONAL INSTITUTES OF HEALTH–ATOMIC ENERGY COMMISSION ZONAL CENTRIFUGE DEVELOPMENT PROGRAM SEMIANNUAL REPORT FOR PERIOD JULY 1–DECEMBER 31, 1963

OAK RIDGE NATIONAL LABORATORY
operated by
UNION CARBIDE CORPORATION
for the
U.S. ATOMIC ENERGY COMMISSION

CENTRAL RESEARCH LIBRARY
DOCUMENT COLLECTION
LIBRARY LOAN COPY
DO NOT TRANSFER TO ANOTHER PERSON
If you wish someone else to see this document, send in name with document and the library will arrange a loan.

LEGAL NOTICE

This report was prepared as an account of Government sponsored work. Neither the United States, nor the Commission, nor any person acting on behalf of the Commission:

A. Makes any warranty or representation, expressed or implied, with respect to the accuracy, completeness, or usefulness of the information contained in this report, or that the use of any information, apparatus, method, or process disclosed in this report may not infringe privately owned rights; or

B. Assumes any liabilities with respect to the use of, or for damages resulting from the use of any information, apparatus, method, or process disclosed in this report.

As used in the above, "person acting on behalf of the Commission" includes any employee or contractor of the Commission, or employee of such contractor, to the extent that such employee or contractor of the Commission, or employee of such contractor prepares, disseminates, or provides access to, any information pursuant to his employment or contract with the Commission, or his employment with such contractor.

ORNL-3656
Special

Contract No. W-7405-eng-26

BIOLOGY DIVISION

THE JOINT NATIONAL INSTITUTES OF HEALTH–ATOMIC ENERGY COMMISSION ZONAL CENTRIFUGE DEVELOPMENT PROGRAM SEMIANNUAL REPORT

For Period July 1–December 31, 1963

N. G. Anderson
Program Coordinator

AUGUST 1964

NOTICE

This document contains information of a preliminary nature and was prepared primarily for internal use. It is subject to revision or correction and, therefore, does not represent a final report. Quotations from or references to this report must not be made in open literature without written permission from the individual authors.

OAK RIDGE NATIONAL LABORATORY
Oak Ridge, Tennessee
operated by
UNION CARBIDE CORPORATION
for the
U. S. ATOMIC ENERGY COMMISSION

OAK RIDGE NATIONAL LABORATORY LIBRARIES
3 4456 0548293 8

cy. 155

ORNL-3656
Errata

THE JOINT NATIONAL INSTITUTES OF HEALTH–ATOMIC ENERGY COMMISSION ZONAL CENTRIFUGE DEVELOPMENT PROGRAM FOR PERIOD JULY 1–DECEMBER 31, 1963

Please note the following corrections to the above report.

Page 32, fourth line from the bottom of column two. Change "B-IX" to read "B-XII."

The figures for Appendixes II and IV are interchanged. The drawings for Appendix II (Drawings of the B-IV System Released Through the Office of Technical Information Extension, AEC, Oak Ridge) can be found on pages 107 through 123. The drawings for Appendix IV [Block Diagram and Schematic Representation of Magnetic Support System for D-I Rotor (Abbot Master Available)] can be found on pages 93 and 94.

Summary

This report, the third under the Joint National Institutes of Health–Atomic Energy Commission Zonal Centrifuge Development Program, describes work on methods for separating subcellular particles, including viruses, being carried out at the Biophysical Separations Laboratory of the Oak Ridge Gaseous Diffusion Plant and at the Biology Division of the Oak Ridge National Laboratory.

The major efforts during this period have been directed toward the development of integrated centrifugal systems for isolating trace quantities of virus from tissues, plasma, and culture fluids. It has been found that when the sedimentation rates of subcellular particles are plotted against the particle banding densities, a vacant area, or "window," appears in the area where most viruses would be plotted. To exploit this "virus window," it has been necessary to develop methods for separating masses of particulate material first on the basis of sedimentation rate and second on the basis of density, and to adapt analytical methods to the description of the separations. To translate these theoretical possibilities into reality, the B-IV zonal centrifuge has been developed, together with methods for multiple-fraction isopycnic banding. The resolution of the system has been studied using a variety of biological materials, and several types of virus particles have been recovered in a high state of purity from tissue breis. The applicability of this system to the problem of searching human tumors for virus-like particles is now being explored. Before this can be effectively done, however, a survey of normal tissue components isolated by these systems is required. By use of a simplified system for particle isolation, virus-like particles have been consistently recovered from human leukemic plasma.

Isolation of virus particles by continuous-flow centrifugation has been examined both theoretically and experimentally. A rotor (B-V) capable of sedimenting particles as small as Echo 28 has been constructed and successfully tested. Since many viruses are inactivated by pelleting, the possibility of devising a high-speed continuous-flow centrifuge in which the virus particles are sedimented into a density gradient has also been examined. Two systems (B-VI and B-VII) designed and built during this period showed both the feasibility of this approach and the difficulties to be overcome. On the basis of this work, rotor B-VIII has been built and successfully tested.

The low-speed A-IX rotor has undergone extensive tests with cell fractions from plant and animal sources, and the high-speed C series rotors have been gradually moved from the level of experimental test systems to that of biological experimentation.

The program continues to be an interesting and a productive experiment in the adaptation of defense-oriented technologies to biomedical purposes.

Contents

SUMMARY iii

I. INTRODUCTION 1

II. BIOMEDICAL APPLICATIONS OF ZONAL CENTRIFUGES 2

A. Isolation of Trace Amounts of Virus from Tissues 2
1. Viruses and Subcellular Particles 2
2. Virus Window 3
3. Detection of Virus Particles 5
4. Determination of Sedimentation Rates 5
5. Rate-Zonal Separations 7
6. Isopycnic Banding 7
7. Virus-Isolation Studies 7
8. S-ρ Plots with Tissue 7
9. Alternate Procedures 9

B. Analytical Studies on Ribosomes Isolated with the B-IV Zonal Ultracentrifuge 9
1. Separation of 30S and 50S Ribosomal Subunits by Zonal Centrifugation 9
2. Separation of Ribosomal Proteins by Disk Electrophoresis 10
3. Radioactivity Determinations 11
4. Discussion 12

C. Virus-Like Particles in Human Leukemic Plasma 12
1. Methods 12

D. Studies on the A-IX Rotor 14

E. Development of Reorienting Gradient Centrifugation Using the A-VIII Rotor 15
1. Resolution 15
2. Separation and Recovery of Pollen Grains 16
3. Effect of Number of Septa 16
4. Prospects for Further Development 18

Bibliography 18

III. THEORETICAL STUDIES 21

A. Continuous-Flow Centrifugation 21

IV. ROTOR DESIGN 23

A. Rigid Rotor Dynamics 24

B. Metallurgical Studies 24

V. LOW-SPEED ZONAL ROTORS 28

A. Rotor A-IX 28

B. Rotor A-X 28

VI. INTERMEDIATE-SPEED ZONAL ROTORS 29
A. B-IV System 29
1. Stability Studies 29
2. Damping Bearing 29
3. Core 30
4. B-IV Instrumentation, Containment, and Operation 32
B. Modifications of the B-IV System for Continuous-Flow Concentration of Particles 32
C. Zonal Rotor Systems Under Development 32
VII. HIGH-SPEED ZONAL ROTORS 33
A. C-II Rotors 33
B. C-III Rotors 33
VIII. ULTRAHIGH-SPEED ROTORS 34
A. D-1 Magnetic Support System 34
IX. CONTINUOUS-FLOW ROTORS 36
A. Rotor B-V 36
1. Principles of Operation 36
2. System 36
B. Continuous Flow with Continuous Isopycnic Banding 40
1. General Principles 40
2. B-VI and B-VII Cores 41
3. Rotor B-VIII 42
X. SEAL DEVELOPMENT 43
A. Type "A" Seals 43
B. Type "B" Seals 45
C. Type "B" Flow-Through Seal 46
XI. GRADIENT MATERIALS 48
A. Preparation of Pure, Sterile Sucrose for Zonal Centrifugation 48
B. Preparation and Recovery of Cesium Compounds 49
1. Experimental Extraction Systems 49
2. Preparation of Organic Compounds of Cesium 49
XII. CONTAINMENT AND STERILIZATION 50
XIII. OPERATING PROCEDURES 53
A. Sample Collection and Homogenization 53
B. Cleaning and Sterilizing 54
C. Assembly of Rotor System 54
D. Gradient Pump Assembly 59
E. Calibration of $\int \omega^2 dt$ Integrator 60
F. Introduction of Gradient and Sample 61
G. Gradient Recovery 64

H. Density and Refractive Index Determinations 66
I. Banding Methods 66
J. Preparation of Samples for Electron Microscopy 72
K. Comments on Operating Procedures 72

XIV. DATA REDUCTION 74
A. Computer Program for the B-IV Zonal Centrifuge 74
1. Program Modifications 74
2. Calculation of Density over Extended Temperature Range 74
3. Viscosity Calculations 75
4. Volume and Radius Formulas for the B-IV Rotor 75
B. Calculation of Viscosity of Sucrose Solutions 75

XV. ANCILLARY STUDIES 78
A. Flame Ionization Analyzer for Determining Total Carbon in Liquid Streams or Solid Samples 78
1. General Considerations 78
2. Operation of Equipment 78
B. Subcellular Fractions of *Astasia longa* as Separated in the Zonal Ultracentrifuge 82

Appendix I. DRAWINGS OF A-IX ROTOR 85

Appendix II. DRAWINGS OF THE B-IV SYSTEM 91

Appendix III. DRAWINGS OF B-II, B-IV, B-VII, AND B-VIII ROTORS AND DAMPER BEARING 95

Appendix IV. BLOCK DIAGRAM AND SCHEMATIC REPRESENTATION OF MAGNETIC SUPPORT SYSTEM FOR D-1 ROTOR 105

I. Introduction

The Oak Ridge installation of the Atomic Energy Commission (AEC) was originally organized to achieve difficult separations. These included the separation of uranium isotopes by two large-scale processes, the separation of plutonium and other fission products, and the isolation of numerous radioisotopes from contaminating substances. It has been of interest to determine whether certain of the skills, techniques, facilities, and individuals associated with these AEC programs could be adapted to the solution of difficult separation problems encountered in biomedical research. The separation of subcellular organelles and viruses presents problems which are comparable in difficulty with some of the isotopic separations. If small virus particles existing at levels as low as, for example, one particle per cell are to be isolated, it will be necessary to achieve purifications ranging from 10^6 to 10^8 fold. The centriole, a key organelle in the process of cell division, has not been isolated from mammalian cells to date owing to the lack of high-capacity high-resolution separation systems. It is not unlikely that other cell components which occupy only a small fraction of the cell mass remain to be discovered.

The common denominator of our present interests is the virus particle. Evidence has accumulated suggesting that ionizing radiation may activate latent oncogenic viruses in animals. The mechanisms involved are obscure. However, virus infection is known to produce chromosome breakage in tissue culture and may conceivably cause the specific chromosomal abnormalities observed in human leukemic cells. The central experimental difficulty is that the definitive experiments which are possible in animals cannot be done in man. The problem of whether human leukemia, for example, may involve a virus released by radiation is not amenable to a simple solution.

The direct approach, that of looking for the virus by physical means, brings to one focus certain of the interests existing in the AEC, the National Cancer Institute, and the Biophysical Separations Laboratory at Oak Ridge. Specifically, the development of virus-isolation techniques is germane to the problems of the cause of human cancer generally, the relation of radiation to human neoplastic disease, especially leukemia, and the physical problem of the separation of particles in centrifugal or other physical systems. From the biophysical viewpoint many virus particles are nearly ideal test objects for the study of separation methods. Viruses can be detected over an extremely wide range of concentrations by biological and physical methods, they exist in a size range which falls within the size spectrum of subcellular particles, and they are, in many instances, both nearly spherical and of uniform size and density. Thus the problem of isolating trace quantities of virus from cells and tissues is of interest from many points of view. The problems to be solved are, for the most part, concerned with the development of separation methods having the highest resolution that can be obtained. Only as the physical, colloid-chemical, mathematical, metallurgical, and engineering problems involved are solved can the parallel biological problems be attacked. Initially, therefore, this program must be concerned with the development of tools, their perfection, and their calibration. As this is accomplished, emphasis can be shifted to their application to pertinent biological problems.

It should be emphasized that concentration on the isolation of one type of subcellular particle – the virus – does not diminish the applicability of the systems developed to the isolation of other subcellular particles. On the contrary, the isolation of particles suspected to be heterogeneous in their physical properties can best be done after it has been demonstrated that the polydispersity observed is not due to low resolution of the isolation system.

II. Biomedical Applications of Zonal Centrifuges

A. ISOLATION OF TRACE AMOUNTS OF VIRUS FROM TISSUES

N. G. Anderson C. L. Burger
W. W. Harris

We shall address ourselves first to the problems of whether, in theory, trace amounts of various types of virus particles can be isolated in a high state of purity from tissues; second, to the various methods by which such separations might be accomplished; and third, to experimental studies with model systems.

1. Viruses and Subcellular Particles

Initially the question must be asked: Are most virus particles sufficiently different from the particles found in broken cell suspensions to allow their isolation by physical methods in a reasonable state of purity? On purely theoretical grounds it is evident that particles having very different densities may have the same sedimentation coefficients in a given solvent. This follows from the fact that the sedimentation rate of a sphere is proportional to the product of the square of the particle radius and the difference in density of the particle and the solvent. In the case of the uniform spherical viruses, we wish to isolate particles of one radius and one density. Separations based on sedimentation rate are sensitive to both parameters, while isopycnic separations depend, obviously, on density alone. To make separations of maximal resolution, therefore, it is necessary to perform both a rate-zonal and an equilibrium, or isopycnic, fractionation. The choice of the order of the separation depends on several considerations. Cell nuclei, which may have the same equilibrium density as certain viruses, are disrupted or extracted by the high salt concentrations employed in most equilibrium centrifugation procedures, including those using cesium chloride. Such extracted nucleoprotein would not behave as do nuclei in subsequent rate-zonal separations. Other cell components may also be altered by salt extraction. An additional disadvantage is that in equilibrium studies with presently available systems, sufficient centrifugal force to band soluble proteins sharply in a relatively short time is not generally available. Banded virus particles may therefore not be free of contamination by smaller particles which have not reached their isopycnic points. Further, the rate separations, which do not involve expensive materials, but which do require relatively large volume gradients, may be done at a lower speed than that usually required for isopycnic banding.

To maximize the particle radius dependence of the rate separations, the difference in density between the particle of interest and the solvent should be maximized, and the separations carried out at the lowest density practicable. This is evident from the fact that the effect of radius on sedimentation approaches zero as the term $(\rho_p - \rho_0)$, where ρ_p is the density of the particle and ρ_0, the density of the solvent, approaches zero (i.e., particles of any radius may band at the same density level if they have the same density). These considerations suggest that the maximal separation for scanning purposes may be obtained by first separating subcellular particles on the basis of sedimentation rate in a zonal centrifuge and then subfractionating the fractions obtained on the basis of density alone. Alternate methods adapted to the problem of isolating specific particles will be discussed in subsequent reports. Of interest here is the question: Will such separations yield relatively pure viruses?

2. Virus Window

Restating the above question more precisely: If all cell constituents, with the exception of viruses, are plotted with the sedimentation rate in water at 20°C along the abscissa and banding density along the ordinate, will there be a vacant space, or "window," in the area where most viruses would fall? If viruses are theoretically separable by such a combination of methods, at what concentration in a tissue can they be detected using available physical detection methods?

Data on the sedimentation rates and densities of viruses and various cell components are given in Fig. II-A-1. The values for the sedimentation coefficients are corrected to water at 20°C. In practice, separations dependent on density alone are made in salt gradients. The isopycnic point of a given particle is not the same in all gradients; it will depend on the degree of hydration of the

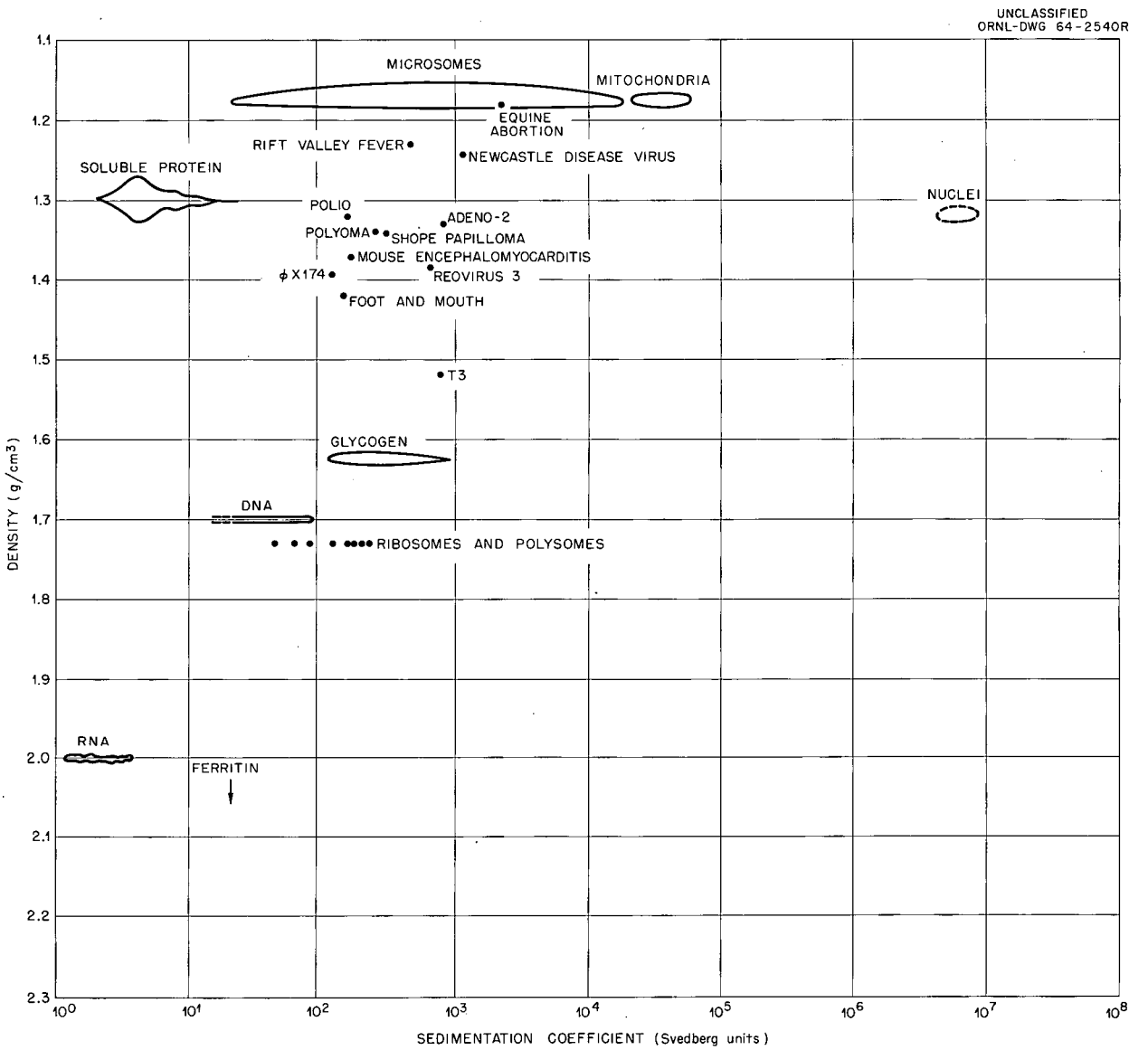

Fig. II-A-1. Sedimentation Coefficients and Banding Densities of Cell Components and Viruses. Sources of data given in text. Note that most virus particles fall in an area, here termed the "virus window," essentially free of cell constituents.

particle in a given medium, the permeability of the particle to the solutes used to make the gradients, and the extent of the solute binding. The banding densities given, unless otherwise stated, are for cesium chloride. In other gradients the values may be numerically different, but the overall distribution of viral and cell component densities would tend to remain the same. The values for the sedimentation rates of proteins are those for rat liver (Anderson and Canning, 1959) which do not differ greatly from the values for rat brain, kidney, and testes. The density ranges for soluble tissue proteins have not been determined in CsCl; however, they probably do not vary greatly from the value of 1.295 reported for bovine serum albumin (BSA) and for human hemoglobin (Cox and Schumaker, 1961). Values for the sedimentation coefficients of ribosomes and polysomes are for rabbit reticulocytes (Gierer, 1963), and the densities are those extrapolated from *Escherichia coli* ribosome data (Tissieres *et al.*, 1959). It is assumed that polysome densities would not be very different. The range of sedimentation coefficients shown for "microsomes" is that observed with rat liver in the zonal ultracentrifuge, and the density range was obtained by banding in CsCl fractions separated in the zonal ultracentrifuge. The sedimentation rates for mitochondria are calculated from the data of de Duve *et al.* (1959) and of Thomson and Klipfel (1958). Nuclear sedimentation coefficients are calculated values assuming diameters ranging from 6 to 12 μ and an average density of 1.040 (Falzone *et al.*, 1962) in dilute buffer. The CsCl density is estimated on the assumption that nuclei contain 77% protein and 19% DNA (Hale and Kay, 1956) and that the isopycnic densities would be the sum of the density of each component times the percentage present. In practice, the nucleoprotein would dissociate, at least partially, and would probably yield several bands. The nuclear isopycnic density is therefore a calculated value given to indicate a region where separations of nuclear from nonnuclear materials would be difficult. The position of glycogen is taken from studies on the distribution of sedimentation coefficients of material isolated from liver (Meyer and Zalta, 1958; Bell *et al.*, 1948; Polglase, Brown, and Smith, 1952). The banding density in CsCl is taken from experimental studies carried out in this laboratory (Anderson, unpublished) using glycogen isolated from rat liver. The value is slightly higher than that previously reported (Bell *et al.*, 1948; Bryce *et al.*, 1958). Ferritin was isolated from human leukemic spleen by zonal centrifugation followed by isopycnic banding.

Deoxyribonucleic acid (DNA), which would not ordinarily be found free in homogenates of mammalian cells, but would be encountered in bacterial homogenates, and might be found extracted from viruses during the preparation of pathological tissues, is also included in Fig. II-A-1. The banding density range is taken from Schildkraut, Marmur, and Doty (1962), and the range of sedimentation rates includes that of single DNA molecules from T2 phage (Hershey, Burgi, and Ingraham, 1962) and a variety of published values. Ribonucleic acid (RNA) has a density in CsCl at the limits of the density available with this salt. The density of 2.0 observed in cesium formate (Davern and Meselson, 1960) has therefore been used. The sedimentation rate range is taken from a number of sources (Cheng, 1962); (Cox and Amstein, 1963). The accurate positioning of cell components from various tissues in the sedimentation rate–banding density (hereafter termed S-ρ) plot will require much additional experimental work, and some of the values used here must be treated with reservation.

Data on the following viruses are taken from published studies: adenovirus 2 (Green, 1962; Kohler, 1962); equine abortion virus (Darlington and Randall, 1963); foot-and-mouth disease virus (Breese, Trautman, and Bachrach, 1960; Trautman and Bachrach, personal communication); mouse encephalomyocarditis virus (Faulkner *et al.*, 1961; Hansen and Schäfer, 1962); Newcastle disease virus (Rott, Reda, and Schäfer, 1963; Stenback, 1963); ϕX 174 (Sinsheimer, 1959; Eigner, 1962); polio virus (Holland *et al.*, 1960; Polson and Levitt, 1963); mouse polyoma (Crawford and Crawford, 1963; Howatson and Crawford, 1963; Mayor, 1961; Melnick, 1962; Winocour, 1963); reovirus 3 (Gomatos and Tamm, 1963); Rift Valley fever virus (Naude, Madsen, and Polson, 1954; Polson and Levitt, 1963); Rous sarcoma (Crawford and Crawford, 1961; Epstein, 1956, 1958; Epstein and Holt, 1958); and Shope papilloma virus (Breedis, Berwick, and Anderson, 1962; Crawford and Crawford, 1963).

It is evident from an examination of Fig. II-A-1 that a "window" appears in the S-ρ plot which includes a minimum amount of nonviral material, and that a large fraction of known viruses would

fall in it. In those instances where a virus has the same banding density as a part of the microsomal fraction, it is evident that the virus cannot be completely separated from contaminating material by centrifugal procedures. Chemical (Kovacs, 1962) or enzymatic dissection may then be necessary. Since the microsomal particles have a wide range of sedimentation rates, however, it should be possible to isolate the virus from the majority of the microsomal mass. The amount of endoplasmic reticulum present which gives rise to microsomes varies widely in different cells and tissues but is low in many tumors and in some cells used for virus production.

These considerations have prompted us to explore methods for large-scale separation of subcellular constituents which would be analogous to the separations shown diagrammatically in Fig. II-A-1.

3. Detection of Virus Particles

Infectivity in a suitable test system will remain the most sensitive method for detecting virus particles. The physical methods for detecting viruses isolated in a reasonable state of purity include absorbance in the ultraviolet, light scattering, electron microscopy, and measurement of fluorescence after conjugation with fluorescent antibodies. The usefulness of each of these methods depends on the concentration of virus achieved. By the use of negative staining techniques, particle counting methods, or sectioning of pellets, it appears that the identification of virus particles on a morphological basis is feasible at the level of one particle per cell if the virus is obtained in a pure form in the same concentration in which it existed in the source tissue. For example, if liver containing 4×10^8 cells/g is used, then the final virus concentration (4×10^8/ml) would be at the lower limits of detection using spray counting methods (Dourmashkin, 1962; Breese and Trautman, 1960) but well within the range of the Sharp counting technique (Sharp and Beard, 1952; Sharp and Overman, 1958; Smith and Benyesh-Melnick, 1961).

For detection of most viruses by ultraviolet absorbance measurements, somewhat larger amounts of virus will be required. The number of optical density units necessary will depend on the optical density of the gradient itself, the length of the light path, and the volume in which the virus is recovered. If the lower limit is 0.1 absorbance unit, then 13×10^{12} particles of the small foot-and-mouth disease virus (Trautman, personal communication), 1.2×10^9 physical particles of poxvirus (Joklik, 1962), or 2.3×10^6 vaccinia particles (Planterose, Nishimura, and Salzman, 1962) would be required. This limit may be lowered by the use of long light path cells (Reimer, personal communication), electronic methods for extending spectrophotometric ranges, or refined small-volume banding methods. The conclusion is, however, that if small virus particles are to be detected by ultraviolet absorbance, the concentration per unit volume must be 10 to 100 times higher than is found in the starting tissue, assuming that only one virus particle is found per cell. For very large viruses, however, the direct absorbance measurements would probably suffice.

Light scattering as a method of detecting virus-sized particles in gradients is capable of much greater sensitivity than absorption measurements. As will be shown in subsequent sections, this method is sensitive below the level where electron microscope counting is ordinarily done. At the arbitrary lower limit of interest here ($\sim 10^8$ particles/ml), light scattering appears to be the gradient monitoring method of choice.

It is concluded that if methods can be developed which will allow only those particles having a narrow range of sizes and densities characteristic of a given virus to be isolated, and if the final concentration is equal to or greater than the concentration in the tissue of origin, then virus particles which exist at a level as low as one particle per cell can be isolated and described. Since the mass of a virus varies from approximately 10^{-6} (Rubin, 1962) to 10^{-8} of that of a cell, the purification (as distinguished from concentration) required is from a million to 10 million fold.

4. Determination of Sedimentation Rates

A computer program (report ORNL-3502 and Chap. XIV of this report) is used to determine the equivalent sedimentation rates (S*), in water at 20°C, which spherical particles which do not behave osmotically would have if found at various points in the gradient after a given period of centrifugation. The basic equation is a modification of that used by Martin and Ames (1961). In a

zonal centrifuge the position of a given particle is determined in the gradient stream recovered from the centrifuge at the end of the run. The term $\omega^2 t$ used in the calculations therefore refers to the centrifugation done during acceleration, at speed, and during deceleration. An electronic system is therefore used to compute $\int \omega^2 \, dt$ continuously during the course of the run.

In experiments designed for searching tissue breis for virus particles, it is desirable to centrifuge long enough to spread known virus particles between the soluble protein zone and the mitochondrial zone. Rat liver mitochondria tend to band isopycnically in sucrose gradients at a density level of 1.203 g/cm^3 (44.5 w/w % sucrose). In practice, virus particles are not allowed to reach this density during rate-zonal centrifugation.

By use of the B-IV computer program, the positions which particles having a range of densities and sedimentation coefficients would have as a function of equivalent centrifuge time at 20,000 rpm were calculated. These are plotted in Fig. II-A-2. With the gradient used for these calculations, a suitable spread is obtained in 1 hr at 20,000 rpm. This speed and time have been used for the majority of the studies made to date.

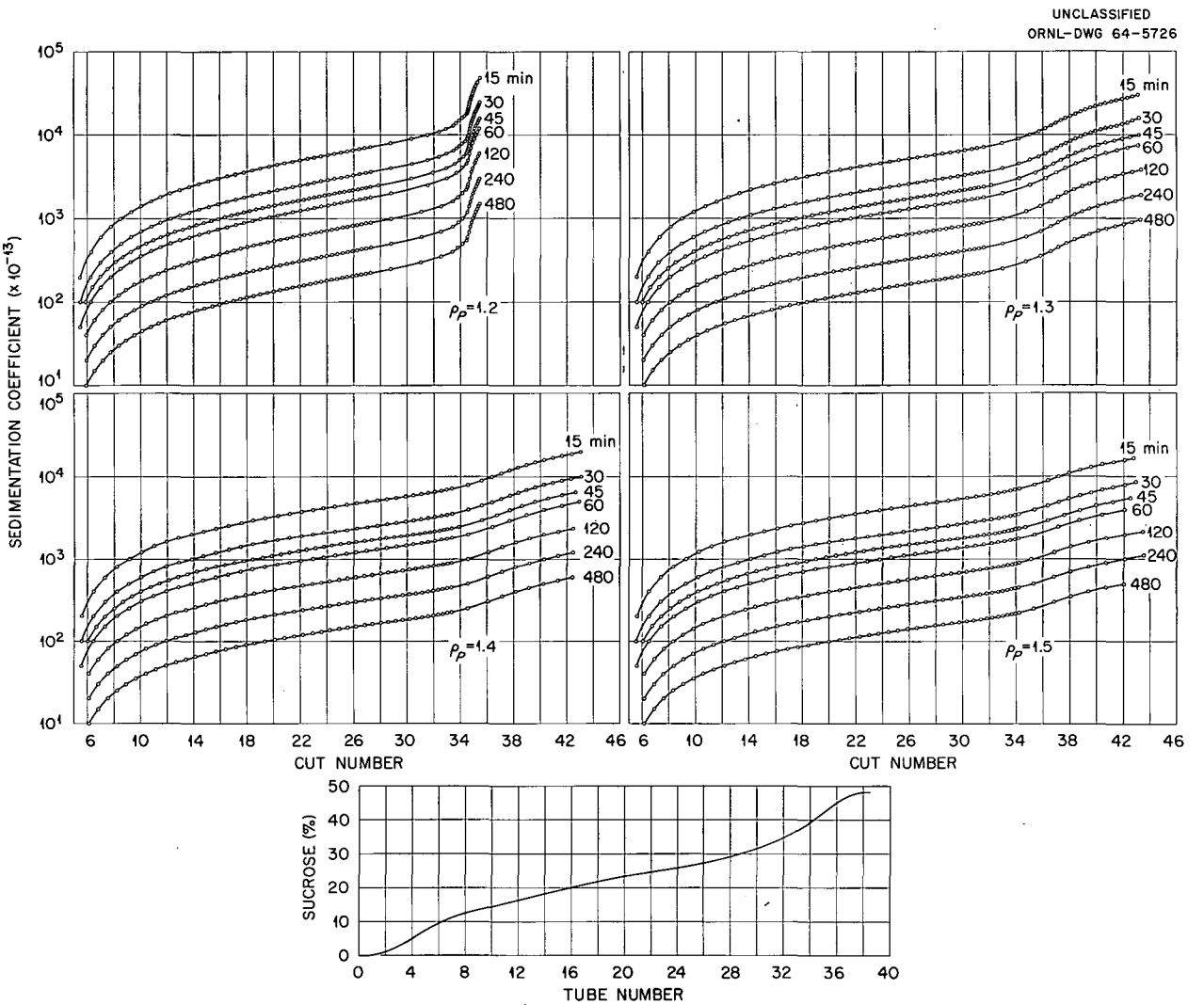

Fig. II-A-2. Positions in a Sucrose Density Gradient in the B-IV Rotor Which Particles Having Indicated Densities and Sedimentation Coefficients Would Have After Centrifugation at 20,000 rpm for Times Indicated (Run 208).

5. Rate-Zonal Separations

From early studies on the use of centrifugal force to stabilize density gradients as they are introduced into centrifuge tubes in a spinning rotor (Albright and Anderson, 1958), it became apparent that the operations of setting up the gradient, introducing the sample layer, separating the various particles in a centrifugal field, and recovering the separated fractions might well be accomplished in a suitable hollow centrifuge rotor *during rotation*. The first zonal rotor built in 1955 (Anderson, 1955, 1956) confirmed this view. Further work resulted in the development of the B-II rotor completed in 1960 (Anderson, 1962). Unfortunately, this rotor was destructively unstable in the region of 31,000 rpm. The steps necessary to redesign this system for operation at 40,000 rpm have resulted in the development of the B-IV system described in Chap. VI of this report. Detailed procedures for operation and calibration are presented in Chap. XIII. Since it is now possible to obtain highly purified and concentrated suspensions of virus particles from human and animal tissues, it has been considered of importance to develop methods for containing as much of the apparatus as possible in Freon-tight glove boxes (see Chap. XI). In addition, all solutions used must be sterile and, as far as possible, particle free (see Chap. XI). The gradient recovered at the end of the run is monitored for ultraviolet absorbance as it flows out of the centrifuge. In addition, total protein (determined by an automated method), refractive index, and physical density are determined on all the fractions collected.

6. Isopycnic Banding

The fractions obtained by rate-zonal centrifugation must now be banded isopycnically (Meselson, Stahl, and Vinograd, 1957) to determine whether particles having different banding densities are present. Since some viruses are known to be inactivated by pelleting, it is not desirable to centrifuge particulate material out of the sucrose solutions and then resuspend it in CsCl or other salt solutions and subsequently centrifuge the CsCl suspensions in swinging-bucket rotors. Rather it is important to band the unpelleted particles as rapidly as possible by a method which would allow as many as 24 samples to be run at once. In previous studies (ORNL-3502) it was shown that the shearing which occurs during the transition from rotation to rest in a liquid density gradient in an angle-head rotor is small and that sharp banding of viruses and DNA could be obtained. Larger particles tend to clump under these conditions but will still band. To generate a large number of gradients rapidly, two methods have been employed. In the first the zonal centrifuge fractions (forty 40-ml tubes) are transferred to Spinco 30 rotor tubes containing 6 to 9 g of dry CsCl. During a 14- to 16-hr centrifugation at 24,000 rpm, the CsCl dissolves to form a steep gradient. In the second method the tubes were half filled with the particle-containing sucrose solutions, and then 10 to 15 ml of saturated CsCl was run to the bottom of the centrifuge tube through a narrow piece of tubing. The tubes were then completely filled with the particle suspension. The latter method requires more time but yields more reproducible gradients. The details of methods for preparing and scanning gradients are discussed in subsequent sections.

7. Virus-Isolation Studies

The amount of material in a tissue brei having the same sedimentation properties as a given virus or virus-like particle limits the purification which can be achieved by rate-zonal centrifugation. In the previous report (ORNL-3502) the results of studies on rat spleen and liver preparations were presented. These findings have now been extended to normal and leukemic mouse spleen, and to human spleen from patients with Hodgkin's disease.

8. S-ρ Plots with Tissue

The development of particle search methods has been guided by a variety of experiments (48 in all during this period with the B-II and B-IV zonal centrifuge rotors) using animal tissues and viruses, bacteriophage, and human autopsy tissue samples. The results confirm the presence of a "virus window" slightly beclouded by a small number of unidentified cell particles. Many hundred electron micrographs have been taken of the fractions obtained. Presentation of these is deferred until all the necessary control experiments have been done

and the interpretations and comparisons are complete. Although the entire search system has been assembled only very recently, the studies to date bear out the early expectations. The results with one complete run using a sample of normal human spleen are shown in Fig. II-A-3. A total of 37.8 g of tissue was homogenized in 151 g of pH 7.5 phosphate-NaCl buffer for 1 min using a Sorvall motor-driven blade-homogenizer. The brei was then centrifuged in 250-ml sterile closed cups

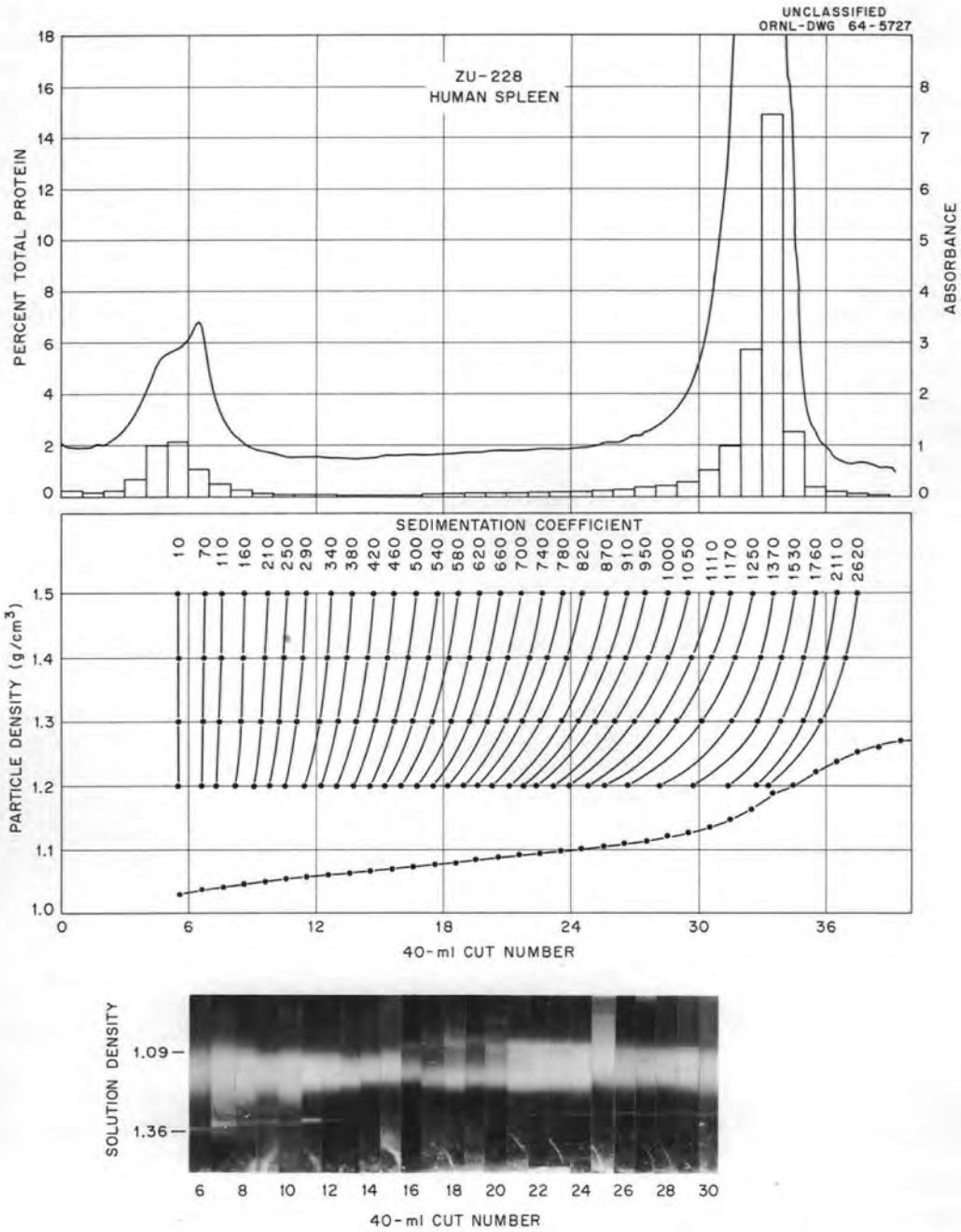

Fig. II-A-3. Fractionation of Normal Human Spleen. Upper plot shows rate zonal centrifugation separation, computer program plot is shown in center, and isopycnic separations in CsCl are shown at the bottom. Preparation of sample described in text.

at 2300 rpm in the International PR-2. The supernatant was removed and centrifuged for 2 hr at 27,000 rpm in the Spinco 30 rotor. The pellets were resuspended and combined in a total volume of 21 ml and used as the sample in a rate-zonal separation run in the B-IV zonal ultracentrifuge using a 1-liter gradient extending from 10 to 30% (w/w) sucrose with a cushion of 55% sucrose (see operating procedure in Chap. XIII). The centrifuge was run 1 hr at 20,000 rpm and unloaded at 5000 rpm. Fractions 6 to 30 were banded at 24,000 rpm for 8 hr using 8 g of dry CsCl per rotor tube. The results are shown in Fig. II-A-3. It should be noted that only a small portion (0.1–0.2%) of the total sample per fraction collected is found in the virus sedimentation rate range. The material present in the lower sharp band in the isopycnic separations was present in an amount too small to be identified as yet by electron microscopy. Under these conditions ferritin is found in a very pure state at the bottom of the CsCl tubes, generally in fractions 6 to 9. These results must now be extended using normal tissues from a variety of sources combined with biochemical analysis to identify the various fractions separated.

9. Alternate Procedures

The method as described here for searching tissues is useful for up to about 4 g of tissue without precentrifugation. By removing nuclei and mitochondria by low-speed centrifugation and subsequently sedimenting virus and microsomes, the initial virus concentration can be increased and masses of tissue as large as 50 to 100 g can be used, depending on the nature of the tissues and the mass of microsomal material present. To process larger amounts of tissue, several other systems are being examined. Theoretical studies on continuous-flow centrifugation (Berman and Anderson, in preparation) suggest that serial or cascaded centrifuge systems can be constructed which will allow the microscopic elements of tissue breis to be removed from multiliter batches of brei, with subsequent sedimentation of the virus in higher-speed continuous-flow rotors such as the B-V recently described (Barringer, Anderson, and Nunley, in preparation; also Chap. V, Sect. A).

In the B-V rotor the virus particles are pelleted onto a vertical surface and must be removed from the rotor at rest. Experiments now in progress demonstrate that continuous-flow centrifugation can be arranged so that the feed stream flows over a density gradient. Particles settling out of the stream are therefore also banded at their isopycnic position. The gradient is recovered from the rotor during rotation. The B-VIII rotor used to demonstrate this principle yields peaks with the viruses thus far studied. These are concentrated into volumes of 40 to 100 ml. The virus may be further reduced in volume by banding in high-speed rotors such as the experimental C-II rotor (141,000 rpm, 310,000 $\times g$ with 110 ml of CsCl solution with an average density of 1.7). The application of these alternate systems to tissues will be described in subsequent papers. To explore the resolution of each S-ρ separation system, a variety of virus-induced tumors and infected tissues must be examined.

B. ANALYTICAL STUDIES ON RIBOSOMES ISOLATED WITH THE B-IV ZONAL ULTRACENTRIFUGE

Eric Schram W. D. Fisher

Although much information is available concerning the role of ribosomes in protein synthesis, little is known about ribosome formation – especially about the synthesis of their structural proteins. The experiments reported here were performed to gain some insight into the specificity and the mechanism of synthesis of these proteins.

1. Separation of 30S and 50S Ribosomal Subunits by Zonal Centrifugation

Since ribosomes are generally contaminated with nascent proteins or with cytoplasmic proteins, the choice of the isolation procedure is a crucial step in the study of ribosomal proteins. Moreover, the quantities of material needed for such a study can be obtained only with large-volume rotors. For preparative separation, use was made of the B-IV zonal rotor described in Chap. VI. *Escherichia coli* were grown in the presence of ^{35}S sulfate so that the proteins could be selectively traced by radioactivity.

The purest ribosomal subunits were obtained by first isolating ribosomes with an *S* value equal to or higher than 70 in a sucrose gradient (see Fig. II-B-1), and by rerunning this fraction in the same gradient after dissociation at low magnesium concentration (see Fig. II-B-2). The optimum gradient for the separation of ribosomal subunits ranged from 13 to 20% (w/w) sucrose. The buffers used had the following compositions: (1) for the homogenization of *E. coli* in the French pressure cell and the isolation of 70S particles, 10^{-2} *M* Tris and 10^{-2} *M* Mg^{2+} (pH 7.4); (2) for the dissociation of the 70S particles and the isolation of their subunits, 10^{-2} *M* sodium-potassium phosphate and 10^{-3} *M* magnesium acetate (pH 7.4).

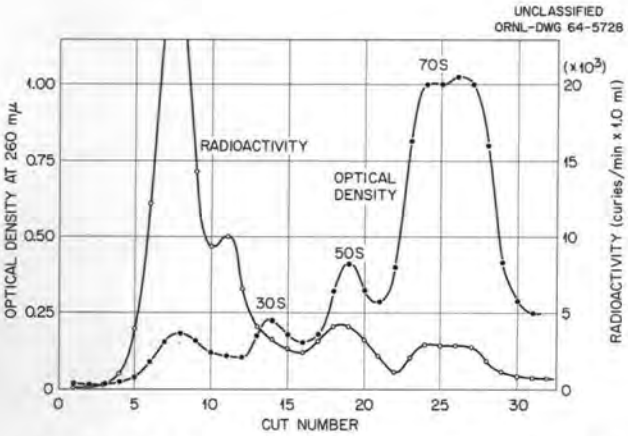

Fig. II-B-1. Zonal Centrifuge Pattern of a Partially Purified Ribosome Pellet from *E. coli*.

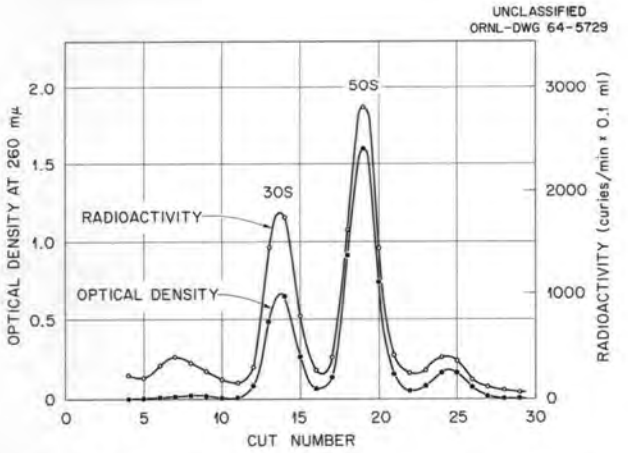

Fig. II-B-2. Zonal Centrifuge Pattern of Dissociated Ribosomes.

The ribosome suspensions obtained by zonal ultracentrifugation were first concentrated by centrifugation in a Spinco 30 rotor, and the proteins were extracted with hydrochloric acid. The efficiency of the separations achieved is indicated by the absence of ribonuclease in the 50S fraction. Previous studies indicate that this enzyme is associated with the 30S fraction.

2. Separation of Ribosomal Proteins by Disk Electrophoresis

In previous studies starch has generally been used for the separation of ribosomal proteins by electrophoresis. To increase the resolution of the separations and to reduce the size of the sample required, we have used polyacrylamide gel columns. As anticipated from the basic properties of ribosomal protein, the best results were obtained using the low-pH buffer system previously used in the separation of other basic proteins (Reisfeld *et al.*, 1962). Each of the patterns observed in the 30S and 50S subunits shows approximately a dozen peaks which appear consistently, but which differ for the two sizes of particles (see Figs. II-B-3 to II-B-5). Minor differences were observed between

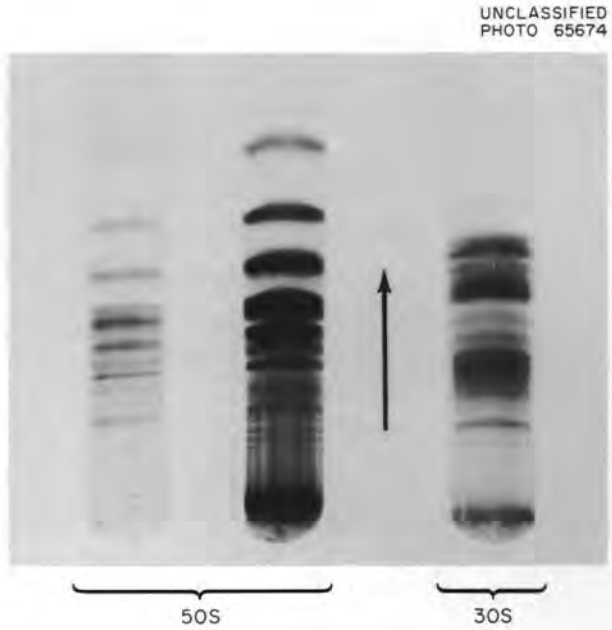

Fig. II-B-3. Disk-Electrophoresis Patterns of Ribosomal Proteins Extracted from 30S and 50S Ribosomal Subunits of *E. coli*.

the patterns for "native" and "derived" 50S particles. No differences were observed between the ribosomes from cultures at rest and those from exponentially growing cultures. The amino acid analyses of these samples are incomplete at this writing.

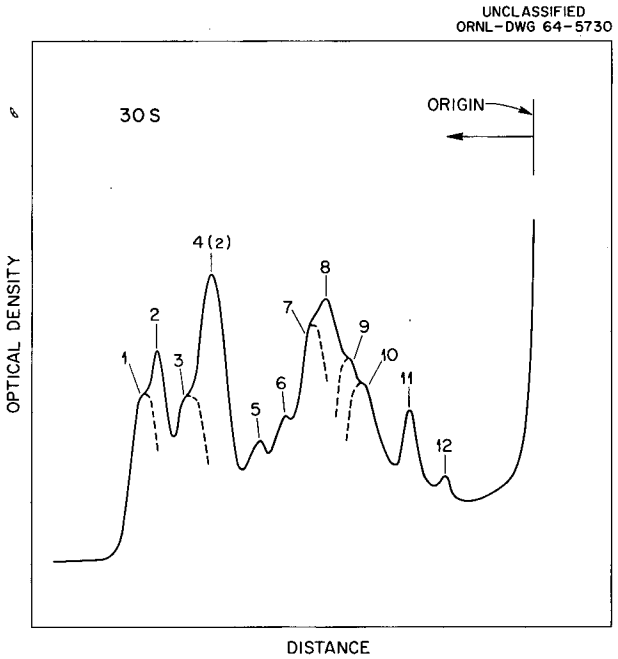

Fig. II-B-4. Absorbance Pattern of Disk-Electrophoresis Analysis of 30S Ribosomal Proteins.

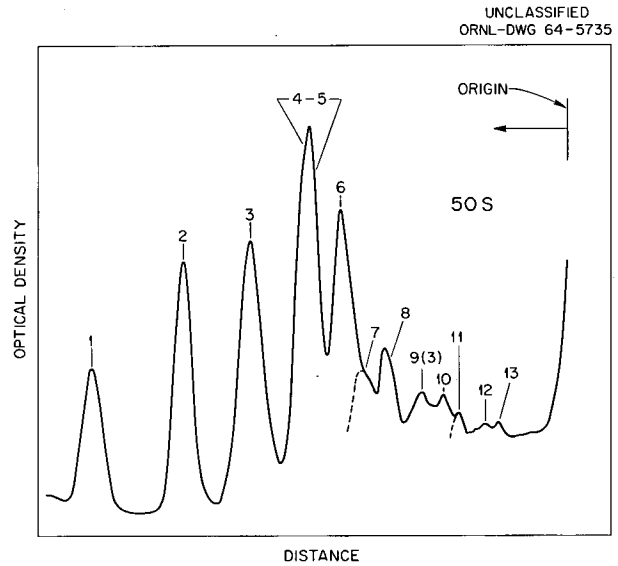

Fig. II-B-5. Absorbance Pattern of Disk-Electrophoresis Analysis of Proteins of 50S Ribosomal Subunits.

3. Radioactivity Determinations

Although not apparent from the ultraviolet absorbance scans of the preparative zonal centrifuge separations nor from the patterns obtained with the analytical ultracentrifuge, contamination of the 30S particles by the overlapping soluble protein peak can be inferred from the radioactivity curves (Fig. II-B-6). Such contamination occurred only when the particles had not been prepared from

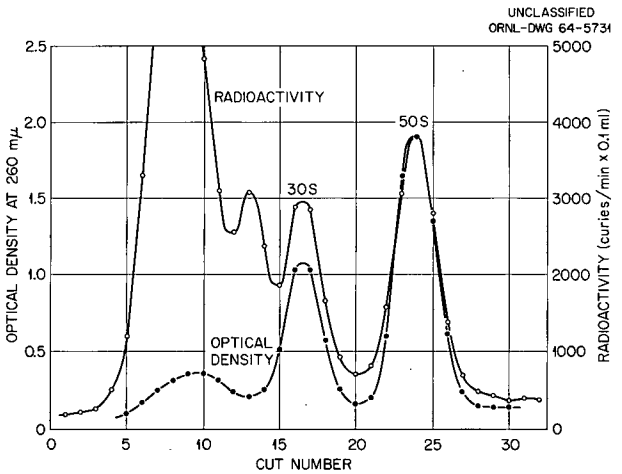

Fig. II-B-6. Zonal Centrifuge Pattern of Dissociated Ribosomal Subunits Prepared Directly from a Differential Centrifugation Pellet Without Prior Isolation of 70S Subunits.

Table II-B-1. Specific Radioactivity of the Ribosomal Subunits from *E. coli* Grown in the Presence of ^{35}S

	Before Chasing	After Chasing
Native 50S	113	42
Derived		
30S	145	26.5
50S	95	17.4
Ratio of native 50S to derived 50S	1.19	2.45
Ratio of derived 30S to derived 50S	1.53	1.52

previously isolated 70S particles and was encountered even when the starting material was a ribosome pellet prepared by differential centrifugation. The importance and the necessity of using zonal centrifugation for preparative work are evident.

It appears from Table II-B-1 that the specific radioactivity (radioactivity vs RNA content) of the 30S subunits is 50% higher than that of the 50S. After chasing with nonradioactive sulfur, the same ratio is observed between the specific radioactivities of the derived subunits, but the specific radioactivity of the native 50S material is now found to be much higher than that of the derived ones. The radioactivity, before and after chasing, of the several fractions isolated by disk electrophoresis is now being studied.

4. Discussion

Green and Hall (1961) have observed differences in the physiological activity and RNA composition of native and derived ribosomal subunits. Such differences do not appear clearly from the electrophoresis data in this study, but the radioactivity data would imply the absence of an equilibrium between the two types of particles (native and derived). Moreover, the higher specific activities found in native 50S after chasing would suggest that these particles are actually derived from the 70S particles. The higher specific radioactivities found in the 30S as compared to that of the 50S may be ascribed to a higher protein content if the proteins from both the 30S and 50S are found to contain the same percentage of cystine and methionine (Spahr, 1962). This view is further supported by the fact that a lower ratio of optical density at 260 mμ to optical density at 235 mμ is consistently found for the 30S particles. Radioactivity measurements now being made on the proteins separated by disk electrophoresis will aid in answering some of the questions raised above and will also indicate whether any of the proteins undergo a higher turnover rate than others.

C. VIRUS-LIKE PARTICLES IN HUMAN LEUKEMIC PLASMA

C. L. Burger N. G. Anderson
W. W. Harris T. W. Bartlett
R. M. Kniseley

During this report period, a total of 250 coded plasma samples from human subjects have been prepared for examination by electron microscopy. Of these, 40 to 50 were from nonleukemic individuals. Microscopy data are presently available on only 140 of these samples. The correlation of particle morphology with diagnosis, treatment, and other parameters will be made by computer analysis.

1. Methods

Samples were prepared as described (Burger *et al.*, 1964). However, banding of the virus pellet has been explored by a number of techniques using greater volumes of plasma per patient to facilitate electron microscopy.

After the resuspended pellets are banded in CsCl, photographs are taken of the banding tubes, and fractions are then recovered by pumping the tube contents through a stainless steel needle and into a spectrophotometer modified with a wave-shifting mechanism to alternately read 260 mμ and 280 mμ. The sample then passes through a Waters refractometer (model 34H), the pump, and finally into a fraction collection tube. The fractions are then prepared for microscopy as reported (Burger *et al.*, 1964).

The gradient analyzer (designed and fabricated by ORGDP Instrument Development Group) used for recovery of banded samples is shown in Fig. II-C-1. The pump used to withdraw the fluid from the tubes is provided with a continuous-speed control (front left, below table holding fraction collector) which varies rate of withdrawal from 0 to 3.7 ml/min, when using $\frac{1}{16}$-in.-ID tubing. The total volume of fluid within the system, from tip of stainless steel needle to end of tubing above collection vessel, is 0.5 ml. The tube holder, an evacuated double-walled chamber which insulates the tube during pumpout, has a light

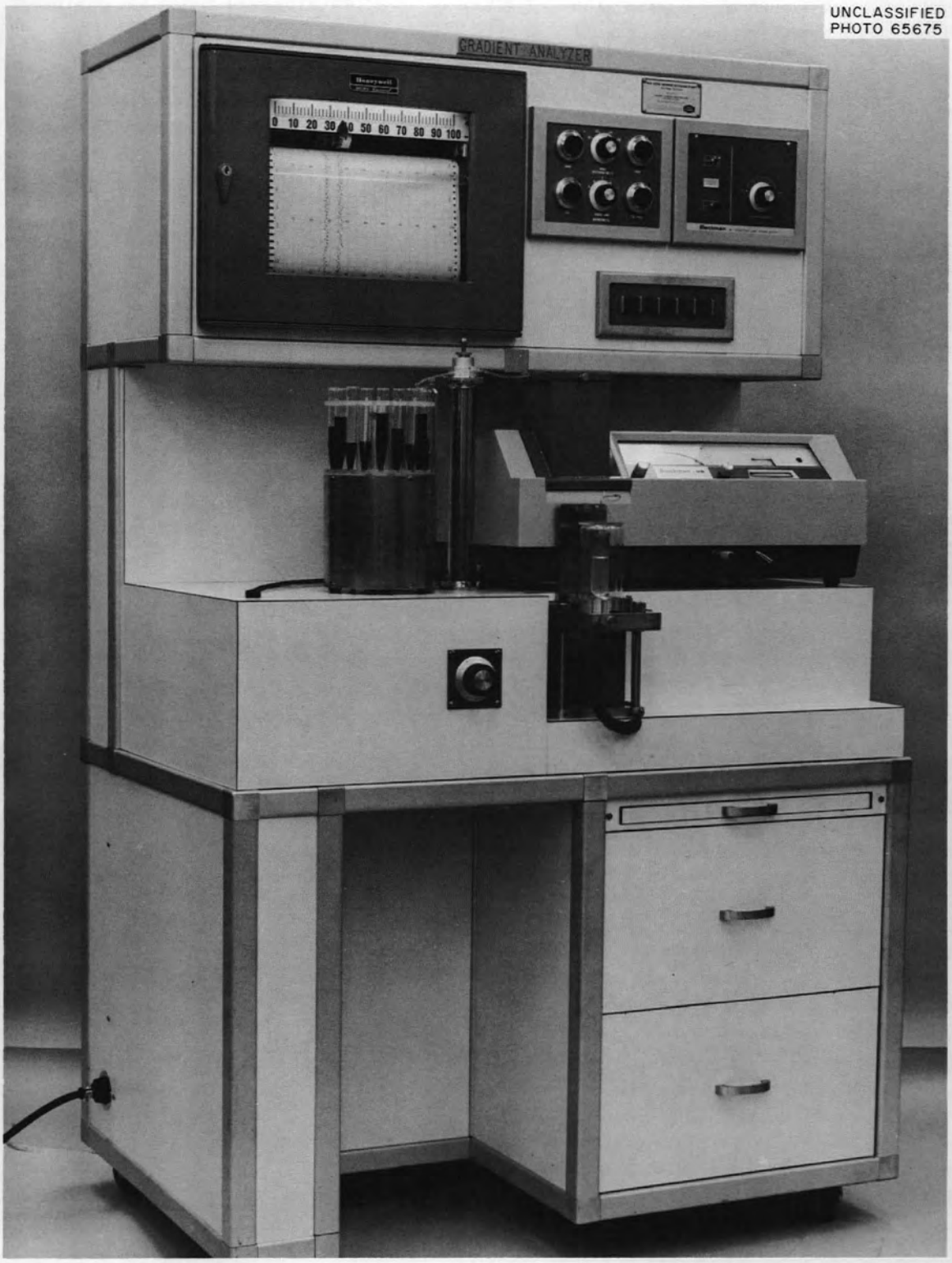

Fig. II-C-1. Gradient Analyzer Used to Recover Virus Banded in Salt Gradients. Absorbance at two wavelengths and refractive index are recorded.

below, permitting visual observation of bands in the tube. The screw is removed from the cap of the Spinco 30 rotor tube, and a plastic adapter is screwed into the opening. The rack holding the tube is then raised, after positioning the needle over the opening in the adapter. The needle is thus positioned at the bottom of the tube, with minimum disturbance of the gradient.

The reference cell of the spectrophotometer has been modified by the addition of a variable slit adjustment. The housing above the cell compartment of the DB contains the refractometer flow cell, modified to reduce the volume and hence the lag time of the instrument. The refractometer has been further altered by the addition of a fine adjustment which permits the operator to set the output voltage of the unit between the settings required through use of the scale and zero adjustment.

The fraction collector provides for eighteen 15-ml centrifuge tubes. An event-recording pen marks the base of the strip chart each time the fraction collector advances, either automatically on a timed basis or manually by depressing a control switch. A visual record of absorbancy at 260 and 280 mμ, refractive index, and tube number is thus obtained for each sample.

The tubing used throughout the system may be washed with formalin between samples, or new tubing may be inserted. The DB and refractometer cells are not at the moment expendable, but disposable DB cells are under study. The important feature is that no "memory" or cross contamination be detected, and none has been observed as checked by comparing leukemic and nonleukemic samples. The recorder is equipped with a 12-point print wheel; two points record refractive index and the others alternate between 260 and 280 mμ.

The panels above the DB contain the hydrogen lamp power supply, zero adjustments for both wavelengths, and the electronic controls for the refractometer. A series of switches include main power, fraction collector power, pump, and sample light. The correlation between virus-like particles observed in plasma and tissues of the same leukemic individuals is under investigation, and results will be reported in future communications. The occurrence of particles other than the "R" and "Q" type previously reported (Burger *et al.*, 1964) will also be described.

D. STUDIES ON THE A-IX ROTOR

R. E. Canning

As each new rotor system is developed, its performance is examined using test particles as a prelude to studies on the separation of more complex biological materials. The A-IX rotor is designed for the separation of cells and for studies on the distribution of drugs, chemical carcinogens, and enzymatic activities among cell fractions. Before this can be done, however, optimal gradients and operating techniques must be developed.

The performance of the A-IX rotor was studied using bovine serum albumin (BSA), rat red blood cells (RRBC), and ragweed pollen. In all cases a 1-liter gradient of 17 to 55% sucrose (ρ = 1.0719 to 1.2663) was used with 55% sucrose as a cushion at the centrifugal end of the gradient. For the overlay, 160 ml of phosphate buffer [pH 7.5, μ (ionic strength) = 0.1] was used.

The effects of movement of the sample zone into and out of the rotor and of disturbances occurring during acceleration and deceleration were studied using BSA (10 ml of 4% BSA in 8.5 w/w % sucrose) as the sample. The sample was introduced into the rotor at 1100 rpm, after which the rotor was accelerated to 4000 rpm (3000 $\times$ g at R_{max}) for 15 min. The rotor was then decelerated to 1100 rpm and unloaded into 40-ml centrifuge tubes through an ultraviolet absorbance monitor. The absorbance recorder chart is shown in Fig. II-D-1. The sample zone was calculated to be

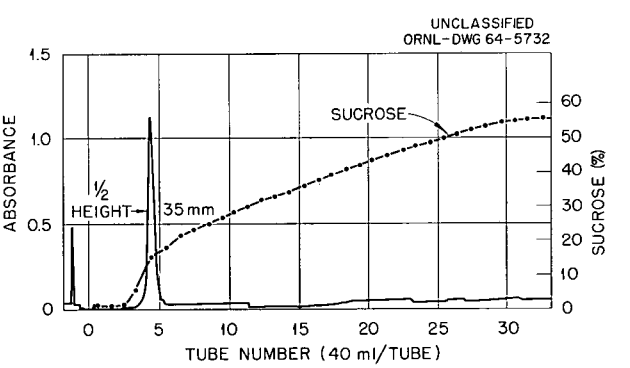

Fig. II-D-1. Run Diagram of Bovine Serum Albumin (BSA) in Rotor A-IX. Ten ml of 4% BSA in 8.5% sucrose; 4000 rpm (3000 $\times$ g at R_{max}), 15 min. Loading and unloading done at 1100 rpm. Scanned at 260 mμ in 0.2-cm light path flow cell.

1 mm wide in the rotor if no zone broadening occurred. The peak width of the sample zone on the recorder chart at one-half height is equivalent to 3.5 mm, indicating that a small amount of broadening had occurred.

Ragweed pollen (200 mg) was washed with alcohol, centrifuged, and suspended in 10 ml of 8.5% (w/w) sucrose. This sample volume was introduced into the rotor at 1100 rpm, and the rotor was accelerated to 4000 rpm for 8 min. After deceleration to 1100 rpm, the rotor was unloaded as described above. Two peaks were observed; one, a yellow pigment at the starting zone which had an equivalent width in the rotor at one-half peak height of 4.0 mm, and the second located at a density level of 1.2304 (50 w/w % sucrose). Upon microscopic examination of the collected fractions, pollen was shown to be localized exclusively in the second peak.

Similar studies were done using 1 ml of packed RRBC diluted to 10 ml with 8.5% sucrose. After 65 min at 1000 rpm the cells were found to band at a level having a density of 1.204 (46% sucrose). Both the pollen and the RRBC appear to have been very close to their isopycnic points.

Preliminary work using the A-IX rotor to separate cell particulates has been concerned with finding the gradient which gives the best separations. It appears that a two-part gradient consisting of 300 ml grading from 12 to 15% (w/w) sucrose and 700 ml of 38 to 50% sucrose with a cushion of 55% sucrose gives a useful separation with a 20% rat liver brei. Ribosomes are not sedimented out of the starting layer with this rotor, but the remaining major cell components are separated. This gradient will be used to explore the feasibility of employing the A-IX rotor for intracellular distribution studies.

E. DEVELOPMENT OF REORIENTING GRADIENT CENTRIFUGATION USING THE A-VIII ROTOR

C. A. Price Gretchian Bostian

Reorienting gradient centrifugation in rotors which do not have spinning seals makes possible the construction of less expensive rotors for low- and intermediate-speed separations and the development of very-high-speed centrifuges (cf. C and D series systems). The actual separation of particles during all types of zonal centrifugation occurs by the same process; reorienting gradient centrifugation differs from zonal centrifugation as previously done only in the manner of loading and unloading samples. The rotor is loaded with the gradient and sample at rest and is then accelerated to the desired speed for the length of time necessary to effect the required separations. At the end of the run the rotor is gradually decelerated to rest, and the gradient is recovered by displacement (see report ORNL-3415, p. 16; Anderson *et al.*, 1964). The principal question is whether, with a given rotor volume and maximum speed, conditions can be found such that negligible mixing occurs during reorientation.

1. Resolution

We have tested reorienting gradient centrifugation with the A-VIII rotor, a large (1.5-liter) hollow-cylinder configuration with a vaned core (Fig. II-E-1). By use of a removable distribution plug and channels in the core, fluids may be conducted either to the base or to the top of the rotor. To study reorientation disturbances, we layered 20 ml of a solution containing 8% (w/w) sucrose and 100 mg of BSA dyed with bromphenol blue (BBSA) on top of a 15 to 40% (w/w) sucrose gradient. An overlay of 200 ml of water was added. The rotor was accelerated to 5000 rpm by various schedules and then decelerated according to the same schedules. The gradient was pumped out at rest and monitored at 280 mμ. The results obtained with several schedules are shown in Fig. II-E-2. The resolution of symmetrical peaks, defined here as Q = (absorbancy of peak)/(width at half height), showed surprisingly that the poorest Q values were obtained with the slowest acceleration schedule. The highest Q values were obtained when the rotor was accelerated rapidly through regions of rotor instability as previously indicated by runout analysis (report ORNL-3502, p. 33). Another surprising feature of this work was that substantial loss of resolution occurred after the rotor had accelerated past 1000 rpm, although reorientation was complete at 500 rpm. Other experiments showed that zones introduced below the top of the gradient suffered less distortion than those inserted at the top of the gradient. These experiments established that

Fig. II-E-1. Components of the A-VIII Rotor System.

acceptable resolution can be obtained in the recovery of a soluble sample introduced near the top of the rotor.

2. Separation and Recovery of Pollen Grains

The separation and recovery of pollen grains was tested using a sample of ragweed pollen mixed with BBSA, made up in 8% sucrose, and layered over a sucrose gradient. Water was used for the overlay. The rotor was then centrifuged for various times. (These experiments were performed before the optimum acceleration schedules had been established.) After 2 hr at 5000 rpm the principal component of ragweed pollen had banded isopycnically. The sharpest bands were obtained with a concave gradient of hyperbolic shape (Fig. II-E-3). A number of minor component bands, including what appeared to be "ghosts," were observed elsewhere in the gradient. The Q values of the recovered peaks were little affected by the size or the volume of the original sample mixture. Longer periods of centrifugation (*e.g.*, 5 and 18 hr) resulted in substantial losses of resolution. These losses may be inherent in the rotor system or may be due to the choice of samples.

3. Effect of Number of Septa

Since the septa of the A-VIII rotor are removable, the effect of removing some or all of the septa may be examined. Preliminary studies indicate that substantial loss of resolution occurs when the number of septa is reduced, suggesting that the optimal number may not be the 18 originally included. Further experimental and theoretical

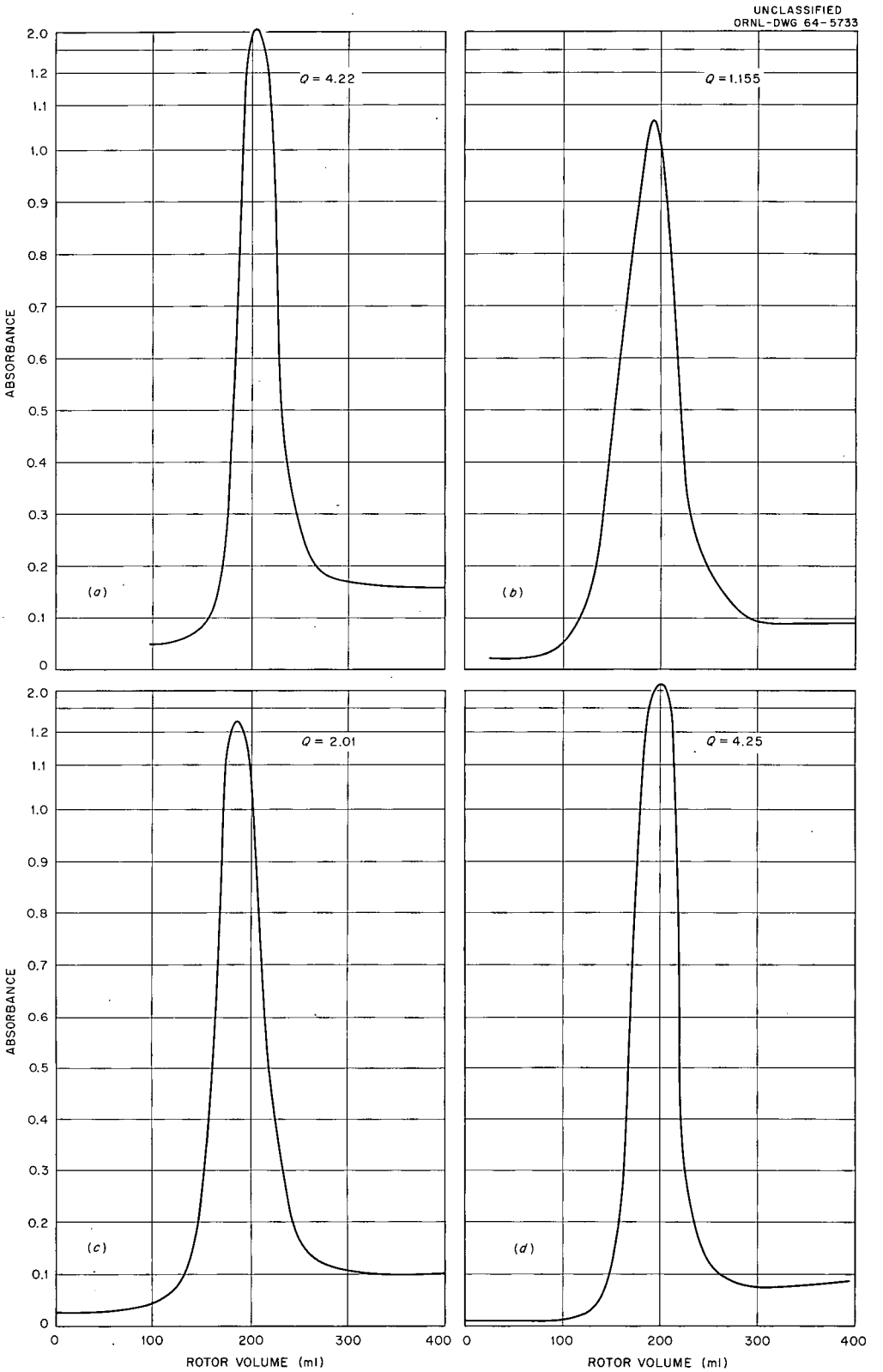

Fig. II-E-2. Resolution of Dyed Bovine Serum Albumin Zone Following Gradient Reorientation. The sample contained 100 mg of protein in 20 ml of 10% sucrose and was followed by a 200-ml overlay. The acceleration and deceleration schedules were as follows: (*a*) to 1000 rpm in 3 min; (*b*) to 1000 rpm in 3 min, then to 5000 rpm in 8 min; (c) to 5000 rpm in 3 min; and (*d*) selective acceleration based on avoiding regions of dynamic instability.

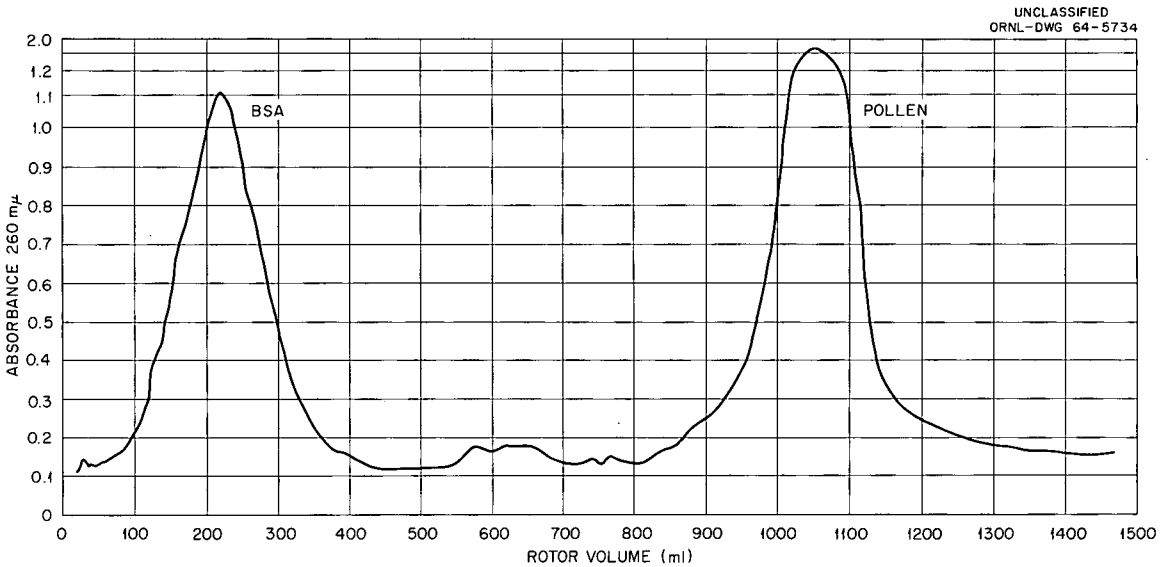

Fig. II-E-3. Banding of Ragweed Pollen in Hyperbolic Sucrose Gradient. Position of starting zone indicated by dyed bovine serum albumin added to the sample. The sample layer contained 15 mg of BSA and 300 mg of ragweed pollen in 20 ml of 8% sucrose. The overlay volume was 200 ml. The rotor was accelerated slowly (during a 3-min interval) to 1000 rpm and then rapidly to 5000 rpm, where it remained for 2 hr.

studies will be required to determine the best internal configuration for reorienting gradient rotors of this size.

4. Prospects for Further Development

The most important conclusion that can be drawn from this study is that bands can be recovered with high resolution after reorienting gradient configuration. This means that a simple and satisfactory principle exists for the recovery of components from high-speed rotors where spinning seals are not practical. Whether rotating-seal systems should be dispensed with in rotors operating below 40,000 rpm must await a detailed comparison of the reorienting made with the conventional mode in other A and B type rotors. No such direct comparisons have been made, but several comments are appropriate.

For speeds below 6000 rpm there are enormous advantages to the disk-shaped, transparent A-IX rotors. The greatest advantage is that of visual observation, so that rate-zonal separations may be clearly distinguished from isopycnic ones. Other advantages are that diffusion cannot easily disturb the gradient even over long intervals and that one may observe transient changes in certain properties of particles during centrifugation. Clearly it will be valuable to learn whether (or how) the reorienting gradient method may be employed with rotors of this shape.

BIBLIOGRAPHY

Albright, J. F., and N. G. Anderson, "A Method for Rapid Fractionation of Particulate Systems by Gradient Differential Centrifugation," *Exptl. Cell Res.* **15**, 271–81 (1958).

Anderson, N. G., "Horizontal Tubeless Centrifuge Head," in *Biol. Div. Semiann. Progr. Rept. Aug. 15, 1955*, ORNL-1953, p. 117.

Anderson, N. G., "New Fractionation Methods for Isolating Cellular Proteins," *Bull. Am. Phys. Soc. Series II* 1, 267–68 (1956).

Anderson, N. G., "The Zonal Ultracentrifuge. A New Instrument for Fractionating Mixtures of Particles," *J. Phys. Chem.* **66**, 1984–89 (1962).

Anderson, N. G., and R. E. Canning, "Studies on Isolated Cell Components. XII. An Ultracentrifugal Analysis of Soluble Proteins from Rat Liver, Brain, Kidney, and Testis," *Exptl. Cell Res.* **17**, 465–71 (1959).

Anderson, N. G., *et al.*, "Analytical Techniques for Cell Fractions. IV. Reorienting Gradient Rotor for Zonal Centrifugation," *Anal. Biochem.* **7**, 1–9 (1964).

Bell, D. J., *et al.*, "Physiochemical Observations on Some Glycogens," *Biochem. J.* **42**, 405–8 (1948).

Breedis, C., L. Berwick, and T. F. Anderson, "Fractionation of Shope Papilloma Virus in Cesium Chloride, *Virology* **17**, 89–94 (1962).

Breese, S. S., Jr., R. Trautman, and H. L. Bachrach, "Analysis by Electron Microscopy and Infectivity of Foot-and-Mouth Disease Virus in Moving Boundary and Zone Ultracentrifugation," *Arch. Biochem. Biophys.* **87**, 1–8 (1960).

Bryce, W. A. J., *et al.*, "Physicochemical Studies on Starches. XII. The Molecular Weight of Glycogens in Aqueous Solutions," *J. Chem. Soc.* **1958**, 711–15.

Burger, C. L., *et al.*, "Virus-Like Particles in Human Leukemic Plasma," *Proc. Soc. Exptl. Biol. Med.* **115**, 151–56 (1964).

Cheng, P.-Y., "Sedimentation and Autoradiographic Analysis of Rapidly Labeled RNAs in Human Amnion Cells," *Biophys. J.* **2**, 465–82 (1962).

Cox, R. A., and H. R. V. Arnstein, "The Isolation, Characterization and Acid-Base Properties of Ribonucleic Acid from Rabbit Reticulocyte Ribosomes," *Biochem. J.* **89**, 574–85 (1963).

Cox, D. J., and V. N. Schumaker, "The Preferential Hydration of Proteins in Concentrated Salt Solutions. II. Sedimentation Equilibrium of Proteins in Salt Density Gradients," *J. Am. Chem. Soc.* **83**, 2439–45 (1961).

Crawford, L. V, and E. M. Crawford, "The Properties of Rous Sarcoma Virus Purified by Density Gradient Centrifugation," *Virology* **13**, 227–32 (1961).

Crawford, L. V., and E. M. Crawford, "A Comparative Study of Polyoma and Papilloma Viruses," *Virology* **21**, 258–63 (1963).

Darlington, R. W., and C. C. Randall, "The Nucleic Acid Content of Equine Abortion Virus," *Virology* **19**, 322–27 (1963).

Davern, C. I., and M. Meselson, "The Molecular Conservation of Ribonucleic Acid During Bacterial Growth," *J. Mol. Biol.* **2**, 153–60 (1960).

de Duve, C., J. Berthet, and H. Beaufay, "Gradient Centrifugation of Cell Particles. Theory and Applications," *Progr. Biophys. Biophys. Chem.* **9**, 325–69 (1959).

Dourmashkin, R. R., "Electron Microscopy of Polyoma Virus: A Review," in *Tumors Induced by Viruses: Ultrastructural Studies* (ed. by A. J. Dalton and F. Haguenau), Academic, New York, 1962.

Eigner, J., *et al.*, "A Study of the 70S Component of Bacteriophage ϕX 174," *J. Mol. Biol.* **6**, 61–84 (1962).

Epstein, M. A., "The Identification of the Rous Virus. A Morphological and Biological Study," *Brit. J. Cancer* **10**, 33–48 (1956).

Epstein, M. A., "Observations on the Rous Virus: Purification and Identification of the Particles from Solid Tumours," *Brit. J. Cancer* **12**; 248–55 (1958).

Epstein, M. A., and S. J. Holt, "Observations on the Rous Virus: Integrated Electron Microscopical and Cytochemical Studies of Fluorocarbon Purified Preparations," *Brit. J. Cancer* **12**, 363–69 (1958).

Falzone, J. A., C. H. Barrows, and M. J. Yiengst, "Fractionation of Rat Liver Nuclei into Diploid and Tetraploid DNA Classes by Continuous Density Gradient Sedimentation," *Exptl. Cell Res.* **26**, 552–61 (1962).

Faulkner, P., *et al.*, "Studies on Protein and Nucleic Acid Metabolism in Virus-Infected Mammalian Cells. 2. The Isolation, Crystallization and Chemical Characterization of Mouse Encephalomyocarditis Virus," *Biochem. J.* **80**, 597–605 (1961).

Gierer, A., "Function of Aggregated Reticulocyte Ribosomes in Protein Synthesis," *J. Mol. Biol.* **6**, 148–57 (1963).

Gomatos, P. J., and I. Tamm, "The Secondary Structure of Reovirus RNA," *Proc. Natl. Acad. Sci. U.S.* **49**, 707–14 (1963).

Green, M., "Studies on the Biosynthesis of Viral DNA," *Cold Spring Harbor Symp. Quant. Biol.* **27**, 219–33 (1962).

Green, M., and B. D. Hall, *Biophys. J.* **1**, 517 (1961).

Hale, A. J., and E. R. M. Kay, "A Comparison of Nuclear Dry Weights Determined by Chemical and by Interferometric Methods," *J. Biophys. Biochem. Cytol.* **2**, 147–58 (1956).

Hansen, P., and W. Schäfer, "Untersuchungen über ein Mäuse-Encephalomyelitis-Virus. Reiniguing and physikalisch-chemische Eigenschaften des Virus," *Z. Naturforsch.* **17**, 15–22 (1962).

Hershey, A. D., E. Burgi, and L. Ingraham, "Sedimentation Coefficient and Fragility Under Hydrodynamic Shear as Measures of Molecular Weight of the DNA of Phage T5," *Biophys. J.* **2**, 423–31 (1962).

Holland, J. J., *et al.*, "Enteroviral Ribonucleic Acid. I. Recovery from Virus and Assimilation by Cells," *J. Expl. Med.* **112**, 821–39 (1960).

Howatson, A. F., and L. V. Crawford, "Direct Counting of the Capsomeres in Polyoma and Papilloma Viruses," *Virology* **21**, 1–6 (1963).

Joklik, W. K., "The Purification of Four Strains of Poxvirus," *Virology* **18**, 9–18 (1962).

Kohler, K., "Gewinnung und Reinigung von Adenovirus-Typ 2 mit Hilfe der CsCl-Gradientrifugation," *Z. Naturforsch.* **17**, 544–47 (1962).

Kovacs, E., "Chemical Dissection of Mammalian Cells with Liberation of Biologically Intact Viruses," *Z. Naturforsch.* **17**, 234–40 (1962).

Martin, R. G., and B. N. Ames, "A Method for Determining the Sedimentation Behavior of Enzymes: Application to Protein Mixtures," *J. Biol. Chem.* **236**, 1372–79 (1961).

Mayor, H. D., "Acridine Orange Staining of Purified Polyoma Virus," *Proc. Soc. Exptl. Biol. Med.* **108**, 103–5, (1961).

Melnick, J. L., "Papova Virus Group," *Science* **135**, 1128–30 (1962).

Meselson, M., F. W. Stahl, and J. Vinograd, "Equilibrium Sedimentation of Macromolecules in Density Gradients," *Proc. Natl. Acad. Sci. U.S.* **43**, 581–88 (1957).

Meyer, F., and J. P. Zalta, "The State of Glycogen in the Liver of Rats," *Compt. Rend.* **247**, 357–59 (1958).

Naude, W. duT., T. Madsen, and A. Polson, "Different Sized Infective Particles of Rift Valley Fever Virus," *Nature* **173**, 1051–52 (1954).

Platerose, D. N., C. Nishimura, and N. P. Salzman, "The Purification of Vaccinia Virus from Cell Cultures," *Virology* **18**, 294–301 (1962).

Polglase, W. J., D. M. Brown, and E. L. Smith, "Studies on Human Glycogen. II. Sedimentation in the Ultracentrifuge," *J. Biol. Chem.* **199**, 105–12 (1952).

Polson, A., and J. Levitt, "Density Determination in a Preformed Gradient of Cesium Chloride," *Biochem. Biophys. Acta* **75**, 88–95 (1963).

Reisfeld, R. A., *Nature* **195**, 281 (1962).

Rott, R., I. M. Reda, and W. Schäfer, "Charakterisierung der verschiedenen, nach Infektion mit Newcastle Disease Virus auftretenden, nichtinfektiösenhämagglutinierenden Teilchen," *Z. Naturforsch.* **18**, 188–94 (1963).

Rubin, H., "Response of Cell and Organism to Infection with Avain Tumor Viruses," *Bacteriol. Rev.* **26**, 1–13 (1962).

Schildkraut, C. L., J. Marmur, and P. Doty, "Determination of the Base Composition of Deoxyribonucleic Acid from Its Buoyant Density in CsCl," *J. Mol. Biol.* **4**, 430–43 (1962).

Sharp, D. G., and J. W. Beard, "Counts of Virus Particles by Sedimentation on Agar and Electron Micrography," *Proc. Soc. Exptl. Biol. Med.* **81**, 75–79 (1952).

Sharp, D. G., and J. R. Overman, "Enumeration of Vaccinia Virus Particles in Crude Extracts of Infected Tissues by Electron Microscopy," *Proc. Soc. Exptl. Biol. Med.* **99**, 409–13 (1958).

Sinsheimer, R. L., "Purification and Properties of Bacteriophage ϕX 174," *J. Mol. Biol.* **1**, 37–42 (1959).

Smith, K. O., and M. Benyesh-Melnick, "Particle Counting of Polyoma Virus," *Proc. Soc. Exptl. Biol. Med.* **107**, 409–13 (1961).

Spahr, P. F., *J. Mol. Biol.* **4**, 395 (1962).

Stenback, W. H., "Host Influence on the Density of Newcastle Disease Virus (NDV)," *Virology* **20**, 545–51 (1963).

Thomson, J. F., and F. J. Klipfel, "Fractionation of Rat Liver Particulates Using Polyvinylprrolidone Gradients," *Exptl. Cell Res.* **14**, 612–14 (1958).

Tissieres, A., *et al.*, "Ribonucleoprotein Particles from *Escherichia coli*," *J. Mol. Biol.* **1**, 221–33 (1959).

Winocour, E., "Purification of Polyoma Virus," *Virology* **19**, 158–68 (1963).

III. Theoretical Studies

A. S. Berman

A. CONTINUOUS-FLOW CENTRIFUGATION

In a previous report,[1] an equation was presented which related flow rates to particle properties, suspending medium properties, centrifuge properties, and the desired fractional particulate removal. The equation can be presented in terms of the sedimentation coefficient, which is defined by

$$S = \frac{(dr/dt)}{\omega^2 r} \times 10^{13} . \qquad (1.1)$$

The flow rate equation, in practical units, is

$$Q_1 = \frac{80 \times 10^{-13}\,(\text{rpm})^2\, V_l S}{G(f,\, r_1/r_2)}, \qquad (1.2)$$

where

Q_1 = flow rate, liters/hr,

rpm = centrifuge speed, revolutions/min,

V_l = rotor volume ($\pi r_2{}^2 L_e$), liters,

S = sedimentation coefficient, Svedberg units,

$G(f,\, r_1/r_2)$ = function of the fractional particulate removal f and the radius ratio r_1/r_2 of the centrifuge,

r_1 = radius of the core,

r_2 = radius of the centrifuge bowl.

The equation for the function G has been given previously and for radius ratios greater than 0.8 is well approximated by

$$G(f,\, r_1/r_2) = f^2(3 - 2f) - \frac{f^2}{2}\left(5f^2 - 8f + 2\left(1 - \frac{r_1^2}{r_2^2}\right)\right) . \qquad (1.3)$$

Figure III-A-1 shows the relationship between sedimentation coefficient and flow rate for various centrifuge speeds for a nominal B-V rotor with r_1 = 4.92 cm, r_2 = 5 cm, L_e = 25 cm, and f = 0.95.

If, in addition to $r_1/r_2 > 0.8$, the fractional particulate removal f is greater than 0.9, a useful

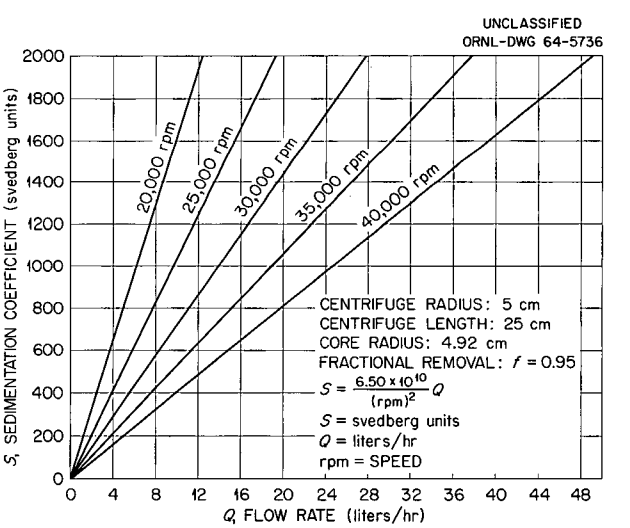

Fig. III-A-1. Relationship Between Sedimentation Coefficients and Flow Rate at Various Speeds.

[1] *Joint NIH-AEC Zonal Centrifuge Development Program Semiann. Rept. January 1–June 30, 1963*, ORNL-3502, pp. 11–14.

approximate equation (maximum error about 10%) is

$$\frac{Q_1}{V_l S} = 80 \times 10^{-13} \text{ (rpm)}^2 , \qquad (1.4)$$

where the symbols have been defined above.

The cluster $(Q_1/V_l S)$ is the flow rate in liters per hour per liter of rotor volume per unit sedimentation coefficient. From Fig. III-A-2, this cluster can be obtained readily for any centrifuge speed. Multiplication of the value so obtained by the machine volume and the sedimentation coefficient gives the estimated flow rate.

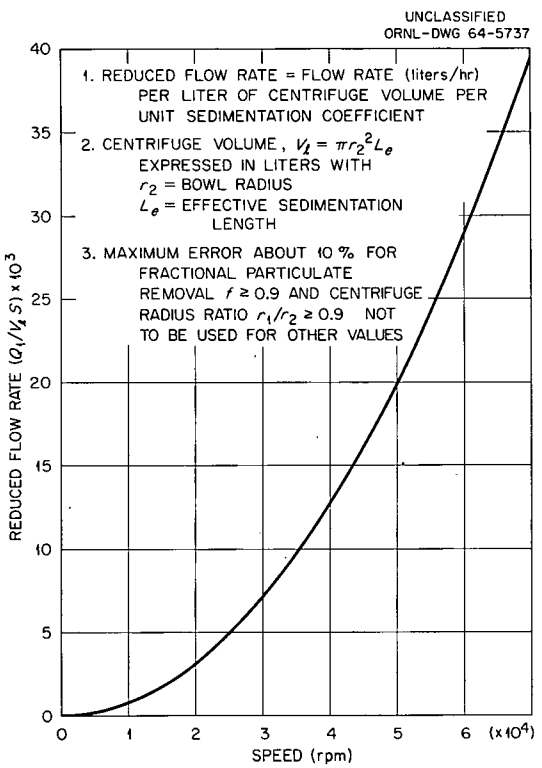

Fig. III-A-2. Relationship Between Speed and Reduced Flow Rate in Continuous Centrifuge Operation (Approximate).

IV. Rotor Design

The rotor systems developed thus far and those in the stage of active planning are shown in Table IV-A-1. The systems developed to determine the limits of resolution which can be obtained are, unfortunately, often complex. However, it is proposed to compare each complex system with the simplest system which can be devised which will achieve comparable centrifugal fields. Therefore the theory and operation of simple reorienting gradient rotors is being explored in parallel with development of dynamically loaded zonal rotors.

Table IV-A-1. Zonal Centrifuge Systems Developed at Oak Ridge

Series	No.	Material	Capacity (ml)	RPM (max)	*g* (max)	Drive	Comments
A	I[a]	Pyrex tubes	2–68	3,000	2,500	PR-2	
A	II[a]	Pyrex bottles	6–250	2,200	1,100	PR-2	
A	III[a]	Aluminum	4000	2,000	939	PR-2	
A	IV[a]	Aluminum	625	18,000	23,545	Spinco K	
A	V[a]	Lucite	1300	1,000	152	PR-2	
A	VI	Aluminum	3000	6,000	7,100	PR-2	
A	VII	Lucite	127	3,000	292	PR-2	
A	VIII	Aluminum	1450	6,000	2,817	PR-2	
A	IX	Lucite	1300	4,000	3,200	PR-2	
A	X	Lucite	300	4,000	3,200	PR-2	Core for A-IX
A	XI	Aluminum/steel	Two 20-ml cells	6,000	7,100	PR-2	
B	I[a]	Aluminum	1450	40,000	125,216	Spinco L	
B	II[a]	Aluminum	1625	20,000	22,738	Spinco L	
B	III	Aluminum	1450	1,500	176	Spinco L	
B	IV	Aluminum	1685	40,000	90,952	Spinco L	New top bearing
B	V	Aluminum	150[b]	40,000	90,952	Spinco L	New top bearing
B	VI	Aluminum	1338[c]	35,000	69,635	Spinco L	New top bearing
B	VII	Aluminum	1012[c]	35,000	69,635	Spinco L	New top bearing
B	VIII	Aluminum	952[c]	35,000	69,635	Spinco L	New top bearing
B	IX	Aluminum	754[c]	35,000	69,635	Spinco L	Design stage
B	X	Aluminum	600	Design stage, removable seals, Spinco L			

Table IV-A-1 (continued)

Series	No.	Material	Capacity (ml)	RPM (max)	g (max)	Drive	Comments
B	XI	Aluminum	1500	Design stage, removable seals, Spinco L			
B	XII	Steel	1700	50,000	142,000	Spinco L	Speed with CsCl, $\rho = 1.7$
C	I[a]	Aluminum	(Not completed)				
C	II	Aluminum	100	141,000	310,000	Direct electric	
C	III	Aluminum	500	81,000	172,000	Direct electric	
C	IV	Aluminum	1000	66,000	143,000	Direct electric	
C	V	Aluminum	5000	40,000	91,000	Magnetic/Spinco	
D	I	Steel	10	400,000	1.2×10^6	Magnetic	

[a]Developed before start of Joint NIH-AEC Zonal Centrifuge Development Program.
[b]Continuous flow.
[c]Continuous flow with banding.

A. RIGID ROTOR DYNAMICS

H. P. Barringer E. F. Babelay

An unclassified theoretical treatment of rigid rotor dynamics applicable to existing centrifuge rotors is now available.[1] The equations of motion derived from a mathematical model are being programmed for an IBM 7090 computer. The use of this program in the design of centrifuge rotors will be described in subsequent reports.

B. METALLURGICAL STUDIES

K. T. Ziehlke

A second C-III centrifuge rotor failed at 81,000 rpm shortly after the rotor was loaded with cesium chloride solution. The rotor had previously operated for several hours at speed when filled with water. Parts of the rotor were examined to determine the origin and cause of the failure. It is concluded that failure was due to stress corrosion caused by beta-phase stringers in the aluminum microstructure and to the use of cesium chloride. The rotor material was 7075 aluminum, an alloy containing 5.6% Zn, 2.5% Mg, 1.6% Cu, and 0.3% Cr. The stock was obtained in the T6 temper, and the rotor was machined without further heat treatment. While the nominal yield strength of this alloy is 73,000 psi, the operating stress in the C-III rotor was calculated to be 52,000 psi.

The fragmentation that developed during the failure was severe, as shown in Fig. IV-B-1, which shows the pieces reassembled in their original relationship. The breaks were predominantly in the radial, longitudinal planes except at the ends, where circumferential parting appeared to have originated at a sharp corner between the thread diameter and the land area that contained the O-ring sealing groove. One of these breaks indicated that the crack originating at the corner propagated in two stages (Fig. IV-B-2). While it is possible that such a crack may have been the start of the failure, it was not possible to pinpoint significant differences between the two zones. Areas of brittle and of ductile failure propagation in both zones were revealed in electron microscope studies.

The longitudinal breaks were in a predominantly radial pattern and were characteristically brittle, even though the 7075-T6 material should have a fair amount of ductility. The photomicrograph of Fig. IV-B-3 illustrates the brittle nature of the failure. Sections taken parallel to the longitudinal failure planes showed microstructures similar to that of Fig. IV-B-4. The elongated beta (zinc)

[1]R. E. Kelley, *Rigid Rotor Dynamics*, TID-19804 (November 1963).

Fig. IV-B-1. Reassembled Pieces of the Second C-III Rotor to Fail at 81,000 rpm. 0.5X. Reduced 50%.

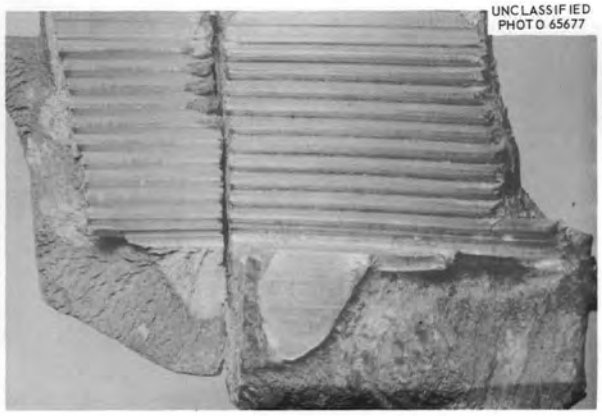

Fig. IV-B-2. Two-Stage Propagation of Crack During Failure of C-III Rotor. The light area just below the bottom thread on the piece on the left appears to have existed as a crack for some time prior to formation of the darker regions. 2X. Reduced 33.5%.

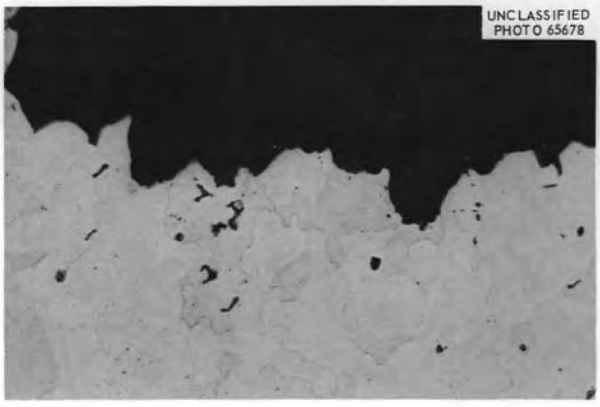

Fig. IV-B-3. Section Through Brittle Failure Area. The edge of the fracture shows little deformation. Tensile tests on 7075-T6 material give about 11% elongation at failure. 250X. Reduced 31%.

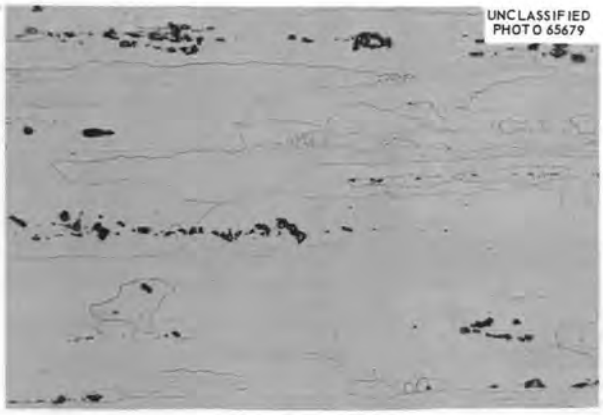

Fig. IV-B-4. Microstructure of Rotor Stock in Longitudinal Direction. The stringers are the residue of the β (zinc-rich) phase in the original ingot structure. The strong orientation effect was produced when the ingot was forged into bar stock. Normal heat-treating cycles would not fully dissolve this massive phase. 250X. Reduced 31%.

Fig. IV-B-5. Crack in β Phase on Inner Surface of Failed Rotor. The principal stress was tensile, at right angles to the stringer direction. 350X. Reduced 26.5%.

phase is brittle and weak in comparison to the matrix. Impact tests on similar material[2] showed that these inclusions severely weakened the 7075-T6 stock, even though hardness tests showed that it had received the recommended heat treatment. Reheat treatment of the earlier stock reduced the volume and continuity of the second phase and markedly improved its impact strength.

Microscopic examination of the inner surface of the rotor showed many small cracks in the zinc-rich beta-phase stringers at the surface. One of these cracks is shown in Fig. IV-B-5. Similar cracks were found in stress-corrosion test samples (Fig. IV-B-6) prepared from the same piece of bar stock as the failed rotor. Samples were stressed to 52,000 psi (rotor operation) and 70,000 psi (about 95% of the yield stress). Those oriented transversely to the bar stock (and rotor) axis failed by stress corrosion in 24 and 20 hr respectively. No failures were encountered in the longitudinal samples in a three-week exposure to saturated cesium chloride.

Examination of the failure pattern and microstructure of the rotor material and the evidence from the stress-corrosion tests indicate that the failure initiated through stress-corrosion cracking.

Fig. IV-B-6. Cracks in β Phase After Stress-Corrosion Test. This sample was loaded to approximately the stress developed in rotor operation. 350X. Reduced 26.5%.

A carefully controlled solution heat treatment, to dissolve the beta-phase residue of the original ingot structure, would minimize the probability of failure from this cause. This conclusion is supported by the results of an earlier stress-corrosion

[2] *Joint NIH-AEC Zonal Centrifuge Development Program Semiann. Rept. January 1–June 30, 1963*, ORNL-3502, pp. 23–30.

test[2] on 7075-T6 sheet stock. The additional mechanical work received by sheet stock in its reduction to sheet thickness effectively broke up the beta phase so that it was readily taken into solution during heat treatment. The relatively random distribution of the remaining beta phase did not furnish paths along which cracks could propagate.

Steel rotors are being considered for high-speed operation with concentrated salt solutions.

V. Low-Speed Zonal Rotors

H. P. Barringer

A. ROTOR A-IX

Drawings suitable for the fabrication of the A-IX rotor and seal have been released to the AEC Division of Technical Information, Engineering Materials Program, for sale as a CAPE package. The drawings are included as Appendix I of this report.

B. ROTOR A-X

The rotor volume (1.3 liters) of the A-IX centrifuge (Fig. V-B-1) is too large for many samples and purposes. A new core, designated A-X, has been fabricated to fit inside the A-IX rotor. The core has two sector-shaped compartments and a usable gradient space of 300 ml. The remainder of the rotor volume is filled by two sector-shaped sections of solid Lucite.

The design of additional rotors in the A series will await the results of comparative studies using the A-VIII and the A-IX rotor to determine the advantages of dynamic loading as compared with the reorienting gradient mode of operation.

In the B-IV rotor, sedimentation rates are calculated from the known position of the starting zone and the position of the separated particle zones in the gradient as recovered at the end of the run. Volume changes due to changes in osmotic pressure experienced by particles sedimenting through the density gradient have been disregarded since they appear to be small in the small spherical viruses. With cells and mitochondria, such as are studied in A series rotors, osmotically induced volume changes are appreciable. Theoretical calculations concerning the osmotic volume changes are based on assumptions concerning the nonosmotic volume of the particles, membrane permeability and distensibility, and particle homogeneity – assumptions which require experimental examination themselves. It is important therefore to be able to measure the sedimentation rates of particles as a function of their position in the gradient. This is best done by measuring sedimentation rates continuously during centrifugation. The A-IX rotor has been designed with this end in view. A scanning system for recording the distribution of particles in the rotor at frequent intervals has therefore been designed. Details of its construction and operation will be included in the next report.

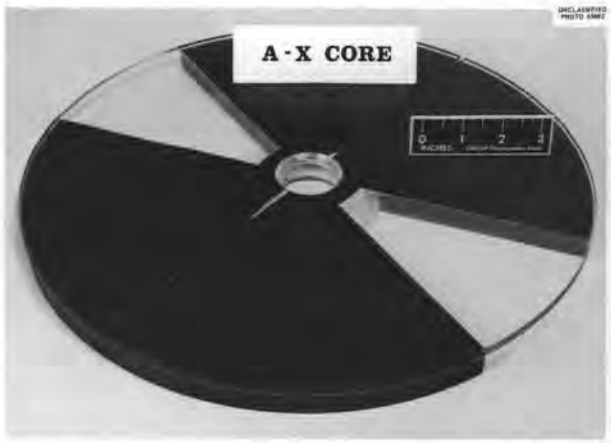

Fig. V-B-1. Core of Rotor A-X Which Fits Inside A-IX. The two section-shaped compartments have a volume of approximately 300 ml. The rest of the rotor volume is solid Lucite.

VI. Intermediate-Speed Zonal Rotors

H. P. Barringer

The B series rotors have been limited to the speeds available with conventional preparative ultracentrifuge drives (~40,000 rpm) and have been designed to separate particles ranging in size down to the smallest subcellular particulates which are the primary subunits of ribosomes (~30S). The approach has been to first explore the limits of resolution and capacity and then to develop the simplest and most inexpensive method for achieving the same (or nearly the same) resolution.

A. B-IV SYSTEM

The B-II rotor[1-3] demonstrated the basic principles but exhibited marked instabilities at speeds of from 26,000 to 31,000 rpm, depending upon the rotors and bearings used. Initially it was thought that fluid movement in the rotor produced the instabilities observed, and a large number of septa (36 in all) were used to achieve a high degree of compartmentation. The septa were removable, subject to deformation, and they increased the load on the rotor wall. In addition, the core was difficult to clean. It was proposed that the rotor be redesigned to simplify the core and to solve, if possible, the stability problem. The latter proved to be the most difficult single problem encountered thus far.

1. Stability Studies

The B-II rotor is driven by a Spinco model L drive in a modified evacuated chamber. The physical constants involved in the centrifuge drive system, rotor, top bearing, and supporting frames were examined for possible sources of excitations which could produce the destructive high-amplitude vibrations observed. Careful experimental measurement, theoretical computations, and redesign studies of the system components were coupled with detailed experimental investigations to obtain the information necessary to reach 40,000 rpm.

Proximity distance detectors were installed inside the centrifuge vacuum chamber to observe and measure movement of the rotor during rotation. Near 31,000 rpm a high-amplitude precessional motion was observed which was superimposed on the normally small amplitude of rotor runout due to minor imbalances. The destructive high-amplitude movements were associated with a natural forward precessional mode of vibration which could exist because of insufficient damping in the upper journal bearing.

2. Damping Bearing

A variety of types of damper bearings were tested in the development of an enclosed journal bearing–seal holder with the proper damping constants. Damping is accomplished by shearing a fluid between parallel plates. One set of plates is attached to the self-aligning journal bearing and is mounted to allow a small translational movement (Fig. VI-A-1). The stationary plates are fastened rigidly to the centrifuge frame. The

[1] N. G. Anderson, *Nature* **199**, 1166 (1963).

[2] *Joint NIH-AEC Zonal Centrifuge Development Program Semiann. Rept. July 1–December 31, 1962*, ORNL-3415.

[3] N. G. Anderson, *J. Phys. Chem.* **66**, 1984 (1962).

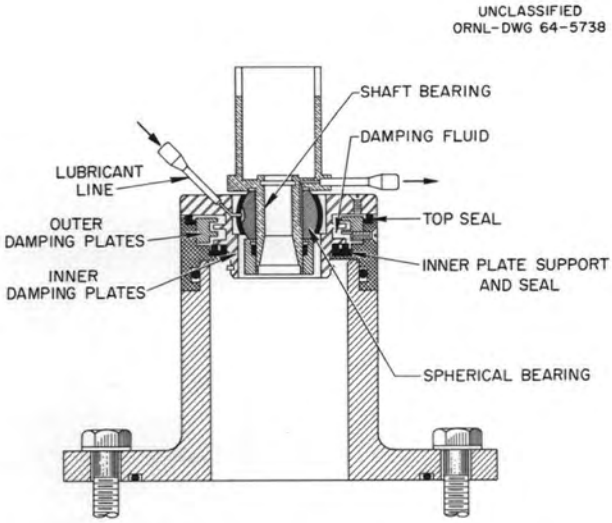

Fig. VI-A-1. Top Damper Bearing for B-Type Rotors.

axial space between the plates is filled with high-viscosity silicone oil. An extension of the upper journal-bearing housing forms a self-aligning holder to position the rotating seal. The completed B-IV bearing is shown in Fig. VI-A-1*a*.

3. Core

The core in a dynamically loaded B series zonal rotor serves three purposes: (1) it compartmentalizes the rotor volume into sector-shaped chambers, (2) it serves to connect the central and peripheral portions of each compartment with the seal, and (3) it serves to funnel the gradient into and out of the rotor with minimal mixing and consequent loss of resolution. When it was found that a high

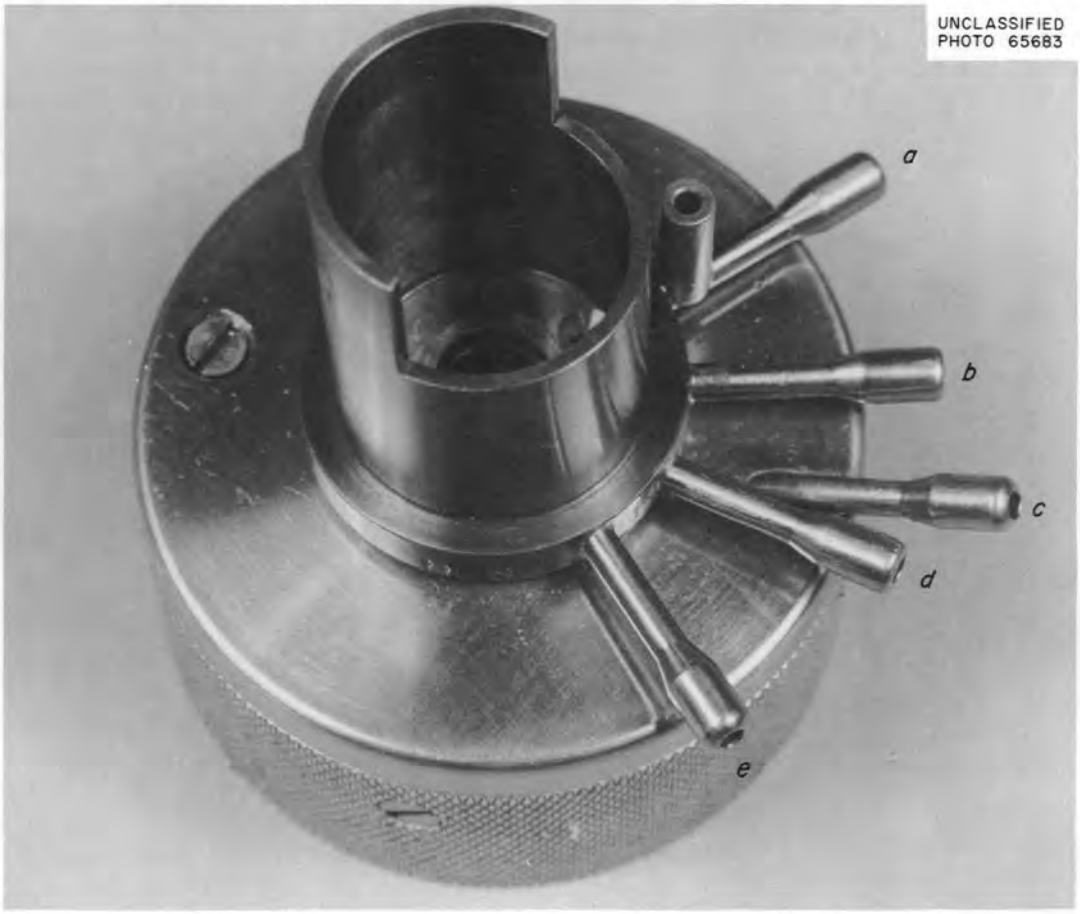

Fig. VI-A-1*a*. B-IV Top Bearing Assembly. (*a*) Overflow oil from bearing; (*b*) cooling water out; (*c*) oil line in, lower bearing; (*d*) oil line in, to shaft; and (*e*) cooling water in.

degree of internal compartmentation was not necessary to achieve rotor stability, the possibility of using a simple four-vaned core was reconsidered. Such a core has the advantage of not bearing against the rotor wall, it can be easily cleaned, and it is simpler to construct.

The surfaces in the B-II core which funnel zones into the exit line are shown in Fig. VI-A-2. A vertical zone approaching the central core surface flows in a vertical direction along the core an average of 3.2 cm, with an average angle of 4° between the zone and the core. The sequence of changes in the cross section of a zone during unloading are shown in Fig. VI-A-2(*b*–*f*). In the B-IV core a different series of surfaces are used to achieve the same effect. The core, shown schematically in Fig. VI-A-3, is machined from two pieces of duraluminum permanently attached to each other. The zones approaching the axis of the centrifuge are moved horizontally as they contact the square central section. The angle of contact between a zone and the portion of the square section next to the vane is 48.9°, decreasing rapidly as the zone reaches the center channel. Fluid flows across the face of this portion of the core and continuously sweeps toward the center into the central vertical groove, that part of each zone which is in contact with the core. As a zone is channeled toward the vertical groove, the rate of horizontal flow is increased, allowing the contact angle to be diminished to nearly 0°. The particle concentration in the film of fluid which is in contact with the core is being continuously decreased by sedimentation. This acts to counteract the effects of laminar flow.

To compare the resolution obtainable with the two systems, a number of experiments have been performed, including the rate separation of T2 and T3 phage under identical conditions with the B-II and B-IV cores. No differences have been noted. To determine whether the starting zone thickness was comparable in the two rotors, bovine serum albumin samples were run into the two rotors under comparable conditions and were unloaded through the ultraviolet absorbance monitor. As shown in Fig. VI-A-4, essentially identical patterns were obtained, showing that the volume occupied by the sample was the same with both rotors.

The B-IV cores have been routinely used for the past five months, at speeds up to 40,000 rpm. All B-II cores have been retired.

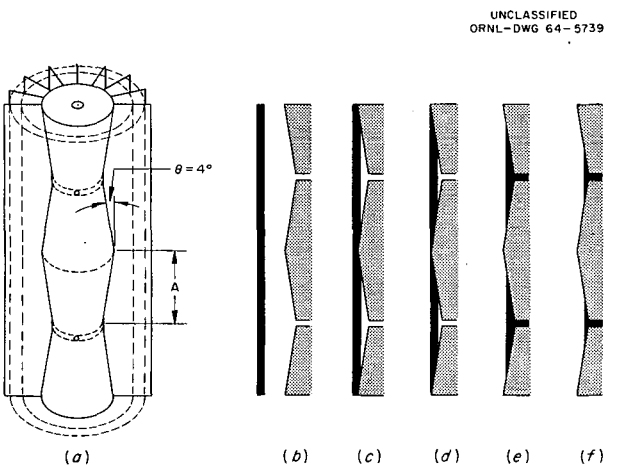

Fig. VI-A-2. Zone Recovery in B-II Core. (*a*) Schematic of B-II core, with some septa removed. (*b*–*f*) Details of zone recovery in B-II core; (*b*) zone approaching core, (*f*) part of zone recovered, part within core.

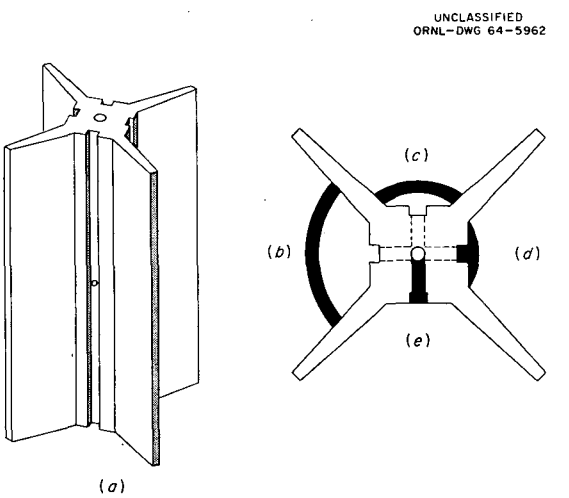

Fig. VI-A-3. Zone Recovery in B-IV Core. (*a*) B-IV core. (*b*–*e*) Zone recovery; (*b*) zone approaching core, (*e*) part of zone recovered, part within core.

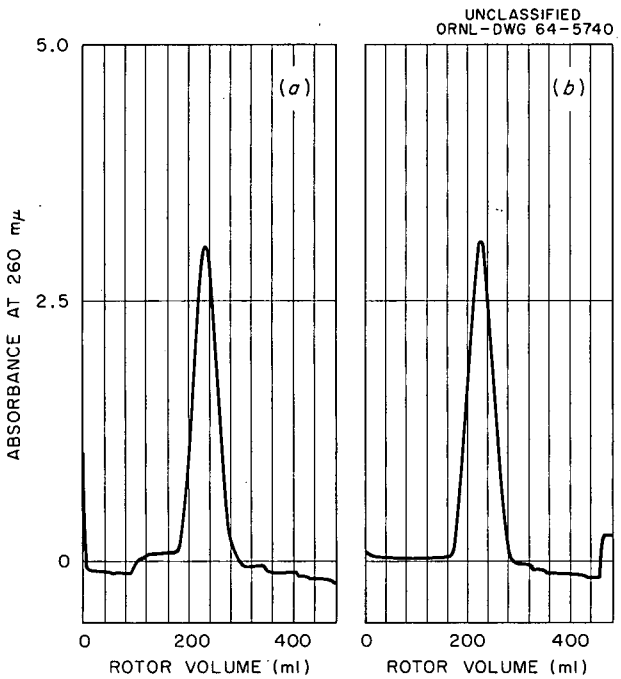

Fig. VI-A-4. Comparison of Widths of Sample Zones in B-II (*a*) and B-IV (*b*) Rotors. Sample: 25 ml of 2.5% bovine serum albumin in 4.2% sucrose; overlay: 216 ml of water; gradient: 17 w/w % sucrose grading into 55 w/w % sucrose; and centrifugation: rotor loaded at 5000 rpm, accelerated to 25,000 rpm, maintained at that speed for 15 min, and unloaded at 5000 rpm.

4. B-IV Instrumentation, Containment, and Operation

The instrumentation and operation of the B-IV rotor system is described in Chapter XIII, and the containment glove box is described in Chapter XII.

B. MODIFICATIONS OF THE B-IV SYSTEM FOR CONTINUOUS-FLOW CONCENTRATION OF PARTICLES

Modifications of the B-IV system for continuous-flow centrifugation of viruses and other small particles are described in Chapter IX. These include the B-V through B-VIII cores.

C. ZONAL ROTOR SYSTEMS UNDER DEVELOPMENT

The basic purpose in the development of the B-IV system has been to devise a high-resolution zonal centrifuge for exploring particle separation in the ultracentrifuge range. As shown in other sections of this report, clean separations of particles having sedimentation coefficients as low as 20S have been obtained. We wish now to explore the possibility of achieving the same resolution with very much simpler rotor systems. Rotors B-X and B-XI are therefore being designed to determine whether the upper bearing can be eliminated from intermediate-speed zonal rotors and to explore the difficulties involved in the use of removable seals suggested previously.[3] Rotor ~~B-IX~~ B-XI, a steel counterpart of the B-IV rotor, will be used to explore protein separations at 50,000 rpm. This rotor will have the highest speed of the B series.

VII. High-Speed Zonal Rotors

A. C-II ROTORS

The C-II rotors have been repeatedly operated at their designed speed of 141,000 rpm. Methods for generating gradients for this rotor and for monitoring the recovered gradient are being investigated. A complete C-II system has been installed in the Biophysical Separations Laboratory to facilitate studies with biological materials. The design of the rotor is discussed in the previous report.[1]

[1] *Joint NIH-AEC Zonal Centrifuge Program Semiann. Rept. July 1–December 31, 1962,* ORNL-3415.

B. C-III ROTORS

Studies on the behavior of gradients in the C series rotors during reorientation to determine the optimal gradient slope and the best level for placement of the sample will be completed before extended studies on the separation of nucleic acids on the basis of sedimentation rate or density are initiated. In the design of the C series rotors, the problem of the effect of shear on high-molecular-weight nucleic acid has been considered, and provision has been made for loading the rotor without requiring the sample to flow through narrow tubes or orifices.

VIII. Ultrahigh-Speed Rotors

At very high gravitational fields a number of interesting possibilities arise. First, if a small rotor with a high rate of acceleration can be built, the resolution of sedimentation rate studies could be increased. Second, banding studies, now limited to materials with very high molecular weights, can be extended to smaller molecules. Third, the effect of high pressure on the buoyant density of biologically important molecules can be examined. We have been interested therefore in the development of an ultrahigh-speed rotor with transparent end caps which would allow observations and measurements to be made during rotation and which would use the reorienting gradient principle to permit the gradient to be recovered and analyzed at the end of the centrifugation period. The D series rotors have been designed to explore these possibilities.

A. D-1 MAGNETIC SUPPORT SYSTEM

The D-1 rotor drive and suspension system is designed to produce a magnetic field which will support the rotor, damp out oscillations, and, at the same time, drive the rotor to the desired speed or decelerate it to zero. It is also necessary to know the exact rotor speed at all times. The supported rotor is shown in Fig. VIII-A-1, with the electrical motor stator surrounding the rotor. A block diagram of the system functions and the electronics schematic diagram are given in Appendix IV.

The system operates as described in the previous report.[1]

The control circuit is built from analog computer elements to make the system inexpensive and reliable. A high-pass filter in the distance detector circuit eliminates control problems encountered by stray flux in the rotor which was introduced by the stator of the drive system. From speed measurements to 90,000 rpm, it appears that the rotor can be accelerated to 400,000 rpm ($1.2 \times 10^6 \times g$ at R_{max}) in less than 30 min.

The most difficult problem associated with operation at a very high speed is the development of the light damping systems which will be required to achieve the full design speed of 400,000 rpm. A prototype damper weighing 1.4 g is being fabricated.

[1] *Joint NIH-AEC Zonal Centrifuge Program Semiann. Rept. July 1—December 31, 1962,* ORNL-3502.

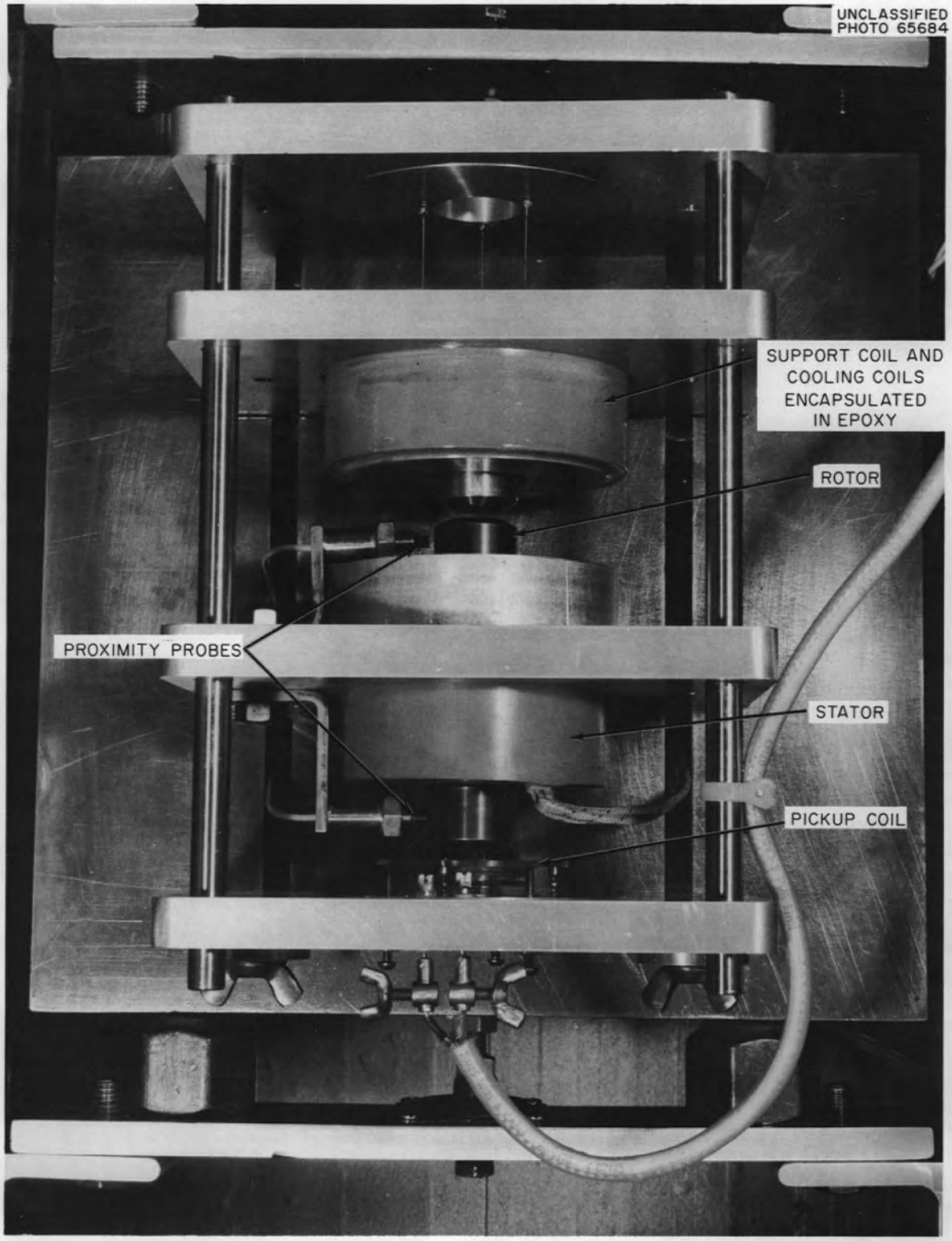

Fig. VIII-A-1. D-1 Rotor in Run Stand. Speed: 400,000 rpm $[(1.2 \times 10^6) \times g]$; capacity: 10 ml; material: steel; and drive: magnetic.

IX. Continuous-Flow Rotors

A. ROTOR B-V

H. P. Barringer C. E. Nunley
N. G. Anderson

Based on theoretical studies previously presented (Chap. III, this report), a continuous-flow centrifuge rotor (B-V of the intermediate-speed series) has been developed to explore the isolation of virus particles from large volumes of culture fluid, extracts of tissues, plasma, or natural waters.

1. Principles of Operation

For the mass isolation of virus particles for experimental or vaccine purposes, a closed continuous-flow centrifuge system is desirable. The requirements are that the feed stream move continuously into the rotor without heating or spraying, that it be accelerated to the tangential velocity obtaining at the edge of the rotor chamber before entering it, that the stream move evenly across the internal rotor wall surface, and that the virus particles separated be easily recovered in sterile containers with no leakage of aerosols to operating personnel.

The chosen configuration is shown diagrammatically in Fig. IX-A-1. The virus-laden fluid is brought into the rotor through a face seal via appropriate channels machined in the core and is released into a small peripheral receiving chamber at the lower end of the rotor. The fluid then flows circumferentially to small axial slots in the lower edge of the core and upward in the annular chamber to the exit ports at the top of the core. The latter ports lead to the face seal, where the fluid is conducted out of the rotor. It should be noted that the four exit channels at the top of the core are rotated 45° with respect to the axial slots at the bottom of the core. The total fluid path is therefore slightly greater than the length of the core.

Close temperature control of the rotor and stream of fluid flowing through it is not obtained in practice. A change from 5°C to 6°C in water flowing through the rotor at 40,000 rpm produces an effective force difference (apparent density difference) of 2.2 g/cm^2. It cannot be assumed therefore that fluid will flow uniformly up the annular space between the core and rotor wall. It is more likely that it will rapidly traverse the length of the rotor either close to the rotor wall if denser than the rotor contents or close to the surface of the core, if lighter. In both cases the fluid will tend to move as a thin sheet. If the thickness of a fluid layer in a centrifugal field is increased, the time required to sediment particles having a given sedimentation rate will also increase. However, the increased dwell time due to the increased cross-sectional area almost exactly compensates for the increased thickness. Therefore, once the distance between the rotor wall and the core has been reduced to the point where the variation in centrifugal force across the gap is negligible, the width of the gap has little effect on rotor performance, provided it is not narrow enough to produce viscous resistance to flow. It is of little consequence, therefore, if the incoming stream flows as a thin sheet along either the core or the rotor wall due to temperature-induced density differences. The quantity of virus in the stream flowing through the rotor is assumed to be so small that removal of the virus causes no perceptible change in fluid density.

2. System

The B-V rotor system includes (1) a hollow centrifuge rotor dimensionally similar to the B-IV zonal rotor described in Chap. VI, (2) an internal

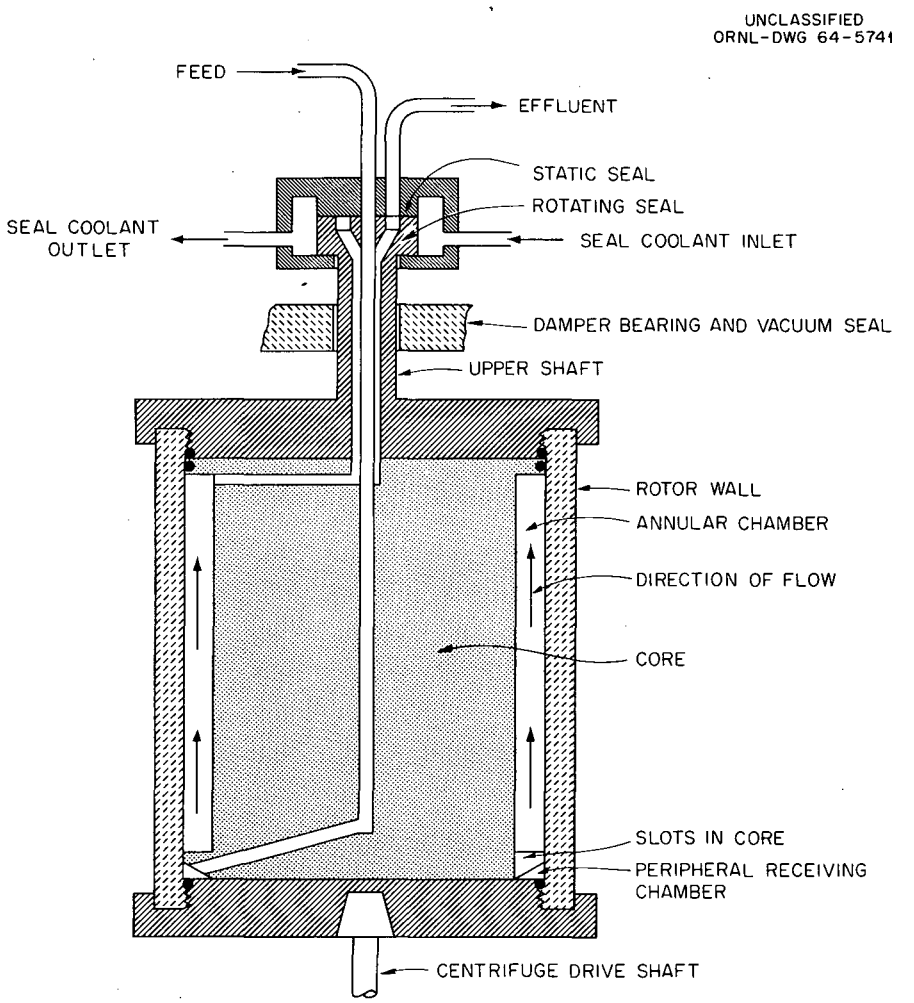

Fig. IX-A-1. Schematic Drawing of B-V Continuous-Flow Centrifuge Rotor.

core which forms an annular cavity inside the rotor (Fig. IX-A-2), and (3) a high-speed contact seal for flowing fluids into and out of the rotor during centrifugation at speeds up to 40,000 rpm. The system, shown diagrammatically in Fig. IX-A-1, is driven by a Spinco model L centrifuge which had been previously modified for use as a zonal ultracentrifuge.

The rotating seal used on the B-V rotor permits one fluid stream to flow on the axis of rotation, while the second stream flows as a concentric annular cylinder outboard of the axis of rotation (see description in Chap. X, section C). Centrifugal force produces a pressure differential between the two fluid lines, as given by the equation

$$\Delta P = \frac{\rho w^2 r_0}{2g}, \qquad (1)$$

where

ΔP = pressure difference between the two seal lines in the rotating part of the seal,
ρ = density of the fluid used,
w = radial velocity in radians per second,
r_0 = radius of outer fluid line,
g = acceleration due to gravity.

The radii of the fluid lines are 1.07 and 3.81 mm. If water is flowing through the rotor at 40,000 rpm, the pressure differential would be 18 psi. It is undesirable to pump against this pressure differential since this would require higher seal face preloads with the accompanying greater wear rates and higher power losses. The preferred flow direction is for the feed stream to move through the center line directly along the axis of rotation and then outward to the bottom of the core. Thus the

particle-containing feed stream has little chance to leak to the outside during continuous-flow centrifugation since it must also leak across the clarified stream flowing in the opposite direction. Rather, such leakage as exists will be more likely to originate from the relatively particle-free effluent stream; and any seal leakage will be trapped in the cooling fluid surrounding the seal.

The seal is provided with two sliding surfaces which preload each other to prevent leakage and

Fig. IX-A-2. Core of B-V Continuous-Flow Rotor. Particles are sedimented to the rotor wall. Speed: 40,000 rpm (90,952 × *g*); capacity: 113 ml; material: aluminum; and drive: Spinco L.

a coolant and disinfectant chamber which contains aerosols that might be produced at high speeds. The seal is attached to the upper shaft of the centrifuge and is located by a holder, which is an integral part of the damper bearing.

The rotor system is shown disassembled in Fig. IX-A-3. The core is 25 cm long and is separated by a distance of 0.08 cm from the inner rotor wall (radius 5.0 cm), giving a ratio of $R_{core}/R_{rotor} = 0.984$. The rotor has been operated with the seal exposed or with the entire upper bearing seal, cooling circuit, and all associated lines in a sealed glove box. The rotor has been operated to 40,000 rpm without excessive vibration using the new B-IV damper bearing.

The absence of vanes in the annular chamber permits the rotor contents to swirl as the rotor is decelerated, thereby tending to resuspend particles clinging to the rotor walls.

To recover the sedimented material, the rotor is removed from the centrifuge and placed in a container (Fig. IX-A-4) having a lower plate which matches the lower rotor end cap and which prevents rotor rotation when the upper end cap is removed. The seal and upper end cap are placed in special stainless steel containers for disinfection and cleaning. The core is removed as shown in Fig. IX-A-4 and placed in the second section of the container. A sterile rubber policeman on a long stainless steel rod is used to wash particle-

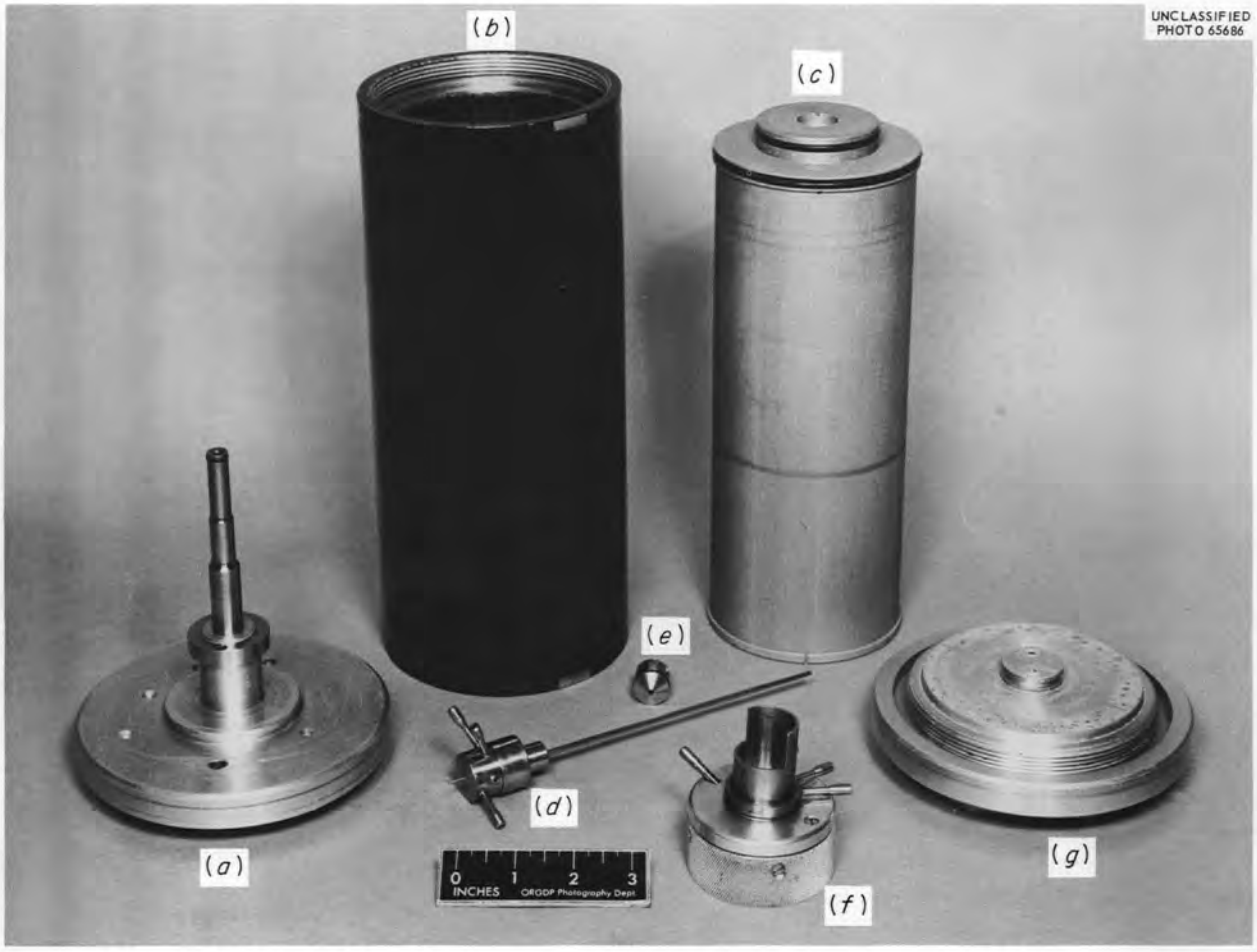

Fig. IX-A-3. Disassembled B-V Rotor System. (*a*) Upper end cap; (*b*) rotor chamber; (*c*) rotor core; (*d*) seal; (*e*) manifold plug; (*f*) upper bearing; and (*g*) upper end cap.

Fig. IX-A-4. Diassembly of B-V Rotor in Containers for Subsequent Disinfection. Photographed in glove box which encloses the top of the centrifuge chamber. (*a*) Core being lifted out of rotor body; (*b*) container for disinfecting core; (*c*) upper end cap in its container; and (*d*) seal container.

containing sediment off the wall and into the 120 ml left in the rotor at the end of the run. The fluid is then aspirated into a sterile vacuum bottle. All containers are then filled with 3% formalin, and the glove box used for the entire procedure is sterilized with ethylene oxide. The coolant line fluid (generally distilled water) is also sterilized with formalin.

An alternate method to be used on multiple runs is to resuspend the sedimented particles by rapidly decelerating the rotor with an accompanying swirling of the fluid to scrub the surfaces of the annular rotor chamber. The rotor contents can then be removed by pumping the fluid out the bottom of the stationary rotor or by displacement with compressed air. Repetitive runs can then be made without disassembly of the rotor.

Results obtained with the B-V rotor are presented in Chap. IX.

B. CONTINUOUS FLOW WITH CONTINUOUS ISOPYCNIC BANDING

N. G. Anderson H. P. Barringer
J. Amburgey

1. General Principles

Many viruses are inactivated by pelleting. In addition, subcellar particles often tend to aggregate after such treatment and are difficult to resuspend. The separations described in this report concern particles which are free in solution; in the sedimentation rate–isopycnic banding studies described in Chap. I, the particles were kept in suspension at all times.

If virus particles are to be concentrated from large volumes of solution by centrifugation but without aggregation, then some means must be found for preventing the virus from colliding with

a solid surface as it is removed from the flowing stream. The possibility has therefore been considered that the particle-laden stream could be made to flow over the surface of a stationary liquid density gradient imprisoned in a spinning rotor. The problems to be solved concern the design of a suitable core which would allow a gradient to be established in the rotor during rotation, would allow the particle-containing stream to flow over the surface of the gradient with minimal turbulence, and would permit the gradient and the banded particles suspended in it to be recovered without loss of resolution at the end of the run.

2. B-VI and B-VII Cores

Both the B-VI (Fig. IX-B-1) and the B-VII (Fig. IX-B-2) cores are tapered cylinders which fit into the B-IV rotor chamber. These were used to study flow in hollow rotors in the presence of gradients. In B-VI the feed stream flows top to bottom in the rotor, while in B-VII it flows in the opposite direction. Pressure differences across the two lines leading through the seal dictate that the feed stream should flow through the center seal line. In order to achieve optimal sedimentation, the feed stream must enter the rotor chamber at the narrow end of the tapered core. In the B-VI core the narrow end of the core is at the top, and a manifold plug is used to cross the fluid lines to make the proper connections. Small air bubbles in the manifold plug interfered with flow through the rotor and caused the pressure required to achieve a given flow rate to rise sharply with rotor speed. To minimize this problem, the B-VII core was so constructed that flow into the rotor was directly down through the center seal line to the bottom of the

Fig. IX-B-1. Core of B-VI Continuous-Flow-Banding Rotor. Core fits chamber of rotor B-II. Speed: 35,000 rpm (69.635 × *g*); capacity: 1338 ml; material: aluminum; and drive: Spinco L.

Fig. IX-B-2. Core of B-VII Continuous-Flow-Banding Rotor. Core fits chamber of rotor B-II. Speed: 35,000 rpm (69.635 × *g*); capacity: 1012 ml; material: aluminum; and drive: Spinco L.

core and then to the rotor chamber. The narrow end of the core is at the bottom.

With the B-VII core, water could be made to flow over a sucrose or cesium chloride gradient with a minimum of difficulty due to back pressure. The gradient, when recovered, gave evidence of considerable mixing in the rotor during unloading. In the absence of septa, Coriolis forces will produce laminar mixing and turbulence as fluid is caused to flow toward the axis at constant rotor speed. It appeared necessary therefore to include septa.

3. Rotor B-VIII

The B-VIII core (Fig. IX-B-3) incorporates certain features of the simpler B-VII core but provides additional flow lines to the edge of the rotor together with four integral fins to prevent swirling of the rotor contents. The feed stream is admitted to the bottom of the core and flows upward along the conical surfaces, which are approximated by 36 facets machined on the core. The fluid exits at the large-diameter (upper) end of the core. By use of this rotor, gradients could be introduced and recovered with relatively little change after many liters of distilled water had been allowed to flow over them. Studies on virus isolation with the B-VIII rotor will be included in the next report.

Fig. IX-B-3. Core of B-VIII Continuous-Flow-Banding Rotor. Core fits chamber of rotor B-II. Speed: 35,000 rpm (69.635 × *g*); capacity: 952 ml; material: aluminum; and drive: Spinco L.

X. Seal Development

C. E. Nunley

Loading and unloading of zonal rotors during rotation and continuous-flow centrifugation require fluid line seals which do not heat, shear, spray, or cross contaminate the suspensions used. In previous reports the development of type "A" seals for low-speed rotors and type "B" seals for intermediate-speed zonal rotors was considered. Modifications based on extended experience continue to be made.

A. TYPE "A" SEALS

In the A-V, A-VI, and early versions of the A-IX rotor, the static seal surface was supported by the

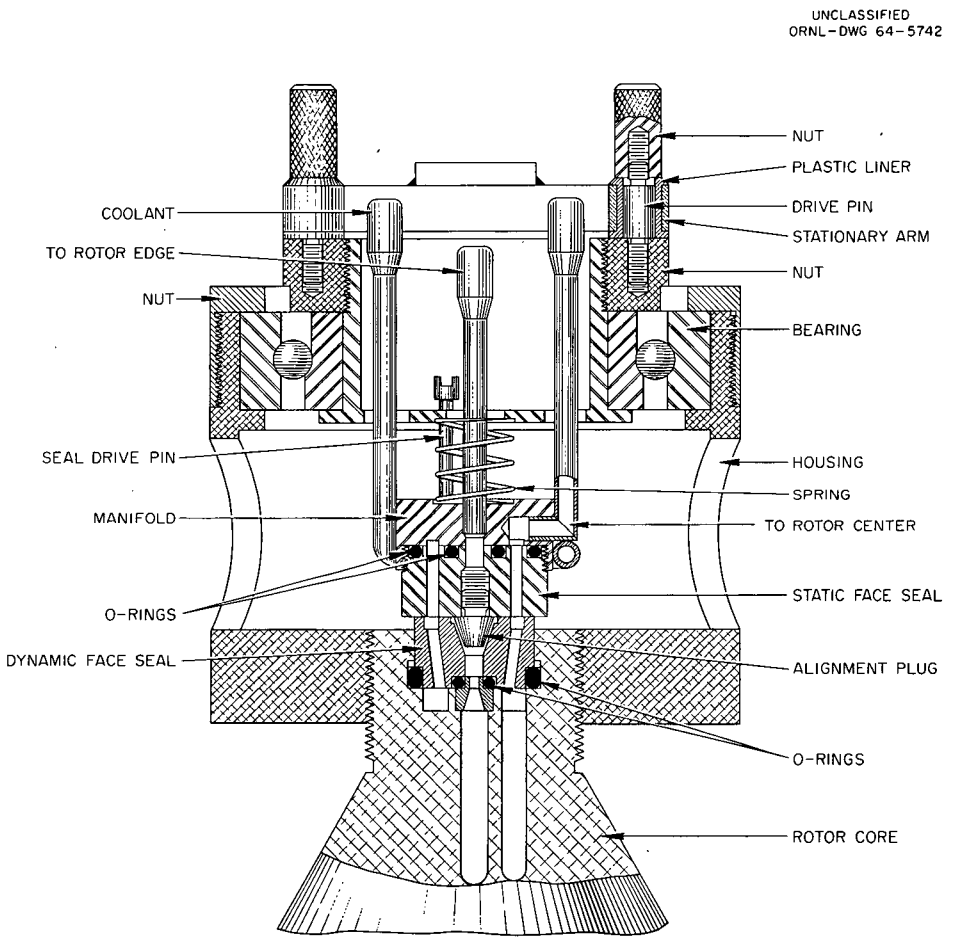

Fig. X-A-1. Type "A" Seal Redesigned to Attach to Rotor. See text. Seal used on low-speed rotors.

centrifuge housing. Small vibrational movements of the rotor and the rotating seal component about its axis were therefore not transmitted to the static seal member. Perfect seal alignment was therefore difficult to maintain.

The "A" seal has therefore been redesigned (Fig. X-A-1), and the entire seal system has been attached to the rotor. The rotating seal housing is threaded on the rotor core and positions the static, or nonrotating, seal face relative to the dynamic, or rotating, seal face through a ball bearing. The nonrotating portion of the seal is flexibly mounted to provide for alignment of the seal faces and sufficient preload to prevent seal leakage. Attached to the static seal is a conical aligning plug and a cooling coil through which chilled water is circulated to remove frictional heat. Components of the seal are shown in Fig. X-A-2.

Modifications being incorporated in the design will allow the seal to be attached to and removed from a rotor during rotation since, in practice, the seal is required only during loading and unloading of the rotor contents. Simpler, smaller-capacity rotors can be designed so that gradient work on smaller scales than reported here would be possible. The ultimate limits of speed in density gradient centrifugation, apart from strengths of materials and rotor mechanics, in any system other than centrifuge tubes, lie in the seal system. A detachable seal will obviate this problem.

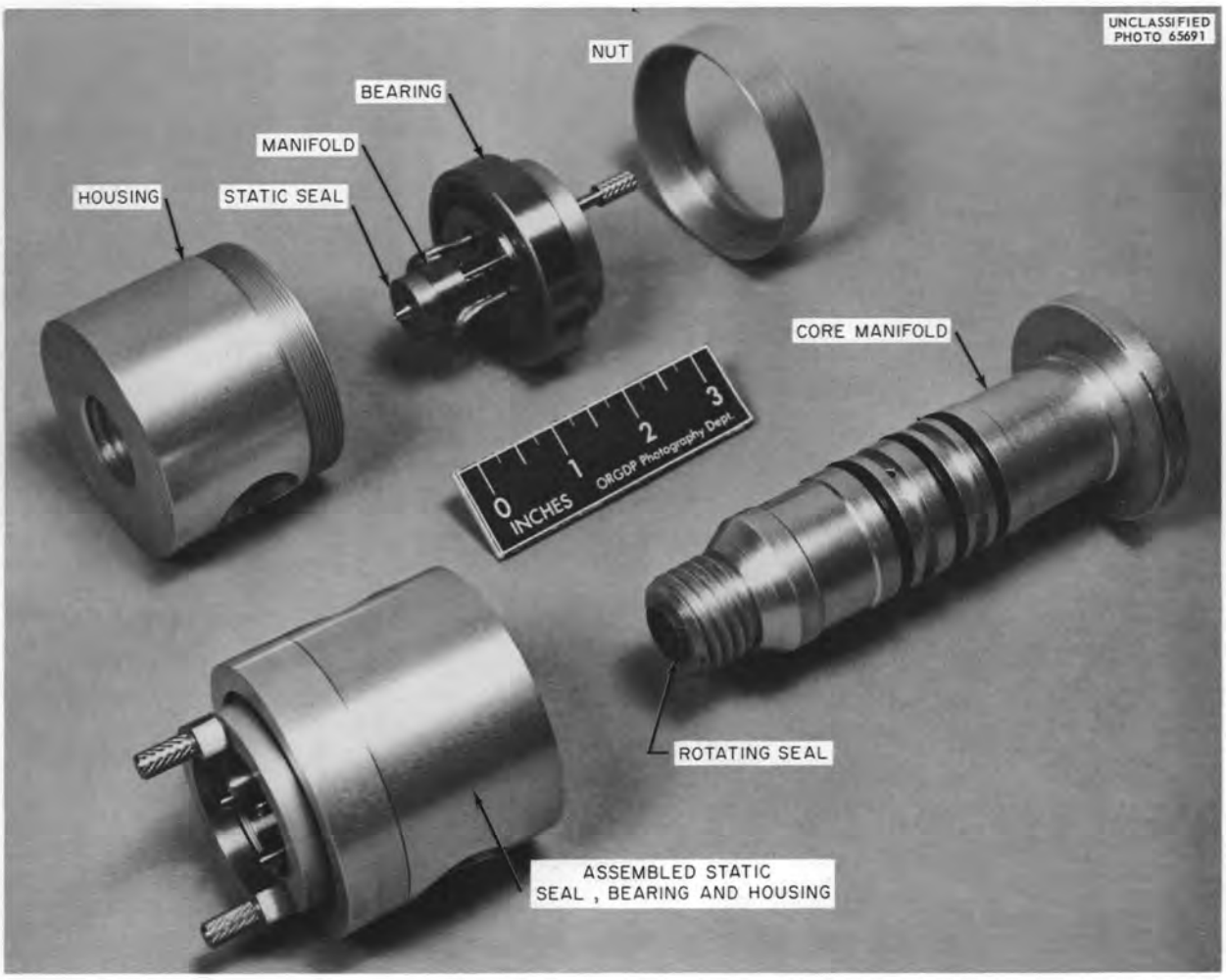

Fig. X-A-2. Components of Type "A" Seal.

B. TYPE "B" SEALS

The "B" seal (Fig. X-B-1) is designed to operate at 40,000 rpm on the B-type rotor systems. The unit (Fig. X-B-2) consists of a housing, a manifold, a two-path seal for rotor feed and outlet stream, and a secondary seal to contain the coolant-disinfectant. The sealing surfaces are preloaded by a coil spring located inside the seal housing. O-ring seals at all connections permit the seal to be readily disassembled for cleaning and inspection without the use of special tools or fixtures.

The life expectancy of the seal has not been established. However, one seal has operated over 100 hr at 40,000 rpm with only minor maintenance. The two-path plastic seal ring was replaced after approximately 50 hr operation; however, inspection of the part indicated negligible wear. This seal is still performing satisfactorily.

Since improved centrifuges will require higher speeds, tests are being conducted to determine the maximum operating speed of the present seal. Satisfactory test results have been obtained at 50,000 rpm.

Biological infectivity tests on material concentrated in the B-V rotor have indicated essentially no cross leakage in the seal. Additional testing will be done at a later date.

UNCLASSIFIED
ORNL-DWG 64-5743

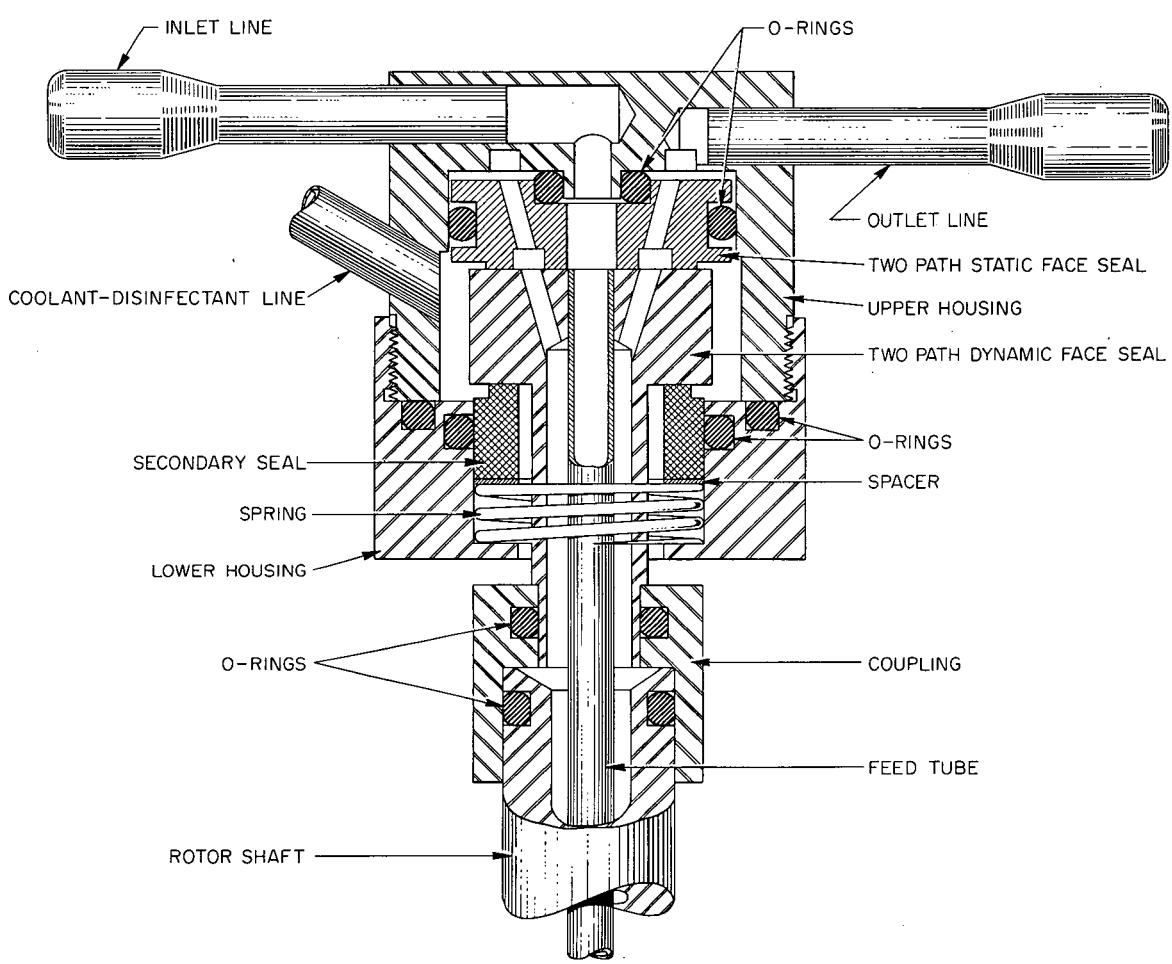

Fig. X-B-1. Type "B" Seal for Intermediate-Speed Rotors. Seal is used routinely at 40,000 rpm; satisfactory test results of seal at 50,000 rpm have been obtained.

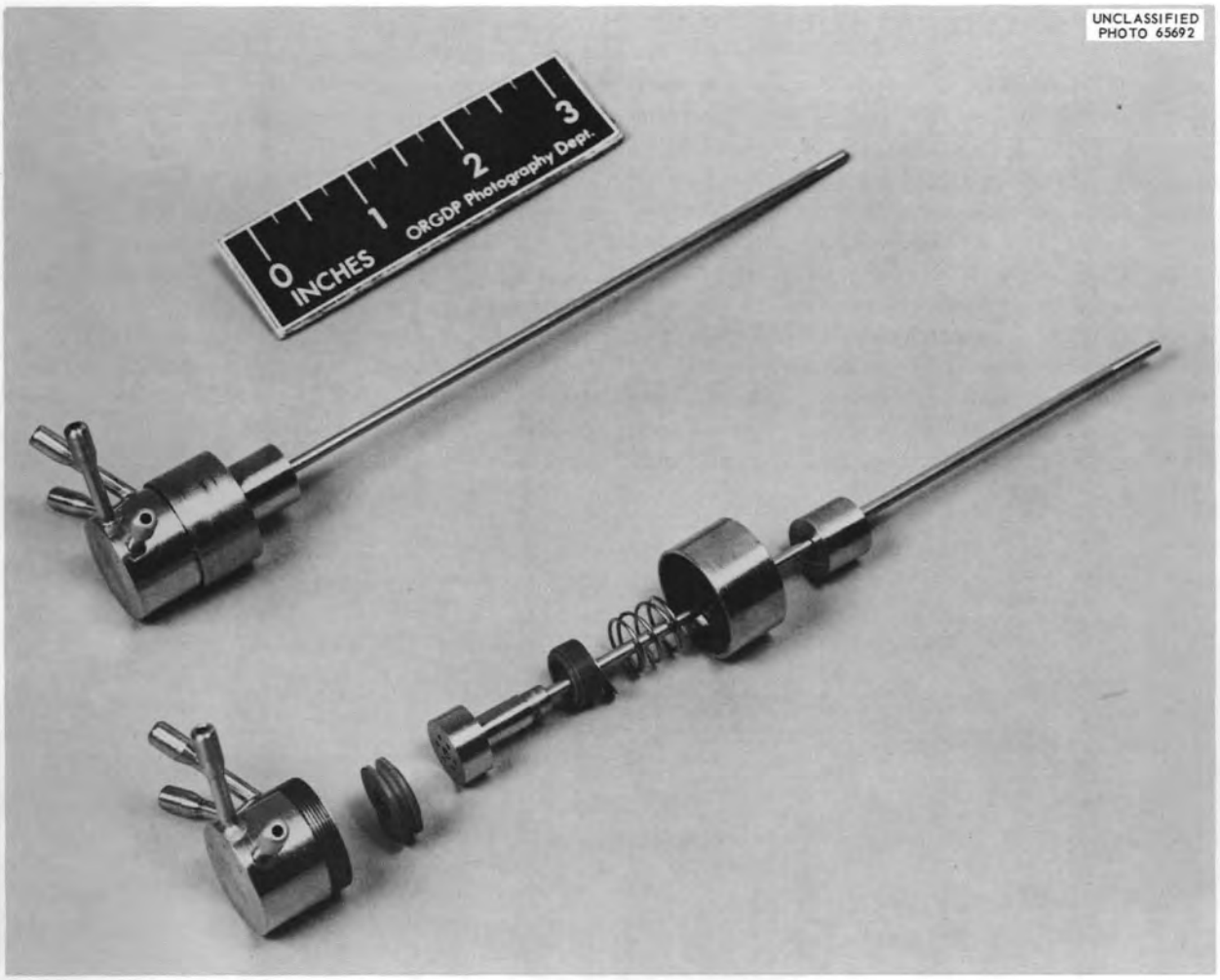

Fig. X-B-2. Type "B" Seal Assembled (Top) and Disassembled (Below). See Fig. X-B-1.

C. TYPE "B" FLOW-THROUGH SEAL

Apparently, gas is centrifuged from the culture fluids; and during continuous-flow centrifugation, it collects in the center of the rotor, blocking the inlet flow of fluid. Thus, for continuous flow of fluid through the rotor running at high speed, it is necessary to eliminate all bubbles from the flow paths inside the rotor. A type "B" seal has been modified (as seen in Fig. X-C-1) to eliminate this problem by the addition of a small-diameter tube which extends into the rotating feed line of the seal to bleed gases from the rotor.

Any gases in the rotor will rise to the top of the seal and form a vortex, so a simple bleed line gives satisfactory results. Tests have shown that air bubbles purposely introduced into the feed line block the inlet flow line when the bleed line is closed, but the block can readily be eliminated by opening the bleed line.

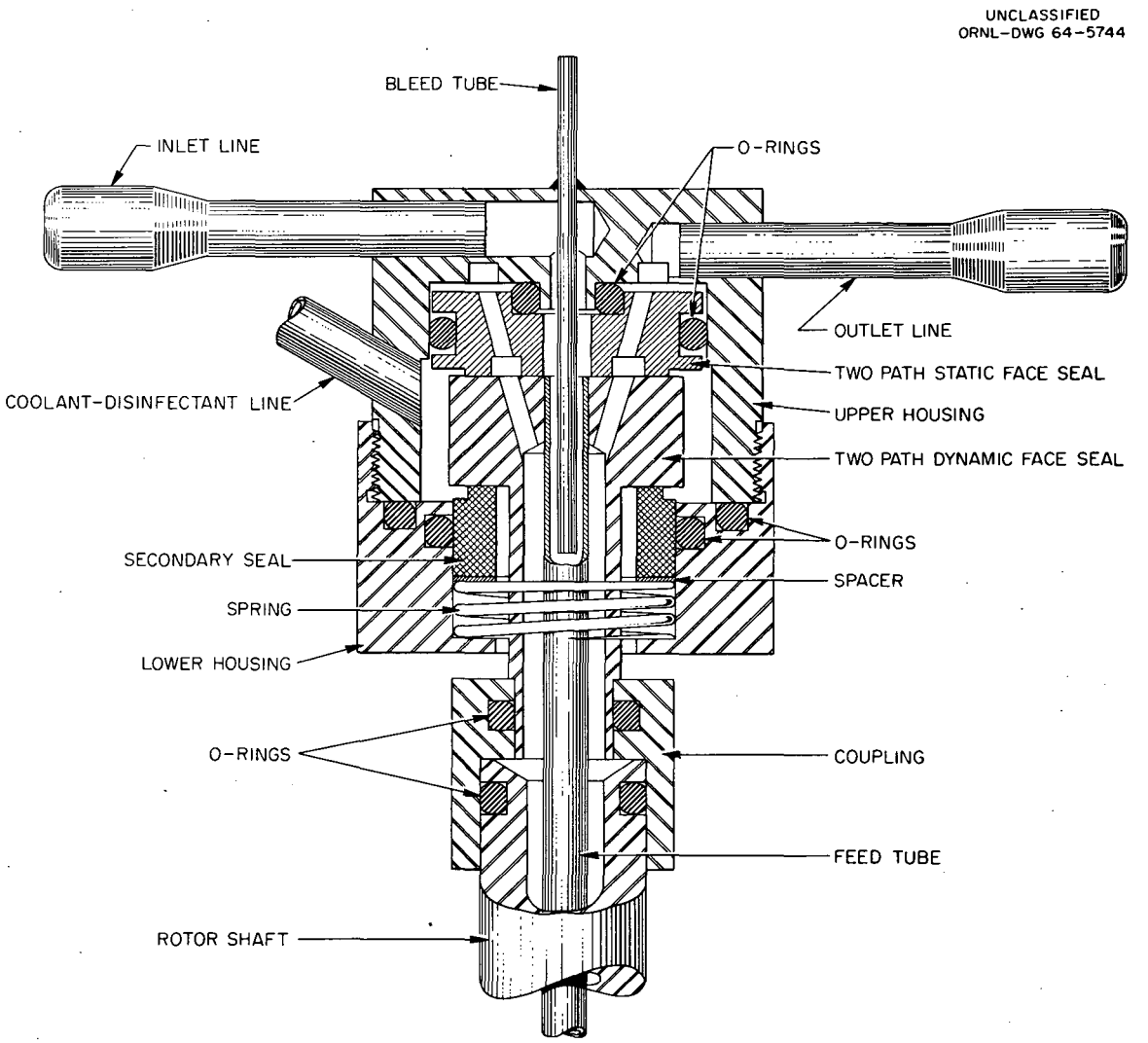

Fig. X-C-1. Seal for Use in Continuous-Flow Rotors. B-type seal has been modified by addition of bleed line to remove trapped gases from rotor.

XI. Gradient Materials

Zonal centrifugation requires a range of gradient materials differing in density, osmotic properties, and physiological effects. At the outset, conventional solutes such as sucrose and cesium chloride have been used. Even with these, the problem of obtaining sterile, particle-free preparations must be solved. In future studies, the preparation and properties of other gradient materials will be considered.

A. PREPARATION OF PURE, STERILE SUCROSE FOR ZONAL CENTRIFUGATION

C. B. Reimer[1]

In terms of mass, most tissue-culture-infected fluids have a very low virus content. In order to avoid the necessity for large preconcentrations of this material, it is advantageous to use all practical measures for extending the sensitivity limits for detecting viruses by physical-chemical means (light scatter, ultraviolet absorption).

Since the various particulate components segregate as zones in the sucrose gradient, it is imperative that background (noise) in these regions be kept as low as possible, so that low virus concentrations (signal) can be detected.

Figure XI-A-1 shows the relative transparency in the ultraviolet of a specially purified sucrose sample, as compared with representative sucrose samples generally considered to be pure. In all cases the optical path length was 100 mm, and the sucrose concentration was 60 g of sucrose per 100 g of solution. These results were obtained by forcing the 60% sucrose solution under 2 atm of air pressure through a 3/4-in.-diam by 5-ft-long carbon column (Pittsburgh decolorizing carbon BPL, 30 × 140, washed free of "fines"). The flow rate remained relatively constant at 4 ml/min (75 min dwell time). This purified material was sterilized by pressure Millipore filtration (0.45-μ filter, with 1.2-μ and glass fiber prefilters). This laboratory process, appropriate for 2 liters, has been successfully scaled up to 100 liters.

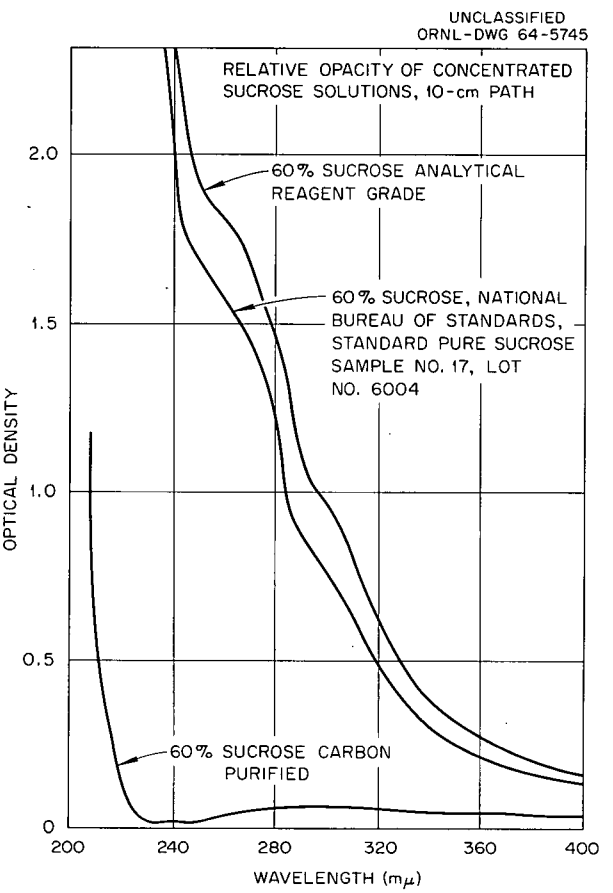

Fig. XI-A-1. Absorbance of Sucrose Solutions Before and After Filtration. As described in text.

[1]Lilly Research Laboratories, Indianapolis 6, Ind.

B. PREPARATION AND RECOVERY OF CESIUM COMPOUNDS

J. A. Carter R. R. Wright
W. S. Pappas C. W. Weber

1. Experimental Extraction System

An experimental production-scale cesium recovery system has been designed and tested using the BAMBP process.[2] The system, shown in Fix. XI-B-1, consists of five Plexiglas contactor stages. As illustrated in Fig. XI-B-2, the organic phase is dispersed into the aqueous phase in each stage by hollow glass centrifugal stirrers. Compartmentalizing each contactor results in a differential organic level between stages, effecting external circulation of the organic phase without the use of external pumps. The organic-aqueous interface serves as a seal to prevent backmixing, thus assuring high stage contact efficiency.

In a demonstration run of cesium chloride plus added impurities, the cesium chloride product was very pure. Concentrations of impurities were comparable to those reported for the laboratory system.[2] The newly designed pumping system performed satisfactorily.

Production rates were limited initially by a persistent emulsion in the scrub stages. Addition of cesium chloride to these stages, as an emulsion breaker, reduced the problem. Contributing to, and possibly responsible for, the emulsion problem is the long-term erosion of the Plexiglas system by the organic materials. A more resistant material may solve the problem.

[2] *Joint NIH-AEC Zonal Centrifuge Development Program Semiann. Rept. January 1–June 30, 1963,* ORNL-3502.

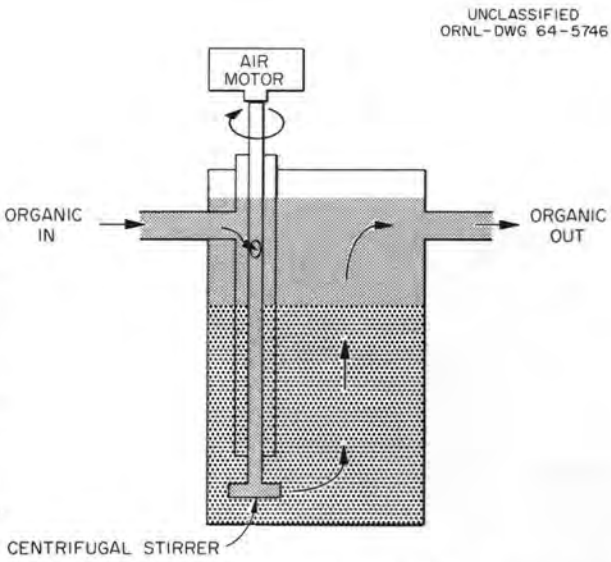

Fig. XI-B-2. Schematic of Flow Within Contactor of Cesium Recovery System.

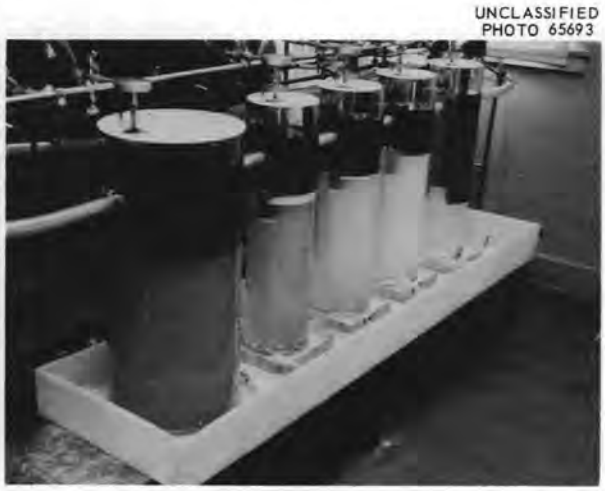

Fig. XI-B-1. Cesium Recovery System. Containers are Plexiglas. See text.

2. Preparation of Organic Compounds of Cesium

Pound quantities of cesium tartrate and cesium citrate have been produced using the experimental extraction system described above. High-purity organic salts were easily prepared by using the appropriate organic acid to strip the cesium from the BAMBP extractant.

XII. Containment and Sterilization

In the development of methods for physically isolating new viruses and for the large-scale isolation of known viruses, the problems of virus release, cross contamination of preparations, and maintenance of sterility must be seriously considered. Initially, the high-concentration phases of experimental work, including zonal centrifugation, have been isolated in glove boxes under negative pressure. Since some of the procedures involve experimentation with new devices under development, complete containment is not feasible at the outset. However, in future research it is important to aim at complete containment of all procedures involving live virus. This means that all steps from the opening of containers to the preparation of electron microscope grids and ampul sealing must be adapted to enclosure conditions. Fortunately, the extensive experience with remotely operated enclosure systems in the Oak Ridge area is available for application here.

The stainless steel biological safety cabinet described in the previous report[1] and used for the initial experiments in contained separation experiments has been replaced by an improved model. The new cabinet is constructed of transparent polyvinyl chloride supported on a framework of aluminum rods. One end panel of stainless steel plate supports a stainless steel exchange compartment. The advantages of the plastic construction are improved visibility, ease of fabrication, and lower cost.

Figures XII-1 and XII-2 are photographic views of two cabinets. The cabinet shown in Fig. XII-1 is in the Biophysical Separations Laboratory in Oak Ridge; that in Fig. XII-2 is at the John L. Smith Memorial Laboratory for Cancer Research, Chas. Pfizer and Co., Maywood, New Jersey.

The cabinet at Oak Ridge is equipped with a forced-air system and pressure controls (Fig. XII-3) to maintain a negative pressure on the inside of the cabinet. The inert air is filtered to minimize cross contamination and dehumidified to prevent condensation on optical surfaces of analytical instruments. The exhaust air is sterilized by an electrically heated incineration system. Two ultraviolet lamps are provided for additional sterilization. The cabinet has been in use for six months with little evidence of deterioration. The two exhaust outlets, one near the top and one near the bottom, may be opened or closed separately. After sterilization of the box by ethylene oxide, the outlets are opened and the residual ethylene oxide is removed by sterile air flow.

A plastic (polyvinyl chloride) dry box similar to that described above was constructed to contain the NCI (Pfizer) centrifuge. This cabinet has a welded aluminum frame with an aluminum bulkhead on each end. The exchange compartment is of plastic construction for better visibility and has two gloves. A second door was provided, at the opposite end, for loading equipment into the box and for cleaning. The spectrophotometer swings from the top frame of the box. With this arrangement a new plastic covering can be more easily installed and less floor space is required. The cabinet will be evacuated by a steam ejector-sterilizer.

Both cabinets are equipped with an electrical service outlet to supply power to any instruments wholly contained in the cabinet (Fig. XII-4).

When operating techniques (see Chap. XIII) become standardized, it is proposed that a single cabinet housing all phases, from sample preparation to virus recovery, be built.

[1] *Joint NIH-AEC Zonal Centrifuge Development Program Semiann. Rept. July 1–Dec. 31, 1962,* ORNL-3415.

Fig. XII-1. Centrifuge and Containment System in Use at Biophysical Separations Laboratory, Oak Ridge, Tennessee. Personnel are dressed for sterile run. Rotor is being passed through exchange port. Sterile collection tubes and gradient pump are on cart.

Fig. XII-2. Centrifuge and Containment System with Control Panels. Units installed at the John L. Smith Memorial for Cancer Research, Charles Pfizer and Co., Maywood, New Jersey.

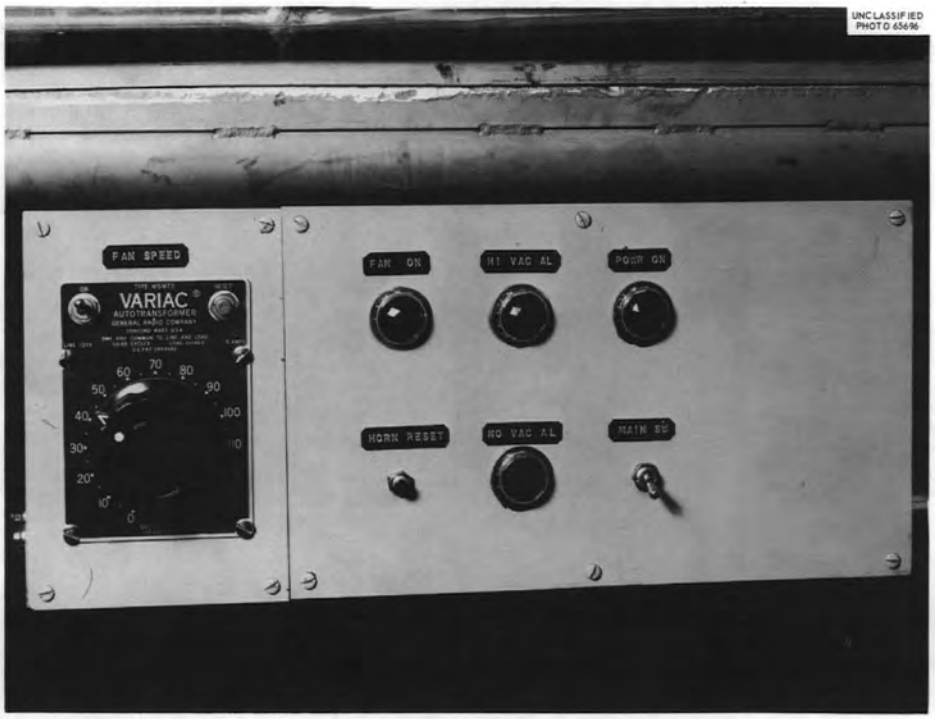

Fig. XII-3. Control Panel on Front of Glove Box in Biophysical Separations Laboratory for Controlling Vacuum Within Box. Pressure is controlled by Variac; horn sounds if pressure changes from predetermined limits.

Fig. XII-4. Panel on Front of Glove Box in Biophysical Separations Laboratory. Ultraviolet light, left; switches for water pump and other outlets within box. Refrigeration switch is for cooling water of seal and damper bearing.

XIII. Operating Procedures

N. G. Anderson C. L. Burger
C. T. Rankin, Jr.

The procedures outlined in this chapter are those currently in use in the Biophysical Separations Laboratory for the S-ρ two-dimensional plot method for searching tissues for virus particles. The technical problems involved are best illustrated by a detailed outline as is given here.

A. SAMPLE COLLECTION AND HOMOGENIZATION

Sterile, particle-free systems are essential when searching for virus or virus-like particles. Any breakdown in the chain of events beginning with sample collection and ending with grid preparation could make the entire operation meaningless. The operation procedures outlined have been designed to minimize contamination by interfering particles.

Tissue samples are obtained under sterile conditions during surgery or autopsy. The problem is to freeze the samples in such a manner as to preserve viral integrity and to develop suitable packages for shipping, weighing, and homogenization. Liquid nitrogen is the storage medium of choice, but seepage of liquified gas into the container will produce a potentially explosive condition. A provisional solution to this problem has been found by using stainless steel homogenizer cups[1] fitted with blowout inserts in the top containing a Millipore filter supported on a porous Teflon disk. If the pressure in the container exceeds 70 psi, the filter will rupture. Since the weight of the container is engraved on the lid, the weight of the tissue sample contained in it may be readily determined. The tissue container may be sterilized by ultraviolet light, opened in a glove box, and the homogenizer top screwed in place to form a closed system. In most instances 9 ml of buffer is added for each gram of tissue before homogenization. A liquid-nitrogen shipping container[2] has been adapted to hold the sample container.

The homogenized sample, if small (4 to 5 g), is inserted directly into the rotor following homogenization. A syringe inserted into the adapter of an intravenous injection set,[3] with one end connected to the rotor center and one end connected to the overlay solution, is used for this purpose (Fig. XIII-F-2).

When the sample is larger than 4 to 5 g, it is precentrifuged at low speed (1500 rpm, 596 × g at R_{max}) in an International PR-2 centrifuge (head No. 259) for 30 to 60 min to remove the heavier components. The supernatant is then sedimented for 1 hr at 30,000 rpm in the Spinco 30 rotor, and the pellets are resuspended and used as the starting sample in the zonal ultracentrifuge. In this way tissue samples weighing up to 150 g can be used without overloading the gradient or monitoring system.

Homogenization of samples has been performed in 8.5% sucrose, in Miller-Golder[4] buffer, a balanced salt solution, or in 0.15 M sodium citrate, pH 6.7. The choice of homogenizing medium is dictated in part by density since the homogenized sample must float on top of the gradient. The overlay solution must in turn be less dense than the sample layer.

[1]Servall No. OM 1047.

[2]Linde container No. BT-2.

[3]Cutter code No. 860-08; Abbott No. 4540.

[4]G. L. Miller and R. H. Golder, *Arch. Biochem.* **29**, 421 (1950).

B. CLEANING AND STERILIZING

All parts of the system in contact with samples or which may become contaminated must be sterilized. At present, reusable components (rotors, e.g.) are treated with formaldehyde where appropriate, washed, and rinsed with distilled water and then either steam or gas sterilized, depending upon the material. The rotor and its components (including seal, damper bearing, gradient engine and associated tubing, Spinco 30 rotor tubes and transfer crooks used in banding, and the glass 40-ml screw-top centrifuge tubes used for gradient recovery) are gas sterilized in a regular steam sterilizer (American Sterilizer Co.) fitted with an ethylene oxide system. Gas sterilization requires approximately 8 hr and is usually done overnight. The components to be sterilized are placed in paper bags which are opened in the glove box or, in the case of the gradient engine, when the tubes leading to the sterile solutions and to the rotor are ready to be attached.

The glove box in which the rate zonal centrifuge is housed is sterilized by overnight exposure to ethylene oxide (two 20-oz cans). The outlet valves from the box are closed during this process; filtered air is pumped through the box, beginning early the next morning, to remove residual gas.

All solutions used are sterilized either by filtration or, when feasible, by steam.

C. ASSEMBLY OF ROTOR SYSTEM

The components of the B-IV rotor are shown in Fig. XIII-C-1. The two end caps of the rotor are sealed with O-rings. The four-vaned core is placed in the rotor after the bottom end cap has been screwed on. The O-ring for the upper end cap is placed in position in the groove in the body of the rotor, and the manifold plug is screwed into position on the under side of the upper end cap (after the guide for the stem of the seal has been inserted). The top end cap is then screwed down, and the end caps are tightened until small bench marks are aligned. The stem guide is essential to avoid displacing or tearing the O-ring, found within the manifold plug, when inserting the seal.

Fig. XIII-C-1. Disassembled B-IV Rotor with Bearing and Seal. (*a*) End cap; (*b*) seal; (*c*) bearing and damper (*d*) bottom end cap; (*e*) rotor chamber; and (*f*) core.

After sterilization, the assembled rotor is placed in the centrifuge (Fig. XIII-C-2), and the upper chamber closure is screwed into position (Fig. XIII-C-3). The damper and bearing are positioned next (Figs. XIII-C-3 and XIII-C-4). The oil lines for the bearing and the cooling water lines for bearing and seal are visible in these figures.

The disassembled seal is shown in Fig. XIII-C-5. Its design is explained in Chap. X. The instructions for use of the seal are as follows:

1. Handle with care at all times.
2. The entire seal assembly (see Dwg. No. LDSP-SK-1881 in Appendix III) plugs into the upper rotor bearing after assembly with rotor. Gently push seal assembly down to running position. DO NOT FORCE. Connect coolant lines and feed lines.
3. Never operate rotor without cooling water on seal and upper bearing.
4. Run rotor at low speed, ~5000 rpm, and check seal for leaks as follows:
   a. Look for excess water in oil drain line. A few drops when rotor is first started are normal.
   b. Check for water in the feed lines, usually rotor center line.
   c. While loading gradient into empty rotor, watch for droplets of liquid in the rotor center line. This indicates leakage across inner sealing dam if the droplets are gradient, or leakage across outer sealing dam if the droplets are coolant.
   d. Check for signs of a bad seal early; this can prevent scrubbing a run in the advanced stages or completely losing a valuable sample.
5. After use, clean the seal thoroughly as follows:
   a. Flow hot tap water through lines with seal removed from rotor but not disassembled.
   b. Take seal housing apart (LEFT-HAND THREAD) and inspect rubbing surfaces. Finish disassembly, by removing part No. 13 from part No. 5; clean spring and lower seal. Dry all parts by blowing with dry air. NOTE: CsCl will corrode the stainless steel runner (part No. 5) if CsCl is used in run. Part No. 5 should be soaked in

Fig. XIII-C-2. Positioning of B-IV Rotor in Centrifuge Chamber Located in Glove Box. Water pump in background (right).

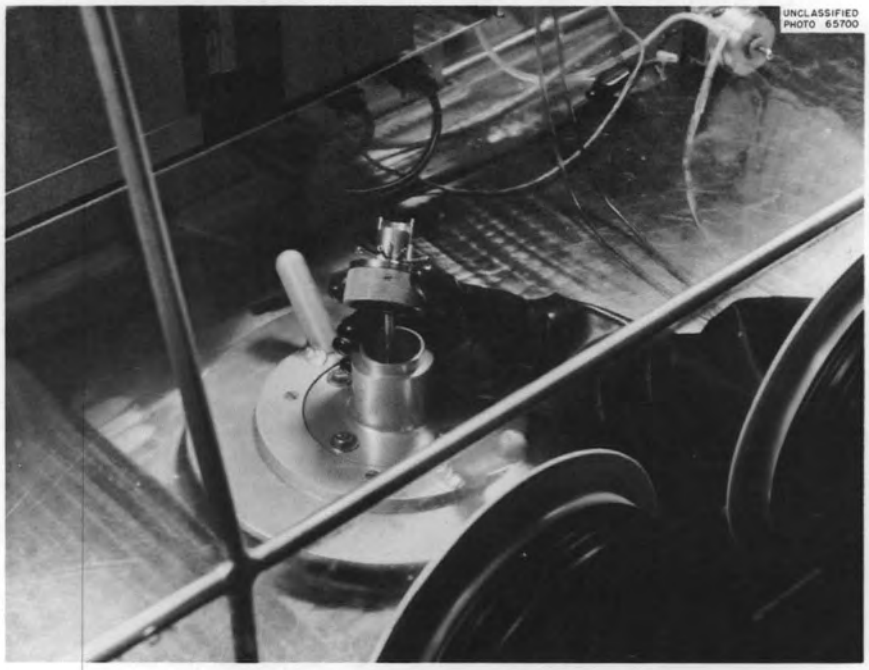

Fig. XIII-C-3. Positioning of Damper Bearing on Rotor.

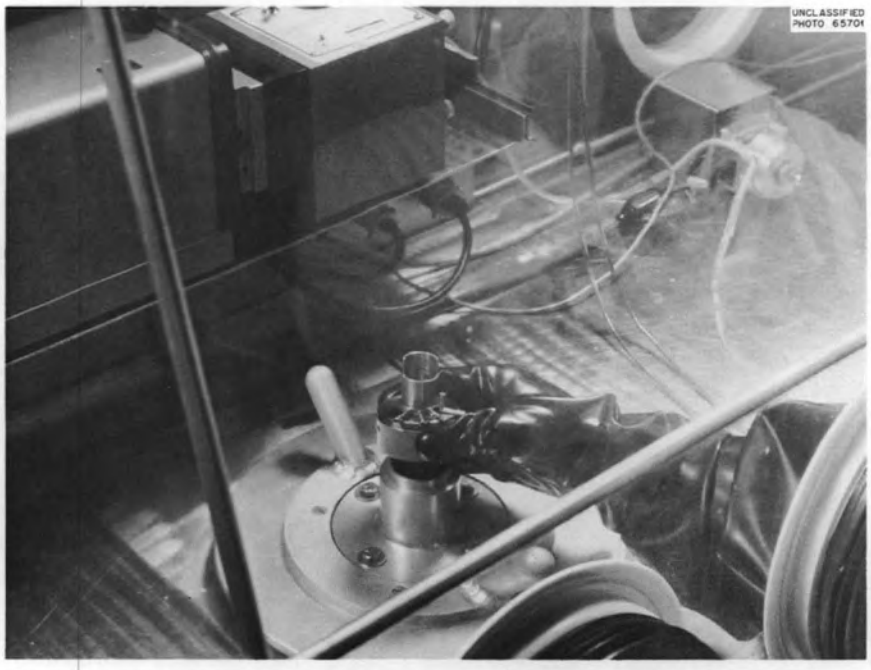

Fig. XIII-C-4. Damper-Bearing Assembly.

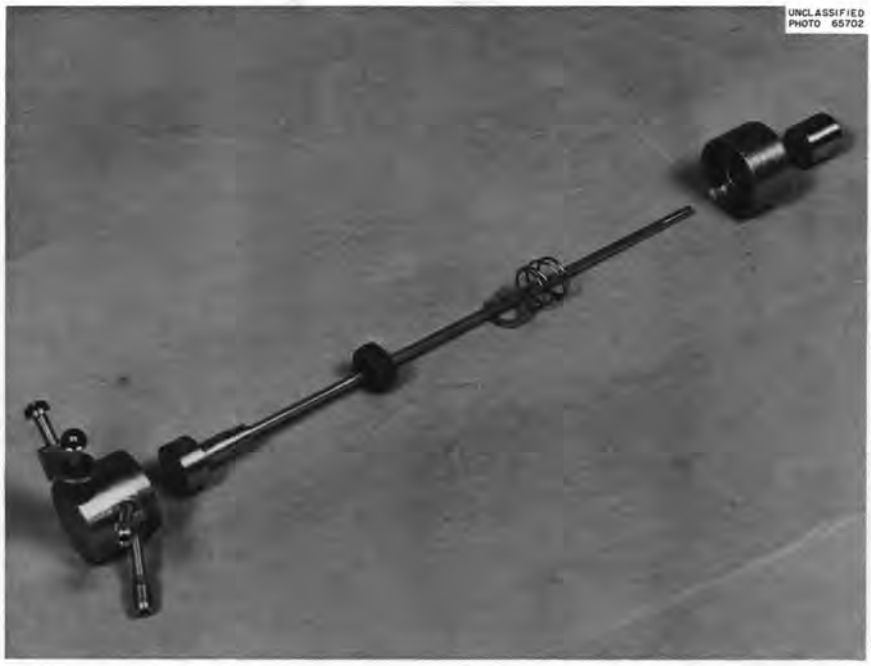

Fig. XIII-C-5. Disassembled Seal. Rotating portion seen on top of shaft. Edge holes there lead to rotor center, center opening to rotor edge. O-ring in coupling (far right) prevents leakage from edge holes of seal to outside.

ethyl alcohol. (See Appendix III for numbered drawing.)

6. Before reassembly for next run, inspect seal rubbing surfaces for scratches or indentations that may cause leaks; then assemble seal with care. NEVER USE SHARP INSTRUMENTS OR FORCE PARTS TOGETHER. Visually check center tube, part No. 14, for straightness before reassembly with rotor.

The assembled seal is positioned by gently inserting the stem through the rotor upper shaft extension and, with gentle pressure, moving it through the O-ring located inside the manifold plug. The upper portion of the seal is supported partially by the metal ring around the damper and bearing (Fig. XIII-C-6). In practice, an O-ring is often used to hold the seal in a given position.

The cooling lines and the oil lines are next connected to the proper outlets provided on the seal and bearing assemblies. The completed assembly at this point is shown in the centrifuge and glove box in Fig. XIII-C-7, and outside the centrifuge in Fig. XIII-C-8. A schematic diagram of the rotor connections is shown in Fig. XIII-F-3.

Cooling water flows, respectively, from the pump[5] (Fig. XIII-C-7) through the upper rotor bearing, seal, graduated reservoir (not visible in photographs), refrigerated heat exchanger, and back to the pump. The cooling water circulates entirely inside the glove box enclosure, while the refrigerant circulates outside. The graduated reservoir indicates the amount of water in the system and provides visual indication of flow rate.

Oil lines from the reservoir within the glove box (see Fig. XIII-C-2) connect to two outlets on the bearing. The oil not only lubricates the bearing but aids in sealing the vacuum chamber. The overflow oil line from the bearing drains inside the glove box into a small plastic bottle.

The rotor, damper bearing, seal, and oil and water lines are shown assembled in Fig. XIII-C-8. The short line seen here is for overflow oil.

[5]Sigma pump model AL 4-300.

Fig. XIII-C-6. Positioning of Seal Through Damper Bearing and into Rotor Extension of End Cap.

Fig. XIII-C-7. Rotor Assembly with Cooling, Oil, Edge, and Center Lines Attached.

Fig. XIII-C-8. Rotor Assembled Outside Centrifuge, Showing Seal, Damper Bearing, and All Lines Attached.

D. GRADIENT PUMP ASSEMBLY

The gradient pump[6] is shown in Fig. XIII-D-1. In use, the pump is sterilized with the pistons partially disassembled to permit ethylene oxide exposure. The program cam used is one producing a 1200-ml gradient linear with rotor volume. Figure XIII-D-1 shows a typical tissue gradient scheme in which the gradient of 1200 ml would range from 10 to 30% sucrose with a 400-ml "cushion" of 55% sucrose. The pump is located outside the glove box. A single Tygon tube carrying the gradient to the rotor leads from the pump and into the glove box through a metal seal located at the rear of the glove box. Gradient solutions are in sterile bottles and are connected to the pump by disposable transfusion tubing connectors.

[6]Available from Beckman Instruments, Spinco Division, Palo Alto, Calif.

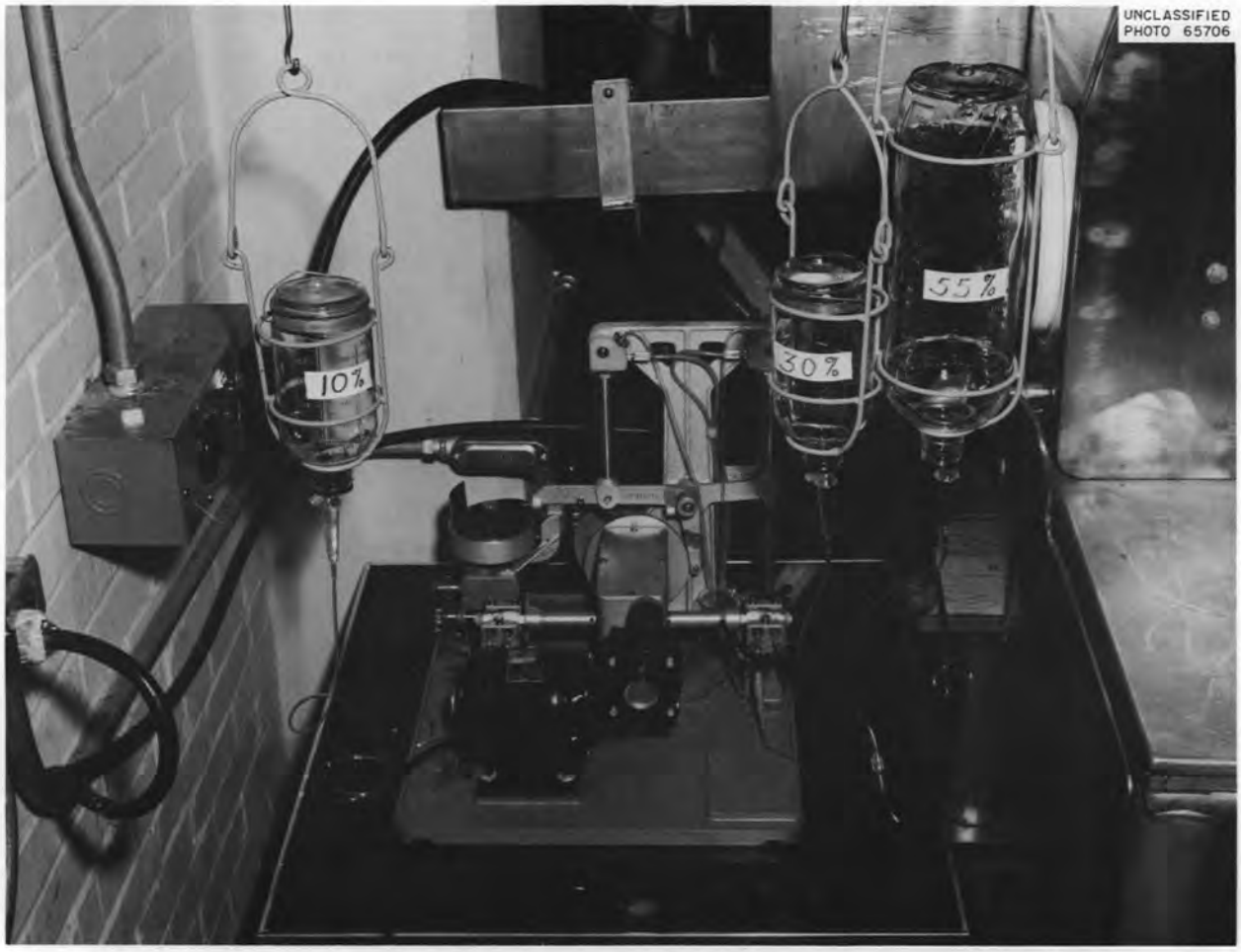

Fig. XIII-D-1. Gradient Pump Assembly, at Rear of Glove Box, with Typical Tissue Gradient Scheme. Program cam, left rear; glove box, right. Lines used for connection of gradient solution to pump are intravenous injection sets (for 10%, cutter No. 860-01 or Abbott No. 4622; for 30–55%, cutter No. 871-00 or Abbott No. 4656).

E. CALIBRATION OF $\int \omega^2 \, dt$ INTEGRATOR

As soon as a sample is placed in a spinning rotor, the particles are subjected to a centrifugal field. Particles sediment not only during the time "at speed" but also during the time required for loading, acceleration, deceleration to unloading speed, and even during the process of unloading the gradient. It is necessary, therefore, to have a measure of the total sedimenting force applied to a given particle during its time in the centrifuge. A system which integrates this parameter with time is used for the rotors developed under this program. The Lectrocount II (Fig. XIII-E-1) has a direct readout for $\int \omega^2 \, dt$ at any given time. The values read are multiples of 10^6.

A proximity probe senses the rpm of the rotor, and a test panel is adjusted to match this frequency. The true reading is displayed on the speed indicator as rpm, and the integrator uses this value in its calculations.

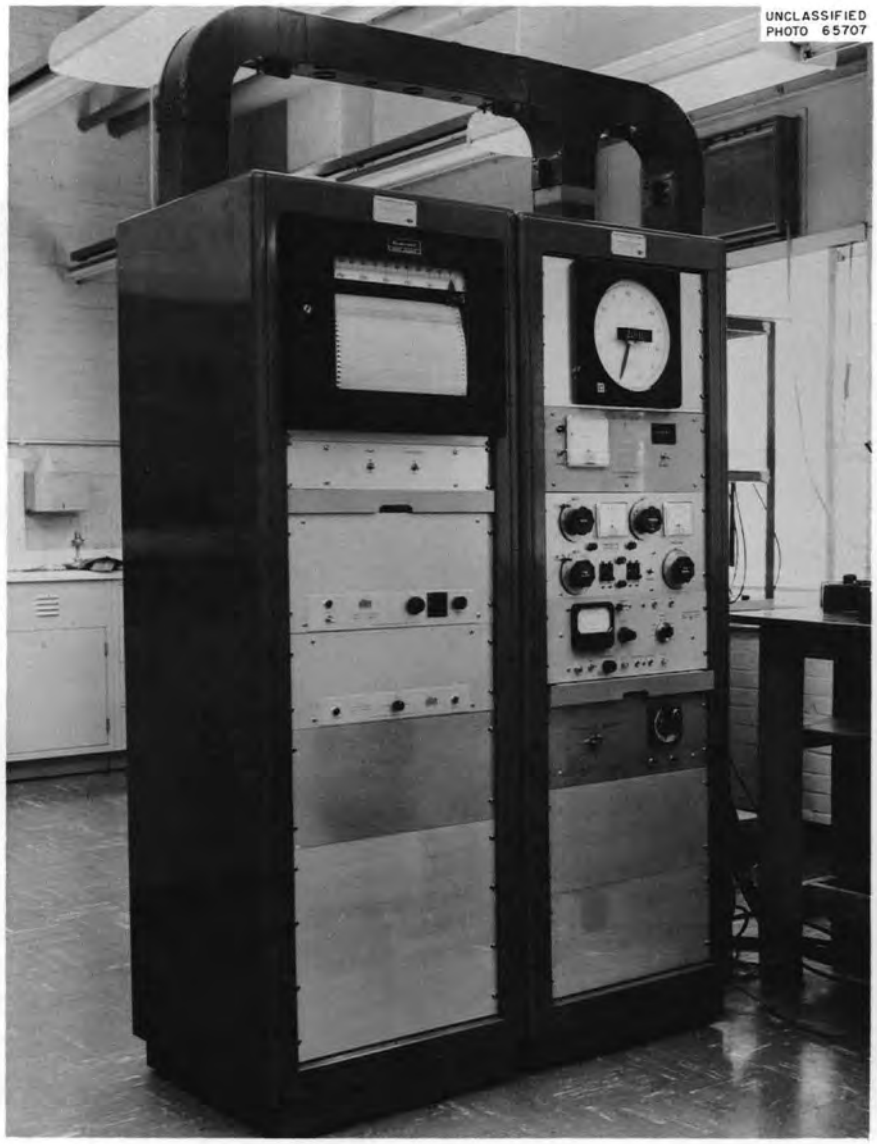

Fig. XIII-E-1. Instrumentation for B- or C-Series Rotors. Left rack contains (top to bottom): (1) recorder, (2) switches for gradient pump and an accessory, (3) optical density converter including range switch, and (4) hydrogen and tungsten lamp controls. Right rack has (top to bottom): (1) Speedomax rpm indicator, (2) Lectrocount integrator panel with counter, (3) centrifuge controls (temperature, pressure, above; speed controls and on-off controls, below), (4) frequency meter, and (5) frequency test panel. (4) and (5) are to calibrate the rpm device.

F. INTRODUCTION OF GRADIENT AND SAMPLE

After the rotor and associated tubing are positioned, the gradient engine is attached to the gradient solution bottles. The line from the gradient pump to the rotor seal edge line connection is provided with a glass T which serves as a bubble trap and drain line when the sample is being introduced into the rotor.

At this time the rotor chamber is evacuated, the refrigeration system (Fig. XIII-F-1) is turned on,

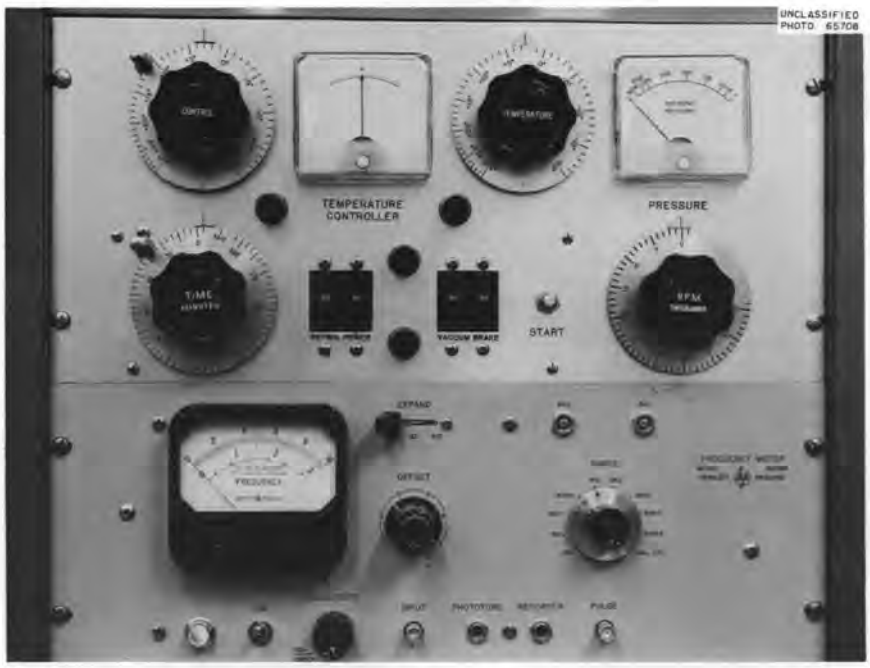

Fig. XIII-F-1. Portion of Control Panels for B-Series Rotors, Showing Centrifuge Panel (Above) and Frequency Meter for Speed Calibration (Below).

and the rotor is accelerated to 3000–5000 rpm. The centrifugal field will stabilize the gradient against the rotor wall. The gradient, light end first, enters the rotor (Figs. XIII-F-2 and XIII-F-3), is distributed uniformly over the rotor wall, and is forced by denser fluid pumped in subsequently toward the center of the rotor. The gradient, normally of 1200 ml, does not fill the rotor completely. A "cushion" of fluid denser than that used to form the gradient is pumped in until the first part of the gradient emerges through the center line. At this point, the gradient pump is stopped, and the gradient line is clamped off. The sample is now ready to be introduced. This is done through the center line (Figs. XIII-F-2 and XIII-F-4), so that the sample will be placed on top (centripetal end) of the gradient. The sample line is part of the intravenous set seen in Fig. XIII-F-2.

A small pump[7] on the sample line between the Y and the rotor ensures constant flow during sample and overlay introduction. The drip-chamber probe is inserted into the overlay bottle and the line is clamped. The needle of the sample syringe is inserted into the medicinal entry, and this line is clamped also. The clamp on the bubble-trap line is removed and placed on the gradient line between the T and the gradient pump, obviating any emergence of solution from the rotor to the exterior of the glove box. The clamp from the sample syringe line is removed, and the sample is introduced into the rotor with the syringe, displacing "cushion" from the edge of the rotor through the bubble-trap line to a waste container inside the glove box. To rinse the sample syringe, the clamps are arranged to allow a small amount of overlay solution to be drawn into the sample syringe, are then rearranged as above, and the rinse is added to the rotor. This rinse should clear the fluid lines of visible sample, at which time the integrator counter is switched on. The sample syringe line is now clamped, the overlay line opened, and the small New Brunswick pump turned on and adjusted to pump from the bottle to the rotor.

Approximately 200 ml of overlay is pumped to the rotor, displacing "cushion" from the edge, to move the sample zone out from the core. An additional 40 ml of overlay is introduced, after

[7]New Brunswick PA-56 pump.

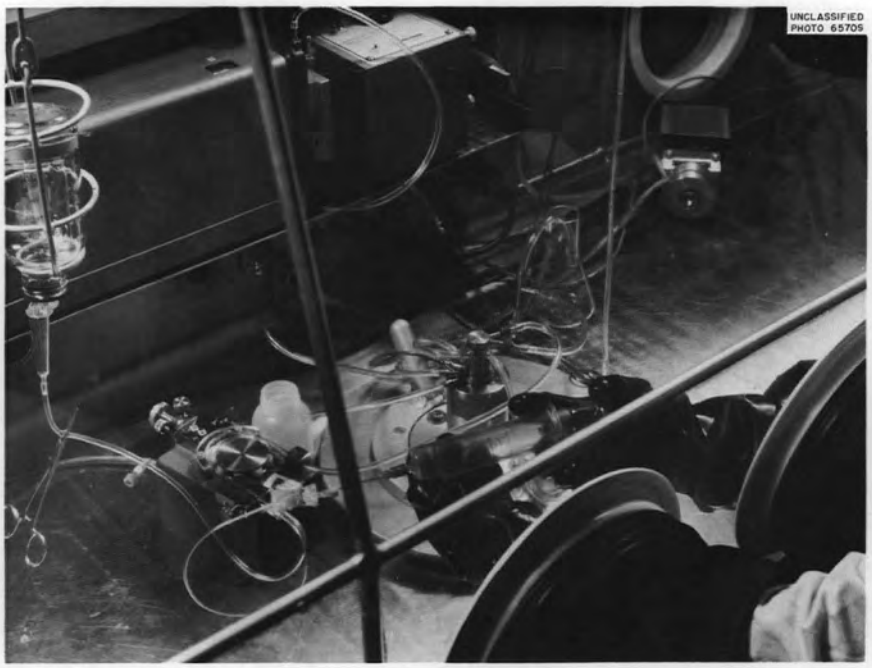

Fig. XIII-F-2. Introduction of Sample Through Center Line of Rotor. Edge line opened to waste container, right rear; overlay solution, left; and DU spectrophotometer with absorbance indicator, rear center.

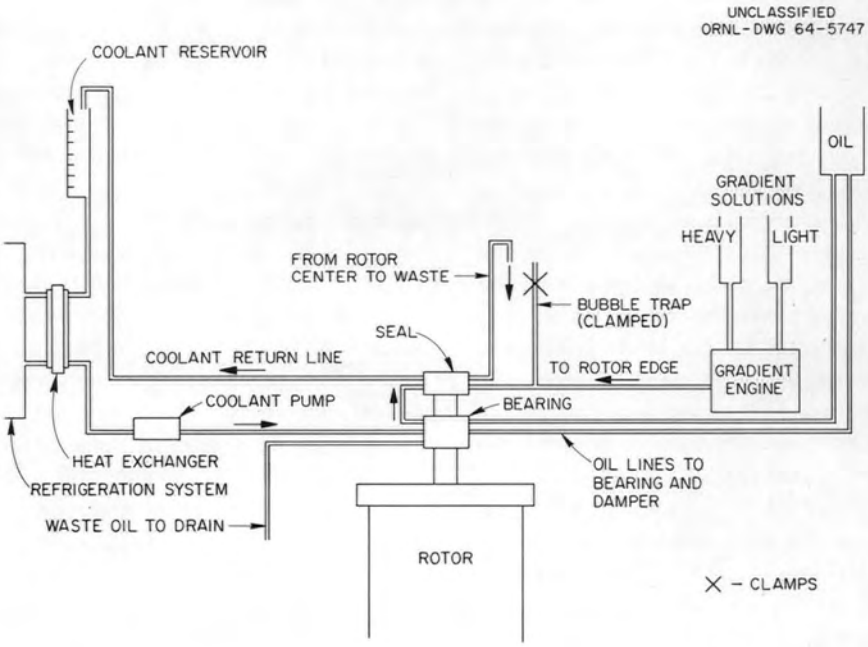

Fig. XIII-F-3. Schematic Diagram of Fluid Lines When Gradient Is Loaded into Rotor.

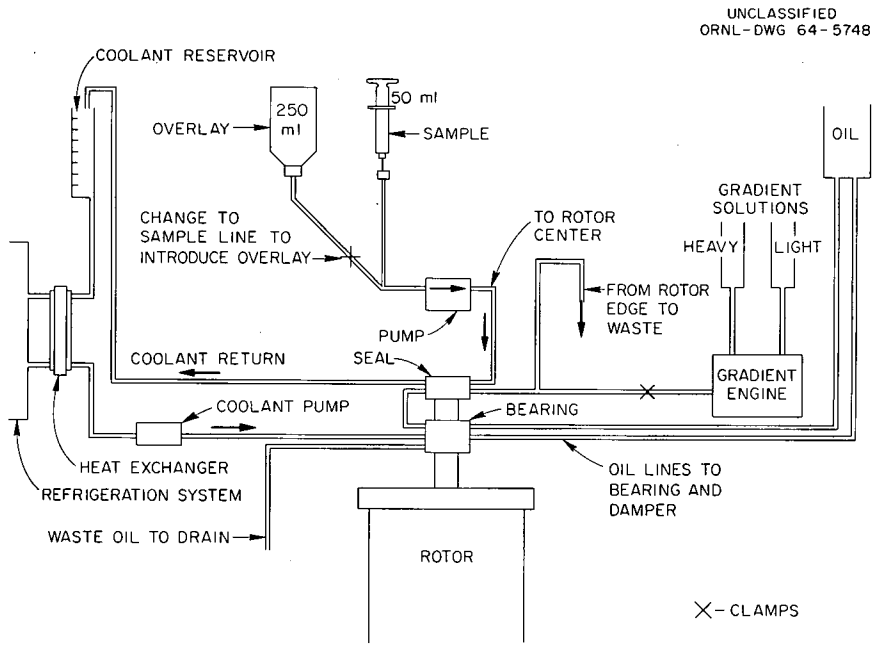

Fig. XIII-F-4. Schematic Diagram of Fluid Lines During Sample Introduction into B-IV Rotor.

which the clamp from the gradient engine is removed and the pump is started. The flow from the edge line of the rotor and from the gradient engine will then both pass through the bubble-trap line to waste. When all overlay solution has entered the rotor, the line from the bottle is clamped, and the New Brunswick pump is turned off and removed from the line. The sample syringe line is opened, and the bubble-trap line is clamped. The flow is now from the gradient engine to the edge of the rotor, displacing overlay from the center to the syringe. By raising the sample line and tapping gently, all air bubbles are removed from the rotor.

When the 40 ml of overlay is recovered in the syringe, the gradient pump is stopped and the pump line is clamped near the rotor. The only line now open to the rotor is that leading from the center to the syringe, which is mounted vertically in a clamp. The rotor is now accelerated to the desired speed for the required time to achieve the separation desired. During the course of a run, the level can be observed in the syringe reservoir and any leakage can be detected. The volume in the syringe will decrease by 5 to 10 ml due to rotor expansion at higher speeds, but after decelerating to unloading speed, the volume should be nearly the same as at the beginning.

G. GRADIENT RECOVERY

The rotor is decelerated to a speed of 3000 rpm, and the separated cell particulates are recovered as a spectrum of particle sizes, smallest first. The line leading to the rotor center, which had been connected to the syringe used for sample introduction during the run, is removed and replaced by a line leading to the quartz flow cell (0.2-cm light path) and through it to the sample collecting tube (Figs. XIII-G-1 and XIII-G-2).

The Gilford absorbance indicator[8] and optical density converter[8] unit used on the Beckman spectrophotometer and instrument panel, respectively, permit readings of 0.25 optical density unit to 2.5 OD units full chart range of the Honeywell recorder. Considering the 0.2-cm flow cell, the actual range becomes 1.25 to 12.5 absorbance units. (The operation of the absorbance units is as described in the Gilford manual.) The gradient is normally scanned at 260 mμ.

The gradient pump is now set to pump only the densest material used (55% sucrose in most virus-isolation studies). The only lines now open are those leading to the rotor edge from the gradient

[8]Gilford No. 220.

Fig. XIII-G-1. Positioning of Flow Cell in DU Spectrophotometer. Rotor contents are displaced through flow cell from bottom to top.

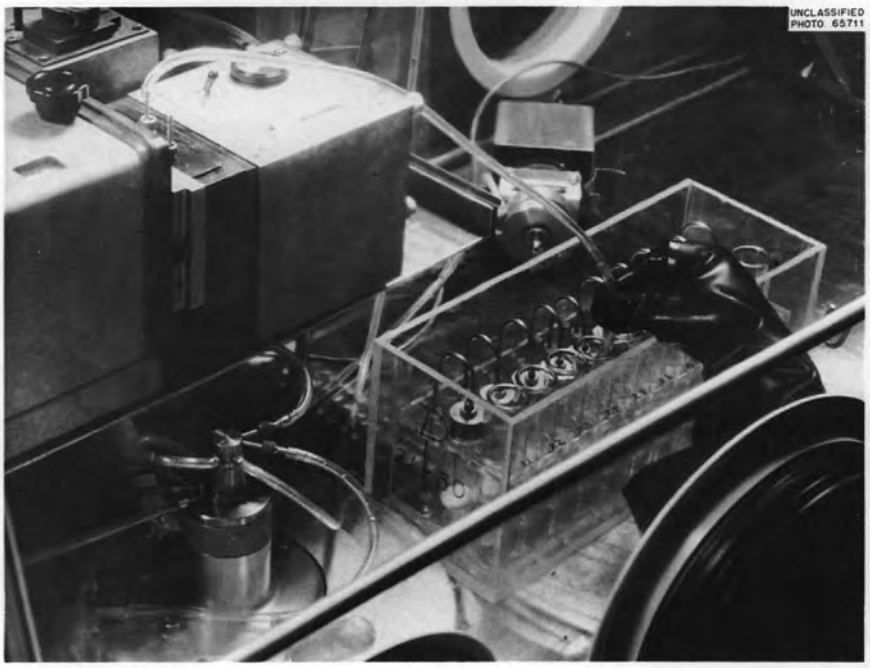

Fig. XIII-G-2. Fraction-Collection Scheme. Beckman DU is moved forward over spinning rotor. Fractions are collected in graduated 40-ml tubes. Rack holds No. 30 rotor tubes with transfer crooks screwed in place.

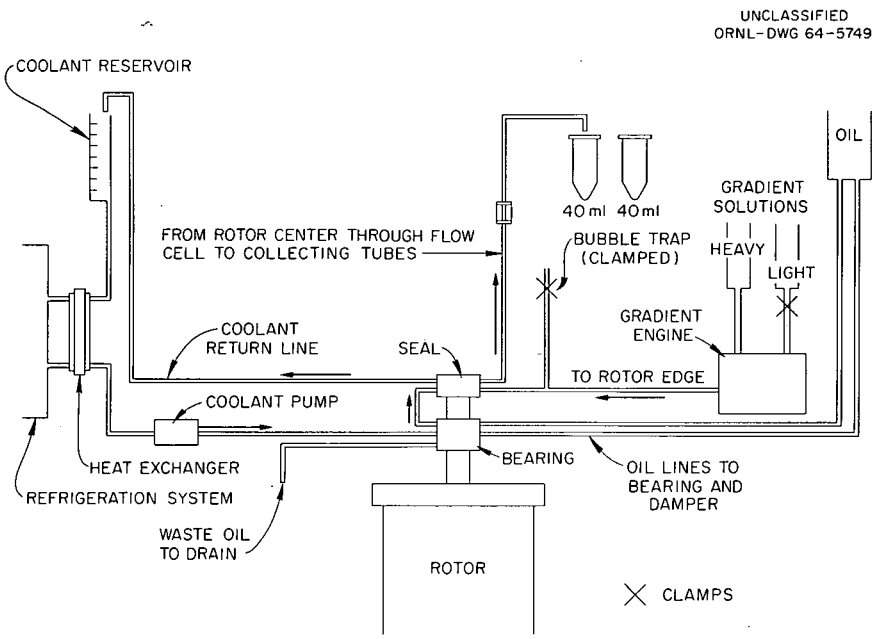

Fig. XIII-G-3. Arrangement of Fluid Lines During Sample Collection.

pump and that leading from the top of the flow cell and connected to the rotor center (Fig. XIII-G-3). As the contents of the rotor are displaced by the 55% sucrose, the fluid running through the DU (Fig. XIII-G-1) is collected in 40-ml centrifuge tubes (Fig. XIII-G-2). As each 40-ml tube is collected, a foot-operated switch is depressed to activate an event marking pen on the strip-chart recorder. This provides a visual record along the base of the chart which may be used to correlate the presence of a given absorbance peak with its location in the recovered fractions.

H. DENSITY AND REFRACTIVE INDEX DETERMINATIONS

Until recently, the density of the recovered fractions was determined by using a manually operated Abbé-type refractometer. It is extremely difficult to do this in an aseptic manner and to ensure that contamination of the operator does not occur. To provide a semiautomatic method for determining the density of the recovered fractions, a torsion balance has been modified (Fig. XIII-H-1), mounted in the glove box, and adjusted to read density directly. The 40-ml fractions are shaken with the screw tops in place, opened, and individually placed under the glass bob (Fig. XIII-H-1). The torsion balance has been modified to electronically read and display the results of the Archimedes measurement on tape (Fig. XIII-H-2) outside the glove box. The printout mechanism is activated by a foot pedal.

I. BANDING METHODS

The results of B-IV runs as described above are given in Chap. II. Such runs separate subcellular particles on the basis of sedimentation rate in relatively short time periods.

To complete the two-dimensional picture, here described as the S-ρ plot (Chap. I), a variety of banding techniques have been explored.

The system used during this report period is one in which the sucrose fractions recovered in the B-IV gradient are pumped into Spinco 30 rotor

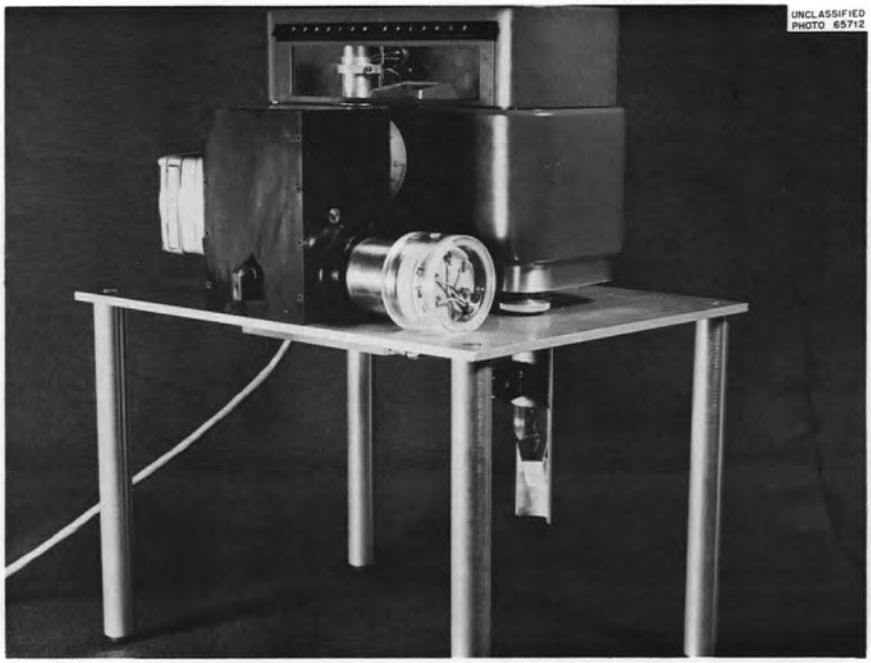

Fig. XIII-H-1. Torsion Balance Unit Located Inside Glove Box for Determining Density of Recovered Fractions. Each 40-ml collection tube is positioned below table with "bob" in fluid. Density is measured on the flotation principle.

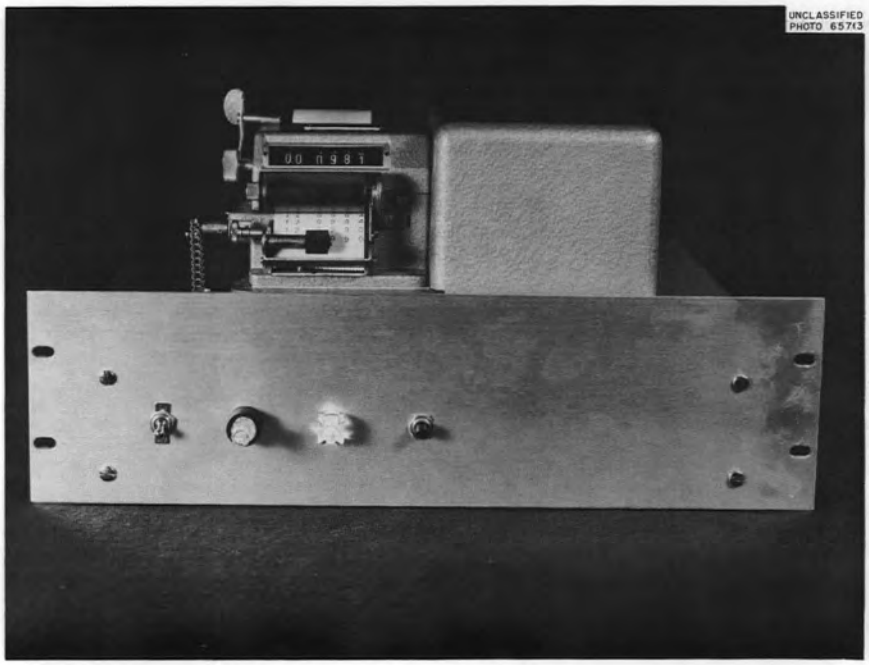

Fig. XIII-H-2. Printout Mechanism for Torsion Balance Densitometer. Unit is located in instrument panel outside glove box and is actuated by foot pedal.

tubes (Fig. XIII-I-1) over dry cesium chloride. Lucite boxes and racks designed to hold ten fraction-collection tubes, ten No. 30 rotor tubes, and ten cap screws were fabricated. Transfer crooks used to fill the No. 30 tubes are shown in Fig. XIII-I-1. The transfer tubes are long enough to reach to the bottom of the glass fraction-collection tubes and have a screw end sealed by an O-ring fitting the top opening of the rotor tubes. The actual transfer is performed as shown in Fig. XIII-I-2. A Lucite transfer chamber, designed to hold the racks described, is closed and evacuated with a vacuum pump. Air is now slowly readmitted to the chamber, and the air pressure on the surface of the liquid in the collection tubes forces the fractions through the transfer tubes and into the evacuated rotor tubes. In practice, the tubes are usually tipped to one side so that the sucrose fractions trickle down the side of the rotor tubes, producing little disturbance.

After the No. 30 centrifuge tubes are full, the rack is carefully removed from the transfer chamber, the transfer tubes are unscrewed, and the regular screws are inserted into the caps.

The tubes are then carefully placed in the No. 30 rotor and spun at 24,000 rpm for 12 to 14 hr. As the CsCl slowly dissolves, a steep gradient is formed. The true density of these gradients is difficult to assess by any method other than direct weighing because of the varying sucrose concentrations in the fractions. Sucrose can be removed by dialysis, but in practice this is not normally done before banding.

Obviously, a particle will have a different apparent density in solutions containing different amounts of sucrose and a constant amount of CsCl. Here, the problem is not that of measuring density per se but rather is that of achieving a separation based on density, whatever that density may be.

At the end of the time required for banding the fractions recovered in the B-IV in the Spinco 30 rotor, the tubes are carefully removed and placed in a rack for photography. The rack and special camera box designed for this purpose are shown in Fig. XIII-I-3. The rack holds 12 tubes, the rotor's capacity. The rack is carefully placed in the slots designed to hold it in the camera box (Fig. XIII-I-4). The light source is in the housing beneath the camera box. The internal arrangement of the tube holder within the box may be seen in Fig. XIII-I-5. Lucite rods were designed with concave surfaces such that when the rack with the

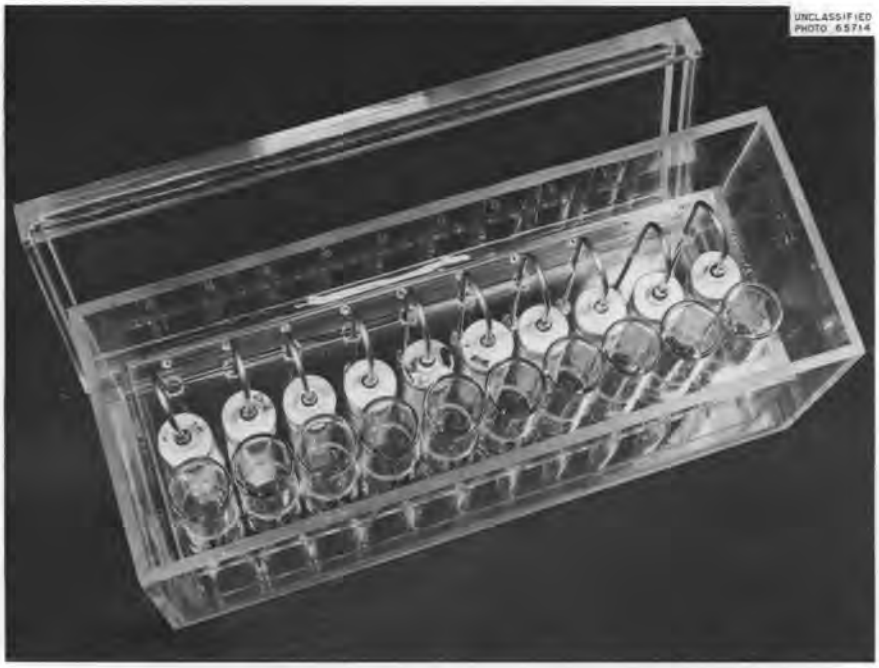

Fig. XIII-I-1. Lucite Rack with Graduated Sample-Collection Tubes (Front), No. 30 Rotor Tubes Fitted with Transfer Crooks, and Screws for Rotor Tube Caps (Rear). Entire assembly is gas sterilized before use.

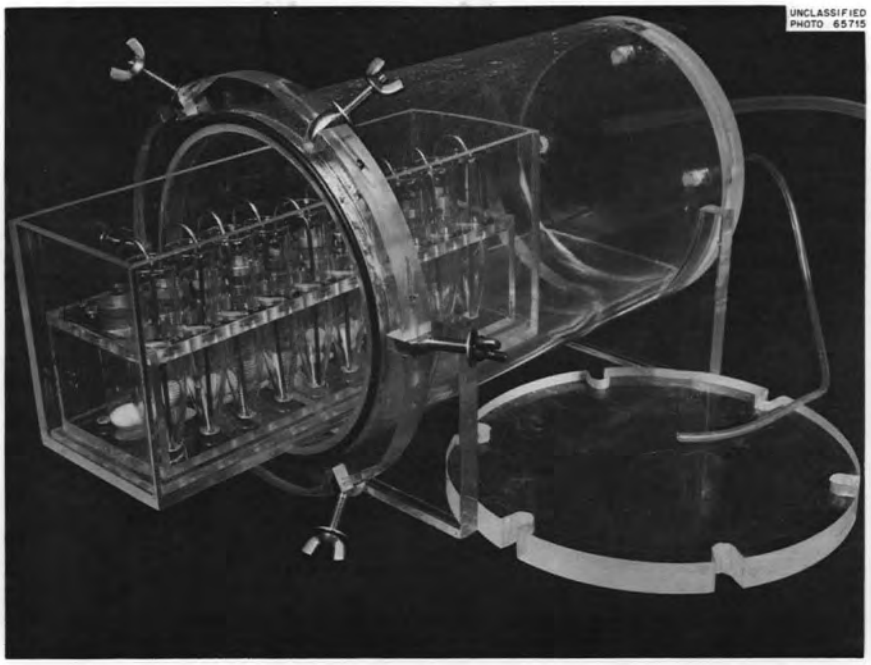

Fig. XIII-I-2. Vacuum Chamber Used in Filling No. 30 Tubes with Recovered Sucrose Gradient Fractions from B-IV. Dry CsCl seen in centrifuge tubes. See text for operation.

Fig. XIII-I-3. Positioning of Rack, with 12 No. 30 Rotor Tubes, in Camera Box. Sucrose fractions from B-IV are banded in CsCl, then photographed.

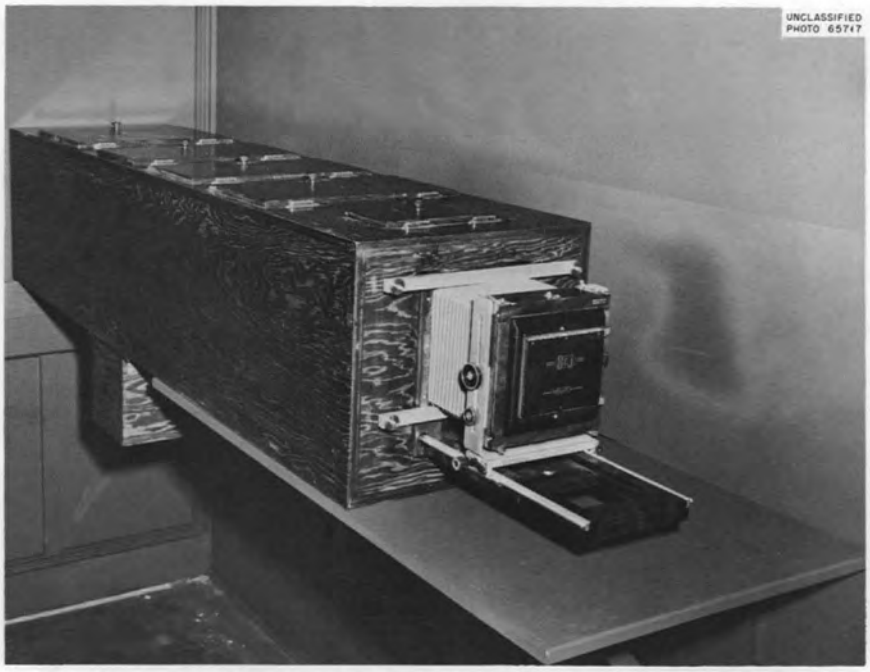

Fig. XIII-I-4. Overall View of Camera Box. Light housing seen projecting below. Top openings allow location of object with respect to camera (front).

Fig. XIII-I-5. Lucite Light Pipes and Rack with Tubes Removed from Camera Box. Lucite rods are painted black except at their ends. Top surface of each is concave to receive centrifuge tube. Rack has black dividers between tubes to prevent light scattering from tube to tube.

tubes is positioned, the tubes rest on those curved surfaces. The Lucite rods are painted black, except for their ends, as is the interior of the box and the tube rack. The light used is a 60-w Lumiline incandescent bulb, which is perpendicular to the Lucite rods.

Gradient recovery is performed in a variety of ways. In general, the sample is pumped through a DB Beckman spectrophotometer and through a Milan refractometer. Recovered fractions, collected in 12-ml glass centrifuge tubes, are then handled as described below. A stainless steel tube which extends to the bottom of the centrifuge tube connects to a 0.2-cm light path flow cell in the DB spectrophotometer by polyethylene, Teflon, or Tygon tubing of small bore.

An alternate technique for band recovery involves the use of a plastic insert (Fig. XIII-I-6) which fits into Spinco SW 25 swinging-bucket centrifuge tubes. The density of the insert is such as to

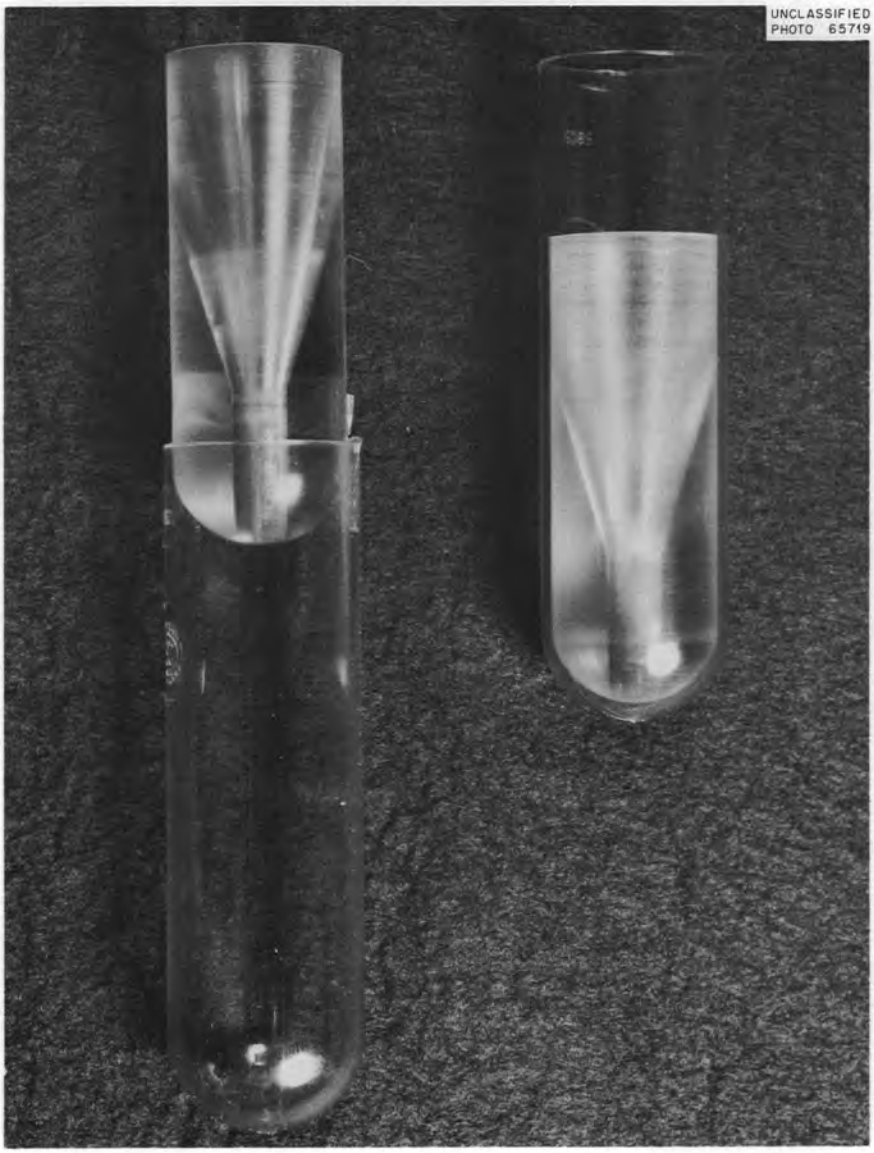

Fig. XIII-I-6. Polycarbonate Centrifuge Tube with Lucite Insert. Insert floats in gradient and bands are therefore restricted to narrow neck of insert, accentuating band. Recovery of an isodense layer is facilitated.

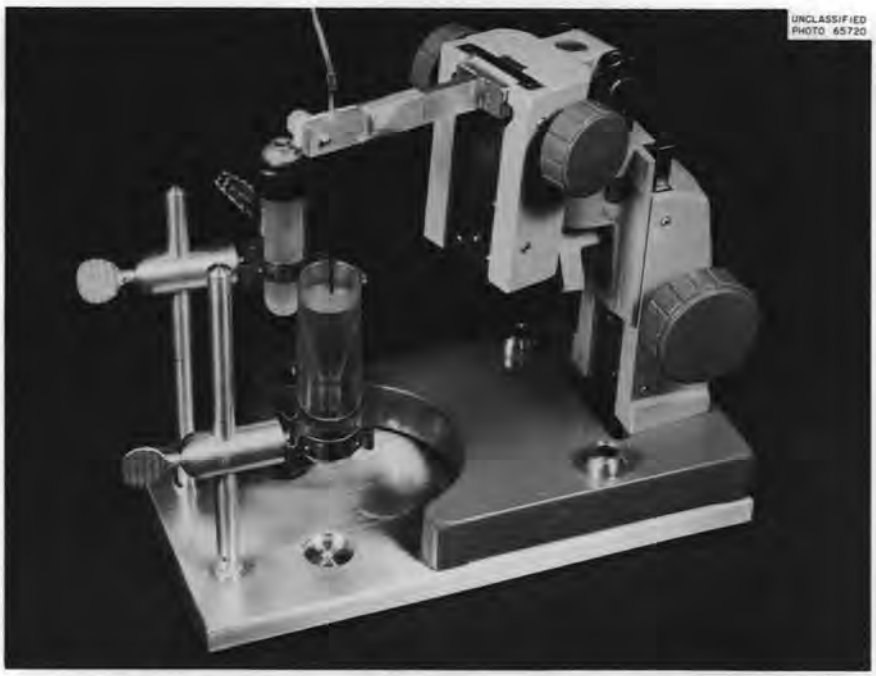

Fig. XIII-I-7. Recovery of Banded Sample. Needle is lowered by rack-and-pinion device to desired level. Pump removes tube contents. Holder (left) for smaller tubes prevents sample warming.

keep it floating in the gradient at a level which ensures that the gradient in the center constriction will be similar from run to run and will be in the range desired for virus separation. Virus particles are therefore constricted into a very small volume, which may be visualized by scattered light, and removed with a fine needle.

The rack shown in Fig. XIII-I-7 has been adapted from a microscope for positioning the stainless steel needle used to recover gradients. In the No. 30 rotor tubes normally used, the needle would enter through the screw hole in the tube cap. The rack-and-pinion device allows exact centering of the needle and also positioning with respect to individual visible bands. Provision is made with this device to keep small tubes (No. 40 or 50) chilled during recovery. The holder for these tubes is also seen in Fig. XIII-I-7.

J. PREPARATION OF SAMPLES FOR ELECTRON MICROSCOPY

Salts of any kind are undesirable in samples being prepared for electron microscopy since the salt background may mask virus or virus-like particles. Samples from the No. 30 rotor tubes prepared as described are therefore routinely dialyzed to remove such salts. Dialysis of recovered fractions is performed as illustrated in Fig. XIII-J-1. The fraction of interest is taken up in a small disposable syringe, the needle removed, and the syringe itself fitted into the top of a nylon adapter to which a length of dialysis tubing has been previously tied. The entire unit is presterilized with steam. The sample is injected into the dialysis sac, and the unit is kept in the refrigerator for the required time. The sample is pulled back into the syringe and either sent to electron microscopy directly or centrifuged in a No. 40 or 50 Spinco rotor to concentrate the material. The grid preparation and techniques used in microscopy will be described in subsequent reports.

K. COMMENTS ON OPERATING PROCEDURES

The rate zonal run diagram, the computer plotter chart, and strips of photographs of cesium chloride

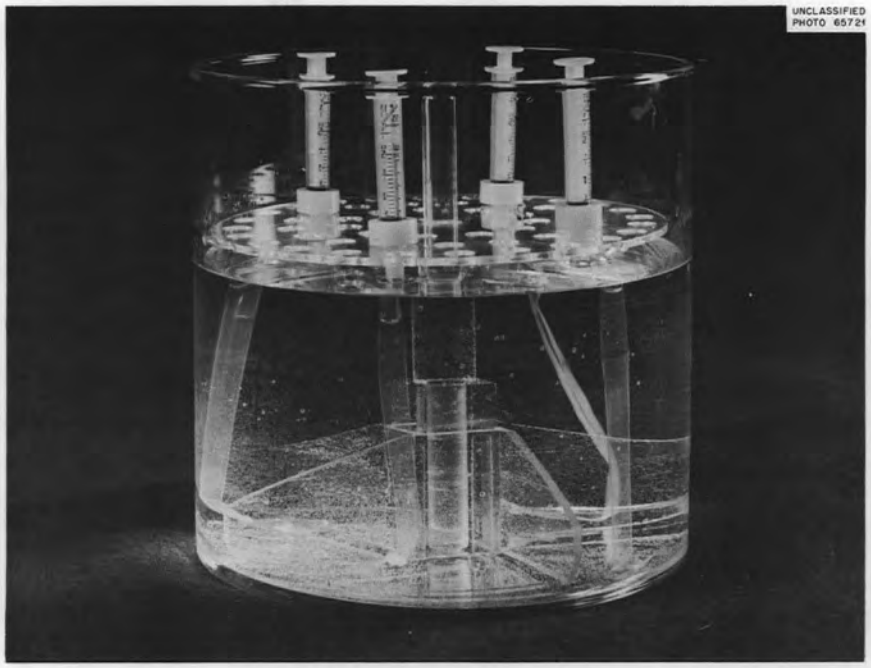

Fig. XIII-J-1. Dialysis Scheme for Removal of CsCl and Sucrose from Recovered Banded Fractions. See text for explanation.

banding tubes are mounted as shown in Fig. II-A-3. The equivalent sedimentation coefficients (S^*), the banding densities, and the absorbance may thus be interrelated.

The techniques described in this chapter for the recovery of fractions in the B-IV rotor followed by banding of the sucrose fractions in CsCl (S-ρ) have evolved during the course of the work. They will be altered as time proceeds in order to improve resolution or to ensure better containment. A number of changes are being tested at the moment to determine if the best methods for recovery are currently employed. These will be described in subsequent reports.

XIV. Data Reduction

A. COMPUTER PROGRAM FOR THE B-IV ZONAL CENTRIFUGE

Barbara S. Bishop

1. Program Modifications

The Zonal Centrifuge Computer Program was revised in the latter part of 1963 to include subroutines for plotting even sedimentation coefficients as a function of tube numbers and density and a new method of calculating even sedimentation coefficients. The density and viscosity equations have also been revised to conform to empirical equations derived by E. J. Barber of the Technical Division at ORGDP. The B-IV rotor for the centrifuge was placed in operation, and the computer program now includes the equations for this rotor as well as the B-II rotor.

The plotting subroutine is labeled PLTSED and is controlled by column 77 of the identification card for each run. If column 77 is 0 or blank, no plotting will occur; if column 77 is 1, the plotting will be given as binary output on Tape 14. The ORGDP Plotting Package for use with the Benson-Lehner plotter is called by PLTSED and includes the subroutines BLSCL, ORBL1, and RANGE.

The new even sedimentation coefficient subroutine is labeled SEDEVN and calculates the even sedimentation coefficient that most nearly approaches the center of the tube with the exception of S-tube where the criterion is the middle of the sample zone. A sedimentation coefficient value is calculated for each tube at the 1.5 density level with other densities calculated for the same coefficient. The previous subroutine used in this manner, labeled EVNSED, gave equally spaced coefficients and did not always include a value for each tube. EVNSED and SEDEVN are both available, and either may be used by a 0 or blank control in column 76 for SEDEVN and a 1 control in column 76 for EVNSED on the identification card.

2. Calculation of Density over Extended Temperature Range

The following equation is valid from 0 to 60°C:

$$\rho = \frac{XM_1 + (1 - X)M_2}{X(B_1 + B_2 t + B_3 t^2) + (1 - X)(A_1 + A_2 t + A_3 t^2)},$$

where

ρ = density,
M_1 = 342.30, mol. wt of sucrose,
M_2 = 18.032, mol. wt of water,
t = temperature, °C,
A_1, A_2, and A_3 = constants determined from density data on pure water (A_1 = 18.027525, A_2 = 4.8318329 × 10^{-4}, A_3 = 7.7830857 × 10^{-5}),
B_1, B_2, and B_3 = constants determined from the solution density data (B_1 = 212.57059, B_2 = 0.13371672, B_3 = −2.9276449 × 10^{-2}),
X = mole fraction sucrose calculated from the relation:

$$X = \frac{\overline{X}/M_1}{\overline{X}/M_1 + (1 - \overline{X})/M_2}$$

$$= \frac{W/M_1}{W/M_1 + (100 - W)/M_2},$$

where $\overline{X}$ is the weight fraction sucrose, and W is the weight percent sucrose.

3. Viscosity Calculations

The following equation is valid from 0 to 80°C:

$$\log_{10} \eta = A + \frac{B}{t + C},$$

where

η = viscosity,
t = temperature, °C,
$C = 146.06635 - 25.251728\,[1 + (X/0.070674842)^2]^{1/2}$,
X = mole fraction.

The general form of the equation for A and B is

$$D_0 + D_1X + D_2X^2\, D_3X^3 + \ldots + D_nX^n,$$

where $D_0, D_1, D_2, \ldots, D_n$ are polynomial coefficients derived from tabulated data. See Table XIV-A-1 for polynomial coefficients.

4. Volume and Radius Formulas for the B-IV Rotor

The equation for volume, in cubic centimeters for a given radius in inches, is

$$V = 164.866(3.35785r^2 - 1.11262r - 0.98510).$$

The equation for radius, in inches for a given volume in cubic centimeters, is

$$r = \sqrt{0.0018061V + 0.032082} + 0.16567.$$

Note: Radii are measured from the center of the rotor.

B. CALCULATION OF THE VISCOSITY OF SUCROSE SOLUTIONS

E. J. Barber P. B. Wood

In the treatment of data from the zonal liquid centrifuge, the density and the viscosity are two of the intensive properties of the sucrose gradient which must be accurately known. Both these intensive properties are functions of the measured properties of temperature and composition at any given point in the centrifuge. Satisfactory equations for calculation of the density of sucrose solutions as a function of the temperature and composition were presented previously.[1] A set of equations for calculation of the viscosity have now been developed to give the viscosity data in the National Bureau of Standards tables.[2]

[1] *Joint NIH-AEC Zonal Centrifuge Development Program Semiann. Rept. January 1–June 30, 1963*, ORNL-3502, pp. 64-66.

[2] J. F. Swindells, *et al.*, *Viscosities of Sucrose Solutions at Various Temperatures; Tables of Recalculated Values, Natl. Bur. Standards (U.S.) Circ. 440* (July 31, 1958).

Table XIV-A-1. Coefficients for Calculations of A and B as Functions of Mole Fraction

Polynomial Coefficients	A		B	
	0 to 48 wt %	48 to 75 wt %	0 to 48 wt %	48 to 75 wt %
D_0	-1.5018327	-1.0803314	2.1169907×10^2	1.3975568×10^2
D_1	9.4112153	-2.0003484	1.6077083×10^3	6.6747329×10^3
D_2	-1.1435741×10^3	4.6066898×10^2	1.6911611×10^5	-7.8716105×10^4
D_3	1.0504137×10^5	-5.9517023×10^3	-1.4184371×10^7	9.0967578×10^5
D_4	-4.6927102×10^6	3.5627216×10^4	6.0654775×10^8	-5.5380830×10^6
D_5	1.0323349×10^8	-7.8542145×10^4	$-1.2985834 \times 10^{10}$	1.2451219×10^7
D_6	-1.1028981×10^9		1.3532907×10^{11}	
D_7	4.5921911×10^9		$-5.4970416 \times 10^{11}$	

Since the tables cover only the composition range from 20 to 75 wt % sucrose over the temperature range 0 to 80°C, viscosity values at 5 wt % intervals between 0 and 20 wt % were developed at 5°C temperature intervals over the range 0 to 80°C using equations of the form developed by the National Bureau of Standards for this purpose:[2]

$$\ln_e \frac{\eta}{\eta_0} = E \frac{X}{1 - X} + FX^2 , \qquad (1)$$

where

η = viscosity of the sucrose,
η_0 = viscosity of pure water at a given temperature,
X = weight fraction sucrose,
E and F = temperature-dependent constants.

Values of E and F were computed from the viscosity data for pure water and the data for sucrose solutions containing 20 and 30 wt % sucrose at the desired temperature intervals. These equations are not valid beyond the range of composition used in their development.

In the approach to fitting the viscosity data, it was recognized that water is an associated liquid containing clusters of molecules with a high degree of structural order and that sucrose is capable of forming hydrogen bonds with the water. Since varying amounts of sucrose may be expected to affect the structural arrangement of the solution more than varying the temperature, an equation was first sought which would accurately describe the change of viscosity at constant composition with temperature. Using the "hole" theory of Eyring and associates,[3] the Antoine or modified Arrhenius equation so successfully used in vapor pressure treatment was tried. This equation as related to viscosity has the form

$$\log_{10} \eta = A + \frac{B}{t + C} , \qquad (2)$$

where η is the viscosity at constant composition and temperature, t is the temperature in °C, and A, B, and C are composition-dependent constants. When this evaluation is carried out, constants A, B, and C are found at any given composition such that the viscosity data as a function of the temperature are reproduced to about three parts per thousand. The Antoine constant, C, is fitted throughout the temperature range as a function of composition only by the right-hand negative leg of a hyperbola having the equation

$$C = 146.06635 - 25.251728 \, [1 + (x/0.070674842)^2]^{1/2}, \qquad (3)$$

where C has the dimensions of temperature on the centigrade scale, and x is the mole fraction sucrose obtained from the relation

$$x = \frac{X/342.30}{X/342.30 + (1 - X)/18.032} ,$$

where X is the weight fraction sucrose. The 342.30 and 18.032 are the molecular weights of sucrose and water respectively.

Assuming that the value of the Antoine or C constant is exactly as calculated from Eq. (3) and allowing errors in the tabulated data at any composition to be distributed between the remaining two constants, values of A and B were found at the same compositions used previously. These reevaluated constants produced equations showing only negligible losses in accuracy at any composition, thus indicating the selection of a satisfactory dependence of the C constant upon composition.

The limiting viscosity (or A constant) and the activation energy (or B constant)[4] so obtained plot as smooth functions of the composition. However, neither constant could be fitted by any simple function,[4] but a high-order polynomial would fit provided the data were fitted in two segments with those below 48 wt % sucrose being fitted by seventh-order polynomials in the mole fraction sucrose and those above 48 wt % sucrose being fitted by fifth-order polynomials. In the procedure used, the A constant was evaluated as a function of composition in such a way that the two equations applicable at 48 wt % gave the same value of A and

[3] S. Glasstone, K. J. Laidler, and H. Eyring, *The Theory of Rate Processes*, Chap. IX, McGraw-Hill, New York, 1941.

[4] See *Joint NIH-AEC Zonal Centrifuge Development Program Semiann. Rept. January 1–June 30, 1963*, ORNL-3502, for explanation of names of constants and type of treatment attempted earlier.

dA/dx at 48 wt %. Assuming that both the A constant and the C constant dependence upon the mole fraction were correct, the best values of the B constant for each tabulated composition were calculated and fitted at functions of the mole fraction in a manner identical to that used in obtaining the A constants. The equations for the A constant and the B constant have the form

$$A = D_0 + D_1x + D_2x^2 + D_3x^3 + \ldots + D_nx^n ,$$

where the D_i's are the coefficients, and x is the mole fraction. The coefficients needed to calculate A and B for the two concentration ranges are given in Table XIV-A-1.

By use of this set of equations the standard deviation in viscosity over the entire range of temperature and composition is 2 parts per thousand, and no individual value is in error by more than 3 parts per thousand in the temperature and composition ranges of primary interest of 5 to 40°C and 5 to 40 wt % sucrose. At temperatures higher than 40°C and compositions above 40 wt % sucrose, some individual values may differ from tabulated values by as much as 8 parts per thousand; but even here the standard deviation from the tabulated data at any given composition is only 3 parts per thousand. The set of equations thus express the viscosity as a function of temperature and composition well within the allowed deviation from the tabulated data of 1%. The equation is also of a form which will allow treatment of the viscosity of sucrose solutions by the "free volume" approach of Doolittle[5] and Miller[6] and may be helpful in elucidating the effect of the addition of sucrose to water upon the structure of liquid water.

[5]A. K. Doolittle, *The Technology of Solvents and Plasticizers*, Chap. 13, Wiley, New York, 1954.

[6]A. A. Miller, *J. Phys. Chem.* 67, 1031–35 (1963).

XV. Ancillary Studies

A. FLAME IONIZATION ANALYZER FOR DETERMINING TOTAL CARBON IN LIQUID STREAMS OR SOLID SAMPLES

R. H. Stevens

1. General Considerations

A rapid and continuous method for determining carbon in solid or liquid organic samples in the 10^{-10}- to 10^{-8}-g range has been investigated as a new analytical tool in research and routine bioanalyses. This method has been successfully used to detect the presence of puffball spores (4 μ) in air when used as an air monitor for organic particulates. It is also a potential instrument for monitoring the eluant from miniature ion exchange columns and for individually analyzing cells and large subcellular particles for carbon content.

The equipment provides for the direct introduction of solid or liquid samples into a hydrogen-flame ionization detector by means of a loop of fine wire which passes slowly through the flame. A brief description of the analyzer and some initial results have been reported.[1]

2. Operation of Equipment

The instrument operates by collecting and measuring the ionization current produced by carbon ions generated during the combustion of the sample in the hydrogen flame. This type of detector is commonly used to monitor the gaseous discharge of chromatographic columns, and its output is essentially a linear function of the amount of carbon present in the sample.

The general operation of the equipment is depicted graphically in Fig. XV-A-1. This arrangement differs from the first version[1] in that a continuous loop of wire has been provided for transporting the sample to avoid the rewinding operation necessary with a single strand. The equipment can be arranged in either of two operating modes: as an air monitor to collect particulates onto the wire from a flowing air stream by the use of an electrostatic precipitator, or as a liquid or solid sampler in which the sample is placed manually or automatically on the wire. Any solvent present is evaporated over a small drying oven. Either sample-acquisition step is immediately followed by movement of the wire into the flame. Figure XV-A-2 is a photograph of the analyzer showing the continuous loop of wire passing axially through a miniature electrostatic precipitator. Figure XV-A-3 is a close-up view of the same equipment except that the precipitator has been replaced by a small drying oven and a microscope has been provided for manipulating small samples.

Dissolved samples are most conveniently handled by "hanging" a 1-μl droplet of solution from the wire and allowing the solvent to evaporate. The drying oven facilitates the latter by providing heated air which flows slowly past the droplet. Several common solvents such as distilled water, absolute ethanol, and methanol have been unsatisfactory as sample carriers since the signals obtained from the nonvolatile residues from 1-μl aliquots of these liquids are usually sufficient to mask the response to 10^{-7} g of sample dissolved in the droplets. Apparent nonlinearities in the analyzer response reported previously[1] for palmitic acid in ethanol were the result of nonvolatile solvent residues contributing to the sample signal by this mechanism. Carbon tetrachloride (RACS grade) may be used as a carrier since its residue

[1]N. G. Anderson and R. H. Stevens, *Joint NIH-AEC Zonal Centrifuge Development Program Semiann. Rept. January 1–June 30, 1963*, ORNL-3502, p. 83.

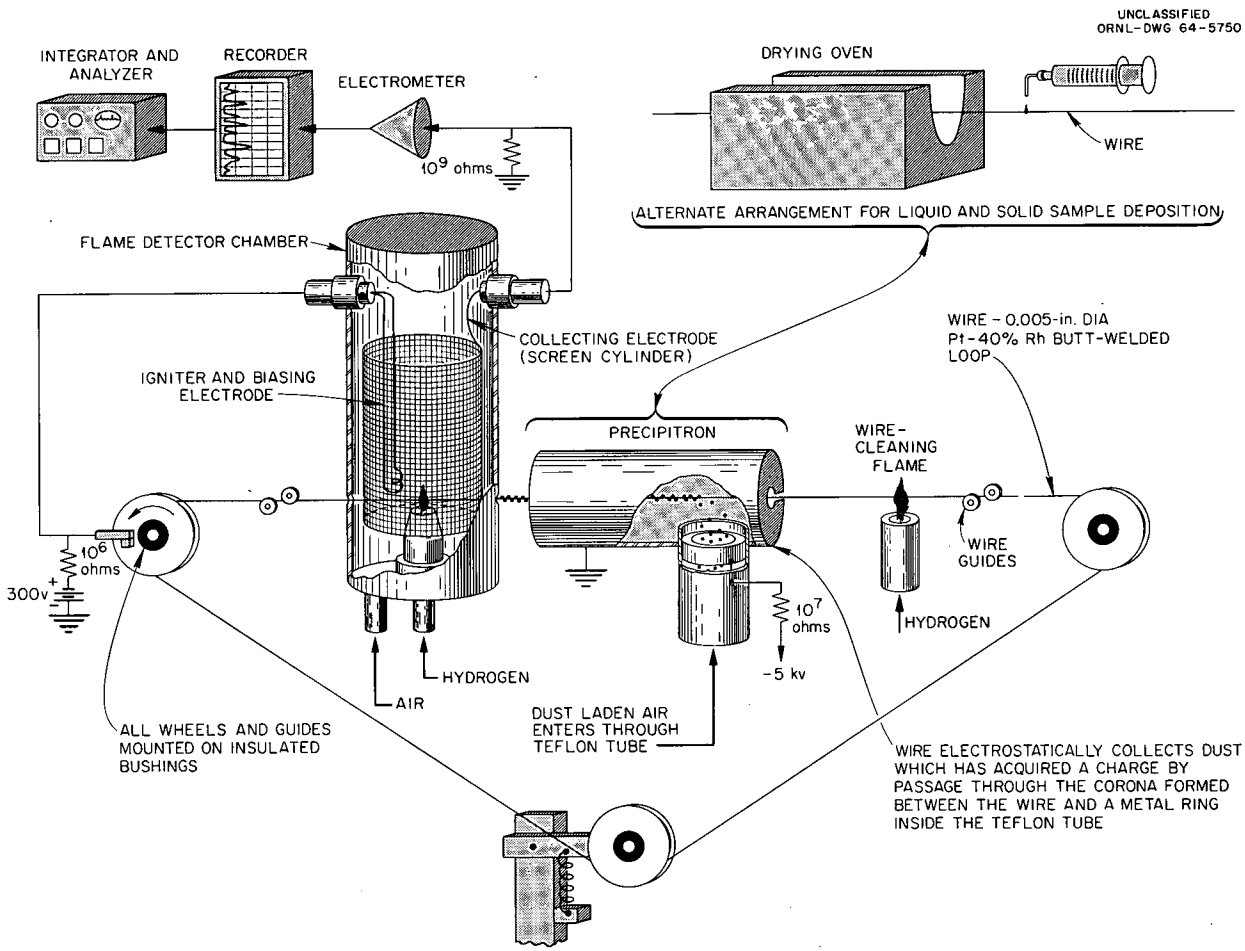

Fig. XV-A-1. Schematic Representation of Flame Ionization Analyzer, for Continuous Carbon Analysis.

is not detectable at the highest sensitivity of the equipment.

An electrical bias of 300 v is applied to the wire with the same polarity as that used for the ionization chamber biasing electrode; this prevents competitive ion or electron collection by the wire which would occur if it were operated at the near-ground potential of the collecting electrode screen. Either the positive or the negative ion current can be collected by selecting the proper polarity of the biasing voltage.

The wire is normally traversed to the left at a lineal speed of $\frac{1}{8}$ to $\frac{1}{4}$ ips during continuous sampling operation. The required in-flame dwell time of the sample for complete combustion is a function of the sample volatility and is generally less than 1 sec, the period experienced by any point on the wire passing through the flame at $\frac{1}{8}$ ips. Large samples having 1 to 3 sec burnoff time frequently require that the wire be stopped in the flame until combustion is complete.

Iridium-rhodium alloy wire, 0.005 in. in diameter, has provided a longer loop service life than the platinum-rhodium alloy wire used in preliminary tests. Wires are precleaned in acid and solvent to reduce the amount of "background" carbon present on the wire surface. A small hydrogen cleaning flame is employed to heat the wire to about 1000°C locally before sample acquisition. This step removes dust and other volatile materials collected by the wire during passage around the wheels and guides. A "run-in" time of several hours is

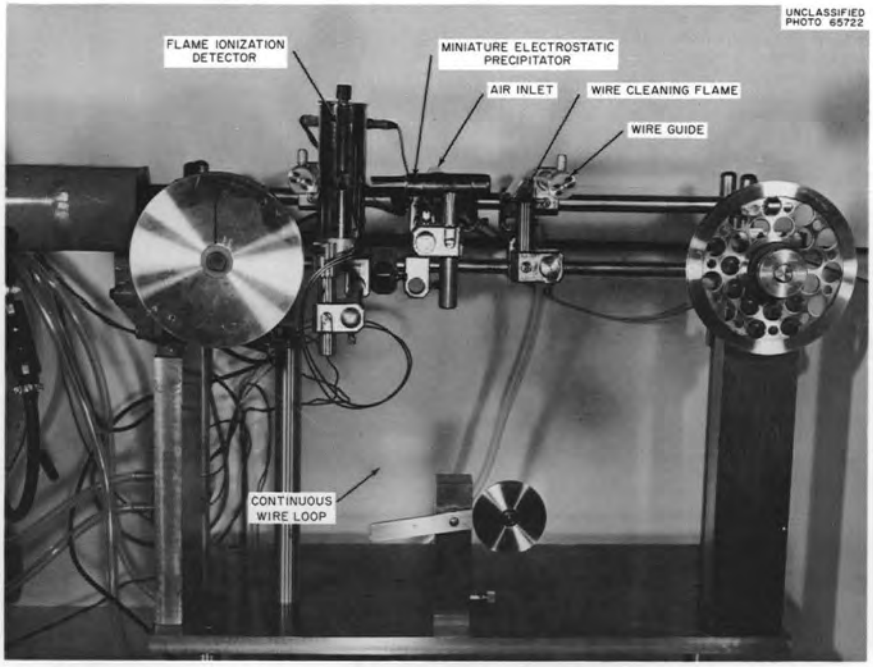

Fig. XV-A-2. Flame Ionization Analyzer Arranged for Air Monitoring of Organic Particulates.

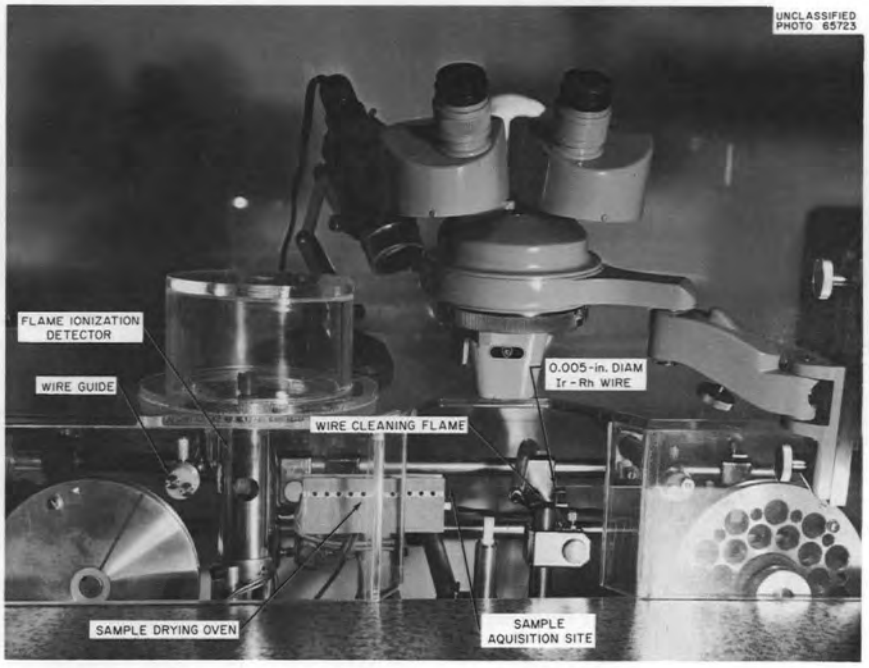

Fig. XV-A-3. Flame Ionization Analyzer Arranged for Solid, Liquid, or Solute Sampling.

UNCLASSIFIED
ORNL-DWG 64-5751

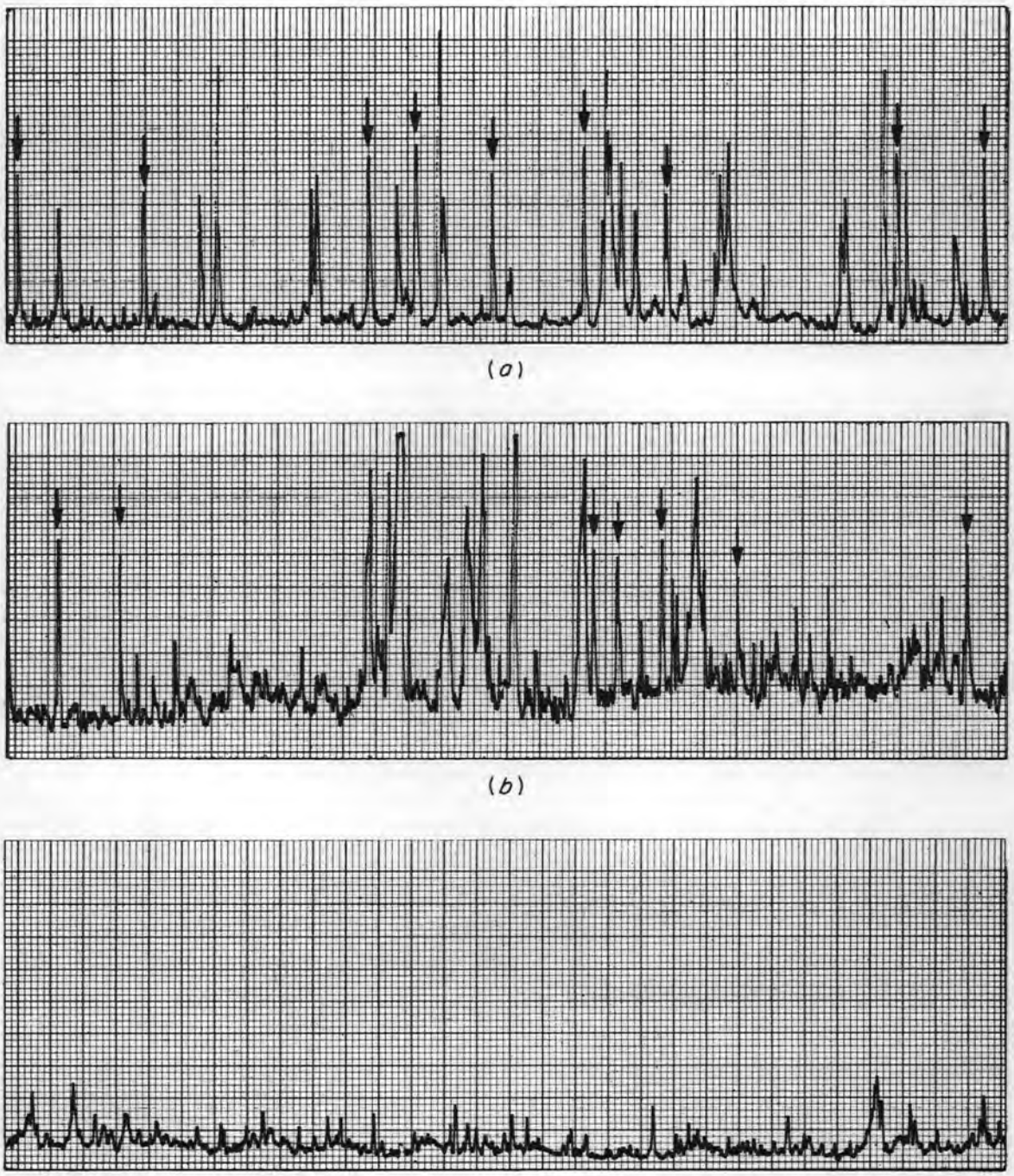

Fig. XV-A-4. Detection of Puffball Spores (4 to 5 μ) in Air Using Flame Ionization Analyzer as an Air Monitor for Organic Particulates. (*a*) Puffball spores dispersed in filtered air. Arrows indicate peaks from individual spores collected on the sample transport wire. (*b*) Puffball spores dispersed in typical unfiltered laboratory air. Arrows indicate individual spore signals identified by peak height. (*c*) Background signal from filtered air and wire noise.

necessary for new wires to remove dissolved contaminants from the wire mass itself by ignition in the cleaning and detector flames. Following this period, spurious signals generated by the wire are infrequent and of small magnitude.

Performance. – The work to date has been to explore the response of the analyzer to carbon and other interfering elements when using a hot wire in the chamber and to determine the sensitivity of the device. Recent work has shown the sensitivity of the analyzer to gaseous samples is within expected limits, namely, 0.003 coulomb per gram of carbon. The response to solid samples, however, is complicated by two effects: precombustion evaporation of the sample from the wire when proximal to the flame, and surface ionization which may provide positive ions of other elements present on the wire when heated in the flame. If the sample can be evaporated from the wire without loss, a sensitivity comparable to that for gas samples is observed. The combustion chamber can be redesigned to overcome the precombustion problem. A dual collection system capable of measuring both positive and negative ionization currents simultaneously will be necessary to study the surface ionization effect.

The existing detector and its associated electrometer are not considered optimum for this work and presently limit the minimum detectable sample weight to a carbon content of about 10^{-10} to 10^{-7} g, depending upon the sample type and the polarity of the ionization current collected. Puffball spores, nominally 4 to 5 μ in diameter, have a calculated carbon content of 2×10^{-11} g/spore. Figure XV-A-4 is a chart record of the detection of individual spores following their collection from air onto the wire using the prototype equipment shown in Fig. XV-A-2. The unexpectedly large response obtained from these spores may be the result of ionization of other elements present in the spore at the time of its combustion on the hot wire.

The basic sensitivity of 0.003 coulomb per gram of carbon applies when using samples evaporated onto the wire by the "hanging-drop" method and negative ionization current collection. The minimum detectable sample carbon weight for these conditions is limited by the sensitivity of the existing electrometer and recorder and by background wire noise to a value of 10^{-7} to 10^{-8} g. Higher-speed electrometers and recorders will be required in future work to respond to the fast current pulses from the detector during the combustion of smaller samples.

B. SUBCELLULAR FRACTIONS OF *ASTASIA LONGA* AS SEPARATED IN THE ZONAL ULTRACENTRIFUGE

P. A. Van Dreal

Subcellular fractions of log-phase-grown *Astasia longa* have been examined in the B-IV zonal ultracentrifuge in preparation for studying changes in these constituents during the cell cycle of the temperature-synchronized cells. Cells were broken by grinding in the cold (4°C) for 30 min in a power-driven mortar and pestle. The homogenate was centrifuged for 10 min at 2400 rpm in an International PR-2 centrifuge. The supernatant was separated in the B-IV rotor in a 10 to 30% sucrose gradient with a 55% sucrose cushion. The rotor was run at 40,000 rpm and unloaded at $101.894 \times 10^6\ \omega^2 t$. Figure XV-B-1 shows the 260- and 280-mμ absorption curves of the material unloaded from the rotor. Under these conditions paramylum granules and nuclei are found on the wall and/or in the initial precipitate. The first peak represents the soluble phase. The next three peaks are

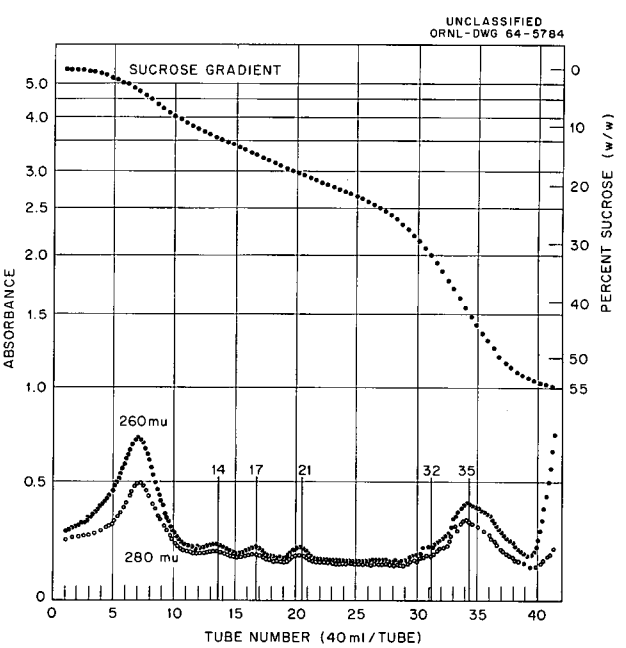

Fig. XV-B-1. Run Monitor of *Astasia longa* Homogenate Separated in B-IV Zonal Ultracentrifuge. Gradient extended from 10 to 30% sucrose (w/w) with a 55% sucrose cushion. Centrifuge unloaded at 101, $894 \times 10^6\ \omega^2 t$.

probably ribosomal. If one assumes a density of 1.5, then the computer predicts that tubes 14, 17, and 21 contain material having sedimentation coefficients of 55, 75, and 102 Svedberg units respectively. The fifth peak contains mitochondria and membrane fractions. Since mitochondria of *Astasia* appear in electron micrographs as elongated structures, it is not surprising that they cannot be isolated unbroken under these conditions.

Appendix I

DRAWINGS OF A-IX ROTOR RELEASED THROUGH THE OFFICE OF TECHNICAL INFORMATION EXTENSION, AEC, OAK RIDGE

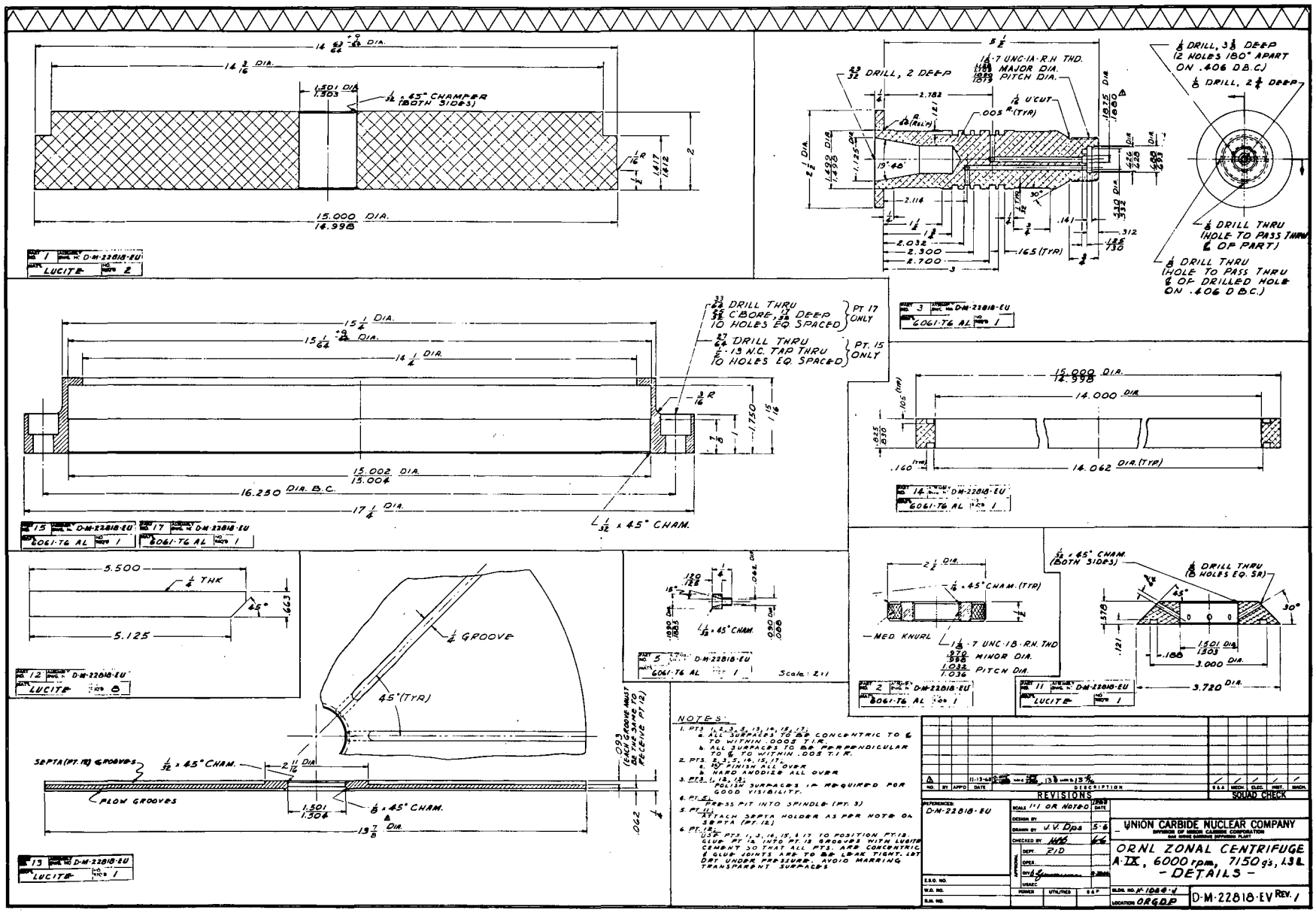
ORNL ZONAL CENTRIFUGE
A-IX, 6000 rpm, 7150 gs, 1.3 L
- DETAILS -
UNION CARBIDE NUCLEAR COMPANY
D-M-22818-EV REV. 1
NOTES:
REVISIONS
SQUAD CHECK
LUCITE
6061-T6 AL
Scale: 2:1

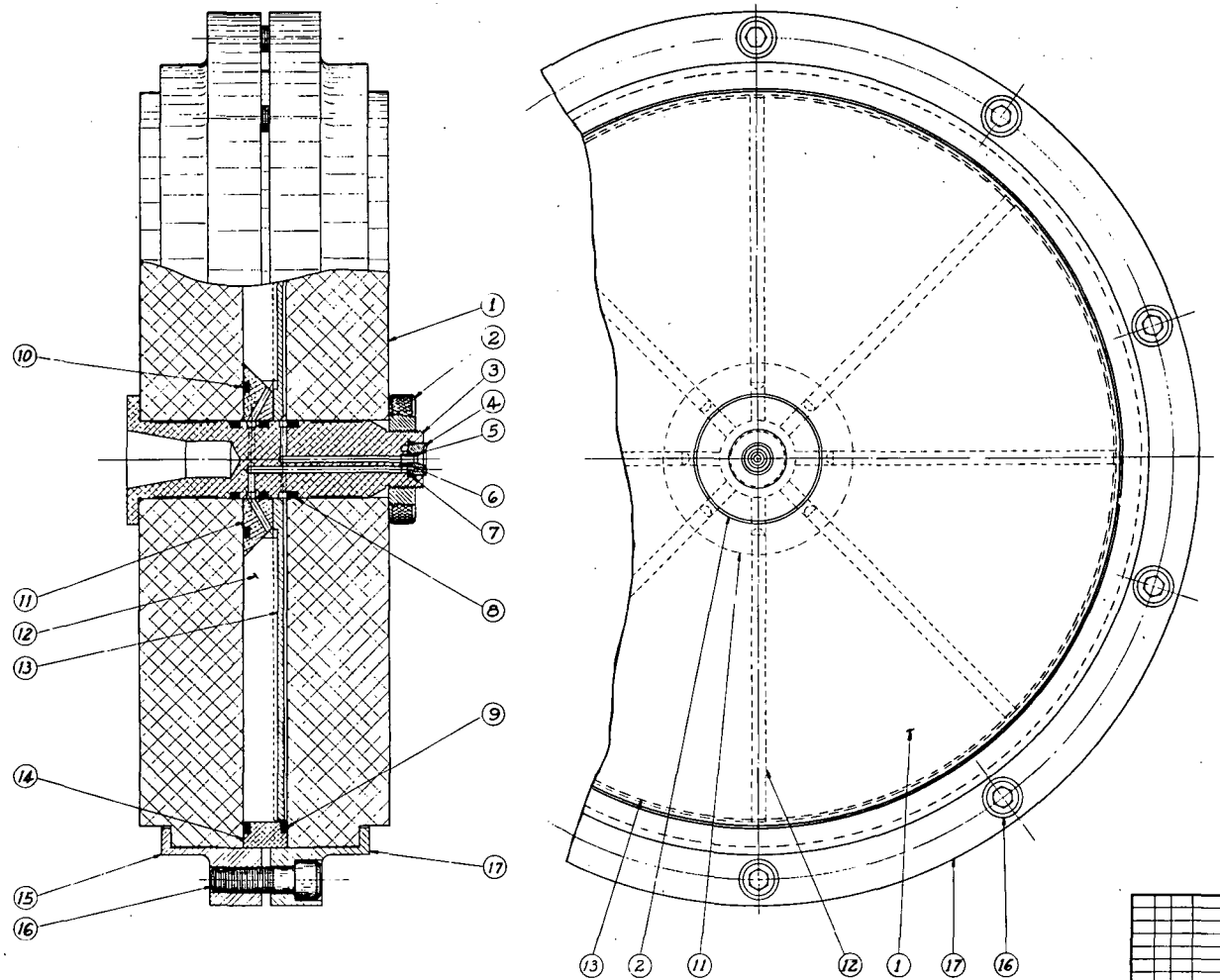

PARTS LIST

PART NO.	NO. REQ'D	DWG. No.	DESCRIPTION
1	2	D-M-22818-EV	END CAPS - LUCITE
2	1	D-M-22818-EV	KNURLED NUT - 6061-T6 AL.
3	1	D-M-22818-EV	TAPERED SPINDLE - 6061-T6 AL.
4	1	———	A-VI SEAL - FURNISHED
5	1	D-M-22818-EV	INSERT - 6061-T6 AL.
6	1	———	O RING - 3/16 x 3/32 x 3/32 (CAT. 07-422-4530)
7	1	———	O RING - 3/8 x 1/8 x 1/16 (CAT. 07-422-5000)
8	3	———	O RING - 1/8 x 1 1/8 x 1 1/8 (CAT. 07-422-5130)
9	2	———	O RING - 1/8 x 14 x 14 3/4
10	1	———	O RING - 1/8 x 2 3/4 x 3 (CAT. 07-422-6000)
11	1	D-M-22818-EV	CORE - LUCITE
12	8	D-M-22818-EV	SEPTA - LUCITE
13	1	D-M-22818-EV	SEPTA HOLDER - LUCITE
14	1	D-M-22818-EV	ROTOR - 6061-T6 AL.
15	1	D-M-22818-EV	COUPLING - 6061-T6 AL.
16	10	———	1/2 - 13 N.C. SCKT HD. CAP x 1 1/4 LG. - STEEL
17	1	D-M-22818-EV	COUPLING - 6061-T6 AL.

NO.	BY	APPD	DATE	DESCRIPTION	S&A	MECH	ELEC	INST.	MACH.

REVISIONS — SQUAD CHECK

REFERENCES: D-M-22818-EV, D-M-22818-FB

SCALE 1:1

DESIGN BY:

DRAWN BY J.V. Dps 5-2

CHECKED BY HMB 6-6

APPROVALS: DEPT. E.A.D. — OPER. — SY — USAEC

E.S.D. NO. — W.O. NO. — S.M. NO. — PRINTER — UTILITIES — S.D.P.

UNION CARBIDE NUCLEAR COMPANY
DIVISION OF UNION CARBIDE CORPORATION
OAK RIDGE GASEOUS DIFFUSION PLANT

ORNL ZONAL CENTRIFUGE
A-IX, 6000 rpm, 7150 g's.
1.3 L. — ASSEMBLY —

BLDG. NO. K-1004-J — LOCATION ORGDP

D-M-22818-EU Rev. 0

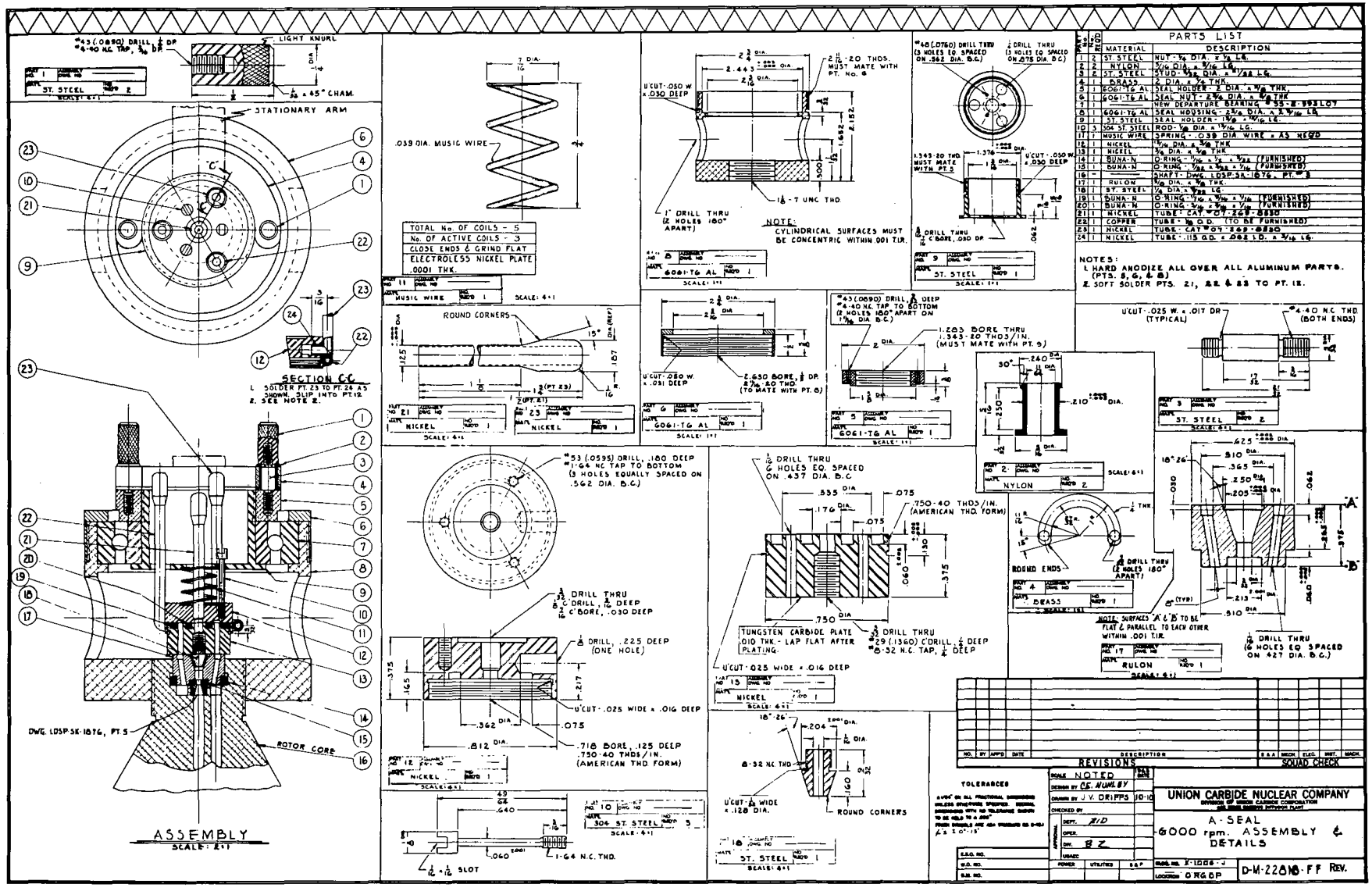
PARTS LIST
MATERIAL
DESCRIPTION
ASSEMBLY
SECTION CC
DWG. LDSP.SK-1876, PT. 5
ROTOR CORE
STATIONARY ARM
LIGHT KNURL
.039 DIA. MUSIC WIRE
TOTAL No. OF COILS - 5
No. OF ACTIVE COILS - 3
CLOSE ENDS & GRIND FLAT
ELECTROLESS NICKEL PLATE
.0001 THK.
ROUND CORNERS
NOTE:
CYLINDRICAL SURFACES MUST BE CONCENTRIC WITHIN .001 T.I.R.
TUNGSTEN CARBIDE PLATE .010 THK. - LAP FLAT AFTER PLATING.
ROUND ENDS
NOTE: SURFACES 'A' & 'B' TO BE FLAT & PARALLEL TO EACH OTHER WITHIN .001 T.I.R.
NOTES:
1. HARD ANODIZE ALL OVER ALL ALUMINUM PARTS. (PTS. 8, 6, & 8)
2. SOFT SOLDER PTS. 21, 22 & 23 TO PT. 12.
TOLERANCES
REVISIONS
SQUAD CHECK
UNION CARBIDE NUCLEAR COMPANY
A-SEAL
6000 rpm. ASSEMBLY & DETAILS
D-M-22818-FF REV.

Appendix II

DRAWINGS OF THE B-IV SYSTEM RELEASED THROUGH THE OFFICE OF TECHNICAL INFORMATION EXTENSION, AEC, OAK RIDGE

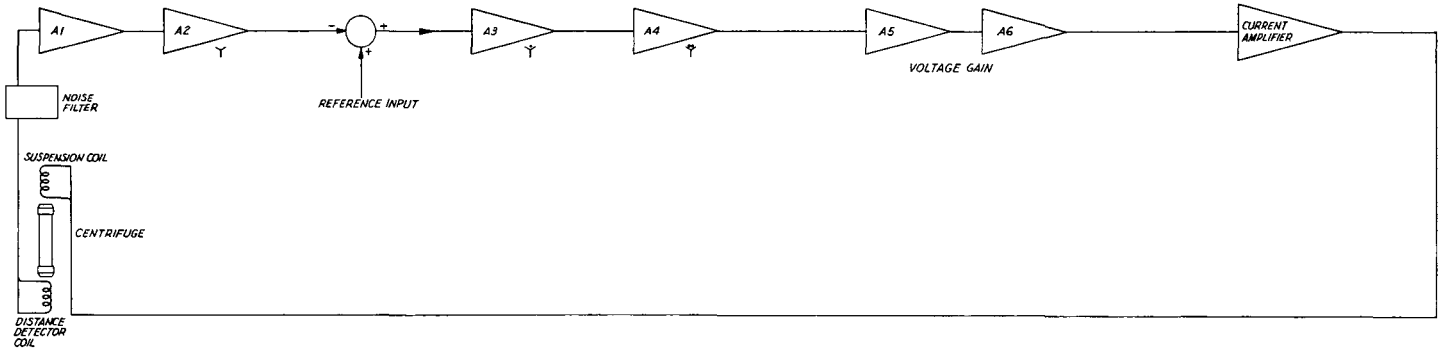

BLOCK DIAGRAM

NO.	BY	APP'D	DATE	DESCRIPTION	CIVIL	MECH.	ELEC.	INST.	MACH.
0									

REVISIONS — SQUAD CHECK

REFERENCES: D-SK-E-64-E SCHEMATIC

SCALE: NONE

		DATE
DESIGN BY	H. P. BARRINGER	10-64
DRAWN BY	W. P. HALE, JR.	11-64
CHECKED BY		
APPROVAL: DEPT.		
OPER.		
DIV.		
SAFETY		

E.S.D. NO.
CHARGE 134065-114
B.M. NO.

UNION CARBIDE CORPORATION
NUCLEAR DIVISION
GAS DIFFUSION PLANT

BIOLOGICAL CENTRIFUGE MAGNETIC SUPPORT
BLOCK DIAGRAM

BLDG. NO. K-1004-J
LOCATION Q.R.E.D.P.

D-SK-E-64-1 REV. 1

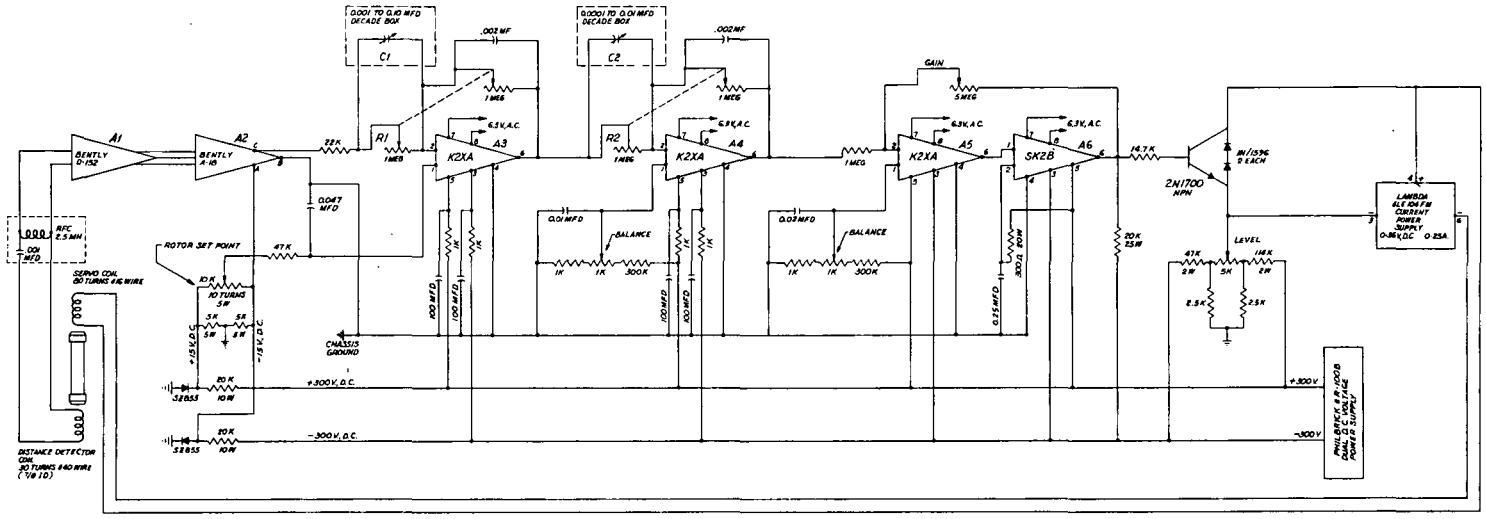

A3, A4, A5 & A6 ARE PHILBRICK ANALOG OPERATIONAL AMPLIFIERS.

* MODIFICATIONS TO LAMBDA POWER SUPPLY:-
1. DISCONNECT CAPACITORS C1, C2O, C21.
2. CONNECT C20 BETWEEN GROUND AND TERMINAL 7.
3. JUMPER TOGETHER TERMINALS 6, 7 & 8.
4. CONNECT ANALOG INPUT TO TERMINALS 3 & 4.
5. CONNECT MAGNET COIL TO TERMINALS 4 & 6.

SCHEMATIC

NO.	BY	APP'D	DATE	DESCRIPTION	CIVIL	MECH	ELEC.	INST.	GNCH
0									

REVISIONS — SQUAD CHECK

REFERENCED: D-SK-E-64-1 BLOCK DIAGRAM

E.S.O. NO.
CHARGE 134065-114
S.M. NO.

SCALE NONE — DATE
DESIGN BY W.W.S. W.S.S.F. N.C.D. H.A.K. 9-10-64
DRAWN BY R. P. HALE, JR. 9-14-64
CHECKED BY
APPROVAL: DEPT. OPER. DIV. SAFETY

UNION CARBIDE CORPORATION
NUCLEAR DIVISION
OAK RIDGE GASEOUS DIFFUSION PLANT

BIOLOGICAL CENTRIFUGE MAGNETIC SUPPORT
SCHEMATIC

BLDG. NO. K-1004-J
LOCATION O.R.G.D.P.

D-SK-E-64-2 REV. 1

Appendix III

DRAWINGS OF B-II, B-IV, B-VII, AND B-VIII ROTORS AND DAMPER BEARING

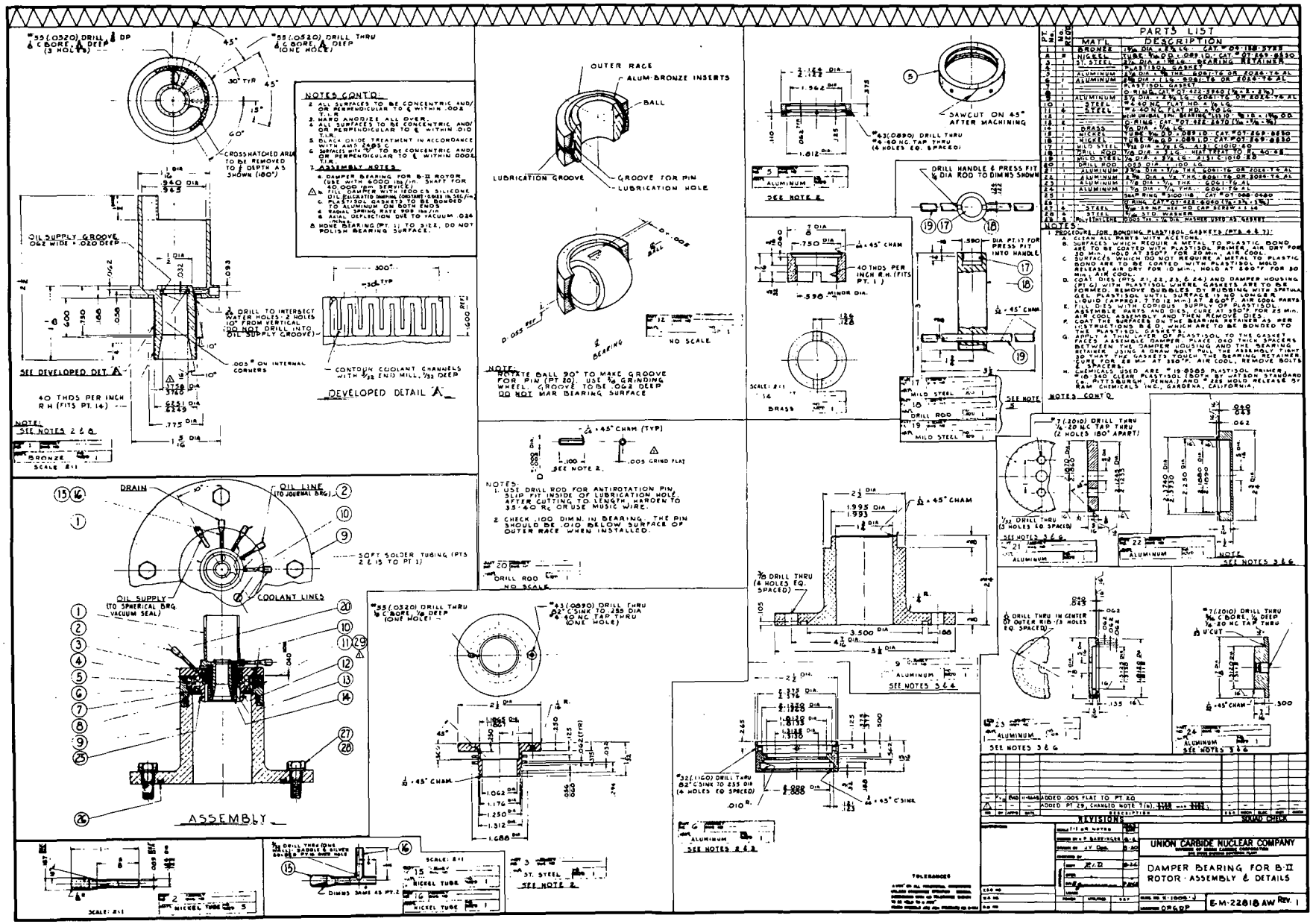
PARTS LIST
NOTES CONT'D
NOTES
DEVELOPED DETAIL A
ASSEMBLY
UNION CARBIDE NUCLEAR COMPANY
DAMPER BEARING FOR B-II ROTOR ASSEMBLY & DETAILS
E-M-22818 AW REV. 1

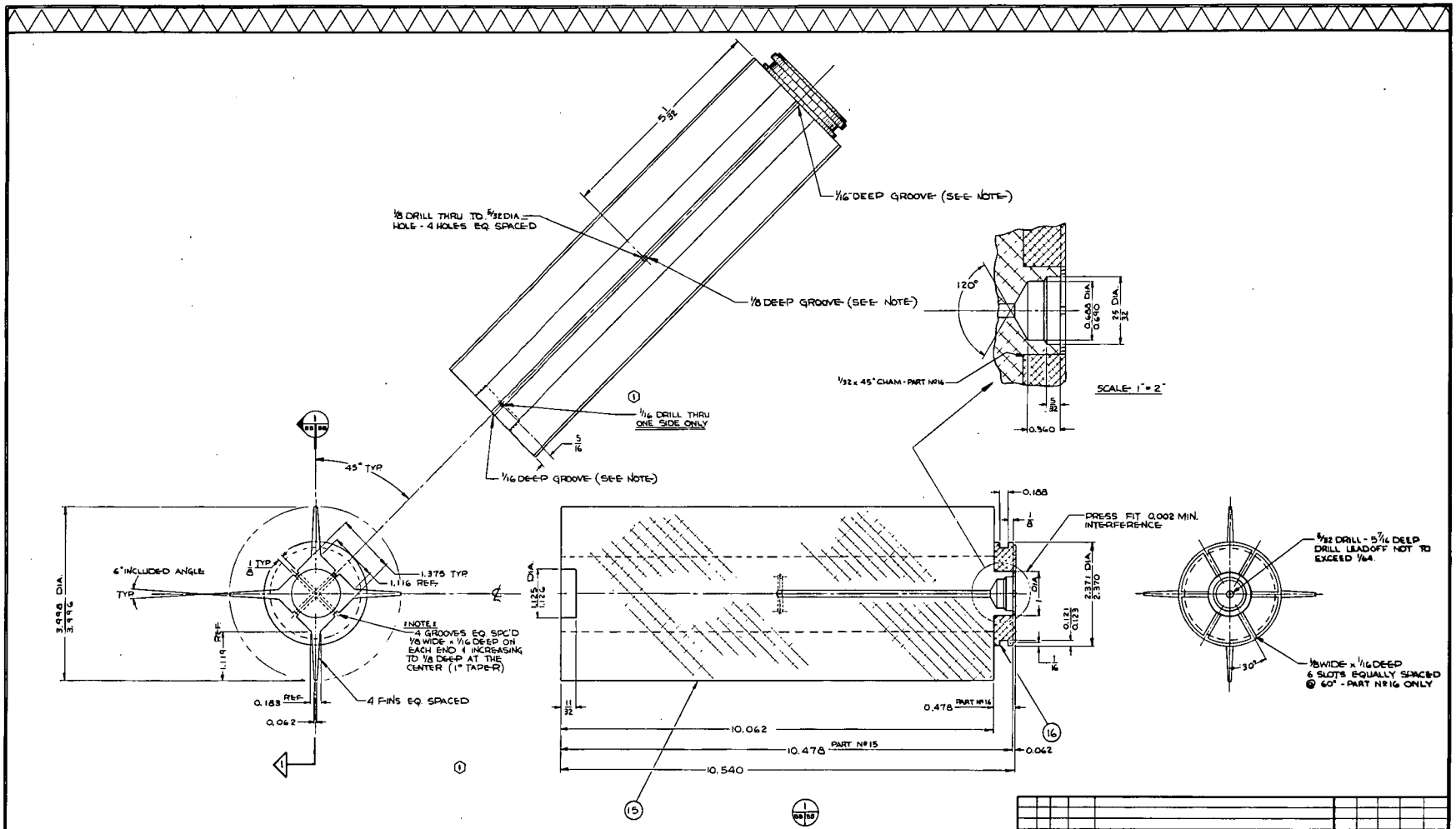

1. ALL SURFACES TO BE CONCENTRIC ABOUT ℄ AND/OR PERPENDICULAR TO ℄ WITHIN 0.0005 T.I.R.
2. HARD ANODIZE ALL OVER.

SECTION & DETAIL KEY

PART NO.	MATERIAL	NOTE	PART NO.	MATERIAL	NOTE
15	D-M-22818-AX		16	D-M-22818-AX	
8	6061-T6 AL	1		6061-T6 AL	1

* STORES #04-009-7252

NO.	BY	APPD	DATE	DESCRIPTION	S&A	MECH.	ELEC.	PROT.	MACH.
1	RLI	FD	9-26-63	ADDED 1/16 DRILL HOLE & REMOVED 5/16 DRILLED HOLES FROM CENTER ON A 1.4 DIA B.C. PART # 15	NONE REQ'D				
0	RLI		9-16-63	DEIG DWG	N.R.				

REVISIONS — SQUAD CHECK

REFERENCES:

SCALE FULL & NOTED — DATE

DESIGN BY

DRAWN BY R.L. INZANA — 9-9

CHECKED BY RMD — 9/16/63

APPROVAL: DEPT. R.L.D. — 9-26-63; OPER.; DIV. A. — 9/16/63; USAEC

E.S.D. NO.
W.O. NO.
S.M. NO.

POWER | UTILITIES | S&P

TECHNICAL DIVISION

UNION CARBIDE NUCLEAR COMPANY
DIVISION OF UNION CARBIDE CORPORATION
OAK RIDGE GASEOUS DIFFUSION PLANT

DETAIL
4 VANE CORE FOR B-IV SYSTEM

SUPS. NO. K-1006 J

LOCATION D.R.G.D.P.

D-M-22818BB REV. 1

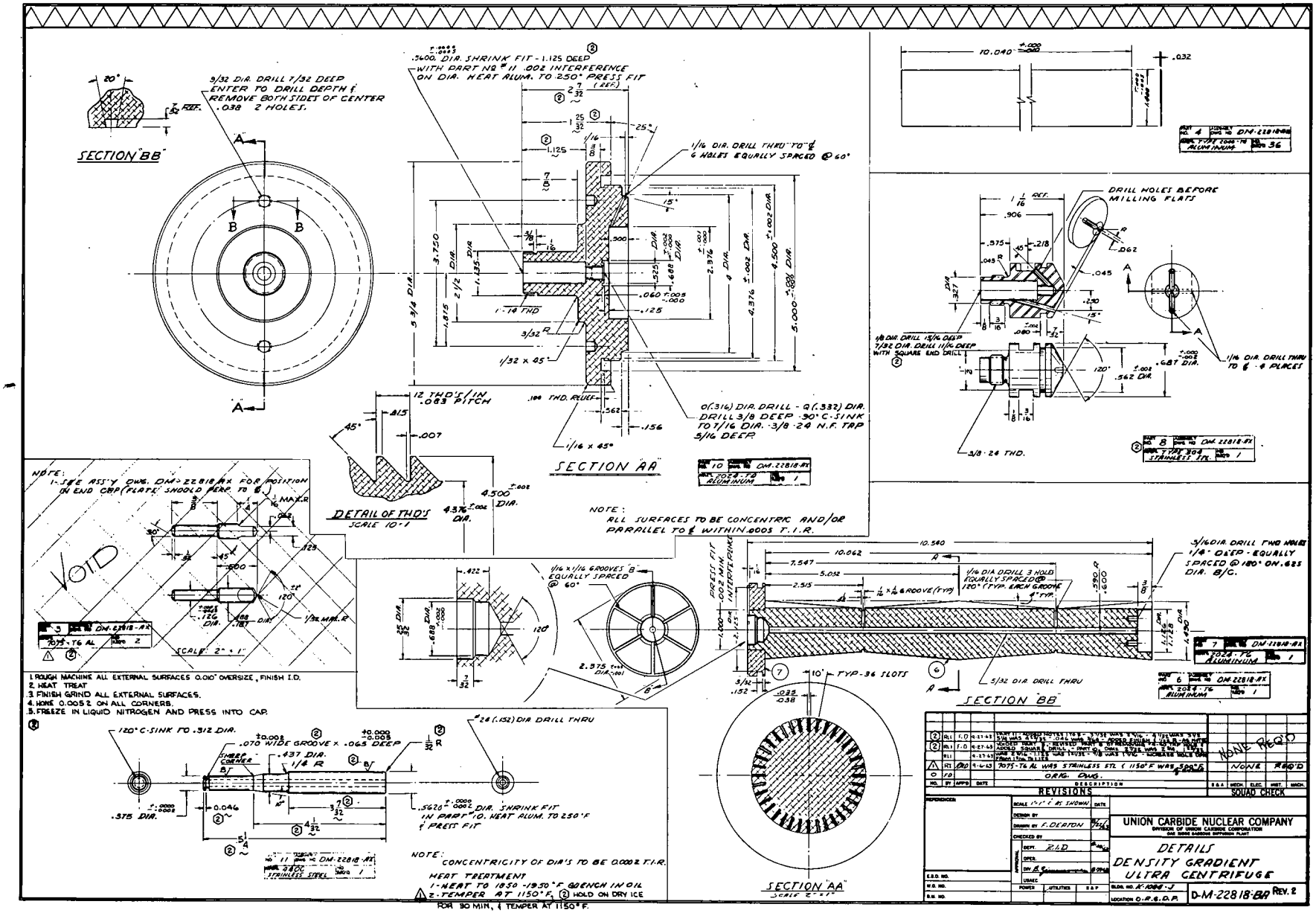
SECTION BB
SECTION AA
DETAIL OF THD'S
SCALE 10:1
VOID
SECTION BB
SECTION AA
UNION CARBIDE NUCLEAR COMPANY
DETAILS
DENSITY GRADIENT
ULTRA CENTRIFUGE
D-M-22818-BA
REV. 2
NONE REQ'D
SQUAD CHECK
REVISIONS
ORIG. DWG.
7075-T6 AL WAS STAINLESS STL (1150°F WAS 950°F)
NOTE:
ALL SURFACES TO BE CONCENTRIC AND/OR PARALLEL TO ℄ WITHIN .0005 T.I.R.
1. ROUGH MACHINE ALL EXTERNAL SURFACES 0.010" OVERSIZE, FINISH I.D.
2. HEAT TREAT
3. FINISH GRIND ALL EXTERNAL SURFACES.
4. HONE 0.005 2 ON ALL CORNERS.
5. FREEZE IN LIQUID NITROGEN AND PRESS INTO CAP.
NOTE:
CONCENTRICITY OF DIA'S TO BE 0.0002 T.I.R.
HEAT TREATMENT
1-HEAT TO 1850-1950°F QUENCH IN OIL
2-TEMPER AT 1150°F, (2) HOLD ON DRY ICE FOR 90 MIN, & TEMPER AT 1150°F.

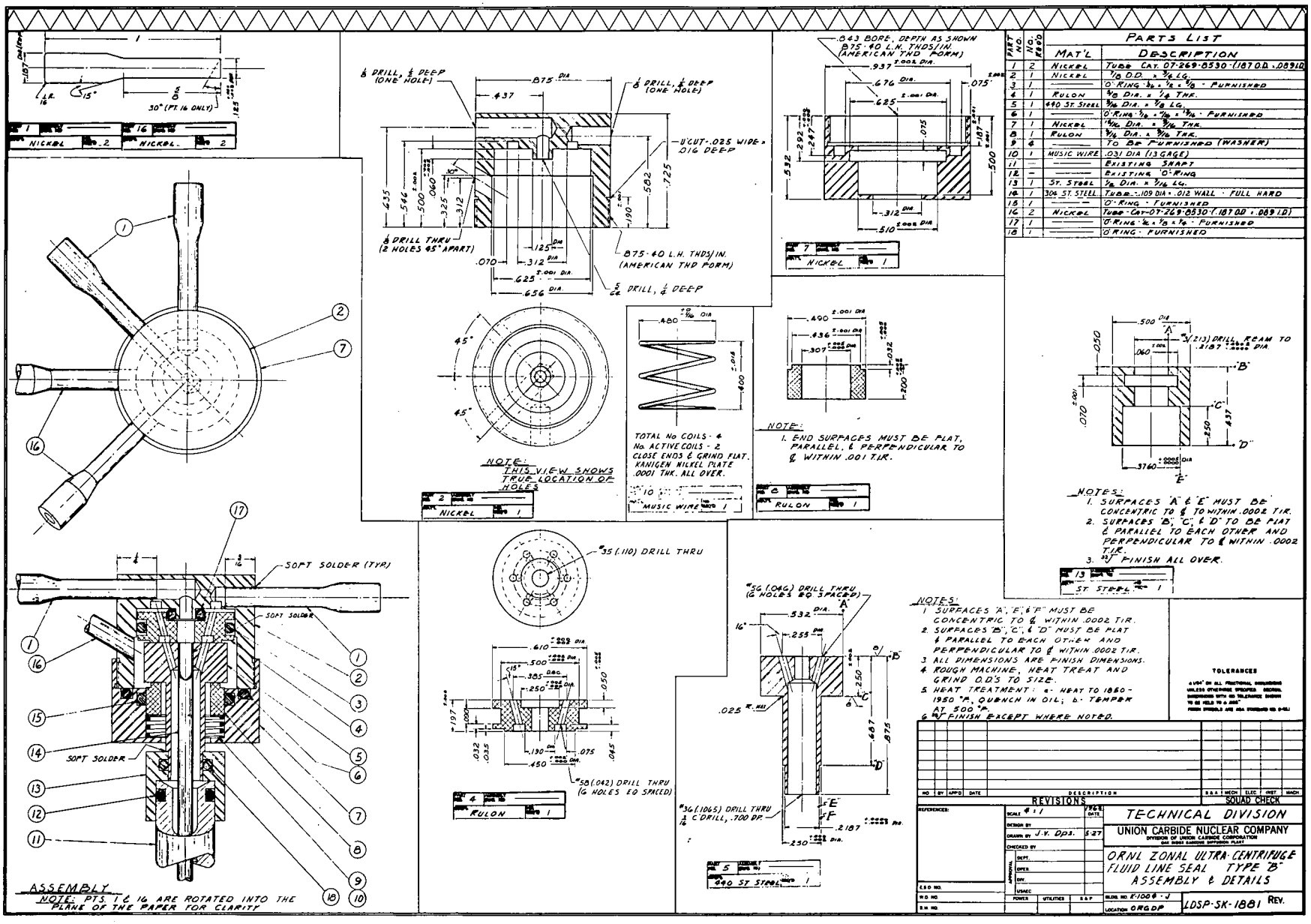
PARTS LIST
PART NO. | NO. REQD | MAT'L | DESCRIPTION
1 | 2 | NICKEL | TUBE CAT. 07-269-8530-(.187 O.D. .089 I.D.)
2 | 1 | NICKEL | 7/8 O.D. x 3/4 LG.
3 | 1 | — | O-RING 3/16 x 7/8 x 1/8 - FURNISHED
4 | 1 | RULON | 5/8 DIA. x 1/8 THK.
5 | 1 | 440 ST. STEEL | 3/16 DIA. x 7/8 LG.
6 | 1 | — | O-RING 7/8 x 1 1/16 x 3/16 - FURNISHED
7 | 1 | NICKEL | 1 5/16 DIA. x 3/16 THK.
8 | 1 | RULON | 3/16 DIA. x 3/16 THK.
9 | 6 | — | TO BE FURNISHED (WASHER)
10 | 1 | MUSIC WIRE | .031 DIA (13 GAGE)
11 | — | — | EXISTING SNAPT
12 | — | — | EXISTING O-RING
13 | 1 | ST. STEEL | 1/2 DIA. x 3/16 LG.
14 | 1 | 304 ST. STEEL | TUBE-.109 DIA x .012 WALL - FULL HARD
15 | 1 | — | O-RING - FURNISHED
16 | 2 | NICKEL | TUBE-CAT-07-269-8530-(.187 OD x .089 ID)
17 | 1 | — | O-RING 3/16 x 7/8 x 3/8 - FURNISHED
18 | 1 | — | O-RING - FURNISHED
NOTE: THIS VIEW SHOWS TRUE LOCATION OF HOLES
NOTE: 1. END SURFACES MUST BE FLAT, PARALLEL, & PERPENDICULAR TO ℄ WITHIN .001 T.I.R.
TOTAL NO COILS - 4
NO. ACTIVE COILS - 2
CLOSE ENDS & GRIND FLAT.
KANIGEN NICKEL PLATE .0001 THK. ALL OVER.
NOTES:
1. SURFACES 'A' & 'E' MUST BE CONCENTRIC TO ℄ TO WITHIN .0002 T.I.R.
2. SURFACES 'B', 'C', & 'D' TO BE FLAT & PARALLEL TO EACH OTHER AND PERPENDICULAR TO ℄ WITHIN .0002 T.I.R.
3. 32 FINISH ALL OVER.
NOTES:
1. SURFACES 'A', 'E', & 'F' MUST BE CONCENTRIC TO ℄ WITHIN .0002 T.I.R.
2. SURFACES 'B', 'C', & 'D' MUST BE FLAT & PARALLEL TO EACH OTHER AND PERPENDICULAR TO ℄ WITHIN .0002 T.I.R.
3. ALL DIMENSIONS ARE FINISH DIMENSIONS.
4. ROUGH MACHINE, HEAT TREAT AND GRIND O.D.'S TO SIZE.
5. HEAT TREATMENT: a- HEAT TO 1850-1950 °F, QUENCH IN OIL; b- TEMPER AT 500 °F.
6. 32 FINISH EXCEPT WHERE NOTED.
TOLERANCES
REVISIONS
TECHNICAL DIVISION
UNION CARBIDE NUCLEAR COMPANY
ORNL ZONAL ULTRA-CENTRIFUGE FLUID LINE SEAL TYPE 'B' ASSEMBLY & DETAILS
LDSP-SK-1881 REV.
ASSEMBLY
NOTE: PTS. 1 & 16 ARE ROTATED INTO THE PLANE OF THE PAPER FOR CLARITY
SOFT SOLDER (TYP)
SOFT SOLDER
NICKEL
RULON
MUSIC WIRE
ST. STEEL
440 ST. STEEL

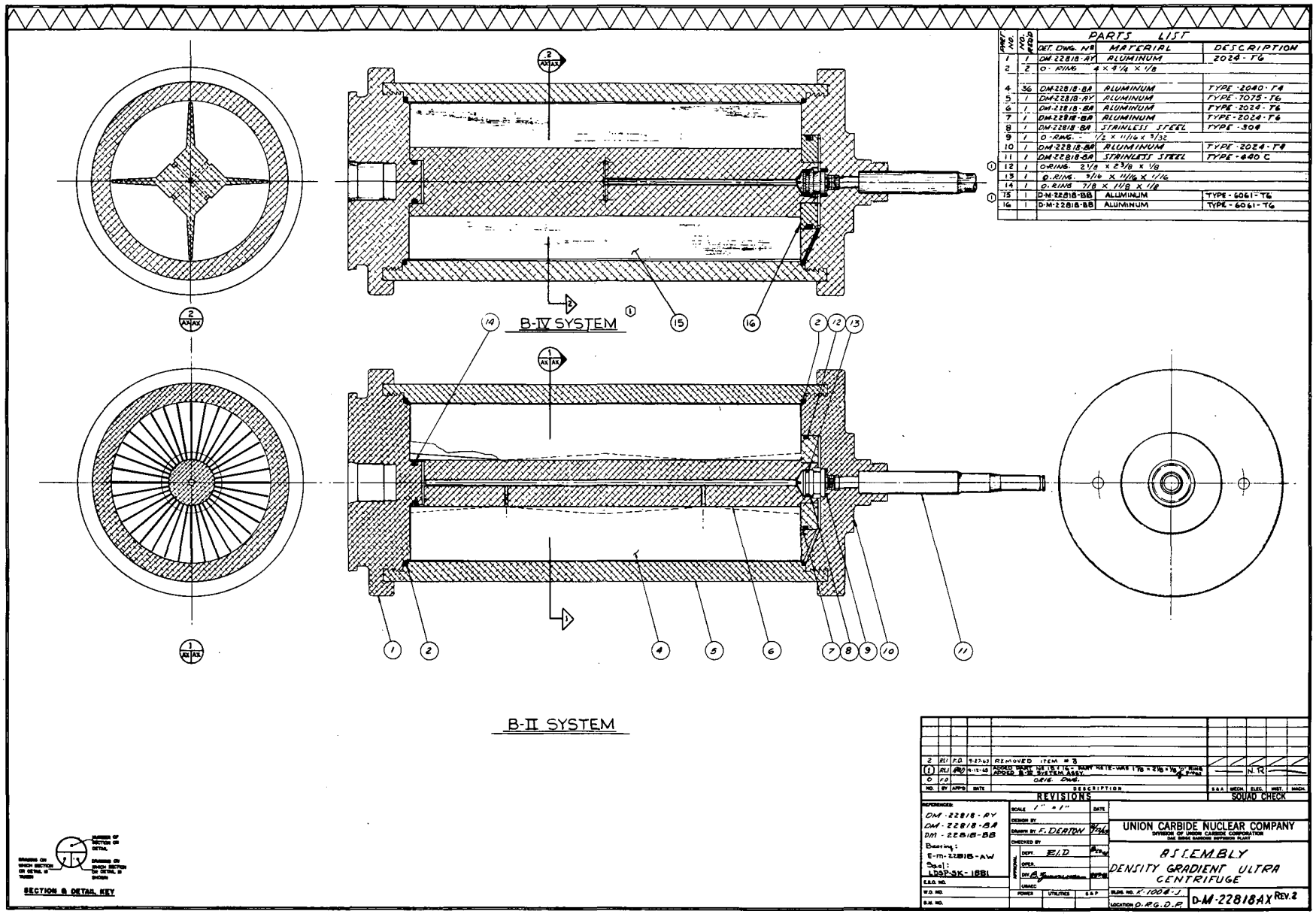
PARTS LIST
PART NO. | NO. REQ'D | DET. DWG. Nº | MATERIAL | DESCRIPTION
1 | 1 | DM-22818-AY | ALUMINUM | 2024-T6
2 | 2 | O-RING | 4 x 4 1/4 x 1/8
4 | 36 | DM-22818-BA | ALUMINUM | TYPE 2040-T4
5 | 1 | DM-22818-AY | ALUMINUM | TYPE 7075-T6
6 | 1 | DM-22818-BA | ALUMINUM | TYPE 2024-T6
7 | 1 | DM-22818-BA | ALUMINUM | TYPE 2024-T6
8 | 1 | DM-22818-BA | STAINLESS STEEL | TYPE 304
9 | 1 | O-RING | 1/2 x 11/16 x 3/32
10 | 1 | DM-22818-BA | ALUMINUM | TYPE 2024-T4
11 | 1 | DM-22818-BA | STAINLESS STEEL | TYPE 440 C
12 | 1 | O-RING | 2 1/8 x 2 3/8 x 1/8
13 | 1 | O-RING | 3/16 x 11/16 x 1/16
14 | 1 | O-RING | 7/8 x 1 1/8 x 1/8
15 | 1 | D-M-22818-BB | ALUMINUM | TYPE-6061-T6
16 | 1 | D-M-22818-BB | ALUMINUM | TYPE-6061-T6
B-IV SYSTEM
B-II SYSTEM
REMOVED ITEM #8
ADDED PART NO 15 & 16 - RUBBER RETE-WAR 1 7/8 x 2 1/8 x 1/16 O' RING
ADDED B-IV SYSTEM ASSY.
ORIG. DWG.
REVISIONS
SQUAD CHECK
DM-22818-AY
DM-22818-BA
DM-22818-BB
Bearing: E-m-22818-AW
Seal: LDSP-SK-1881
SCALE 1" = 1"
DESIGN BY
DRAWN BY F. DEATON
CHECKED BY
DEPT. E.I.D.
UNION CARBIDE NUCLEAR COMPANY
DIVISION OF UNION CARBIDE CORPORATION
OAK RIDGE GASEOUS DIFFUSION PLANT
ASSEMBLY
DENSITY GRADIENT ULTRA CENTRIFUGE
SLIDE NO. K-1008-J
LOCATION O.R.G.D.P.
D-M-22818AX REV. 2
SECTION & DETAIL KEY

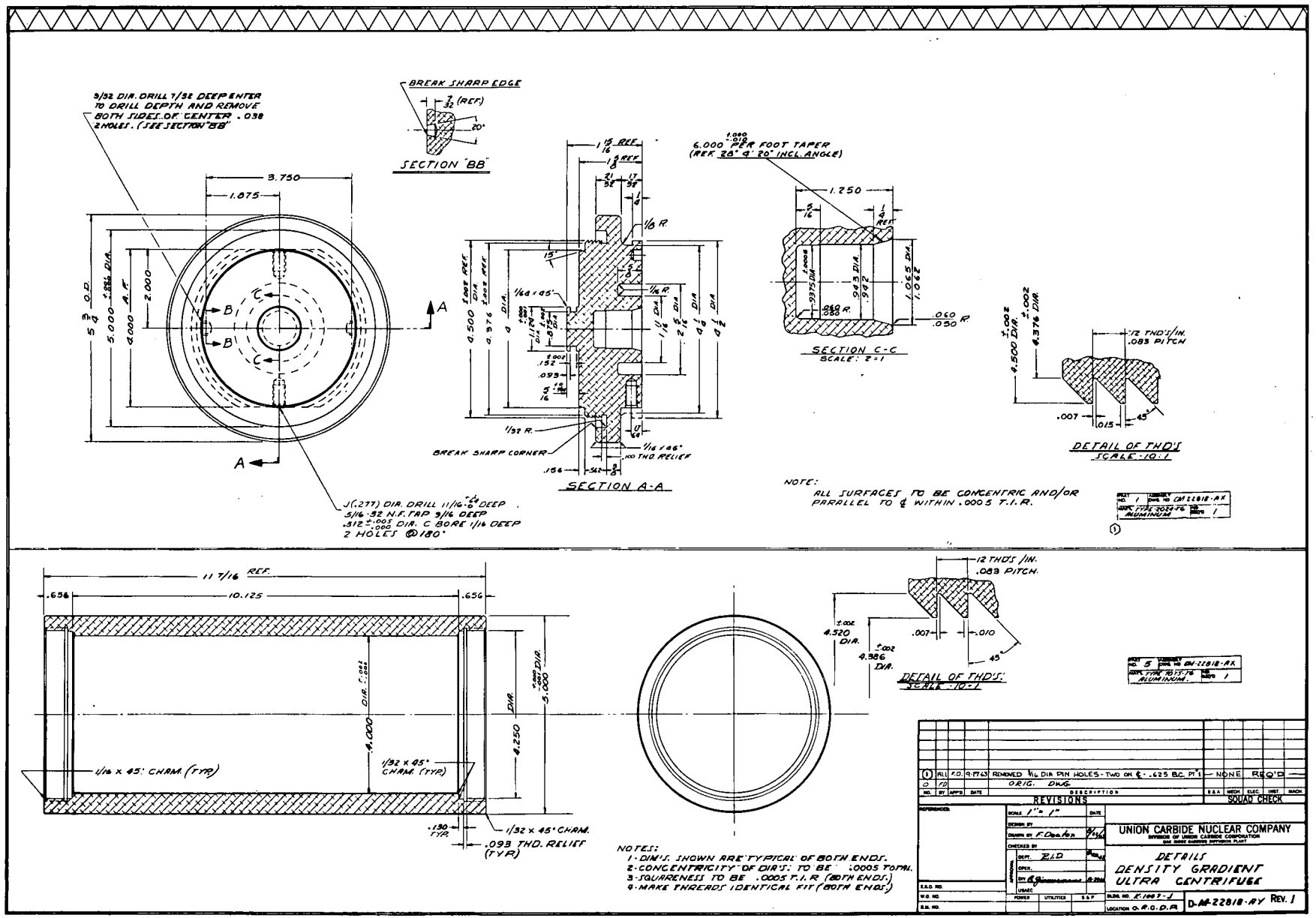
3/32 DIA. DRILL 7/32 DEEP ENTER TO DRILL DEPTH AND REMOVE BOTH SIDES OF CENTER .038 2 HOLES. (SEE SECTION "BB")
BREAK SHARP EDGE
SECTION "BB"
3.750
1.875
5 3/4 O.D.
5.000 ±.002 DIA.
4.000 A.F.
2.000
J(.277) DIA. DRILL 11/16 DEEP
5/16-32 N.F. TAP 3/16 DEEP
.312 +.005 -.000 DIA. C BORE 1/16 DEEP
2 HOLES @180°
BREAK SHARP CORNER
.100 THD. RELIEF
SECTION A-A
6.000 +.010 -.010 PER FOOT TAPER
(REF. 28° 4' 20" INCL. ANGLE)
SECTION C-C
SCALE: 2:1
12 THD'S/IN.
.083 PITCH
DETAIL OF THD'S
SCALE: 10:1
NOTE:
ALL SURFACES TO BE CONCENTRIC AND/OR PARALLEL TO ℄ WITHIN .0005 T.I.R.
11 7/16 REF.
10.125
1/16 x 45° CHAM. (TYP)
1/32 x 45° CHAM. (TYP)
.093 THD. RELIEF (TYP)
4.520 DIA.
4.386 DIA.
DETAIL OF THD'S
SCALE: 10:1
NOTES:
1. DIM'S. SHOWN ARE TYPICAL OF BOTH ENDS.
2. CONCENTRICITY OF DIA'S. TO BE .0005 TOTAL
3. SQUARENESS TO BE .0005 T.I.R. (BOTH ENDS.)
4. MAKE THREADS IDENTICAL FIT (BOTH ENDS.)
REVISIONS
NONE REQ'D
SQUAD CHECK
UNION CARBIDE NUCLEAR COMPANY
DETAILS
DENSITY GRADIENT
ULTRA CENTRIFUGE
D-M-22818-AY REV. 1

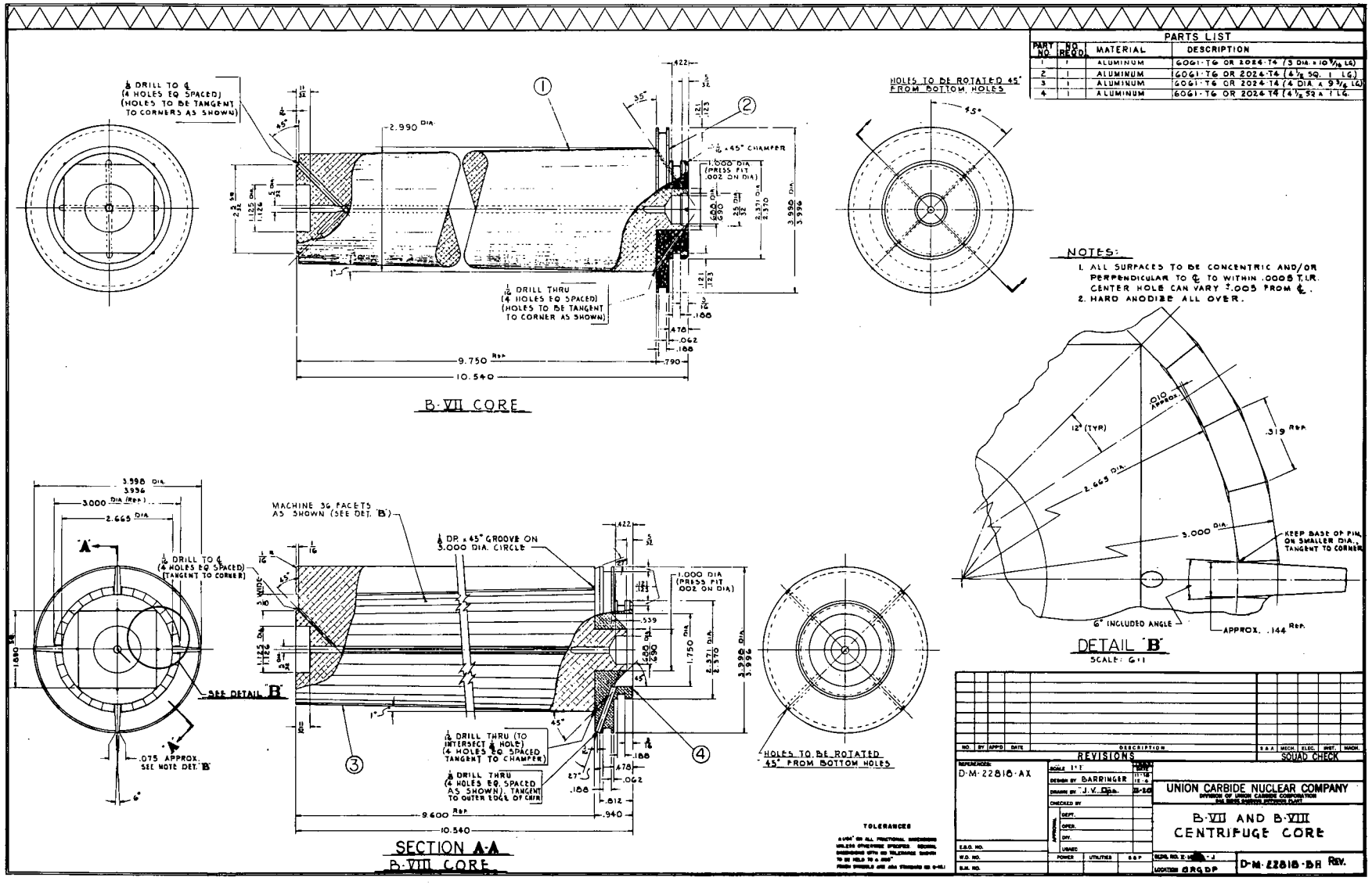
PARTS LIST
PART NO. | NO REQ'D. | MATERIAL | DESCRIPTION
1 | 1 | ALUMINUM | 6061-T6 OR 2024-T4 (3 DIA. x 10 5/16 LG)
2 | 1 | ALUMINUM | 6061-T6 OR 2024-T6 (4 1/2 SQ. 1 LG)
3 | 1 | ALUMINUM | 6061-T6 OR 2024-T4 (4 DIA. x 9 3/8 LG)
4 | 1 | ALUMINUM | 6061-T6 OR 2024-T4 (4 1/2 SQ. x 1 LG.
B-VII CORE
SECTION A-A
B-VII CORE
DETAIL "B"
SCALE: 6:1
NOTES:
1. ALL SURFACES TO BE CONCENTRIC AND/OR PERPENDICULAR TO ℄ TO WITHIN .0005 T.I.R. CENTER HOLE CAN VARY ±.005 FROM ℄.
2. HARD ANODIZE ALL OVER.
HOLES TO BE ROTATED 45° FROM BOTTOM HOLES
SEE DETAIL "B"
MACHINE 36 FACETS AS SHOWN (SEE DET. "B")
1/8 DR. x 45° GROOVE ON 3.000 DIA. CIRCLE
1/16 DRILL TO ℄ (4 HOLES EQ SPACED) (TANGENT TO CORNER)
1/8 DRILL TO ℄ (4 HOLES EQ SPACED) (HOLES TO BE TANGENT TO CORNERS AS SHOWN)
1/8 DRILL THRU (4 HOLES EQ SPACED) (HOLES TO BE TANGENT TO CORNER AS SHOWN)
1/16 DRILL THRU (TO INTERSECT 1/8 HOLE) (4 HOLES EQ SPACED TANGENT TO CHAMFER)
1/8 DRILL THRU (4 HOLES EQ. SPACED AS SHOWN) TANGENT TO OUTER EDGE OF CAVITY
1.000 DIA (PRESS FIT .002 ON DIA)
1/8 x 45° CHAMFER
.075 APPROX. SEE NOTE DET. "B"
6° INCLUDED ANGLE
APPROX. .144 REF.
KEEP BASE OF PIN ON SMALLER DIA., TANGENT TO CORNER
HOLES TO BE ROTATED 45° FROM BOTTOM HOLES
TOLERANCES
REVISIONS
SQUAD CHECK
D-M-22818-AX
UNION CARBIDE NUCLEAR COMPANY
B-VII AND B-VIII CENTRIFUGE CORE
D-M-22818-BA REV.

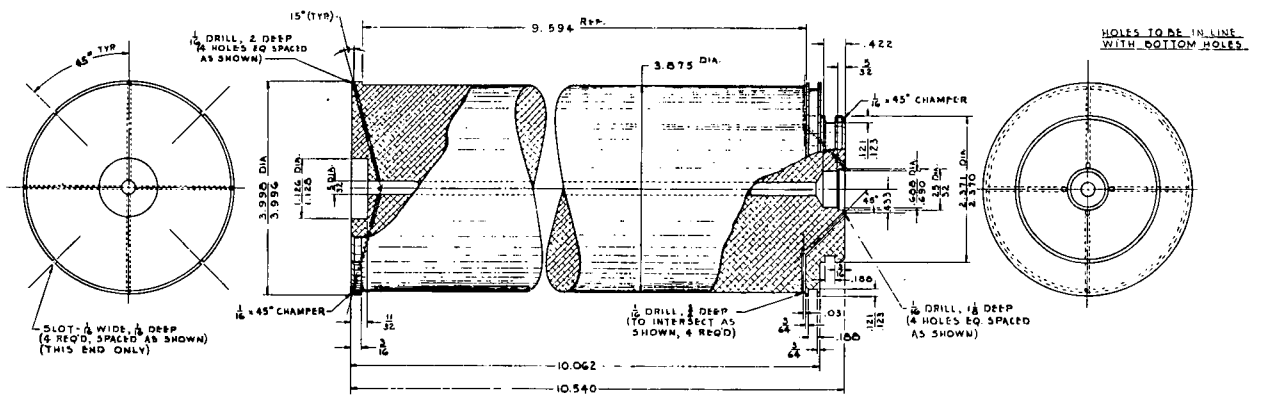

PART #1 - B·V CORE

PARTS LIST			
REF. NO.	NO. REQ'D	MATERIAL	DESCRIPTION
1	1	ALUMINUM	2024-T4 OR 6061-T6 (5 DIA. x 10 9/16 LG)
2	1	ALUMINUM	2024-T4 OR 6061-T6 (2 1/2 DIA x 10 9/16 LG)
3	1	ST. STEEL	TYPE 304 (1 1/16 DIA. x 1 7/16 LG.)
4	1	ALUMINUM	2024-T4 OR 6061-T6 (4 1/2 SQ. x 1 LG.

NOTES:
1. ALL SURFACES (PT. #3) TO BE CONCENTRIC AND/OR PERPENDICULAR TO THE ℄ TO WITHIN .001 T.I.R. EXCEPT 1/4 DIA. CENTER HOLE (PT. 1)
2. ALL SURFACES (PTS. 2 & 4) TO BE CONCENTRIC AND/OR PERPENDICULAR TO THE ℄ TO WITHIN .0005 T.I.R. CENTER HOLE MAY LEAD OFF BY ±.005.
3. HARD ANODIZE ALL OVER. (EXCEPT PT 3))

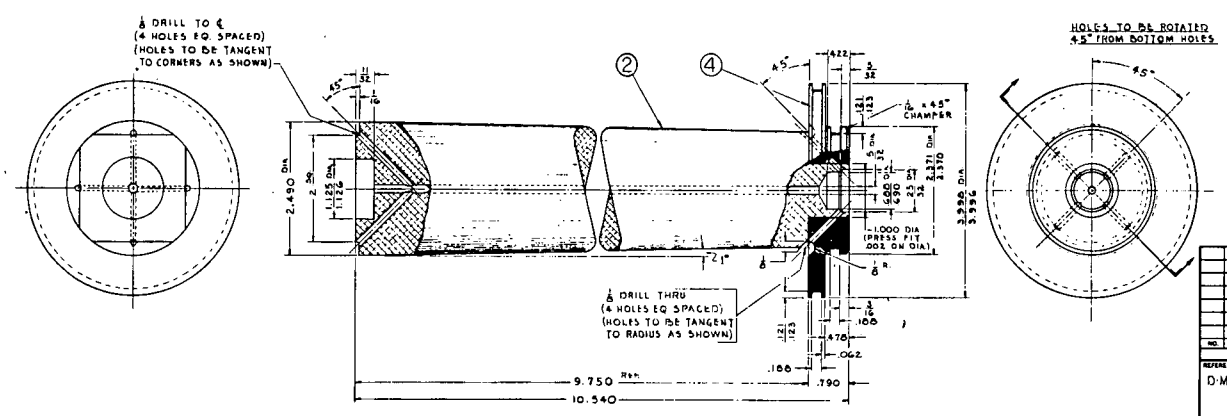

B·VI CORE

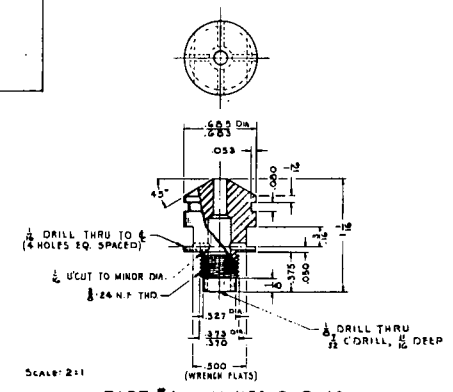

PART #3 - MANIFOLD PLUG

TOLERANCES
±.005" ON ALL FRACTIONAL DIMENSIONS UNLESS OTHERWISE SPECIFIED. DECIMAL DIMENSIONS WITH NO TOLERANCE SHOWN TO BE HELD TO ±.005"
FINISH STRESS ARE ASA STANDARD NO. B-46.1

NO.	BY	APP'D	DATE	DESCRIPTION	S & A	MECH.	ELEC.	INST.	MACH.
REVISIONS					SQUAD CHECK				

REFERENCES: D-M-22818-AX

SCALE 1:1 OR NOTED
DESIGN BY BARRINGER
DRAWN BY J.V. Dpa.
CHECKED BY
APPROVAL: DEPT. OPER. DIV. USAEC
E.R.D. NO.
W.O. NO.
S.R. NO.
POWER | UTILITIES | S & P

UNION CARBIDE NUCLEAR COMPANY
DIVISION OF UNION CARBIDE CORPORATION
OAK RIDGE GASEOUS DIFFUSION PLANT

B·V, B·VI CENTRIFUGE CORE AND MANIFOLD PLUG

BLDG. NO. K-1006-J
LOCATION ORGDP

D-M-22818-BG REV.

Appendix IV

BLOCK DIAGRAM AND SCHEMATIC REPRESENTATION OF MAGNETIC SUPPORT SYSTEM FOR D-1 ROTOR (ABBOT MASTER AVAILABLE)

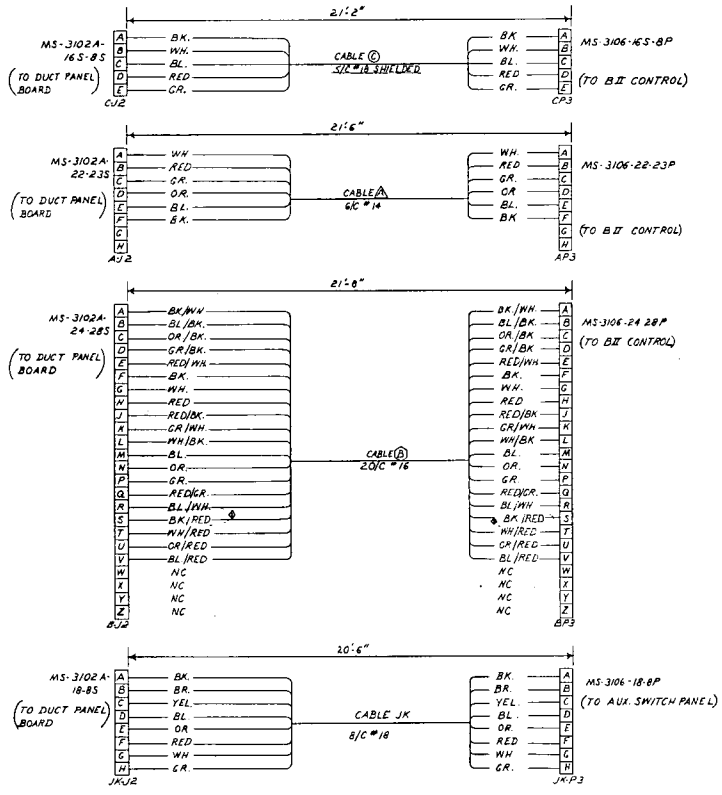

NOTE: A B C
COINCIDE WITH SYMBOLS ON
B II MACHINE SCHEMATIC D-I-30399B

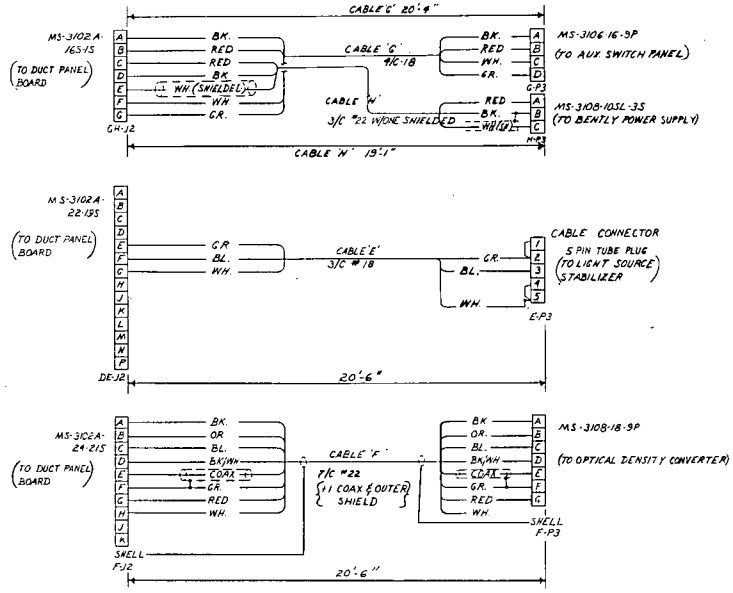

NO.	BY	APP'D	DATE	DESCRIPTION	S&A	MECH	ELEC	INST.	MACH
1	CRDJJ	7/16/63		Revised Wire Colors.	✓	✓	✓	✓	✓
0					✓	✓	✓	✓	✓

REVISIONS — SQUAD CHECK

REFERENCES: A-I-30399Z1

SCALE NONE — DATE

DESIGN BY BJB

DRAWN BY JCR 7-3-62

CHECKED BY BJB 7/16/63

APPROVAL: DEPT. DJJ 7/16/63; OPER. BJB 7/16/63; DIV. 7/16/63

UNION CARBIDE NUCLEAR COMPANY
DIVISION OF UNION CARBIDE CORPORATION
OAK RIDGE GASEOUS DIFFUSION PLANT

BIOLOGICAL ULTRA-CENTRIFUGE
B II MACHINE
DUCT CABLE DETAILS

E.S.D. NO. — W.O. NO. — E.N. NO. — USAEC — POWER — UTILITIES — S & P — BLDG. NO. — LOCATION

D-I-30399K REV. 1

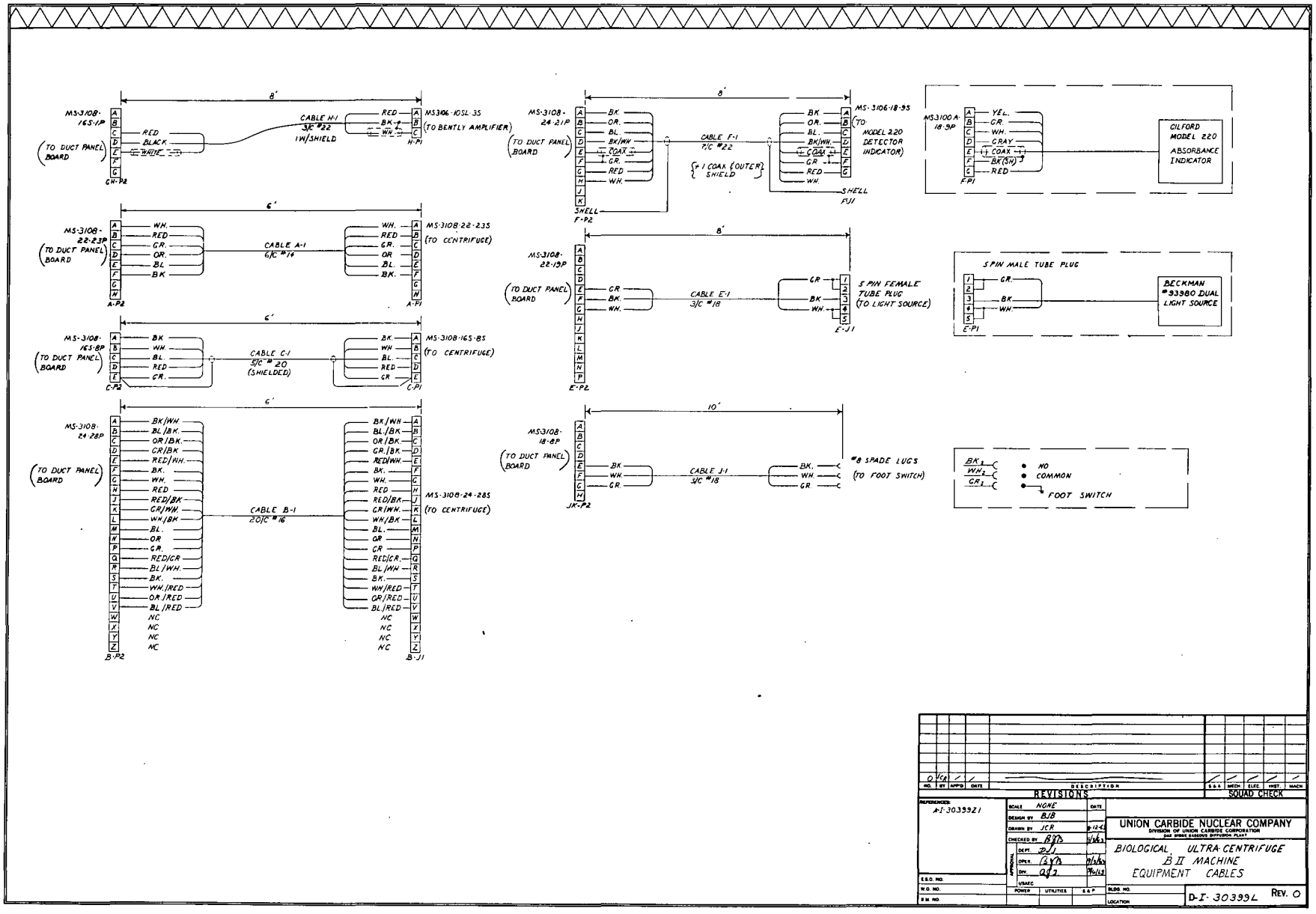
MS-3108-16S-1P
(TO DUCT PANEL BOARD)
GH-P2
RED
BLACK
WHITE
CABLE H-1
3/C #22
1W/SHIELD
MS3106-10SL-3S
(TO BENTLY AMPLIFIER)
H-P1
MS-3108-22-23P
(TO DUCT PANEL BOARD)
A-P2
CABLE A-1
6/C #14
MS-3108-22-23S
(TO CENTRIFUGE)
A-P1
MS-3108-16S-8P
(TO DUCT PANEL BOARD)
C-P2
CABLE C-1
5/C #20
(SHIELDED)
MS-3108-16S-8S
(TO CENTRIFUGE)
C-P1
MS-3108-24-28P
(TO DUCT PANEL BOARD)
B-P2
CABLE B-1
20/C #16
MS-3108-24-28S
(TO CENTRIFUGE)
B-J1
MS-3108-24-21P
(TO DUCT PANEL BOARD)
F-P2
CABLE F-1
7/C #22
+1 COAX (OUTER) SHIELD
MS-3106-18-9S
(TO MODEL 220 DETECTOR INDICATOR)
SHELL
F-J1
MS-3100A-18-9P
F-P1
GILFORD MODEL 220 ABSORBANCE INDICATOR
MS-3108-22-19P
(TO DUCT PANEL BOARD)
E-P2
CABLE E-1
3/C #18
5 PIN FEMALE TUBE PLUG
(TO LIGHT SOURCE)
E-J1
5 PIN MALE TUBE PLUG
E-P1
BECKMAN #93980 DUAL LIGHT SOURCE
MS-3108-18-8P
(TO DUCT PANEL BOARD)
JK-P2
CABLE J-1
3/C #18
#8 SPADE LUGS
(TO FOOT SWITCH)
NO
COMMON
FOOT SWITCH
REVISIONS
SQUAD CHECK
REFERENCES: A-I-303399Z1
SCALE NONE
DESIGN BY BJB
DRAWN BY JCR
CHECKED BY BJB
UNION CARBIDE NUCLEAR COMPANY
DIVISION OF UNION CARBIDE CORPORATION
PAD GASEOUS DIFFUSION PLANT
BIOLOGICAL ULTRA-CENTRIFUGE
B II MACHINE
EQUIPMENT CABLES
D-I-303399L
REV. 0

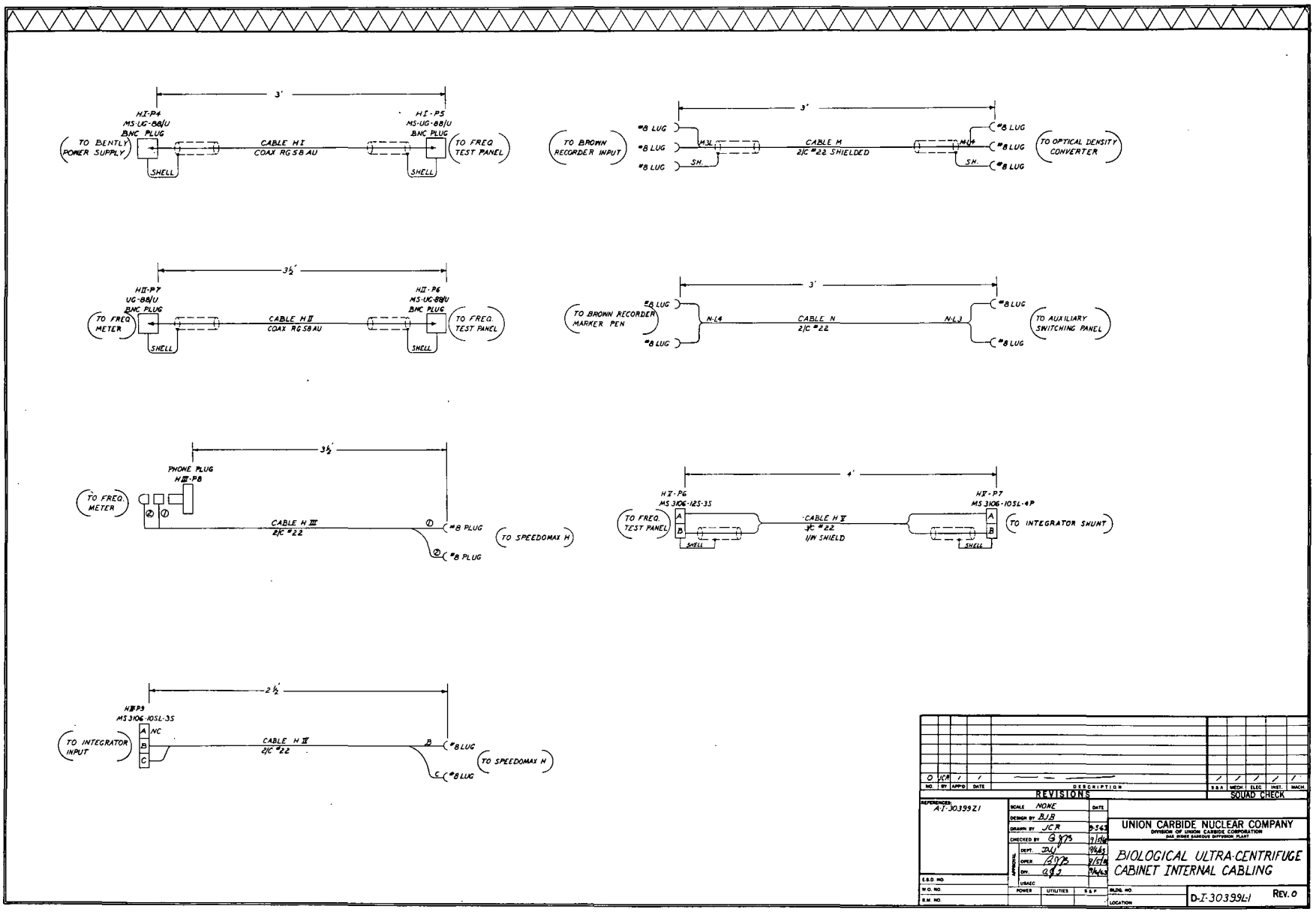
3'
H I-P4
MS-UG-88/U
BNC PLUG
TO BENTLY POWER SUPPLY
SHELL
CABLE H I
COAX RG58AU
H I-P5
MS-UG-88/U
BNC PLUG
SHELL
TO FREQ TEST PANEL
3'
#8 LUG
#8 LUG
#8 LUG
TO BROWN RECORDER INPUT
M-L1
SH.
CABLE M
2/C #22 SHIELDED
M-L4
SH.
#8 LUG
#8 LUG
#8 LUG
TO OPTICAL DENSITY CONVERTER
3½'
H II-P7
UG-88/U
BNC PLUG
TO FREQ METER
SHELL
CABLE H II
COAX RG58AU
H II-P6
MS-UG-88/U
BNC PLUG
SHELL
TO FREQ. TEST PANEL
3'
#8 LUG
#8 LUG
TO BROWN RECORDER MARKER PEN
N-L4
CABLE N
2/C #22
N-L3
#8 LUG
#8 LUG
TO AUXILIARY SWITCHING PANEL
3½'
PHONE PLUG
H III-P8
TO FREQ. METER
②
①
CABLE H III
2/C #22
①
#8 PLUG
②
#8 PLUG
TO SPEEDOMAX H
4'
H I-P6
MS 3106-125-3S
TO FREQ. TEST PANEL
A
B
SHELL
CABLE H V
3/C #22
1/W SHIELD
H V-P7
MS 3106-10SL-4P
A
B
SHELL
TO INTEGRATOR SHUNT
2½'
H III-P9
MS 3106-10SL-3S
TO INTEGRATOR INPUT
A
B
C
NC
CABLE H III
2/C #22
B
#8 LUG
C
#8 LUG
TO SPEEDOMAX H
0
JCR
NO.
BY
APP'D
DATE
DESCRIPTION
REVISIONS
S&A
MECH.
ELEC.
INST.
MACH.
SQUAD CHECK
REFERENCES:
A-I-30399Z1
SCALE NONE
DESIGN BY BJB
DRAWN BY JCR
CHECKED BY
DEPT.
OPER.
DIV.
APPROVALS
USAEC
POWER
UTILITIES
S & P
E.S.D. NO.
W.O. NO.
B.M. NO.
BLDG. NO.
LOCATION
UNION CARBIDE NUCLEAR COMPANY
DIVISION OF UNION CARBIDE CORPORATION
OAK RIDGE GASEOUS DIFFUSION PLANT
BIOLOGICAL ULTRA-CENTRIFUGE
CABINET INTERNAL CABLING
D-I-30399L-1
REV. 0

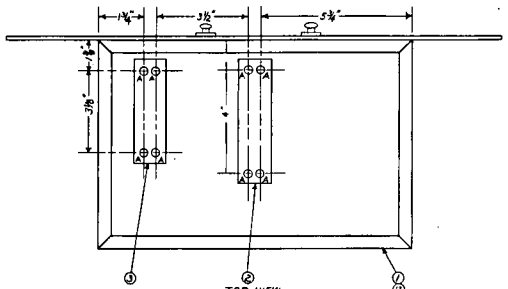

TOP VIEW
(COVER PLATE REMOVED)

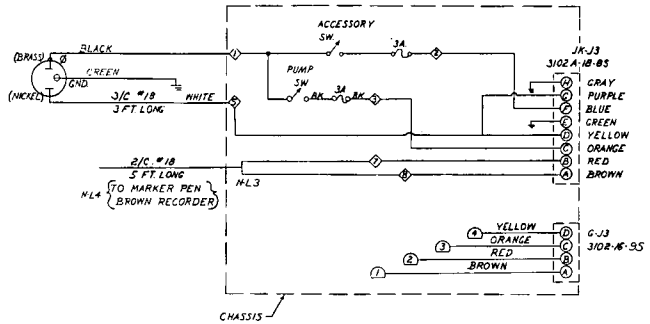

WIRING SCHEMATIC
SCALE - NONE

NOTES:

1. ◇ DENOTES CONNECTION AT 8 TERMINAL JONES STRIP
2. ⌒ DENOTES CONNECTION AT 6 TERMINAL JONES STRIP
3. ENGRAVE CHARACTERS ON FRONT PANEL ⅛" LETTERS FILL WITH BLACK PAINT- AFFIX CHARACTERS TO REAR OF CHASSIS USE ⅛" HIGH LETTERS.

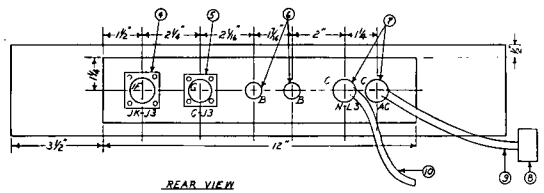

REAR VIEW

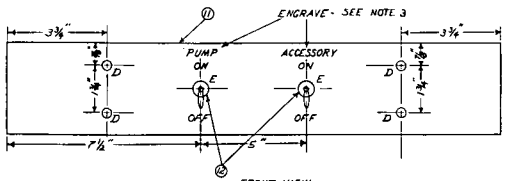

FRONT VIEW
SCALE - 1-2

HOLE SCHEDULE		
LOC.	SIZE	QUAN.
A	5/32 DIA.	8
B	5/8 DIA.	2
C	7/8" DIA.	2
D	#7 DRILL	4
E	15/16" DIA.	2
F	DET. 1	1
G	DET. 2	1

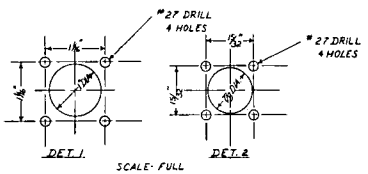

DET. 1 DET. 2
SCALE - FULL

ITEM	DESCRIPTION	QUAN.	REMARKS
13	CHASSIS COVER PLATE	1	12"x8"x 1/16" STEEL CAD. PLATE
12	TOGGLE SWITCH	2	C-H D.P.D.T.
11	PANEL-ALUMINUM	1	19"x 3½"x ⅛" CLEAR ANODIZED
10	2/C #18 CABLE	5 FT.	
9	3/C #18 CABLE	3 FT.	
8	HUBBELL MALE CAP	1	NEMA STD 10 V. AC 15 AMP
7	CABLE CLAMP	2	½" CONDUIT SIZE
6	FUSE HOLDER	2	BUSSMAN WITH 3 AMP FUSE
5	BOX CONNECTOR	1	MS-3102A-16-9S
4	BOX CONNECTOR	1	MS-3102A-18-18S
3	TERMINAL BLOCK	1	6 POINT-CINCH-JONES
2	TERMINAL BLOCK	1	8 POINT-CINCH-JONES
1	CHASSIS 12"x8"x2½"	1	STEEL CADMIUM PLATE

NO.	BY	APP'D	DATE	DESCRIPTION	B&A	MECH.	ELEC.	INST.	MACH.
0									

REVISIONS — SQUAD CHECK

REFERENCED: A-I-3039921

SCALE AS NOTED
DESIGN BY B.J.B.
DRAWN BY J.C.R.
CHECKED BY
DEPT. 7-41
OPER.
DIV.
USAEC
E.S.O. NO.
W.O. NO.
B.M. NO.
POWER | UTILITIES | B&P
BLDG. NO.
LOCATION

UNION CARBIDE NUCLEAR COMPANY
DIVISION OF UNION CARBIDE CORPORATION
OAK RIDGE GASEOUS DIFFUSION PLANT

BIOLOGICAL ULTRA-CENTRIFUGE
B II MACHINE
AUXILIARY SWITCHING PANEL

D-I-30399M REV. 0.

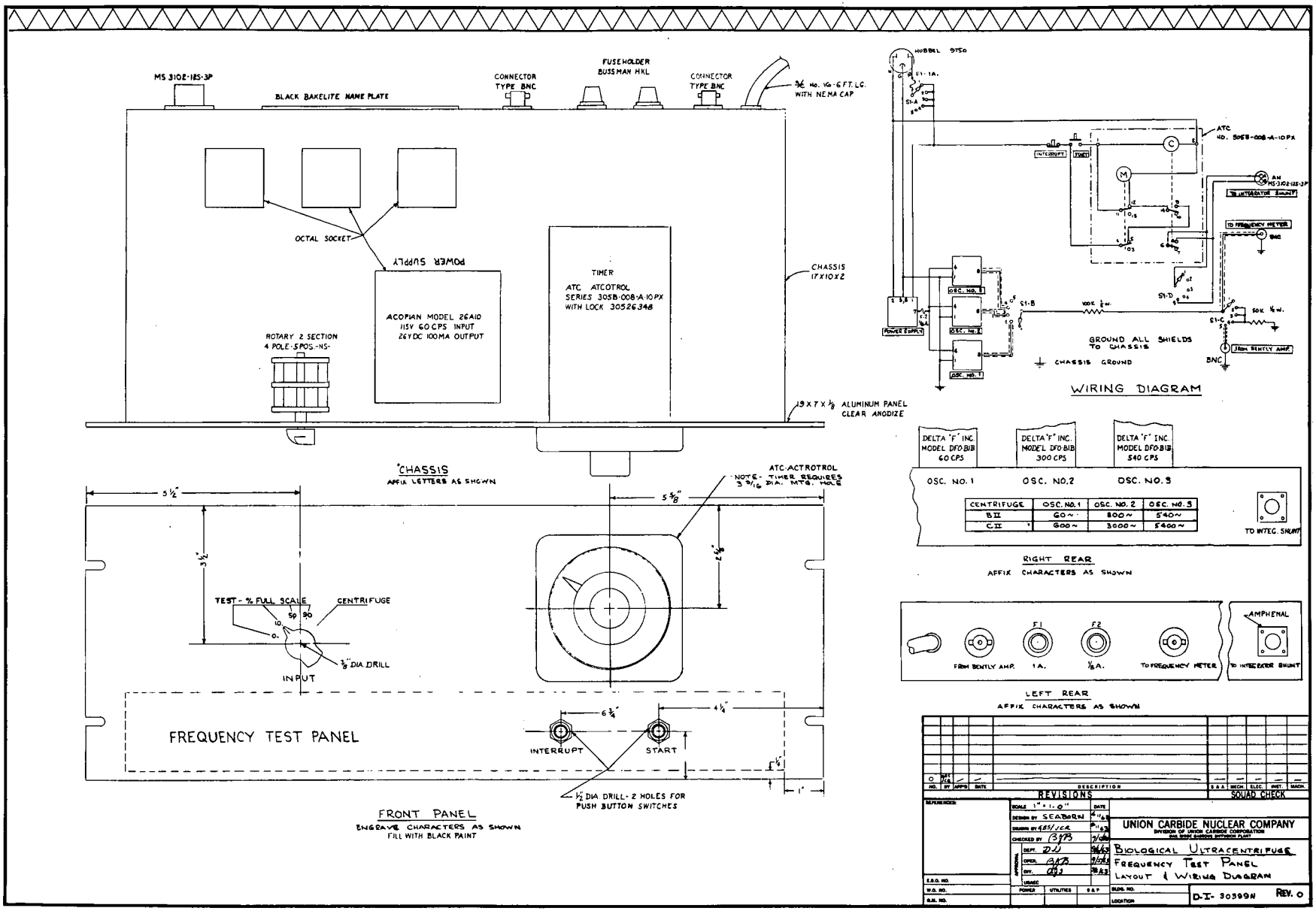
MS 3102E-12S-3P
BLACK BAKELITE NAME PLATE
CONNECTOR TYPE BNC
FUSEHOLDER BUSSMAN HKL
CONNECTOR TYPE BNC
3/8 No. 16-6 FT. LG. WITH NEMA CAP
OCTAL SOCKET
POWER SUPPLY
ACOPIAN MODEL 26A10 115V 60 CPS INPUT 26VDC 100MA OUTPUT
TIMER
ATC ATCOTROL SERIES 305B-008-A-10PX WITH LOCK 30526348
ROTARY 2 SECTION 4 POLE-5 POS.-NS-
CHASSIS 17X10X2
19 X 7 X 1/8 ALUMINUM PANEL CLEAR ANODIZE
CHASSIS
AFFIX LETTERS AS SHOWN
NOTE- TIMER REQUIRES 3 5/16 DIA. MTG. HOLE
ATC-ACTROTROL
5 1/2"
5 5/8"
3 1/2"
2 5/8"
TEST - % FULL SCALE
CENTRIFUGE
INPUT
3/8" DIA DRILL
FREQUENCY TEST PANEL
INTERRUPT
START
6 3/4"
4 1/4"
1 1/4"
1"
1/2 DIA DRILL - 2 HOLES FOR PUSH BUTTON SWITCHES
FRONT PANEL
ENGRAVE CHARACTERS AS SHOWN
FILL WITH BLACK PAINT
HUBBELL 9750
F1-1A.
S1-A
INTERRUPT
TIMER
ATC NO. 305B-008-A-10PX
AM MS 3102-12S-3P
TO INTEGRATOR SHUNT
TO FREQUENCY METER
BNC
OSC. NO. 3
OSC. NO. 2
OSC. NO. 1
POWER SUPPLY
S1-B
100K 1/4 W.
S1-D
S1-C
50K 1/4 W.
FROM BENTLY AMP.
GROUND ALL SHIELDS TO CHASSIS
CHASSIS GROUND
WIRING DIAGRAM
DELTA "F" INC. MODEL DFO-B1B 60 CPS
DELTA "F" INC. MODEL DFO-B1B 300 CPS
DELTA "F" INC. MODEL DFO-B1B 540 CPS
OSC. NO. 1
OSC. NO. 2
OSC. NO. 3
CENTRIFUGE | OSC. NO. 1 | OSC. NO. 2 | OSC. NO. 3
B II | 60~ | 300~ | 540~
C II | 600~ | 3000~ | 5400~
TO INTEG. SHUNT
RIGHT REAR
AFFIX CHARACTERS AS SHOWN
F1
F2
FROM BENTLY AMP.
1A.
1/8A.
TO FREQUENCY METER
AMPHENAL
TO INTEGRATOR SHUNT
LEFT REAR
AFFIX CHARACTERS AS SHOWN
REVISIONS
NO. BY APPD DATE DESCRIPTION
SQUAD CHECK
SCALE 1" = 1.0"
DESIGN BY SEABORN
DRAWN BY
CHECKED BY
APPROVAL
UNION CARBIDE NUCLEAR COMPANY
DIVISION OF UNION CARBIDE CORPORATION
OAK RIDGE GASEOUS DIFFUSION PLANT
BIOLOGICAL ULTRACENTRIFUGE
FREQUENCY TEST PANEL
LAYOUT & WIRING DIAGRAM
D-I-30399N
REV. 0

PARTS LIST				
PART NO.	DWG. NO.	NO. REQD.	DESCRIPTION (NAME, SIZE, ETC.)	MATERIAL
1	E-I-13017E	1	SHAFT EXTENSION, 2 15/32" LG. x 0.3125" DIA.	STEEL
2	"	1	SPACER PLATE, 2" LG. x 1 1/4" W x 3/4" H	ALUMINIUM
3	"	1	SPACER ROD, 2" LG. x 1/2" DIA.	ALUMINIUM
4	"	2	COLLAR, 5/8" LG. x 5/8" DIA.	BRASS
5	"	1	SPROCKET, (1 EA.) FURNISHED BOSTON GEAR #CA-12, 12 TEETH, STORES Nº 07-DRO-0630	STEEL
6	"	6	SCREW, ROUND HEAD, 8-32 NF x 1/2" LG.	STEEL
7	"	1	HOUSING, SPEEDOMETER RATIO ASSEMBLY, STEWART WARNER #7778, RATIO 1.1110 VENDOR: R.T. CLAPP 2016 MAGNOLIA AVE. KNOXVILLE	
8	"	2	8-32 NF x 1/8" HOLLOW POINT HEADLESS SET SCREW	STEEL
9	"	1	10-32 NF x 1/8 HOLLOW POINT HEADLESS SET SCREW	STEEL

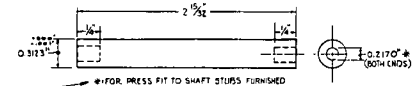

BEFORE PRESS FITTING SHAFT STUBS, SKIM GRIND SMALLER DIAMETER CONCENTRIC WITH LARGER DIA. SHAFT STUBS MUST BE CONCENTRIC WITH SHAFT EXTENSION AFTER PRESS FITTING

SHAFT EXTENSION

PART (1)

STEEL

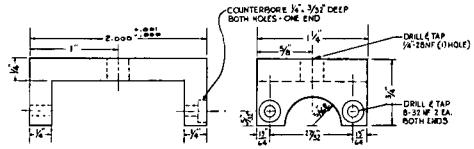

SPACER PLATE

PART (2)

ALUMINIUM

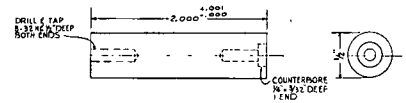

SPACER ROD

PART (3)

ALUMINUM

NOTES:

(1) REMOVE RETAINING RING FROM 0.175" END OF SHAFT SOCKET.

(2) ASSEMBLE WITH SHAFT SOCKETS
a) 0.203" I.D. ON MALE END OF HOUSING TO PERMIT 0.187" END OF INSERT TO PROJECT OUT OF HOUSING.
b) 0.1875" I.D. ON FEMALE END OF HOUSING

(3) CUT 1/4" FROM KEYWAY END OF MATING FLEXIBLE SHAFT TO FIT FEMALE SHAFT SOCKET END

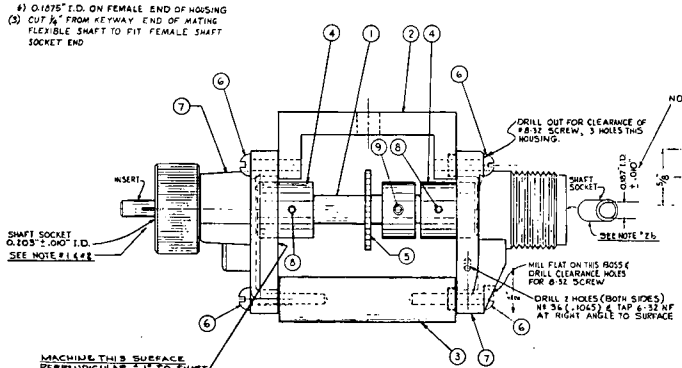

ASSEMBLY

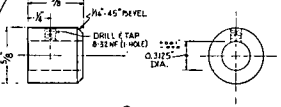

COLLAR

PART (4)

BRASS

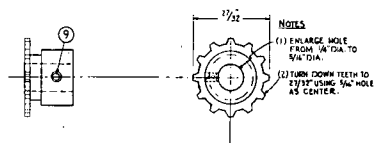

NOTES

(1) ENLARGE HOLE FROM 1/4" DIA. TO 5/16" DIA.

(2) TURN DOWN TEETH TO 27/32" USING 5/16" HOLE AS CENTER.

SPROCKET

PART (5)

STEEL

NO	BY	APPD	DATE	DESCRIPTION	E.S.A.	MECH	ELEC	INST	MACH

REVISIONS

SQUAD CHECK

REFERENCES: A-I 30399Z1

SCALE: TWICE SIZE

DESIGN BY: TECH. DIV.

DRAWN BY: JCR / RJM

CHECKED BY: CSB

APPROVALS: DEPT. JJJ; OPER. ASB; ENG. CSB

UNION CARBIDE NUCLEAR COMPANY
DIVISION OF UNION CARBIDE CORPORATION
OAK RIDGE GASEOUS DIFFUSION PLANT

CENTRIFUGE TACHOMETER ADAPTOR

E-I-30399P REV. 0

TOLERANCES

E.S.D. NO

W.O. NO

S.W. NO

POWER | UTILITIES | S.A.P.

BLDG. NO

LOCATION

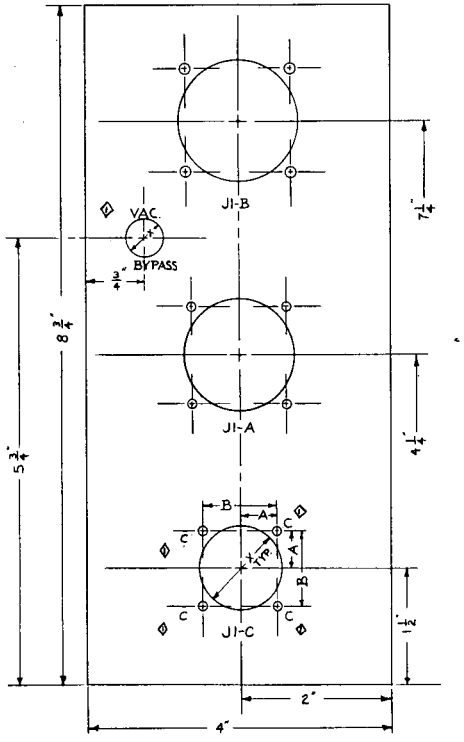

CENTRIFUGE MACHINE CONNECTOR PANEL

MATERIAL: 1/8" THICK HARD ALUMINUM
SOCKET LETTER IDENTIFICATION 1/8" BLACK

CONNECTOR INS.	X	A	B	C
J1-B MS3102-24-28S	1 9/16"	11/16"	1 3/8"	0.147"
J1-A MS3102-22-23S	1 7/16"	5/8"	1 1/4"	0.120"
J1-C MS3102-16S-8S	1 1/16"	31/64"	31/32"	0.120"
VAC. BYPASS SPST TOG. SW	1/2"			

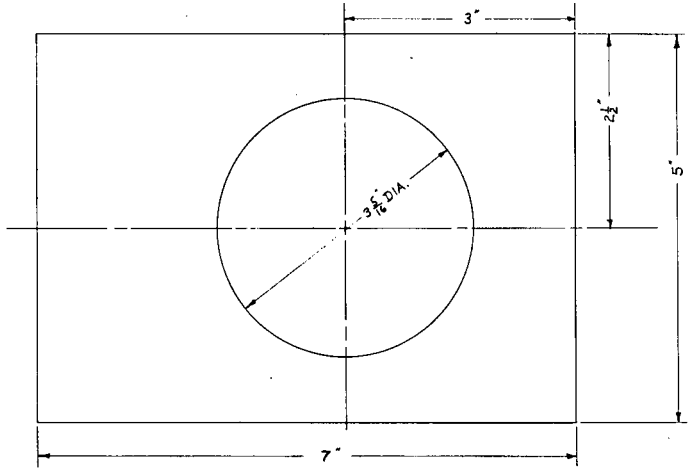

CENTRIFUGE TACHOMETER METER PANEL

MATERIAL: 1/8" THICK HARD ALUMINUM

NO.	BY	APPD.	DATE	DESCRIPTION
1	JCR	RW	9/27/63	REV. HOLE DESIG. & ADDED SWITCH

REVISIONS

S & A / MECH. / ELEC. / INST. / MACH.
SQUAD CHECK

REFERENCES: A-I-303982
E. S. O. NO.
W. O. NO.
B. M. NO.
POWER | UTILITIES | S & P

		DATE
SCALE	FULL	
DESIGN BY	BJB	
DRAWN BY	JCR	5-23-63
CHECKED BY	BJB	9-25-63
APPROVAL DEPT.	DJJ	9/25/63
OPER.	BJB	9/25/63
DIV.	DJJ	9/25/63
USAEC		

UNION CARBIDE NUCLEAR COMPANY
DIVISION OF UNION CARBIDE CORPORATION
OAK RIDGE GASEOUS DIFFUSION PLANT

BIOLOGICAL ULTRA-CENTRIFUGE
BII MACHINE CONNECTOR PANELS

BLDG. NO. –
LOCATION –

C-I-30399R REV. 1

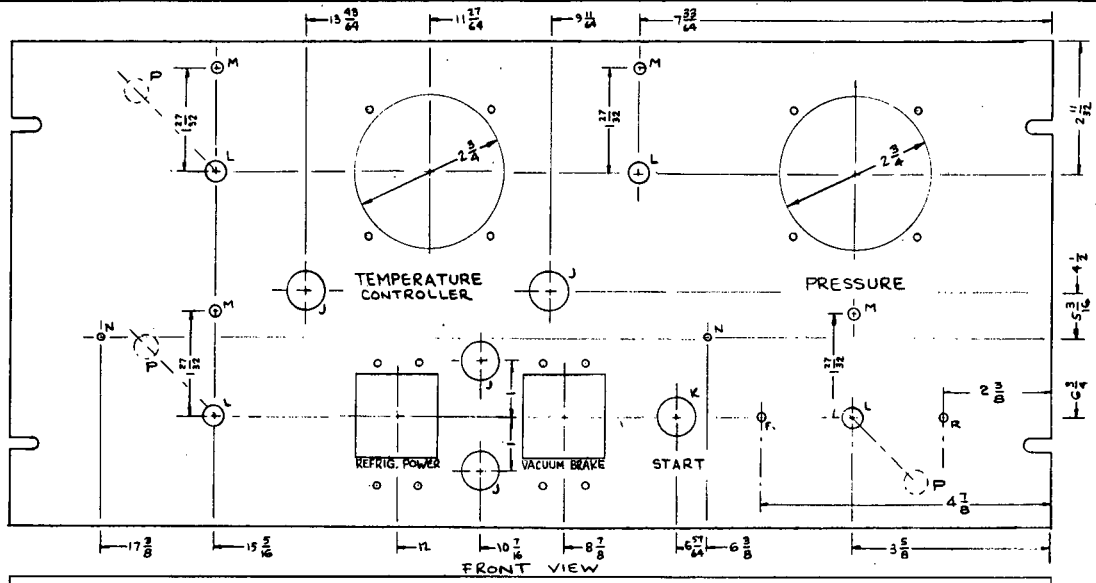

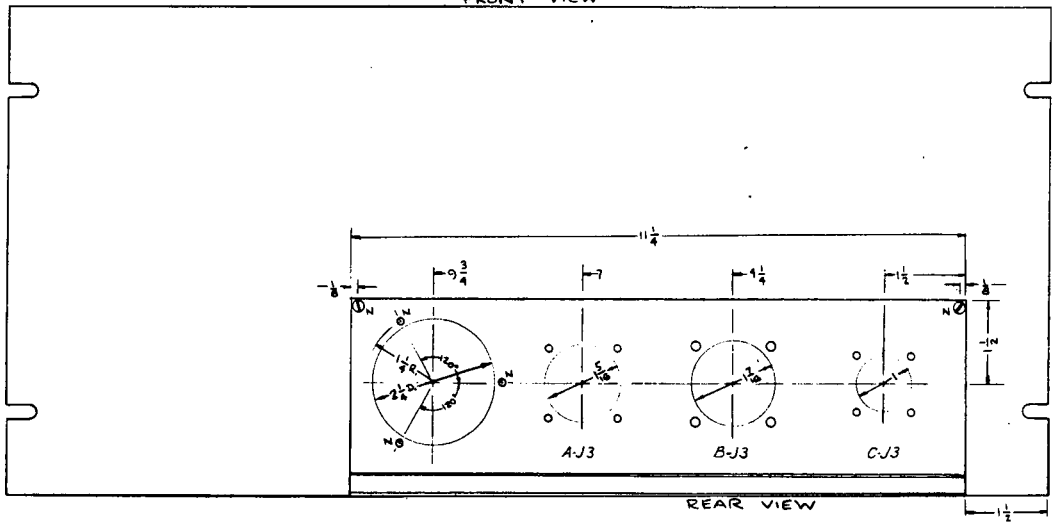

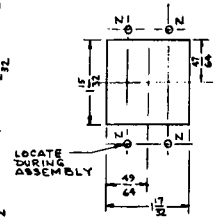

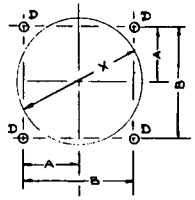

X	A	B	D
2 3/4	1 1/8	2 1/4	25
1 3/16	5/8	1 1/4	30
1 7/16	11/16	1 3/8	25
1	31/64	31/32	30

LETTER	HOLE SIZE
J	11/16
K	1/2
L	3/8
M	NO. 7
N	NO. 25
P	SEE NOTE 5
R	3/16

NOTES
1. SPOT WELD ITEM 2 TO ITEM 1.
2. TAP ENDS OF ITEM 3 - 6-32 × 1/2
3. AFTER FABRICATION, PAINT HAMMERTONE GRAY.
4. ENGRAVE AS SHOWN, FILL WHITE.
5. DRILL HOLE AT ASSEMBLY & INSTALL DIAL LOCKS.

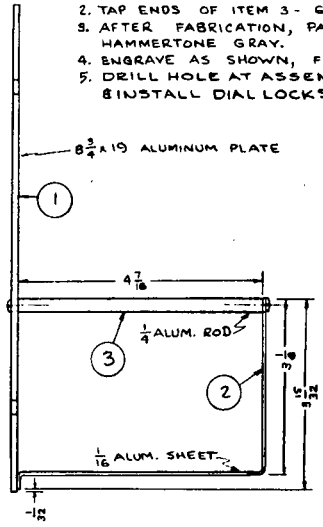

NO.	BY	APPD.	DATE	DESCRIPTION
0	JCR	—	—	

REVISIONS

SQUAD CHECK: S&A, MECH., ELEC., INST., MACH.

POWER | UTILITIES | S&P

REFERENCES: A-I-30399 Z1

E.S.O. NO. —
W.O. NO. —
B.R. NO. —

APPROVAL		DATE
SCALE 3/4" = 1.0"		
DESIGN BY GBS		1-24-63
DRAWN BY JCR		8/7/63
CHECKED BY RBB		8/7/63
DEPT. DJJ		8/8/63
OPER. RBB		8/8/63
DIV. QJJ		8/8/63
USAEC		

UNION CARBIDE NUCLEAR COMPANY
DIVISION OF UNION CARBIDE CORPORATION
OAK RIDGE GASEOUS DIFFUSION PLANT

BIOLOGICAL ULTRACENTRIFUGE
B-II CONTROL PANEL

BLDG. NO.
LOCATION

C-I-30399 H REV. 0

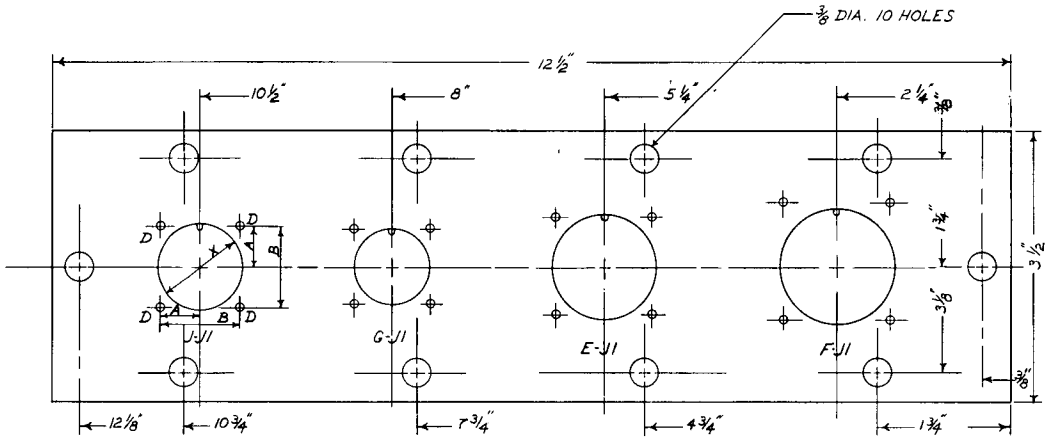

CONN.	INSERT	X	A	B	D
J-J1	18-8S	1 3/16	17/32	1 1/16	0.120
G-J1	16S-1S	1 1/16	3/64	3/32	0.120
E-J1	22-19S	1 1/16	5/8	1 1/4	0.120
F-J1	24-21S	1 3/16	11/16	1 3/8	0.147

GLOVE BOX CONNECTOR PANEL

MATERIAL: STAINLESS STEEL 16 GA.

NOTE: 1. AFFIX CONNECTOR CHARACTERS AS SHOWN

2. CONNECTOR KEYWAY TO BE VERTICAL AT THE TOP (MS-3102)

3. WIRE AND POT CONNECTORS PER INSTRUCTIONS AT ASSEMBLY

NO.	BY	APPD.	DATE	DESCRIPTION	S&A	MECH.	ELEC.	INST.	MACH.
0	JCR	/	/		/	/	/	/	/

REVISIONS — SQUAD CHECK

REFERENCES: A-I-303932I

E. S. O. NO. –

W. O. NO.

B. M. NO.

POWER	UTILITIES	S & P

APPROVAL		DATE
SCALE 1:1		
DESIGN BY BJB		8/23/63
DRAWN BY JCR		8-28-63
CHECKED BY RJM		9/1/63
DEPT. LJJ		9/1/63
OPER. RSD/B		9/1/63
DIV. agj		9/4/63
USAEC		

UNION CARBIDE NUCLEAR COMPANY
DIVISION OF UNION CARBIDE CORPORATION
OAK RIDGE GASEOUS DIFFUSION PLANT

BIOLOGICAL ULTRA-CENTRIFUGE GLOVE BOX CONNECTOR PANEL

BLDG. NO.

LOCATION

C-I-30399J-1 REV. 0

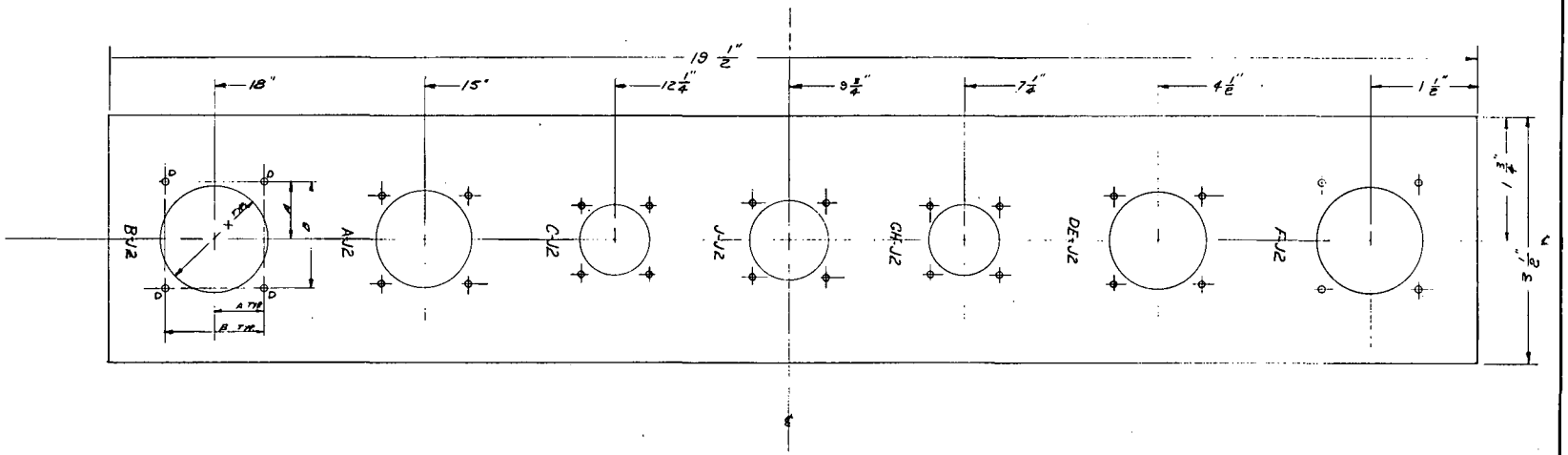

DUCT CONNECTOR PANEL

MATERIAL: HARD ALUMINUM 1/8" THICK

NOTE: 1. AFFIX CONNECTOR CHARACTERS AS SHOWN
2. CONNECTOR KEYWAY TO BE VERTICAL AT THE TOP
3. CHASSIS CONNECTORS TO BE MS-3102 WITH INSERTS AS LISTED

CONN.	INSERT	X	A	B	D
B-J2	24-28S	1 9/16	11/16	1 3/8	0.147
A-J2	22-23S	1 7/16	5/8	1 1/4	0.120
C-J2	16-8S	1 5/16	31/64	31/32	0.120
J-J2	18-8S	1 9/16	27/32	1 1/16	0.120
GH-J2	16S-1S	1 5/16	51/64	29/32	0.120
DE-J2	22-19S	1 7/16	5/8	1 1/4	0.120
F-J2	24-21S	1 9/16	11/16	1 3/8	0.147

NO.	BY	APPD.	DATE	DESCRIPTION	S&A	MECH.	ELEC.	INST.	MACH.
1	JCR	BJB	8-29-63	ADDED NOTE 3	/	/	/	DJJ	/
0	JCR	—	—	—	/	/	/	/	/

REVISIONS — SQUAD CHECK

REFERENCED: A-I-3039921
E. S. O. NO. –
W. O. NO. –
B. R. NO. –
POWER | UTILITIES | S & P

		DATE
SCALE	1 = 1	
DESIGN BY	RJTB	6/11/63
DRAWN BY	JCR	8/7/63
CHECKED BY	RJTB	8/7/63
APPROVAL DEPT.	DJJ	8/8/63
OPER.	RJB	8/8/63
DIV.	DJJ	8/8/63
USAEC		

UNION CARBIDE NUCLEAR COMPANY
DIVISION OF UNION CARBIDE CORPORATION
OAK RIDGE GASEOUS DIFFUSION PLANT

BIOLOGICAL ULTRACENTRIFUGE
DUCT CONNECTOR PANEL

BLDG. NO.
LOCATION

C-I 30399 J REV. 1

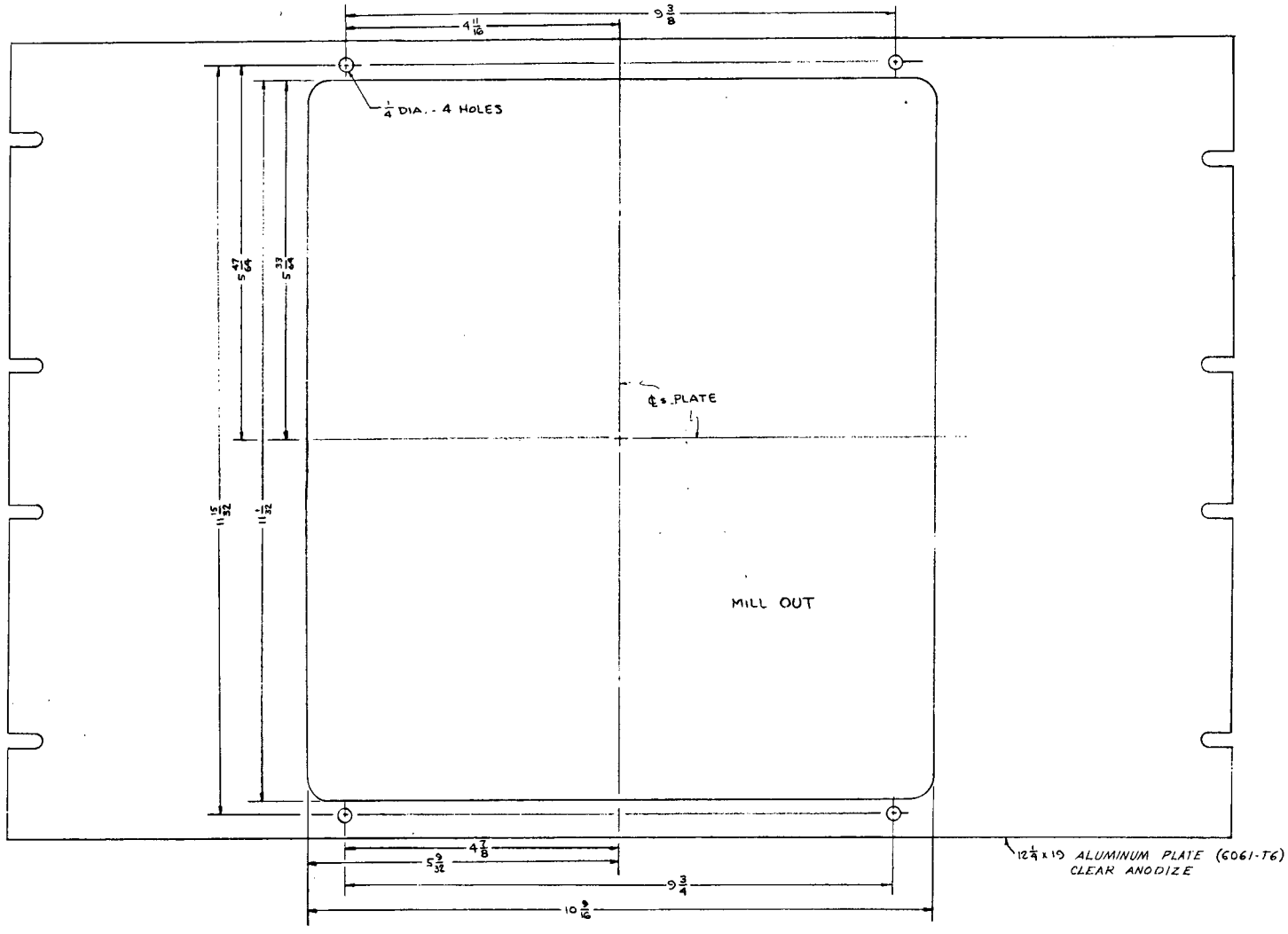

NO.	BY	APPD.	DATE	DESCRIPTION

REVISIONS

S & A	MECH.	ELEC.	INST.	MACH.

SQUAD CHECK

REFERENCED: A-I-3039921

E. B. O. NO. —
W. O. NO. —
B. N. NO. —

POWER	UTILITIES	S & P

		DATE
SCALE FULL		
DESIGN BY GBS		1/24/63
DRAWN BY JCA		8/7/63
CHECKED BY GBS		8/7/63
APPROVAL DEPT. DJV		8/7/63
OPER. BDS		8/11/63
DIV. GSJ		8/11/63
USAEC		

UNION CARBIDE NUCLEAR COMPANY
DIVISION OF UNION CARBIDE CORPORATION
OAK RIDGE GASEOUS DIFFUSION PLANT

BIOLOGICAL CENTRIFUGE
SPEEDOMAX PLATE

BLDG. NO.
LOCATION

C-I-303996 REV. 0

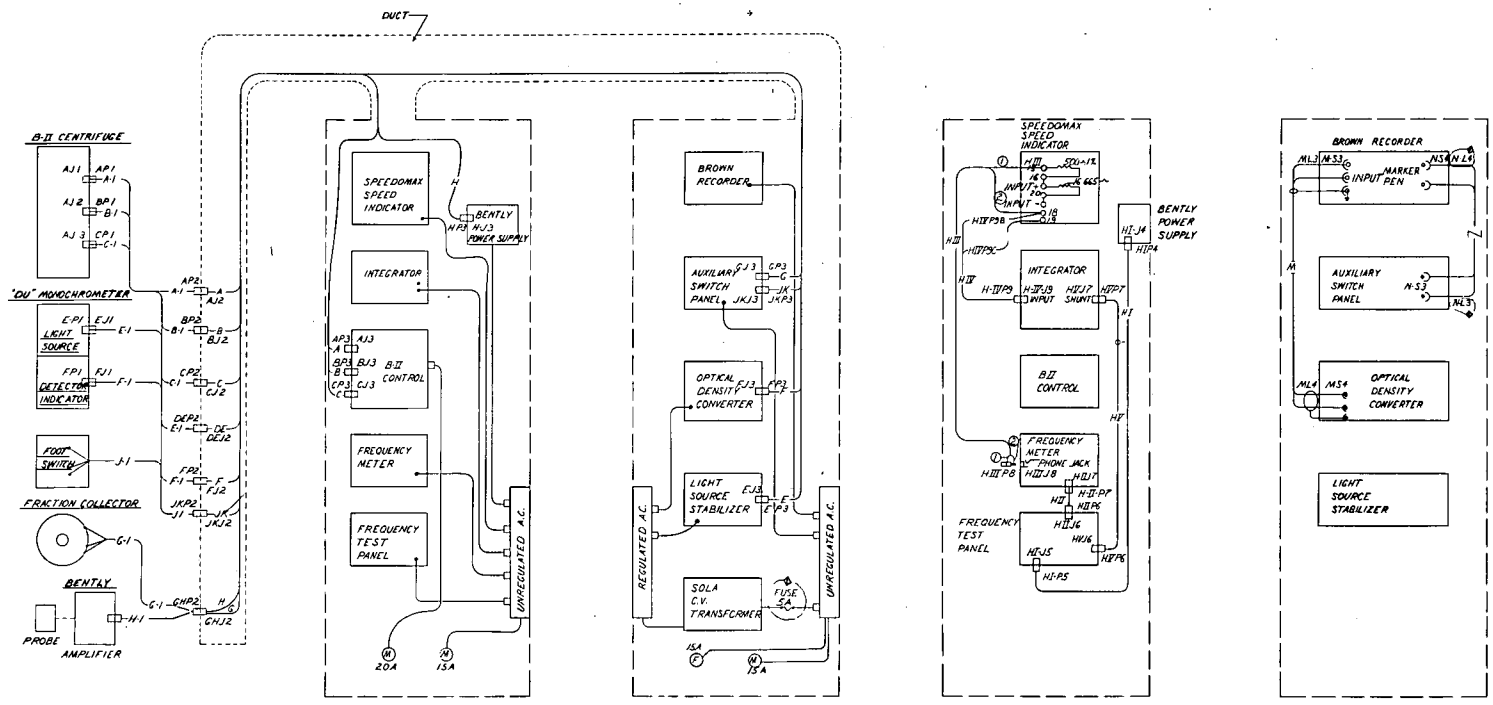

CONTROL CABINET REAR VIEW

ANALYTICAL CABINET REAR VIEW

CONTROL CABINET INTERNAL REAR CABLING VIEW

ANALYTICAL CABINET INTERNAL REAR CABLING VIEW

NO.	BY	APP'D	DATE	DESCRIPTION	E&A	MECH.	ELEC.	INST.	MACH.
1	HF	DJ	7/17/63	Revised wire basis & added chart	✓	✓	✓	✓	✓
0	—	—	—		✓	✓	✓	✓	✓

REVISIONS — SQUAD CHECK

REFERENCES: A-1-303393I

SCALE	NONE	DATE
DESIGN BY	BJB	—
DRAWN BY	JCR	9-1-63
CHECKED BY	BJB	9/1/63
APPROVAL DEPT.	DJ	9/16/63
APPROVAL OPER.	BJB	9/16/63
APPROVAL SFT.	DJ	9/16/63
APPROVAL USNEC		

E.S.D. NO. —
W.O. NO. —
B.M. NO. —

POWER | UTILITIES | S&F

BLDG. NO.
LOCATION

UNION CARBIDE NUCLEAR COMPANY
DIVISION OF UNION CARBIDE CORPORATION
OAK RIDGE GASEOUS DIFFUSION PLANT

BIOLOGICAL ULTRA-CENTRIFUGE B-II SYSTEM
INTERCONNECTION CABLE DIAGRAM

D-I-303393B REV. 1

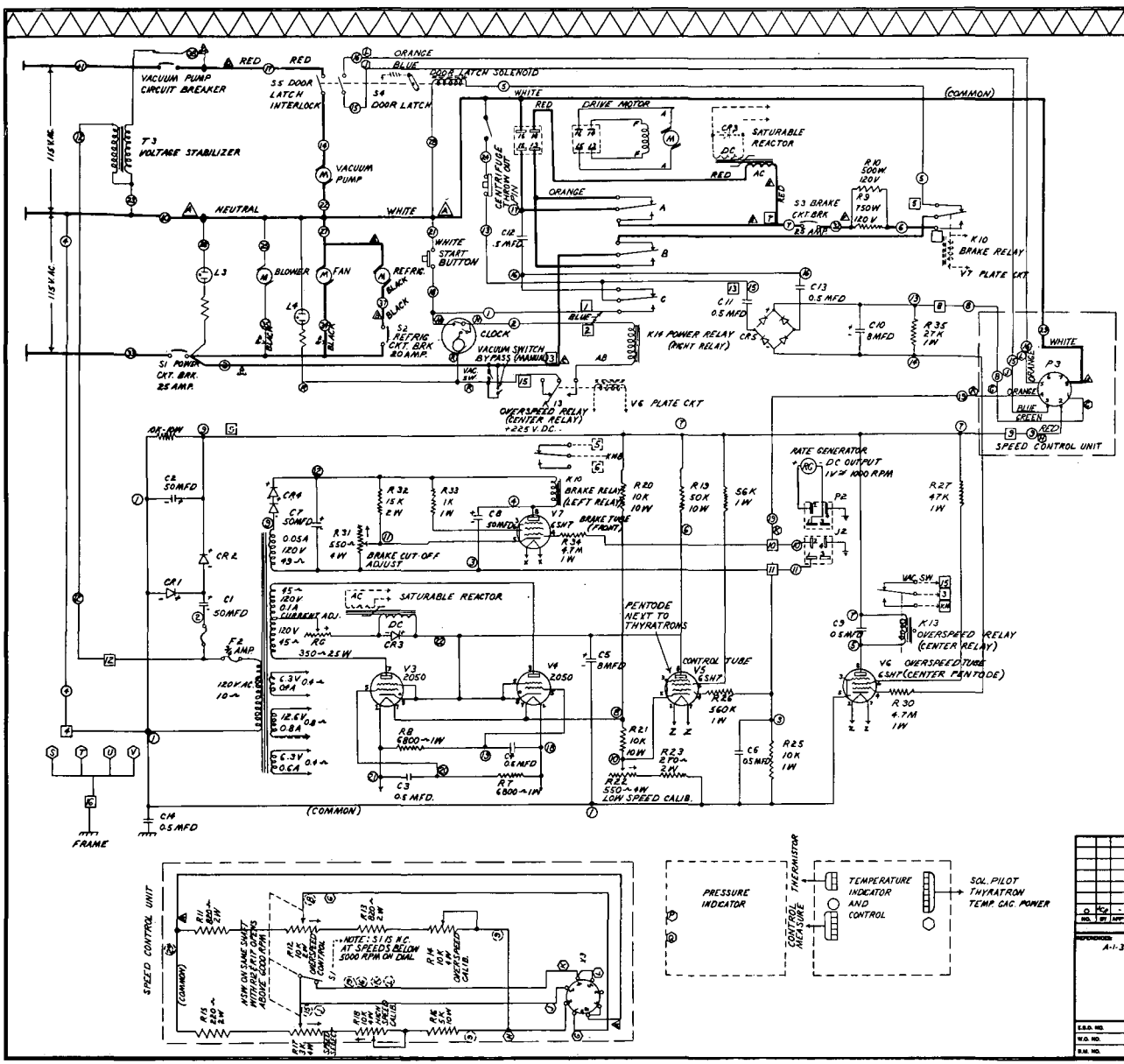

CONTROL CIRCUIT ADJUSTMENTS

A milliammeter used in conjunction with an adapter plugged in between any one of the three pentode tubes and the speed control chassis will allow control circuit adjustments to be made at the tube, rate generator, and various relays.

Following is a list of typical plate current values and their interpretation:

I. Speed Control V_5 (Pentode next to Thyratrons)

Plate current 2 to 2.5 ma. at any controlled speed. Maximum current during acceleration should not exceed 9 ma. and should taper smoothly to normal controlling current as selected speed is reached. Erratic variations in current at controlled speed indicated poor rate generator commutation or an improperly grounded machine. Insufficient current (under 2 ma.) can indicate an open rate generator circuit. A shorted rate generator circuit is indicated by the plate current not tapering off as set speed is reached.

II. Over Speed Circuit V_6 (Center Pentode)

Normal operating current of tube V_6 should never exceed 9 ma. Relay K13 (center relay) should close at 5 to 6 ma. and open at 2 to 3 ma. (Observe closing current as tube warms up.)

R14 (over speed cal.) should be adjusted so that the plate current decreases and relay K13 opens at a speed of 22 - 23,000 rpm. with a selected speed of 20,000. For purposes of overspeed circuit adjustment, rate generator plug should be removed and leads shorted. This will cause machine, once started, to run out of control.

Premature opening of relay can be caused by:

a) Improper adjustment of R_6 max. accelerating current set too high (above 16 amps.).
b) Poor vacuum
c) Poor tube V_6.

Tardy opening can be caused by accelerating current too low (below 14 amps.).

III. Brake Circuit V_7 (Front Pentode)

Normal operating current of tube V_7 should never exceed 9 ma. Relay (left relay) K10 should close at 5 to 6 ma. and open at 2 - 3 ma. Erratic variations in plate current of V_7 at low speed indicates poor rate generator commutation.

Relay K10 should pull in at speeds over 5000 rpm. and drop out at speeds below 500 rpm.

-LEGEND-

- INDICATES NO 18 WIRE.
- INDICATES NO.14 OR LARGER WIRE.
- INDICATES A NUMBER ON A WIRE.
- INDICATES A NO TERMINAL ON THE TERMINAL BOARD ASSEM IN THE ELECTRONIC CHASSIS.
- INDICATES A NO TERMINAL ON THE TERMINAL STRIP TO THE ELECTRONIC CHASSIS.
- INDICATES 'B' CABLE TERMINAL NO. (MOTOR CONTROL)
- INDICATES 'A' CABLE TERMINAL NO. (POWER CABLE)
- INDICATES 'C' CABLE TERMINAL NO. (TEMP. CONTROL & INDICATOR)

WIRES 1 2 3 4 5 6 7 8 9 10 11 12 ARE CONNECTED TO A COMMON TERMINAL STRIP ON REAR OF MACHINE.

NOTE: THIS SCHEMATIC (REVISED) PERTAINS TO MODEL 'U2U' SERIAL NO.1153 AND UP (MARCH 1958). BECKMAN DWG # X 401-93.

NO.	BY	APP'D	DATE	DESCRIPTION	S&A	MECH.	ELEC.	INST.	MACH.
				REVISIONS	SQUAD CHECK				

REFERENCED: A-I-303393I

SCALE: NONE
DESIGN BY: B.J.B.
DRAWN BY: J.C.R.
CHECKED BY: 2-7-58
APPROVAL: DEPT. 3-3-58; OPER. 3-7-58; DIV. 3-7-58; USAEC

E.S.D. NO.
W.O. NO.
S.M. NO.
POWER | UTILITIES | S&P

UNION CARBIDE NUCLEAR COMPANY
DIVISION OF UNION CARBIDE CORPORATION
GAS DIFFUSION PLANT

BIOLOGICAL ULTRA-CENTRIFUGE B II MACHINE SCHEMATIC

BLDG. NO.
LOCATION

D-I-303393C REV. 0

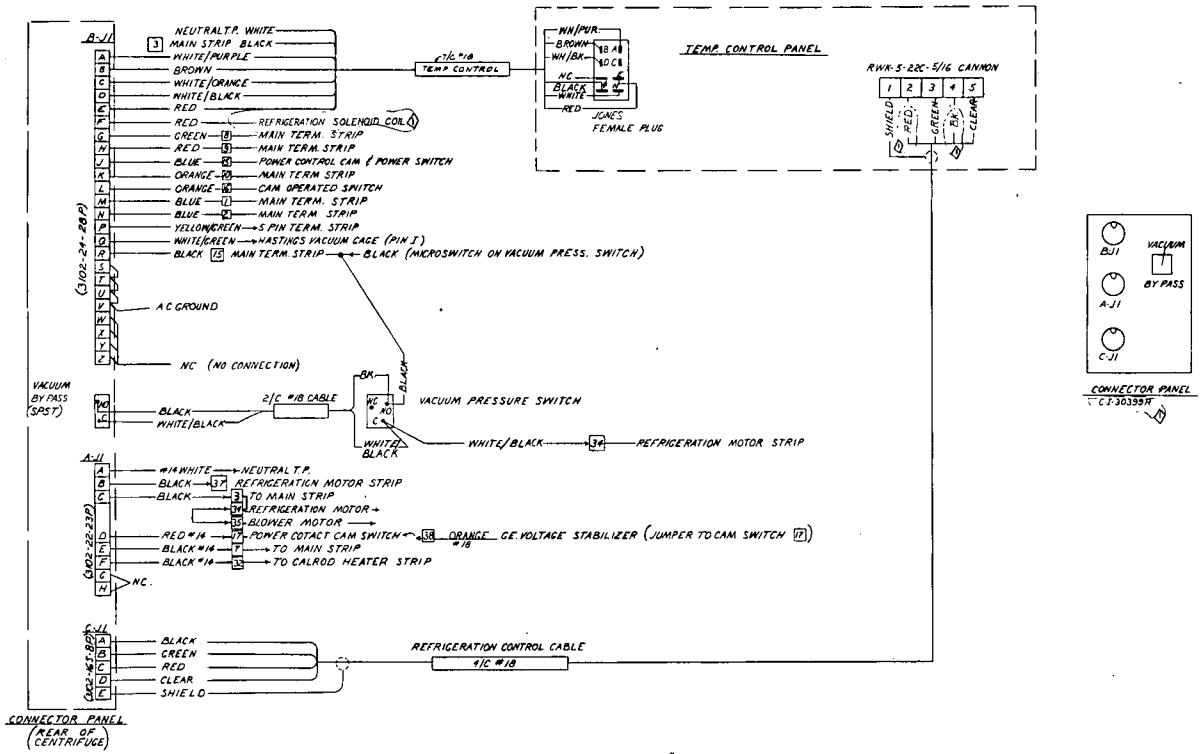

NOTE: ALL WIRE NOT DESIGNATED # 16 AWG.

NO.	BY	APP'D	DATE	DESCRIPTION	S&R	MECH	ELEC	INST.	MACH.
1	JCB	BJJ	7/[illegible]/63	REVISED WIRE COLORS & WIRE DESIG. & REF.					
0	JCB	-	-						

SQUAD CHECK

REVISIONS

REFERENCE: A-1-30399Z1

SCALE	NONE	DATE
DESIGN BY	BJB	
DRAWN BY	J.C.B.	8-7-63
CHECKED BY	BJB	8-8-63
APPROVAL DEPT.	DJJ	8/16/63
APPROVAL OPER.	BJB	8/16/63
APPROVAL DIV.	BJJ	8/16/63
USAEC		
POWER	UTILITIES	S.&P.

E.S.O. NO.
W.O. NO.
S.D. NO.

UNION CARBIDE NUCLEAR COMPANY
DIVISION OF UNION CARBIDE CORPORATION
OAK RIDGE GASEOUS DIFFUSION PLANT

BIOLOGICAL ULTRA-CENTRIFUGE
BII MACHINE
CABLING

SLDG. NO.
LOCATION

D-I-30399D REV. 1

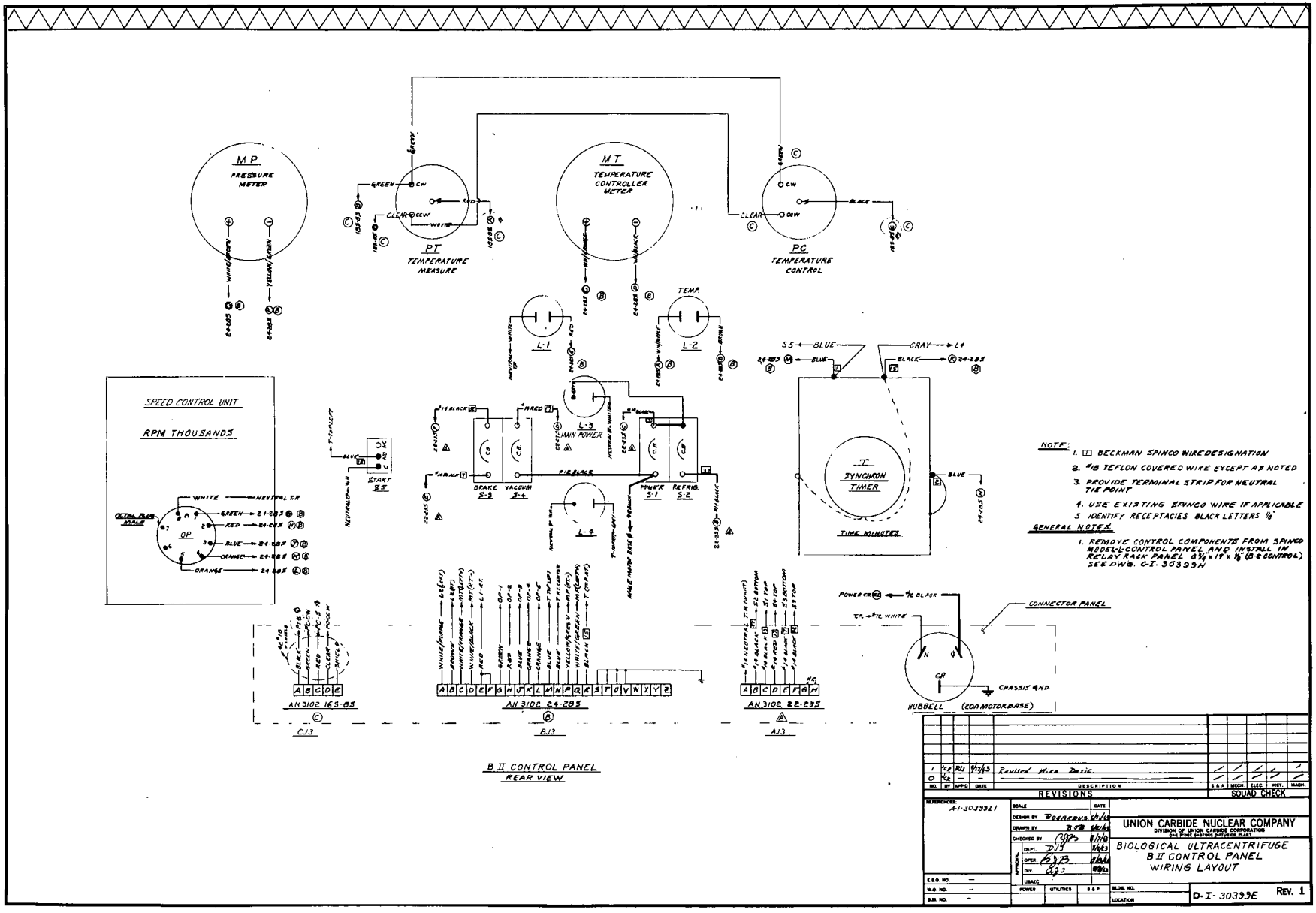

B II CONTROL PANEL
REAR VIEW

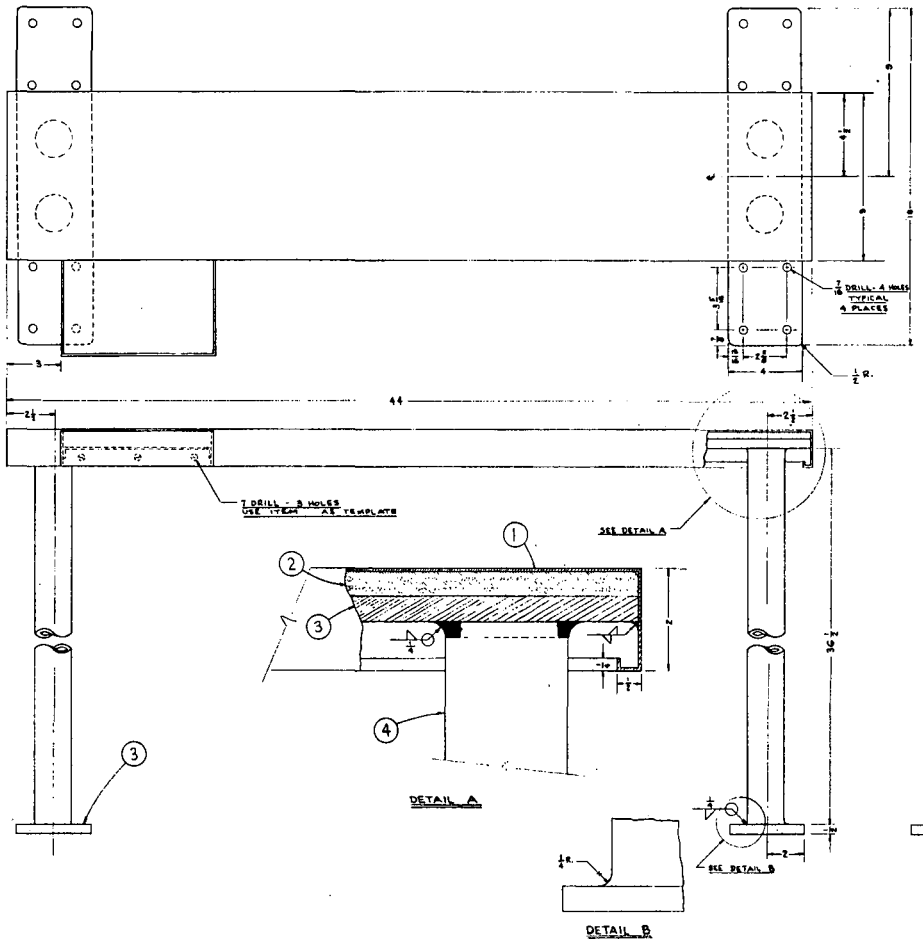

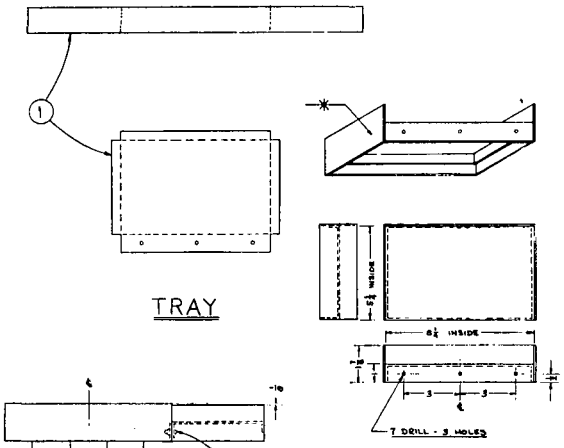

GENERAL NOTES:

1. GRIND WELD SMOOTH AT DETAIL B. BLEND CONTOURS.
2. ITEM 2 MAY BE SCREWED TO ITEM 3 IF DESIRED.
3. FILL ALL IMPERFECTIONS IN TABLE TOP (ITEM 1) BEFORE PAINTING.
4. PAINT TABLE AND TRAY SEPARATELY.
5. PAINT GRAY HAMMERTONE. FINISHED SURFACES TO BE SMOOTH & FREE OF BURRS, SHARP EDGES & CORNERS, HOLES, CRACKS, & RIPPLES.

ITEM	QUANTITY	DESCRIPTION
8	2	WASHER, LOCK, NO. 10, SHAKEPROOF
7	3	WASHER, FLAT, BRASS, NO. 10
6	3	NUT, 10-32, BRASS, HEX.
5	3	SCREW, 10-32 x 3/8, ROUND HD., BRASS
4	15 FT.	TUBING, 1 IN. O.D. x 1/8 WALL, 1100H14 ALUM.
3	4 SQ. FT.	PLATE, ALUMINUM, 1/8 IN., 1100F
2	8 SQ. FT.	PLYWOOD, FIR, 1/2 IN.
1	6 SQ. FT.	SHEET, 16 GA., STAINLESS STEEL

REFERENCES: A-I-3039921

UNION CARBIDE NUCLEAR COMPANY
A DIVISION OF UNION CARBIDE AND CARBON CORPORATION
X-10 PLANT

BIOLOGICAL CENTRIFUGE SPECTROPHOTOMETER TABLE

D- I - 30339F REV 0

SCALE 1/8" = 1.0"
DRAWN BY G.B.S.-K.S. 9/16/62
CHECKED BY R.M. 10/16/62
DSTT. 11/14/62
DFTD. 12/14/62
P.E.D. 12/21/62
SUBD. NO.
LOCATION

REVISIONS

NO.	BY	DATE	APPD.	DATE	DESCRIPTION
0	1/62	—	—	—	

SEE DRAWING NO. A-I-3039921 FOR ALL DIMENSIONS NOT SHOWN HERE

S.E.D. NO. — E.R. NO. —
E.N. NO. —
ACCT. CHG. —
W.O. NO. —

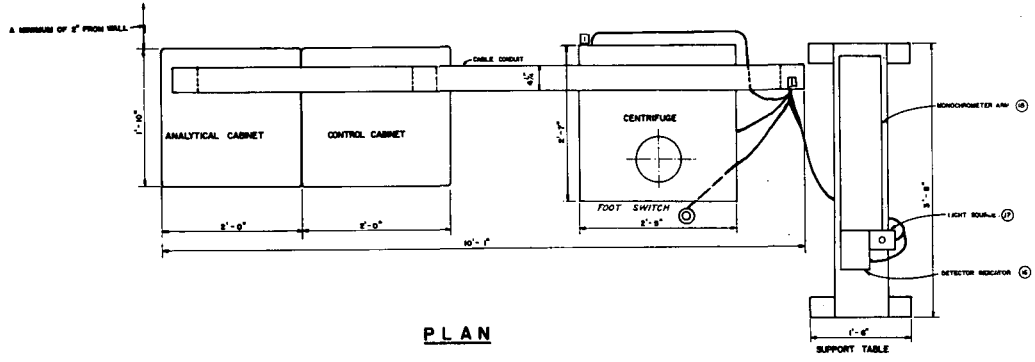

PLAN

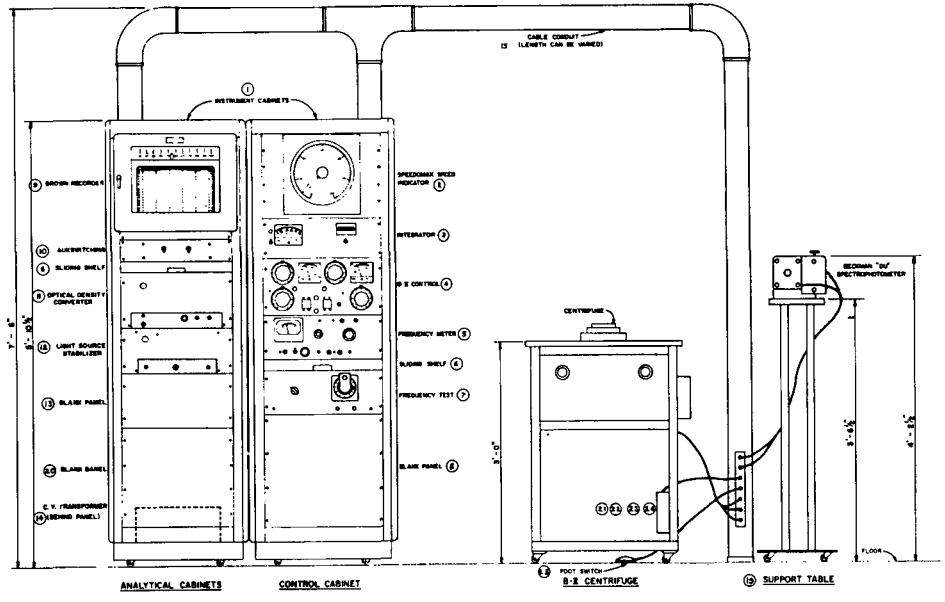

FRONT ELEVATION

ITEM	DESCRIPTION	QUAN.	MATERIAL
1	RELAY RACK CABINET	2	69 7/8" x 24 1/16" x 22" PANEL SPACE 61 1/8" BUD 60-2806SG
2	SPEED INDICATOR	1	INDICATOR - LAN SPEEDOMAX H - ROUND FACE NO RECORD 0-10 MV.
3	ELECTRONIC INTEGRATOR	1	ROYSON LECTRO COUNT II BULLETIN #31 RACK MTD. 6 DIGITS
4	B-II CONTROL PANEL	1	UCNC DWGS: D-I-30399E; C-I-30399N
5	FREQUENCY METER	1	HEWLETT PACKARD MODEL 500B/R RACK MOUNT
6	SLIDING DESK TOP	2	BUD 60-2361SG
7	FREQUENCY TEST PANEL	1	UCNC DWG. D-I-30399N
8	BLANK PANEL	1	19" x 17 1/2" x 1/8" ALUMINUM CLEAR ANODIZED
9	OPTICAL DENSITY RECORDER	1	BROWN ELECTRONIC STRIP CHART - SINGLE PEN 0-10 MV - NO. 153X12X-X-6A
10	AUXILIARY SWITCHING PANEL	1	UCNC DWG. D-I-30399N
11	OPTICAL DENSITY CONVERTER	1	GILFORD MODEL 220 RACK MTD. POWER CONVERTER UNIT
12	LIGHT SOURCE STABILIZER	1	GILFORD MODEL 205 RACK MTD. LIGHT SOURCE STABILIZER
13	BLANK PANEL	1	19" x 8 3/8" x 1/8" ALUMINUM CLEAR ANODIZED
14	C.V. TRANSFORMER	1	SOLA TYPE CUS NO. 23-22-150
15	4" x 4" WIREWAY	As Req.	NATIONAL ELECTRIC CO. 4 x 4 WIRE WAY W/HINGED COVERS
16	ABSORBANCE INDICATOR	1	GILFORD MODEL 220 ABSORBANCE INDICATOR
17	DUAL SOURCE UNIT	1	BECKMAN NO. 6871
18	TYPE "DU" MONOCHROMETER	1	BECKMAN NO. 12703
19	SUPPORT TABLE	1	UCNC DWG. D-I-30399F
20	BLANK PANEL	1	19" x 15 3/8" x 1/5" ALUMINUM CLEAR ANODIZED
21	DISTANCE DETECTOR	1	BENTLY MODEL D-152
22	ENERGIZER	1	BENTLY MODEL E-15
23	SENSING HEAD	1	BENTLY MODEL HT-084-3
24	TACHOMETER ADAPTER	1	UCNC DWG. P-E-I-30399
25	FOOT SWITCH	1	SQUARE D CO. NO. 9002-AW2 110V - 1 N.O.

1. POINTS 1 ARE CONNECTED BY 6 FOOT FLEXIBLE CABLES.
2. CENTRIFUGE MAY BE MOVED TO ANY DESIRED POSITION WITHIN LIMITS OF THE 6 FOOT FLEXIBLE CABLE.
3. POWER REQUIREMENTS:
   ONE 110 V, 30A A.C., 1 PHASE CIRCUIT
   ONE 110 V, 15A A.C., 1 PHASE CIRCUIT
4. COOLING REQUIREMENTS:
   300-400 ML. H_2O/MIN. AT 8°C.
   APPROXIMATELY 100 BTU/MIN. HEAT LOAD.

NO	BY	APP'D	DATE	DESCRIPTION	S&A	MECH	ELEC	INST	MACH
2	JCR	DJJ	7/11/63	Changed circuit rating					
1	JCR	DJJ	9/6/63	ADDED MATERIAL LIST - REVISED NOTES &					
0	JCR								

REVISIONS — SQUAD CHECK

REFERENCES: A-I-30399E1

SCALE: None
DESIGN BY: BJB
DRAWN BY: JCR
CHECKED BY: BJB
APPROVAL: DJJ, BJB, GJS

UNION CARBIDE NUCLEAR COMPANY
DIVISION OF UNION CARBIDE CORPORATION
OAK RIDGE GASEOUS DIFFUSION PLANT

BIOLOGICAL ULTRA-CENTRIFUGE INSTALLATION PLAN AND ELEVATION

D-I-30399A REV. 2

ORNL-3656
Special

INTERNAL DISTRIBUTION

1. S. I. Auerbach
2. R. Baldock
3. R. E. Biggers
4. A. L. Boch
5. D. S. Billington
6. E. P. Blizard
7. C. J. Borkowski
8. G. E. Boyd
9-10. Clark E. Center (ORGDP)
11-12. D. D. Cowen
13. C. J. Collins
14. F. L. Culler
15. P. B. Dunaway
16. J. L. Fowler
17. J. H Frye, Jr.
18. R. F. Hibbs (Y-12)
19. A. S. Householder
20. J. S. Johnson
21. R. W. Johnson
22. W. H. Jordan
23. K. A. Kraus
24. M. T. Kelley
25. J. A. Lane
26-27. C. E. Larson
28. T. A. Lincoln
29. S. C. Lind
30. R. S. Livingston
31. K. Z. Morgan
32. D. J. Nelson
33. M. L. Nelson
34. J. S. Olson
35-36. R. B. Parker
37. M. E. Ramsey
38. R. M. Rush
39. M. J. Skinner
40. J. A. Swartout
41. E. H. Taylor
42. A. M. Weinberg
43. G. C. Williams
44. H. I. Adler
45-64. N. G. Anderson
65. W. A. Arnold
66. R. H. Baum
67. M. A. Bender
68. F. J. Bollum
69. C. L. Burger
70. S. F. Carson
71. E. H. Y. Chu
72. G. B. Cline
73. W. E Cohn
74. C. C Congdon
75. F. J. de Serres
76. D. G. Doherty
77. J. L. Fairley
78. W. D. Fisher
79-81. C. J. Whitmire, Jr.
82. A. H. Haber
83. A. Hollaender
84. S. Karasaki
85. M. A. Kastenbaum
86. R. F. Kimball
87. S. P. Leibo
88. D. L. Lindsley, Jr.
89. T. Makinodan
90. P. Mazur
91. G. D. Novelli
92. T. T. Odell, Jr.
93. G. M. Padilla
94. A. P. Pfuderer
95. M. L. Randolph
96. W. L. Russell
97. R. B. Setlow
98. G. E. Stapleton
99. A. C. Upton
100. E. Volkin
101. R. C. von Borstel
102. S. Wolff
103. T. Yamada
104. E. F. Babelay
105. E. J. Barber
106. H. P. Barringer
107. J. C. Barton
108. A. S. Berman
109. H. A. Bernhardt
110. Barbara S. Bishop
111. H. D. Culpepper
112. J. T. Dalton
113-127. E. C. Evans
128. J. Farquharson
129. R. L. Farrar, Jr.
130. W. W. Harris
131-133. W. L. Harwell
134. E. T. Henson
135. A. P. Huber

136. G. R. Jamieson
137. E. C. Johnson
138. T. J. Lewis
139. E. F. Martin
140. J. R. Mahoney
141. L. L. McCauley
142. C. E. Nunley
143. P. R. Vanstrum
144. D. A. Waters
145. C. W. Weber
146. S. J. Wheatley
147. W. J. Wilcox, Jr.
148. E. Chargaff (consultant)
149. R. D. Hotchkiss (consultant)
150. Curt Stern (consultant)
151. M. M. Wintrobe (consultant)
152. P. C. Zamecnik (consultant)
153-154. Biology Library
155-157. Central Research Library
158. Reactor Division Library
159-160. ORNL – Y-12 Technical Library Document Reference Section
161-201. Laboratory Records Department
202. Laboratory Records, ORNL, R.C.
203. Laboratory Shift Supervisor

EXTERNAL DISTRIBUTION

204. Justin Andrews, NIAID (Director), Bethesda, Maryland
205. R. W. McNamee, Union Carbide Corporation, New York
206. G. A. Andrews, ORINS
207. C. Baker, National Cancer Institute, Bethesda, Maryland
208. F. Baronowski, AEC Production Division, Washington, D.C.
209. N. F. Barr, Atomic Energy Commission, Washington, D.C.
210. N. Berlin, National Cancer Institute, Bethesda, Maryland
211. H. E. Bond, U.S. Naval Radiological Defense Laboratory, San Francisco, California
212. Myron Brakke, U.S. Department of Agriculture, Agriculture Research Service, Plant Physiol. Department, University of Nebraska, Lincoln 3, Nebraska
213. H. D. Bruner, Atomic Energy Commission, Washington, D.C.
214. W. R. Bryan, National Cancer Institute, Bethesda, Maryland
215. J. C. Bugher, Puerto Rico Nuclear Center, Rio Piedras, P.R.
216. W. W. Burr, Jr., Atomic Energy Commission, Washington, D.C.
217. R. M. Chanock, National Institute of Allergy and Infectious Diseases, Bethesda, Maryland
218. R. A. Charpie, Union Carbide Corporation, New York
219. M. A. Churchill, Chief, Stream Sanitation Staff, Edney Bldg., TVA, Chattanooga, Tennessee
220. W. D. Claus, Atomic Energy Commission, Washington, D.C.
221. Helen Coates, National Institute of Allergy and Infectious Diseases, Bethesda, Maryland
222. B. T. Cole, Department of Zoology, University of South Carolina, Columbia, S.C.
223. E. Dapper, U.S. Army Chemical Corps, Fort Detrick, Maryland
224. C. M. Davidson, Environmental Hygiene Branch, Edney Bldg., TVA, Chattanooga, Tennessee
225. W. W. Davis, Eli Lilly Co., Indianapolis, Indiana
226. O. M. Derryberry, Director of Health and Safety, Edney Bldg., TVA, Chattanooga, Tennessee
227. Harold S. Diehl, Sr., Vice President for Research in Medical Affairs, American Cancer Society, 521 W. 57th St., New York 19, New York
228. C. L. Dunham, Atomic Energy Commission, Washington, D.C.
229. K. M. Endicott, National Cancer Institute, Washington, D.C.
230. S. G. English, Assistant General Manager for Research and Development, AEC, Washington, D.C.
231. J. L. Fahey, National Cancer Institute, Bethesda, Maryland
232. E. Frei, National Cancer Institute, Bethesda, Maryland
233. F. E. Gartrell, Assistant Director of Health and Safety, Edney Bldg., TVA, Chattanooga, Tennessee
234. H. Bentley Glass, Johns Hopkins University, Baltimore, Maryland
235. Donald A. Glaser, Virus Lab., U. of Calif., Berkeley 5, Calif.
236. H. N. Glassman, U.S. Army Chemical Corps, Fort Detrick, Maryland

237. E. Grabowski, AEC Production Division, Washington, D.C.
238. S. T. Grey, Food and Drug Administration, Washington, D.C.
239. N. S. Hall, University of Tennessee, Knoxville
240. John Harris, AEC Public Relations Division, ORO
241. Fred J. Hodges, University of Michigan, Medical Center, Ann Arbor
242. E. C. Horn, Department of Zoology, Duke University, Durham, N.C.
243. J. G. Horsfall, Connecticut Agricultural Experimental Station, New Haven
244. R. D. Housewright, U.S. Army Chemical Corps, Fort Detrick, Maryland
245. R. J. Huebner, National Cancer Institute, Bethesda, Maryland
246. J. S. Kirby-Smith, Atomic Energy Commission, Washington, D.C.
247. R. M. Kniseley, ORINS Medical Division
248. K. W. Kohn, National Cancer Institute, Bethesda, Maryland
249. P. Kotin, National Cancer Institute, Bethesda, Maryland
250. E. L. Kuff, National Cancer Institute, Bethesda, Maryland
251. W. T. Lammers, Davidson College, Davidson, N.C.
252. A. D. Langmuir, Chief, Epidemiology Branch, Communicable Disease Center, Atlanta, Georgia
253. R. E. Learmouth, National Cancer Institute, Bethesda, Maryland
254. J. L. Liverman, Atomic Energy Commission, Washington, D.C.
255. R. F. Loeb, College of Physicians and Surgeons, Columbia University, New York
256. W. H. Magruder, National Cancer Institute, Bethesda, Maryland
257. W. E. McMahon, Atomic Energy Commission, ORO
258. R. G. Meader, National Cancer Institute, Bethesda, Maryland
259. J. L. Melnick, Department of Virology and Epidemiology, Baylor University, College of Medicine, Houston, Texas
260. G. R. Mider, National Cancer Institute, Bethesda, Maryland
261. Carl V. Moore, Washington University, St. Louis, Missouri
262. P. T. Mora, National Cancer Institute, Bethesda, Maryland
263. J. E. Moynahan, National Institutes of Health, Bethesda, Maryland
264. M. A. Mufson, National Institute of Allergy and Infectious Diseases, Bethesda, Maryland
265. W. G. Pollard, ORINS
266. C. A. Price, Department of Plant Physiol., Rutgers-The State University, New Brunswick, N.J.
267. R. Quimby, National Aeronautics and Space Administration, Washington, D.C.
268. H. M. Roth, Research and Development Division, AEC, ORO
269. W. P. Rowe, National Institute of Allergy and Infectious Diseases, Bethesda, Maryland
270. P. S. Sarma, National Institute of Allergy and Infectious Diseases, Bethesda, Maryland
271. John Schacter, Union Carbide Corporation, New York
272. D. G. Sharp, University of North Carolina, Department of Biophysics, Chapel Hill
273. Byron T. Shaw, Administrator, Agricultural Research Service, U.S. Department of Agriculture, Washington, D.C.
274. C. S. Shoup, Atomic Energy Commission, Oak Ridge
275. R. G. Smith, Food and Drug Administration, Washington, D.C.
276. H. A. Sober, National Cancer Institute, Bethesda, Maryland
277. Sol Spiegleman, Department of Microbiology, University of Illinois, Urbana
278. W. M. Stanley, Virus Laboratory, University of California, Berkeley
279. S. R. Tipton, Department of Zoology, University of Tennessee, Knoxville
280. John Totter, Atomic Energy Commission, Washington, D.C.
281. Rodes Trautman, Plum Island Lab., USDA, Greenport, L.I., New York
282. Shields Warren, New England Deaconess Hospital, Boston, Massachusetts
283. A. G. Wedum, U.S. Army Chemical Corps, Fort Detrick, Maryland
284. J. White, National Cancer Institute, Bethesda, Maryland
285. H. G. Wood, Western Reserve University, Cleveland, Ohio
286. M. Zelle, Argonne National Laboratory, Argonne, Illinois

287-291. C. G. Zubrod, National Cancer Institute, Bethesda, Maryland
292. Atomic Energy Commission, Washington, D.C.
293. General Electric Company, Richland, Washington
294. New York Operations Office
295. AEC Patent Branch, Washington, D.C.
296-300. Division of Technical Information Extension, Oak Ridge
301. UCLA Medical Research Laboratory